

**Cultivation of microalgae:  
effect of light/dark cycles on biomass yield**

**Marcel Janssen**

Cultivation of microalgae:  
effect of light/dark cycles on biomass yield

Promotor:

Prof. Dr. Ir. J. Tramper

*Hoogleraar in de Bioprocestechnologie, Wageningen Universiteit*

Co-promotoren:

Dr. Ir. R. H. Wijffels

*Universitair hoofddocent sectie Proceskunde, Wageningen Universiteit*

Prof. Dr. L. R. Mur

*Hoogleraar in de Aquatische Milieubiologie, Universiteit van Amsterdam*

Samenstelling promotiecommissie:

Prof. Dr. E. J. R. Südholtzer (*Wageningen Universiteit*)

Prof. Dr. Ir. A. J. M. Stams (*Wageningen Universiteit*)

Dr. L. Sijtsma (*ATO-DLO*)

Dr. J. C. P. Matthijs (*Universiteit van Amsterdam*)

Prof. Dr. E. Molina Grima (*Universidad de Almeria*)

Marcel Gerard Jozef Janssen

Cultivation of microalgae:  
effect of light/dark cycles on biomass yield

**Proefschrift**

Ter verkrijging van de graad van doctor  
op gezag van de rector magnificus  
van Wageningen Universiteit,  
Prof. Dr. Ir. L. Speelman,  
in het openbaar te verdedigen  
op maandag 25 maart 2002  
des namiddags te vier uur in de Aula.

M. Janssen - Cultivation of microalgae: effect of light/dark cycles on biomass yield – 2002  
Thesis Wageningen University, Wageningen, The Netherlands – with summary in Dutch –  
184 p.

Keywords: microalgae, cultivation, light regime, light/dark cycles, biomass yield,  
photosynthetic efficiency, photobioreactors, scale-up.

ISBN: 90-5808-592-9

Printed by: Ponsen & Looijen BV, Wageningen, The Netherlands

*Dit proefschrift is opgedragen aan Jan, Riek  
en Anja Janssen*

# Contents

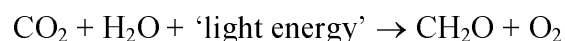
<b>Chapter 1</b>	Introduction	9
<b>Chapter 2</b>	Specific growth rate of <i>Chlamydomonas reinhardtii</i> and <i>Chlorella sorokiniana</i> under medium-duration light/dark cycles: 13 – 87 s	29
<b>Chapter 3</b>	Efficiency of light utilization of <i>Chlamydomonas reinhardtii</i> under medium-duration light/dark cycles: 6 – 25 s	45
<b>Chapter 4</b>	Efficiency of light utilization of <i>Chlamydomonas reinhardtii</i> and <i>Dunaliella tertiolecta</i> under medium-duration light/dark cycles: 15 s	69
<b>Chapter 5</b>	Microalgae cultivation: modeling biomass yield on light energy as a function of light-gradient/dark cycles: 10 - 100 s	91
<b>Chapter 6</b>	Efficiency of light utilization of <i>Dunaliella tertiolecta</i> under short light/dark cycles: 0.19 - 6 s	107
<b>Chapter 7</b>	Enclosed outdoor photobioreactors: light regime, photosynthetic efficiency, scale-up and future prospects	123
	<b>Summarizing Discussion</b>	159
	<b>References</b>	165
	<b>Samenvatting</b>	175
	<b>Nawoord</b>	179
	<b>Curriculum Vitae</b>	183

# 1. Introduction

## Micro-algae and cyanobacteria

Microalgae and cyanobacteria, also called blue-green algae, are most widely known as a nuisance to the public. Algae stick to the wall of your aquarium and cyanobacterial blooms can spoil surface waters just because the water does not look very attractive anymore and smells. Cyanobacteria even can release toxins dangerous for humans. But these unicellular microorganisms can also be exploited in many different ways as will be explained later. For this they need to be cultivated in controlled and preferably closed systems with sufficient supply of light energy. In this introduction a theoretical background is given on microalgae, microalgal cultivation and enclosed photobioreactors. At the end of this chapter an outline of the thesis is presented.

Microalgae and cyanobacteria are oxygenic photoautotrophic microorganisms. They are able to use sunlight to metabolize carbon dioxide (CO<sub>2</sub>) inside energy-rich organic compounds (CH<sub>2</sub>O) under liberation of oxygen (O<sub>2</sub>). The organic compounds, represented by CH<sub>2</sub>O, are used as building blocks for microalgal growth; for brevity the term microalgae is also used for cyanobacteria. As can be seen in the following generalized equation, water (H<sub>2</sub>O) is needed as an additional substrate:



This process of light-driven biomass growth is called photosynthesis, which is the only biological process of importance that can harvest energy from the sun.

### *Oxygenic photosynthesis*

Microalgae, including cyanobacteria, have the capacity to absorb light energy, photons, and to store it as chemical energy via the formation of chemical bonds. The basic unit of the photosynthetic apparatus is the photosystem. Light energy, i.e. photons, is absorbed by carotenoid and chlorophyll pigments of the photosystem antenna complex. In Figure 1.1 the operation of photosystem II is shown schematically. The excitation energy is funneled through the pigment bed towards the reaction center (P680), which is brought to a higher energy level (P680<sup>\*</sup>). Almost 95 to 99 % of the excitations can be transferred to the reaction center. The transfer of energy is that efficient because the excitations 'fall' inside an 'energy hole' with



the reaction center at the bottom. During transport the excitations lose some energy and this is the reason reverse transport is not possible. Inside the reaction center the remaining excitation energy activates the reaction center ( $P680 \rightarrow P680^*$ ) by promoting an electron from the highest-energy filled orbital to the lowest-energy unfilled orbital. The electron is quickly transferred to an acceptor generating an oxidant and reductant, respectively, and this process is called charge separation.

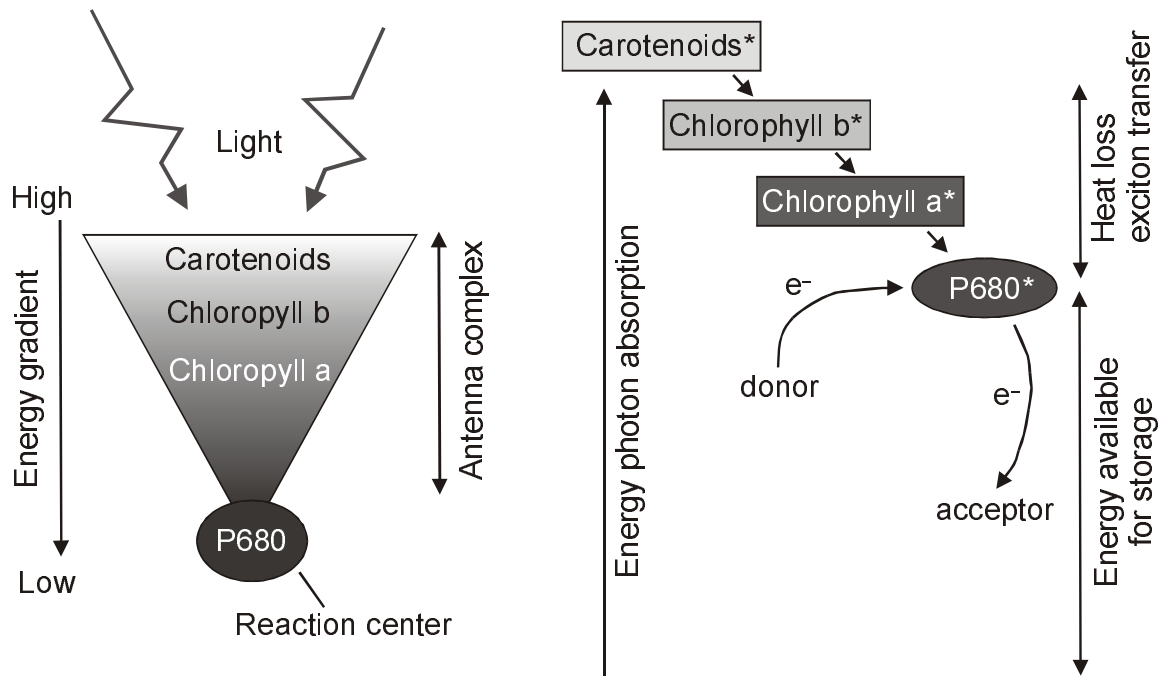


Figure 1.1. The photosystem, funneling of light-induced excitations from the antenna complex to the reaction center; light-induced excitation energy is marked with '\*'.

A considerable diversity exists among the carotenoid and chlorophyll pigments. The different divisions of microalgae are characterized by a specific pigment composition. In Figure 1.2, characteristic absorption spectra of a green alga (Chlorophyta), a diatom (Chrysophyta) and a cyanobacterium (cyanophyta) are shown. The absorption peaks between 650 and 700 nm, the red region, are caused by chlorophyll absorption. Carotenoids, also called accessory pigments, absorb most strongly in the blue region (400-500 nm) and transfer the excitation energy to the chlorophylls, making photosynthesis efficient over a wider range of wavelengths. In addition to chlorophylls and carotenoids, cyanobacteria have other pigments called phycobilisomes. This enables the blue-green algae to absorb a part of the solar spectrum (600-650 nm) more strongly than the other microalga (Figure 1.2).

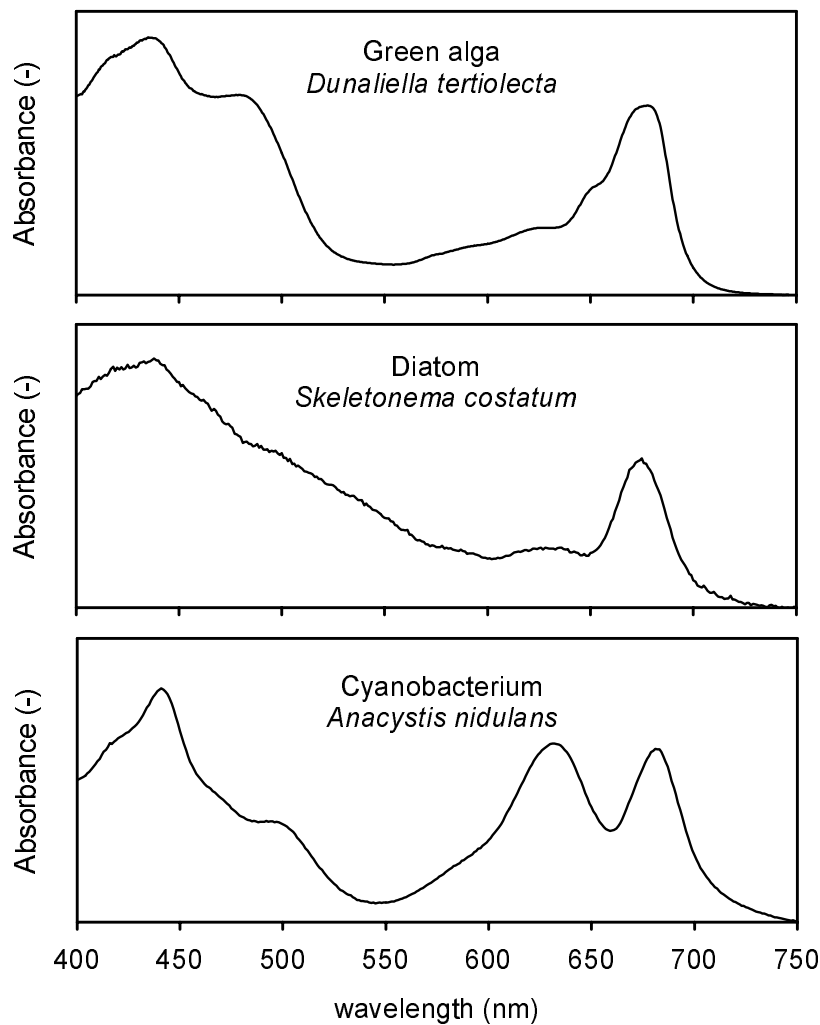


Figure 1.2. Characteristic absorption spectra of microalgae: a green alga, *Dunaliella tertiolecta*, a diatom, *Skeletonema costatum* (Courtesy of Kromkamp and Limbeek, 1993) and a cyanobacterium, *Anacystis nidulans* (Courtesy of Louis Aubriot).

In addition to light harvesting, carotenoids have other functions in the cell. They protect the photosynthetic system in the situation algae are exposed to high light intensities. An overdose of excitation energy can lead to production of toxic species (e.g. singlet oxygen) and to photosystem damage (Vacha, 1995; Barber, 1994). Carotenoids are capable of scavenging toxic photoproducts (Vacha, 1995; Edge, et al., 1997). More important, they can prevent the formation of these products because an overdose of excitation energy can be dissipated as heat by carotenoids in the antenna complex (Demmig-Adams, et al., 1995; Gilmore, 1997; Niyogi, et al., 1997b; Casper-Lindley and Björkman, 1998; Masojidek, et al., 1999). This process of heat dissipation is always present, but additional capacity can be induced after long-term exposure to high light intensity. Also carotenoids (e.g. astaxanthin) can accumulate

and possibly act as a 'sun-shade' during high-light exposure in combination with other stress factors (Masojidek, et al., 2000). But the exact role of carotenoids in these processes is still under discussion. Moreover, the exact mechanisms of heat dissipation are diverse.

In oxygenic photosynthesis two photosystems, Photosystem II (PSII) and photosystem I (PSI), operate in series (Figure 1.3). The reaction center of PSII shows the strongest absorption at 680 nm and is called P680. Practically this means that the excitation energy of every photon with a wavelength smaller than 680 nm, absorbed by the antenna pigments, can be transferred to P680. Accordingly, the PSI reaction center, P700, absorbs most strongly at 700 nm. PSII generates a strong oxidant capable of liberating electrons from water. The reductant delivers the reducing equivalents via a series of electron carriers and the cytochrome  $b_6f$  complex to the oxidized reaction center of PSI. The light energy absorbed by PSI is not only used to oxidize the reaction center, but is also used to produce a strong reductant capable of reducing oxidized nicotinamide adenine dinucleotide phosphate (NADP<sup>+</sup>) to NADPH.

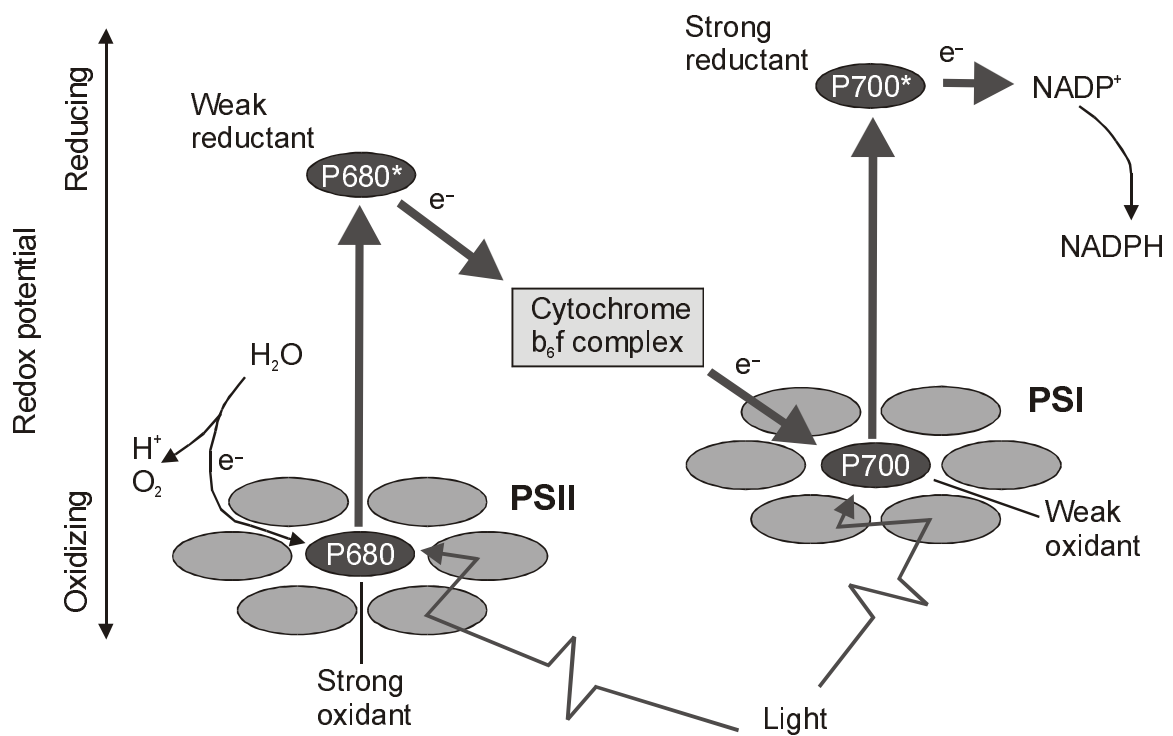


Figure 1.3. The 'light reactions' of oxygenic photosynthesis, production of reduced nicotinamide adenine dinucleotide phosphate (NADPH); light-induced excitation energy is marked with '\*'.  
 Redox potential

In Figure 1.4 the structure of the photosynthetic machinery is shown in more detail. Both photosystems are inserted in the lipid bi-layer of the so-called thylakoid membranes. The thylakoid membranes enclose an inner space called the lumen. The strong oxidant formed

after excitation of the PSII reaction center induces splitting of water into oxygen, electrons and protons. The protons are left in the lumen. In a continuous process electrons are used to reduce the reaction center, and, after renewed excitations, they are transported to plastoquinone (PQ). Protons are picked up from the surrounding medium (stroma) producing fully reduced plastoquinone ( $\text{PQH}_2$ ). This membrane-soluble protein diffuses to the cytochrome  $b_6f$  complex. Via the cytochrome complex electrons are transferred to the water-soluble electron carrier plastocyanin (PC). A special mechanism inside this complex allows for additional pumping of protons across the lipid bilayer (Figure 1.4). Via the lumen, plastocyanin diffuses to PSI, which acts as an oxidant after light-induced excitation. One by one, the electrons released by plastocyanin reduce the reaction center, and, after renewed light-induced excitations, they are transported to the electron carrier ferredoxin (Fd). Finally,  $\text{NADP}^+$  is reduced to NADPH via the action of ferredoxin-NADP reductase (Fp). The proton gradient across the thylakoid membrane drives adenosine triphosphate (ATP) production via the action of ATP synthase.

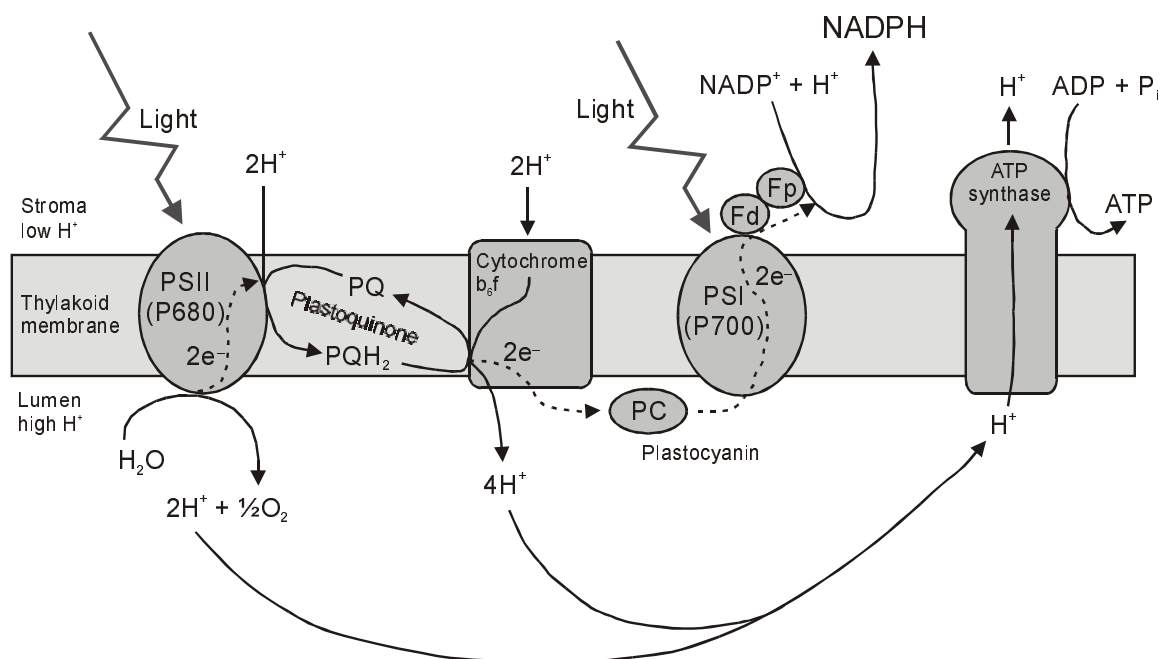


Figure 1.4. The site of the 'light reactions': the thylakoid membrane, linear electron transport and production of adenosine triphosphate (ATP) via a proton motive force.

In the eukaryotic microalgae the thylakoid membranes are found in the chloroplast. In the prokaryotic cyanobacteria the site of photosynthesis is the plasma membrane or membranes derived from it. The energy and reducing power derived as ATP and NADPH is used to fix

carbon dioxide via the action of ribulose-biphosphate carboxylase (Rubisco) in the Calvin cycle. The carbon reduction reactions take place in the aqueous region of the chloroplast, the stroma, or in the cytoplasm (cyanobacteria). The product of the Calvin cycle is phosphoglyceraldehyde (triose P) and this is the building block for synthesis of fats, fatty acids, amino acids and carboxylic acids. In addition, triose P is the starting point for synthesis of hexose P, followed by carbohydrate synthesis. Carbohydrates (e.g. starch) are stored and used later as energy source (respiration) and building blocks.

### ***Products from microalgae***

The process of photosynthesis itself may be very interesting, but this is not the reason why photoautotrophic microorganisms are cultivated. Microalgae are rich in many specific and attractive compounds (Cohen, 1986; Benemann, 1990; Apt and Behrens, 1999). Long-chain polyunsaturated fatty acids are one category of potential products. Eicosapentaenoic acid (EPA) has a significant effect on the vascular status of humans because of the antithrombotic and antiaggregatory effects. In addition, docosahexaenoic acid (DHA) is a dominant fatty acid in neurological tissue, i.e. the gray matter of the human brain. These compounds are very interesting as nutritional supplements. Other nutraceuticals already derived from microalgae are  $\beta$ -carotene (pro-vitamin A) and astaxanthin (antioxidant) and these two processes are scaled to a commercial scale (Borowitzka, 1992 and 1999; Olaizola, 2000). But also other vitamins and antioxidants can be derived from microalgae (Cohen, 1986; Benemann, 1990; Borowitzka, 1992).

Because of the large photosynthetic machinery, microalgae are very rich in pigments. Especially cyanobacterial phycobilisomes (e.g. phycocyanin) are interesting because of their excellent fluorescent properties (Apt and Behrens, 1999). Photoautotrophic microorganisms as microalgae, including cyanobacteria, are also capable to carry out very specific conversions. Because microalgae incorporate inorganic carbon ( $\text{CO}_2$  and  $\text{HCO}_3^-$ ), they are very useful for production of isotopically labeled  $^{13}\text{C}$ -compounds. In addition to carbon, it is easy to produce labeled  $^2\text{H}$ - or  $^{15}\text{N}$ -compounds from nitrate ( $^{15}\text{NO}_3^-$ ) and water ( $^2\text{H}_2\text{O}$ ) (Apt and Behrens, 1999).

Moving further into the pharmaceutical market microalgae contain sterols, which could be used as building blocks for pharmaceuticals (hormones). Moreover, cyanobacteria are a potential source of compounds with biomedical applications (anti-microbial, -viral or anti-cancer compounds) (Cohen, 1986; Borowitzka, 1995; Apt and Behrens, 1999).

Finally, photosynthesis is the only biological process of importance in which light energy is fixed as chemical energy by means of production of energy-rich carbon compounds. Microalgae therefore have the potential to be used for bioenergy production (Casadevall, et al., 1985; Braun and Reith, 1993). Although this has been studied extensively, large-scale application is not yet feasible because of the complications involved with the scale-up of photobioreactors (Chapter 7). Possibly new insights could be gained in the future as a spin-off of the potential commercial exploitation of microalgae described above.

## Cultivation of microalgae

Cultivation of microalgae seems quite easy. Only simple nutrients need to be provided such as ammonium or nitrates, phosphates, trace amounts of certain metals and, most importantly, the greenhouse gas carbon dioxide. Because algae are autotrophic they can grow on these simple and cheap media. The only problem is that algae are phototrophic and that light energy is the growth limiting ‘substrate’. This is nice on one hand because the energy source can be for free: sunlight! But, on the other hand, it is very difficult to expose your culture to a sufficient amount of light energy and to utilize this energy efficiently for biomass production.

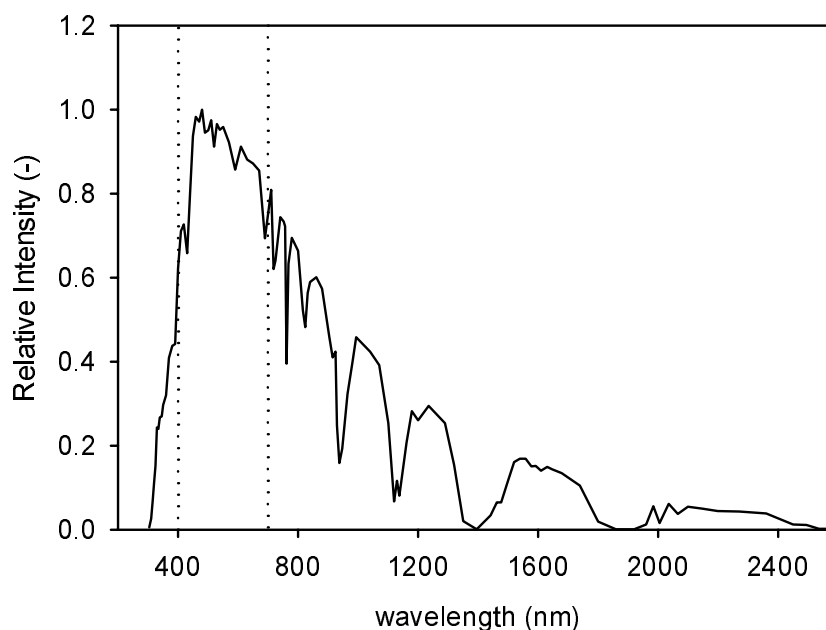


Figure 1.5. Relative intensity on energy basis of sunlight at ground level (American Society for Testing and Materials, ASTM, spectrum E892).

### Light as the substrate

Sunlight is the ultimate energy source for microalgae. In Figure 1.5 the relative light intensity of sunlight at ground level is shown. Although the wavelength range of solar radiation is very broad, only radiation between 400 and 700 nm can be used by microalgae (Figure 1.2). This part of the solar spectrum is called 'Photosynthetic Active Radiation' (PAR) and is enclosed with dotted lines in Figure 1.5. On an energy basis 43 % of the solar radiation is in the PAR region (Thimijan and Heins, 1983).

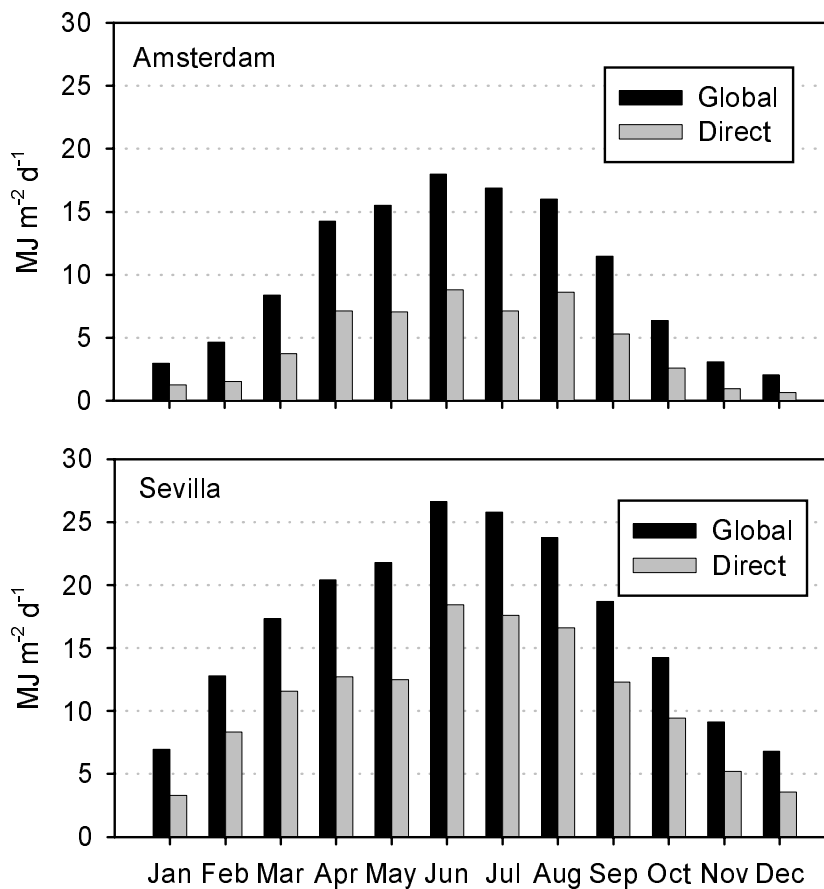


Figure 1.6. Horizontal global and direct daily irradiance on ground level in: Amsterdam 52°21'N and Sevilla 37°22'N in 1996 and 1997 according to The European Database of Daylight and Solar Radiation (Fontoynt, et al., 1998).

The magnitude of solar radiation is dependent on the geographical position on Earth and the climatological conditions at that position. As an illustration the irradiance on a horizontal surface at two different geographical locations is shown in Figure 1.6: Amsterdam and Sevilla. Global irradiance is the sum of direct beam irradiance and diffuse irradiance. Diffuse irradiance is caused by scattering of light by small aerosols in the atmosphere and water

droplets (clouds). In June global irradiance in Amsterdam is  $18.0 \text{ MJ m}^{-2} \text{ d}^{-1}$ , which is 68 % of that in Sevilla,  $26.6 \text{ MJ m}^{-2} \text{ d}^{-1}$ . In Sevilla much more than half of the global radiation (69 % in June) reached ground level as direct beams. In Amsterdam this is less than half (49 % in June) because of more days with overcast skies.

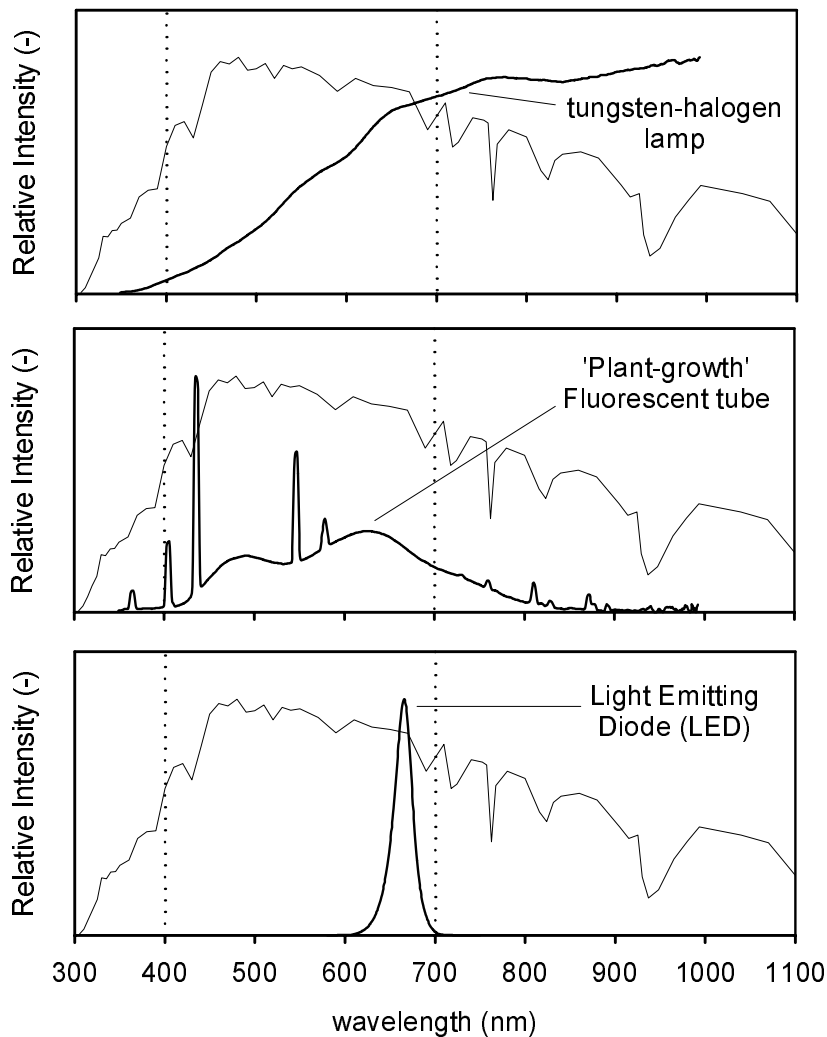


Figure 1.7. Relative intensity on energy basis of artificial light: Tungsten-halogen lamp (Philips Halotone, 300 W, 230 V, R7s), 'plant-growth' fluorescent tube (Osram-Sylvania, Britegro 2023, 36 W) and a Light Emitting Diode, LED (Kingbright, L-53SRC-F). In all graphs the relative intensity of sunlight is presented as a reference.

Studies on microalgae are preferable done under controlled conditions. Since outdoor sunlight cannot be controlled, microalgae are usually studied indoors under artificial illumination. Many different types of lamps are available. The cheapest and simplest to use are fluorescent lamps and tungsten-halogen lamps. Both were used in the experiments leading to this thesis. Fluorescent tubes can be specially adapted to provide more homogeneous illumination in the



PAR region. An example of such a 'plant-growth' fluorescent spectrum is shown in Figure 1.7, together with the spectrum of a tungsten-halogen lamp.

The tungsten-halogen lamp shows a low intensity in the blue region (400-500 nm) but intensity increases strongly at higher wavelengths and a large part of the radiation is composed of wavelengths higher than 700 nm. In addition to these lamps, light-emitting diodes (LEDs) were used. LEDs show a very narrow emission peak. In this thesis LEDs peaking between 660 and 665 nm were used, which coincides with the chlorophyll absorption peaks (Figure 1.7 and Figure 1.2). LEDs are very robust and can be alternately switched on and off at higher frequencies than tungsten-halogen lamps, which was important in the experiments of this thesis.

It is clear that light is not a simple substrate for algae as is glucose for yeast, for example. Depending on the light source the exact composition of light is different (Figure 1.7). Also light absorption by microalgae is wavelength dependent (Figure 1.2). But, to be able to quantify light intensity in a single number it is common practice to sum all contributions between 400 and 700 nm of the light source (see dotted lines in Figure 1.7). This wavelength range is chosen because this is the part of the spectrum which can be absorbed and utilized by microalgae, hence the name 'photosynthetic active radiation' (PAR). In addition it is common practice to express light intensity as the photon flux density (PFD): the number of photons impinging on a flat surface per unit of time,  $\mu\text{mol m}^{-2} \text{s}^{-1}$ . Light sensors in photosynthesis research are adapted in such a way that every photon in the PAR range results in the same output.

The reason not to use energy units ( $\text{W m}^{-2}$ ) is the fact that photosynthesis is a quantum process. Every PAR-photon absorbed by the antennae can be used inside the reaction center to induce charge separation (Figure 1.1). This is illustrated in Figure 1.8. For two different microalgae, *Chlorella* (green alga) and *Navicula minima* (diatom), the quantum yield is shown as a function of wavelength. A quantum yield of 0.1 corresponds to a quantum requirement of 10, which means that one molecule of oxygen is produced upon absorption of 10 photons. It can be seen that the quantum requirement is more or less constant in the PAR range. This means that every photon absorbed results in an equal photosynthetic output although the affinity for absorption is different (Figure 1.2).

Whenever irradiance on a surface is expressed on energy basis (e.g. Figure 1.6) and the spectral distribution of the light source is known it is possible to calculate the corresponding photon flux density. In the case of Amsterdam in summertime, daily irradiance on a horizontal surface is  $16.0 \text{ MJ m}^{-2} \text{ d}^{-1}$ . Assuming a 12 hours day period this corresponds to

$370 \text{ W m}^{-2}$ . Combining the solar spectrum (Figure 1.5) and Planck's Law this can be recalculated to a PFD of  $818 \mu\text{mol m}^{-2} \text{ s}^{-1}$  in the PAR range.

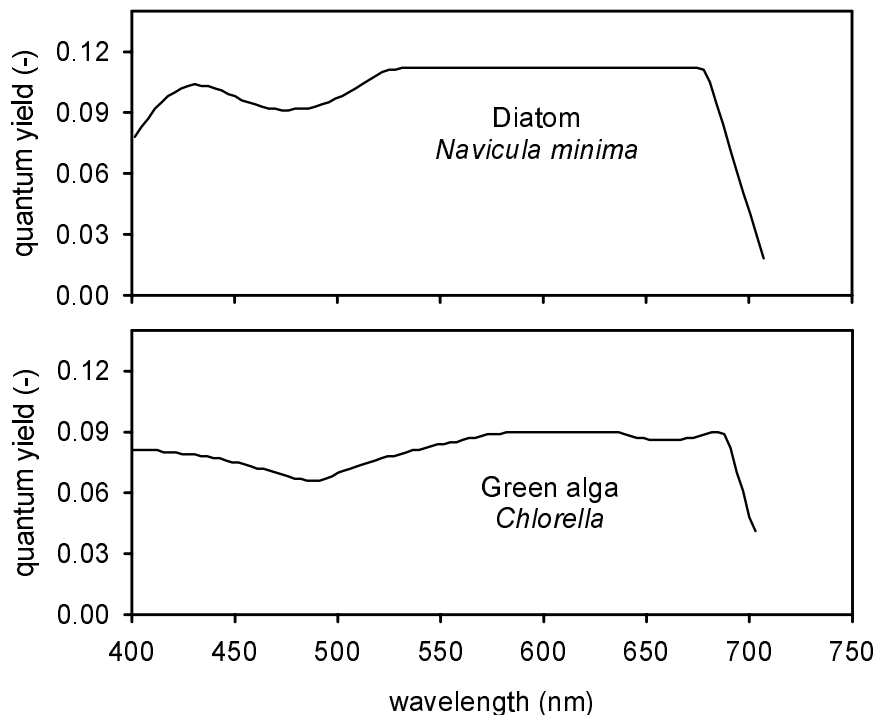


Figure 1.8. Quantum yield (oxygen basis) as a function of wavelength in two microalgae: *Chlorella* (green alga, after Emerson and Lewis, 1943) and *Navicula minima* (diatom, after Tanada, 1951).

Photosynthesis, i.e. microalgal growth, is strongly dependent on the photon flux density (PFD). This dependency can be determined in short-term oxygen production experiments. Photosynthesis can be measured as the specific oxygen production rate under increasing PFDs (Figure 1.9). Under low PFDs oxygen production increases linearly with the PFD, illustrated with the dashed line in Figure 1.9. At PFDs higher than  $100 \mu\text{mol m}^{-2} \text{ s}^{-1}$  the increase of the oxygen production rate slows down and, eventually, the alga reaches its maximal oxygen production rate. This phenomenon is called light-saturation of photosynthesis. The discrepancy between the straight dashed line and the curved solid line is a measure of the PFD that cannot be utilized by the alga although this photon flux is absorbed. In other words light energy is only utilized efficiently under low PFDs; lower than approximately  $100 \mu\text{mol m}^{-2} \text{ s}^{-1}$  in this case.

At high PFDs the antenna complexes of the photosystems (Figure 1.1) absorb too much light. A considerable part of the excitation energy cannot be utilized in the reaction centers because

their capacity is limited. As a result, the surplus of excitation energy is predominantly dissipated as heat in the antenna. For this reason, the determination of the (maximum) quantum yield, as shown in Figure 1.8, is always done under low light intensities.

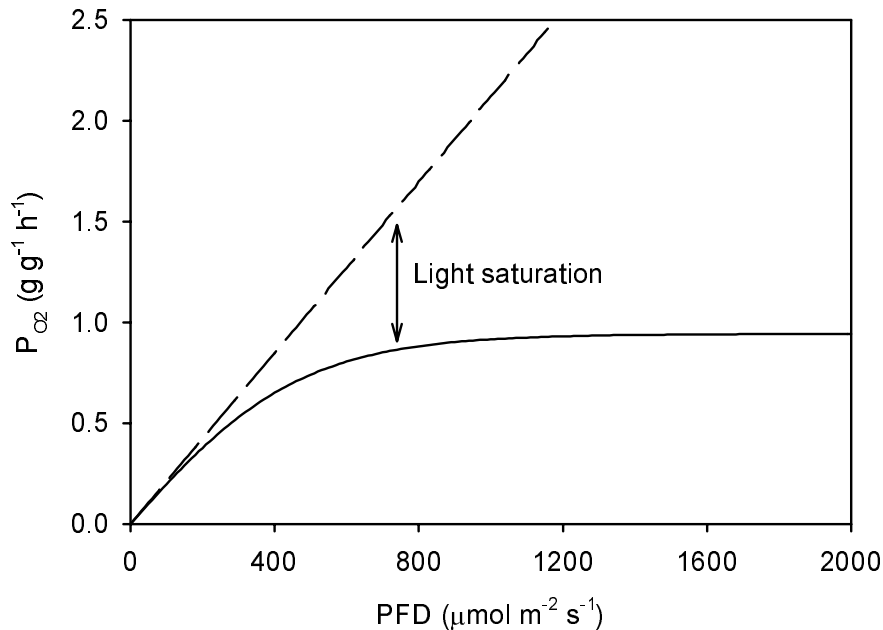


Figure 1.9. Specific oxygen production rate ( $P_{O_2}$  in  $g\ g^{-1}\ h^{-1}$ ) on a protein basis as a function of the photon flux density (PFD in  $\mu\text{mol}\ m^{-2}\ s^{-1}$ ). Data obtained for *Chlamydomonas reinhardtii* (green alga) cultivated under continuous light of 600 - 700  $\mu\text{mol}\ m^{-2}\ s^{-1}$ , Chapter 3.

### ***Cultivation, productivity and photosynthetic efficiency***

A huge variety of very interesting cultivation systems for microalgae have been developed. The only one used on a large scale and a commercial basis is the shallow open raceway-pond (Figure 1.10). These ponds are usually no more than 30 cm deep and the water with nutrients and microalgae is circulated with a paddle wheel. Sunlight impinges on the surface and is absorbed inside the culture; the photon flux density will decrease with increasing depth. This is visualized in Figure 1.11 for a pond depth of 30 cm and a photon flux density of 1000  $\mu\text{mol}\ m^{-2}\ s^{-1}$ . The attenuation coefficient was estimated at 0.15  $m^{-1}$ , but in reality this is determined by the actual biomass density and the specific absorption of the biomass. The largest part of the volume is exposed to very low PFDs (Figure 1.11). In this zone the light energy will be utilized efficiently. Close to the reactor surface, however, the PFD is very high and there light efficiency will be very low (Figure 1.9). This is a general problem in microalgal cultivation systems. Reduction of the irradiance level will lead to more efficient

utilization of the remaining light energy. But, of course, shading is not an option in microalgal biotechnology because overall light input, and hence volumetric productivity, will decrease.



Figure 1.10. Shallow open raceway pond (Courtesy of Cyanotech Inc., Hawaii, USA).

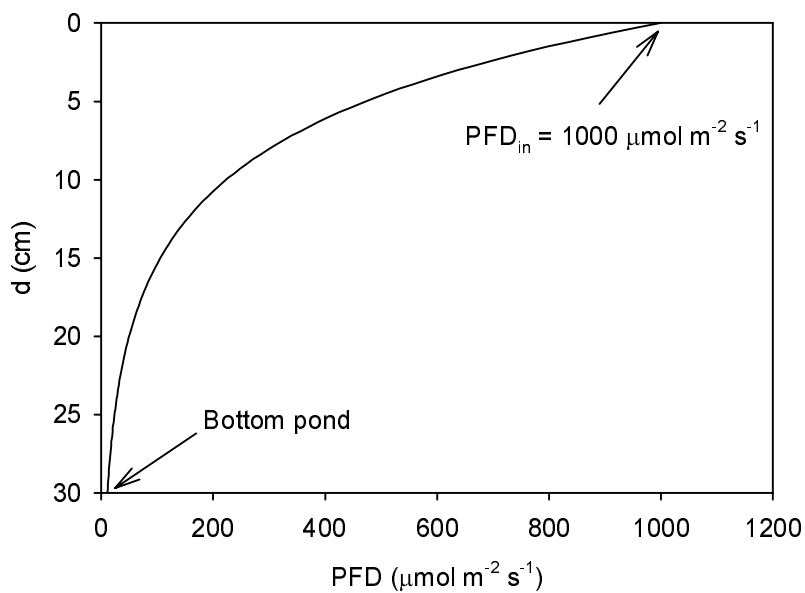


Figure 1.11. Photon flux density (PFD in  $\mu\text{mol m}^{-2} \text{s}^{-1}$ ) as a function of the distance to the light-exposed surface ( $d$  in cm). The PFD is estimated using Beer's law and an attenuation coefficient of  $0.15 \text{ m}^{-1}$ .

From this open pond example it is clear that two parameters are very useful to characterize the efficiency of microalgal cultivation systems: the volumetric productivity and the efficiency of light utilization. The volumetric productivity is the product of the biomass density and the specific growth rate. A high volumetric productivity is beneficial because this means you can suffice with a small cultivation system. Moreover, a high volumetric productivity usually is accompanied with a high biomass density, which is more attractive with respect to downstream processing. These considerations are very common in the field of bioprocess engineering. But, working with photosynthetic microorganisms, the efficiency of light utilization should be considered too. An increase in the efficiency of light utilization will lead to an increase of the volumetric productivity. Light energy is the growth limiting substrate and light falling on the cultivation system should be used as efficiently as possible.

The efficiency of light utilization for photoautotrophic growth can be expressed in several ways. In algal biotechnology the term photosynthetic efficiency (PE) is widely used and it is equal to the ratio between the caloric value of biomass produced and the light energy absorbed. The photosynthetic efficiency is usually expressed as a percentage. On the other hand, the efficiency of light utilization can also be expressed as the biomass yield on light energy in grams of dry weight or protein produced per amount of light energy absorbed ( $Y_{dw,E}$  or  $Y_{prot,E}$ ). If light energy is expressed as mol quanta in the PAR range (400-700 nm) this yield can be determined easily using widely available PAR-based quantum sensors.

Returning to the open pond design it is known that the volumetric productivity is poor because of the long light path, tens of centimeters. The photosynthetic efficiency on the other hand is reasonable (Richmond, 1996). Nevertheless, this is a very successful concept because of the simplicity and the low costs. However, only a few species can be grown in these systems open to the environment: *Dunaliella salina* at high salinity, *Spirulina platensis* at high alkalinity and fast-growing *Chlorella* species. Many other microalgae species are also promising for the production of a large variety of compounds. To be able to grow such monocultures for extended time, enclosed photobioreactors should be used to prevent contamination with other (micro)organisms. A closed production system will be even more important when the possibility exists to improve algal strains using genetic techniques.

## **Enclosed photobioreactors**

Many different type of lab-scale and pilot-scale photobioreactors have been developed (Pulz and Scheibenbogen, 1998; Tredici, 1999). Also a few have been scaled to a production level

size (Olaizola, 2000; Pulz, et al., 2001). These designs, however, will not be introduced here. In Chapter 7 the most important designs are covered in a detailed study. In this introduction only one important common aspect of enclosed photobioreactors will be covered.

### ***Liquid mixing and light/dark cycles in photobioreactors***

An example of a photobioreactor is shown in Figure 1.12: an outdoor air-lift column with internal draught tube and transparent wall. Only the outer surface is exposed to sunlight, the so-called photic zone. This light will be absorbed by the algal culture inside, and, depending on the biomass concentration, a certain part of the interior of the bioreactor can be considered a 'dark zone'. This is illustrated in Figure 1.12 where the dark zone comprises the volume occupied by the draught tube of the air-lift reactor, which is called the 'riser'. Due to the air-lift type of mixing, algae will travel through the dark and the 'photic' zones. In other words the algae will experience a fluctuating light regime or light/dark cycles.

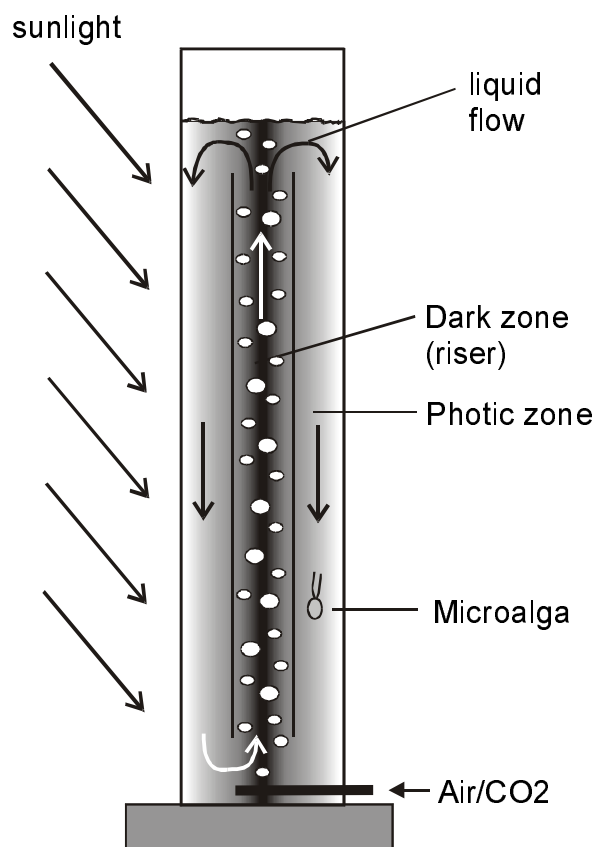


Figure 1.12. Example of outdoor enclosed photobioreactor: air-lift column with internal draught tube and transparent wall.

Although this example is based on an air-lift reactor the fluctuating light regime experienced by microalgae is a general characteristic of all types of photobioreactors. The interior of a

photobioreactor will always be dark because it is not interesting operating photobioreactors at biomass densities at which the light gradient is low. First of all because this implies that not all the light energy entering the reactor is absorbed. Secondly, the biomass density is too low under these circumstances to be commercially interesting, considering the costs of managing large volumes of cultivation liquid. As a third, the efficiency of light utilization is low under high light intensities, i.e. low biomass densities.

Based on the example given above it is easy to imagine that each type of photobioreactor is characterized by a typical light regime. The light regime is characterized by the light gradient when going from the light-exposed surface to the interior of the reactor. This light gradient is dependent on reactor design and biomass density. A second characteristic is the frequency of the light/dark fluctuations, which is dependent on reactor design and the intensity of mixing of the reactor liquid.

### ***Light/dark cycles, productivity and photosynthetic efficiency***

The efficiency of light utilization is very important for an optimal photobioreactor design because light energy is the growth-limiting energy source. Inside photobioreactors algae are exposed to light/dark cycles with high light intensities close to the reactor surface and darkness in the interior of the reactor. But, as was already shown on page 20 the photosynthetic efficiency is low under high light intensities. The fact that light energy cannot be stored and homogenized in a volume with photosynthetic microorganism is the one and only factor limiting the application of these microorganisms.

It was demonstrated, however, that very fast alternations between high light intensities and darkness could greatly enhance the photosynthetic efficiency under these high light intensities. This is called the flashing light effect and was observed under very short light/dark cycles from less than 40  $\mu$ s up to 1 s (Kok, 1953; Phillips and Myers, 1954; Terry, 1986; Matthijs, et al., 1996; Nedbal, et al., 1996). This effect was more pronounced under the shorter cycles in this range. Also the dark period should be considerably longer than the light period. The short cycle-time flashing light effect is thought to result from the fast reduction of the e-acceptors,  $Q_A$  and  $Q_B$ , associated to PSII (Figure 1.4), followed by their oxidation in the dark period (Matthijs, et al., 1996). This will result in a maximum 'photon-accepting capacity' of PSII during light flashes. The flashing light effect observed under relatively long cycle times, 100 ms to 1 s, can be explained by a similar mechanism: the alternating reduction and oxidation of the large pool of membrane-soluble plastoquinone molecules (Figure 1.4) during light and dark periods, respectively (Matthijs, et al., 1996; Nedbal, et al., 1996). But,

for the plastoquinone pool to be completely oxidized in the 'dark' a certain level of background light would still be necessary to drive PSI (Figure 1.4).

On the other hand, it was suggested that some microalgae were able to maintain the maximal growth rate under dark periods of almost 10 seconds (Lee and Pirt, 1981; Merchuk, et al., 1998). It was thought energy-rich compounds were stored during the light period to be utilized during the dark period (Lee and Pirt, 1981). And it was also suggested photoinhibitory damage was less pronounced under light/dark cycles (Merchuk, et al., 1998). In addition, evidence was provided that photosynthesis in higher plants is limited by sucrose synthesis (Stitt, 1986; Sharkey, et al., 1986a). Carbon dioxide is fixed and phosphorylated during the light period. In the following dark period Triose P is metabolized further to sucrose, liberating inorganic phosphate ( $P_i$ ). As a result of the higher availability of  $P_i$  the photosynthetic capacity in the following light period also is higher.

The flashing light effect did not seem to be suitable to profit from in large-scale photobioreactors (Powell, et al., 1965). However, if it would be possible to obtain similar effects applying longer light/dark cycles of several seconds to tens of seconds (medium duration), this would be very interesting. Mixing-induced light/dark cycles of this length are much easier to apply in photobioreactors. Liquid circulation in air-lift reactors (Figure 1.12), for example, is in this order of magnitude. This was the reason the relation between medium-duration light/dark cycles and the efficiency of light utilization by microalgae is the subject of this thesis.

## Outline

In this thesis growth and efficiency of light utilization of different species of microalgae were studied under light/dark cycles. In Chapter 2 the specific growth rate of the green freshwater algae (chlorophyta) *Chlamydomonas reinhardtii* and *Chlorella sorokiniana* was determined under different square-wave light/dark cycles (Figure 1.13). *C. reinhardtii* was chosen because it is a well-studied model organism. *C. sorokiniana* was also used because this organism was originally used by Lee and Pirt (1981) who suggested this microalga was able to store sufficient energy during a light period to maintain maximal growth in dark periods up to 10 seconds. In this chapter it is shown that this is not possible. Even more, evidence is provided more light energy is wasted during the light period of a light/dark cycle than during continuous illumination.



*C. reinhardtii* was studied further under square-wave light/dark cycles of 6 to 25 s ( $t_c$  in Figure 1.13) and this is described in Chapter 3. The efficiency of light utilization was directly measured as the yield of biomass (grams of protein) on light energy (moles of PAR). In addition, the quantum yield of photochemistry was determined using pulse-amplitude-modulation (PAM) fluorometry. Both determinations showed that the efficiency of photosynthesis generally is lower during the light period of light/dark cycles in comparison to continuous illumination.

In Chapter 4 these experiments were extended to higher photon flux densities (PFDs), 600 - 700  $\rightarrow$  1100 - 1200  $\mu\text{mol m}^{-2} \text{s}^{-1}$ . In addition, also a green marine alga, *D. tertiolecta*, was tested. Again it was demonstrated that the efficiency of light utilization does not change or even decreases after introduction of a dark period ( $t_d$  in Figure 1.13) in a continuous light regime.

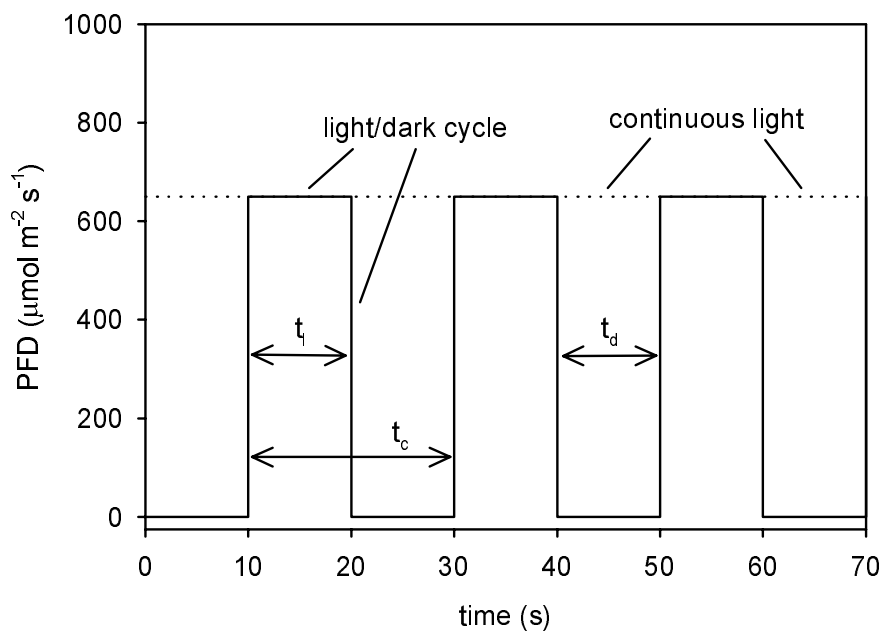


Figure 1.13. Typical example of a square-wave light/dark cycle applied in lab-scale experiments of this thesis:  $t_c$ , duration of complete cycle;  $t_l$ , duration of light period;  $t_d$ , duration of dark period.

As described in Chapter 5, the relation between light/dark cycles of 10 to 100 s and the biomass yield on light energy was studied more extensively for *D. tertiolecta*. A statistical model and a corresponding experimental design were used to quantify this relation. In these experiments the light/dark cycles were not artificial square-wave cycles, but mixing-induced light-gradient/dark cycles as will be encountered in photobioreactors.

Because it was clearly shown that light/dark cycles of several seconds to tens of seconds did not result in enhanced photosynthetic activities, short light/dark cycles were checked too. In Chapter 6 experiments are presented of *D. tertiolecta* grown under short, 0.19 and 6 s, square-wave light/dark cycles. An increase in efficiency was observed under 0.19 s cycles in comparison to continuous illumination. These results are discussed with respect to the performance of short light-path photobioreactors operated at high biomass densities.

Finally, in Chapter 7, The light regime and the photosynthetic efficiency in characteristic examples of state-of-the-art pilot-scale photobioreactors were analyzed. In short light-path systems, high efficiencies can be reached at high biomass concentrations. It is demonstrated, however, that these and other photobioreactor designs are poorly scalable and/or not applicable for cultivation of monocultures. That is the reason new photobioreactor designs are proposed in which light capture is physically separated from photoautotrophic cultivation.



## 2. Specific growth rate of *Chlamydomonas reinhardtii* and *Chlorella sorokiniana* under medium-duration light/dark cycles: 13 – 87 s

### Abstract

The specific growth rate of *Chlamydomonas reinhardtii* and *Chlorella sorokiniana* decreased under square-wave light/dark cycles of medium duration, 13 - 87 s, in comparison to continuous illumination. Three experiments were done in three different turbidostats at saturating and sub-saturating light intensities during the light period, 240 - 630  $\mu\text{mol m}^{-2} \text{s}^{-1}$ . Within each experiment the light intensity during the light periods of the intermittent light regimes was equal and this intensity was also applied under continuous illumination.

The specific growth rate decreased proportional or more than proportional to the fraction of time the algae were exposed to light; this light fraction ranged from 0.32 to 0.88. We conclude that under these light regimes the chlorophyta *C. reinhardtii* and *C. sorokiniana* are not able to store light energy in the light period to sustain growth in the dark period at the same rate as under continuous illumination.

*C. reinhardtii* increased its specific light absorbing surface by increasing its chlorophyll-*a* content under light/dark cycles of 13 s duration and a light fraction of 0.67 at 240  $\mu\text{mol m}^{-2} \text{s}^{-1}$ . The chlorophyll-*a* content was twice as high under intermittent illumination in comparison to continuous illumination. The combination of a higher specific light absorption together with a lower specific growth rate led to a decrease of the yield of biomass on light energy under intermittent illumination.

This chapter has been published as: Janssen M, Kuijpers TC, Veldhoen B, Brik Ternbach M, Tramper J, Mur LR and Wijffels RH. Specific growth rate of *Chlamydomonas reinhardtii* and *Chlorella sorokiniana* under medium duration light/dark cycles: 13 – 87 s. Journal of Biotechnology, Vol. 70, p. 323-333, 1999.

## **Introduction**

The possibility of using photo-autotrophic micro-organisms has been recognized in biotechnology. Microalgae are produced on a commercial scale for the production of single-cell protein, polysaccharides, health-food compounds such as polyunsaturated fatty acids and vitamins. In addition, algae are capable of accumulating heavy metals (Becker, 1994). Other promising applications of photo-autotrophic micro-organisms are the production of hydrogen gas from water and (sun)light (Rao and Hall, 1996; Schulz, 1996) and the fixation of carbon dioxide (Yoshihara, et al., 1996; Akimoto, et al., 1997; Hu, et al., 1998a).

Large-scale cultivation of photo-autotrophic micro-organisms, however, is still limited by scale-up problems and economical considerations. Development of cheaper and more efficient photobioreactors is a key issue. Light energy often limits reactor productivity and therefore light should be used at the highest possible efficiency. But in high-density cultures only algae close to the illuminated surface, the so-called photic zone, are exposed to light. Algae outside the photic zone receive no light. Moreover, a considerable part of the light energy absorbed in the photic zone will be dissipated as heat because the capacity at which algae fix light energy is limited. This heat-dissipated light energy cannot be used anymore by the algae outside the photic zone.

It has been shown that faster mixing of high-density cultures increases the yield of biomass on light energy at high light intensities (Laws, et al., 1983; Hu and Richmond, 1996; Hu, et al., 1996a). Mixing results in movement of algae through the culture and, as such, they are exposed to an intermittent light regime. In other words, algae are alternately exposed to light and no light at all. As a result of faster mixing, algae are exposed to high light intensities more often, but the time of exposure is shorter. These shorter light/dark cycles probably have caused the reported higher biomass yields on light energy (Richmond, 1996) because less energy is wasted in the photic zone.

The duration of the light/dark cycles in the above studies was in the range of 0.2 to 1 s. For providing these fast fluctuations reactors were developed with a short light path and a fast mixing rate provided by intense aeration. It would be interesting to investigate the effect of longer light/dark cycles on algal productivity. Light/dark cycles of medium duration, 10 to 100 s, can be applied more easily in closed photobioreactors. Reactor types in which the suspension is circulated in a manner resembling plug flow, such as air-lift loop reactors, are suitable for this. Only part of the reactor volume needs to be exposed to (sun)light. The algae

are intermittently illuminated as they circulate through the reactor. Such systems can be better temperature controlled, as the dark part of the reactor is not exposed to sunlight and can be cooled more easily. Furthermore, the dark/light cycle can be controlled well by controlling the superficial liquid circulation velocities. Finally, there is a lot of knowledge available on hydrodynamics, mass transfer and scale up of air-lift systems (Chisti, 1989).

The influence of medium duration light/dark cycles is not clear. In short term oxygen evolution experiments with non-acclimated *Chlorella* and *Scenedesmus* no influence of fluctuating light, of equal time-averaged irradiance, (1 - 0.0038 Hz, 1 - 263 s cycle duration) was found on specific oxygen production and carbon fixation (Grobbelaar, 1989 and 1991; Grobbelaar, et al., 1992). However, an increase in specific oxygen production was observed after three hours of exposure to fluctuating light and apparently physiological changes took place under fluctuating light (Grobbelaar, 1991). Others observed a decrease of the specific growth rate of the chlorophyta *Chlamydomonas*, *Oocystis*, *Dunaliella*, *Chlorella* and *Scenedesmus* at frequencies of 0.2 - 0.1 Hz (5 - 10 s cycle duration) in comparison to continuous illumination of the same time-averaged irradiance (Walsh and Legendre, 1982; Quéguiner and Legendre, 1986; Nedbal, et al., 1996).

On the contrary, Pirt (1986) suggested that *Chlorella sorokiniana* was able to store sufficient ATP and reducing power to sustain maximal growth for about 9 s in darkness. In addition, Merchuk et al. (1998) showed that the red microalga *Porphyridium* sp. could sustain maximal growth in darkness for 6 s during light/dark cycles of 27 s. It is also suggested that photosynthesis in green plants is limited by carbon metabolism and that short dark periods (up to 30 seconds) following a saturating light fleck can result in enhanced carbon fixation (Stitt, 1986; Sharkey, et al., 1986a and b).

With respect to photobioreactor design it would be very interesting to elucidate the effect of medium duration light/dark cycles on algal productivity. Therefore we measured the specific growth rates of two green algae (chlorophyta) under square-wave light/dark cycles. For comparison the specific growth rate was also determined under continuous illumination. We used *Chlamydomonas reinhardtii* and *Chlorella sorokiniana* and they were cultivated in three different systems. The cycle duration ranged from 13 to 87 s and the fraction of time the algae were exposed to light during a cycle ( $\epsilon$ ) ranged from 0.32 to 0.88.

## Materials and methods

Three different cultivation systems were used in three different experiments: 1) *C. reinhardtii* was cultivated in two air-lift loop reactors under continuous illumination and under a 8.5/4.4 s light/dark cycle at  $240 \mu\text{mol m}^{-2} \text{s}^{-1}$ . 2) *C. sorokiniana* was cultivated in a bubble column under continuous illumination at four different light intensities. At the highest and lowest intensity a 30/10 s square-wave light/dark cycle was applied; 3) *C. sorokiniana* was cultivated in a flat panel reactor under five different square-wave light/dark cycles at 250 - 290  $\mu\text{mol m}^{-2} \text{s}^{-1}$  which are presented in Table 2.1. Within each experiment the light intensity during the light periods of the intermittent light regimes was equal and this intensity was also applied under continuous illumination.

Table 2.1. Experimental design specific growth rate determination of *Chlorella sorokiniana* in flat panel turbidostat under different light/dark cycles.

cycle duration, $t_c$ (s)	light fraction, $\varepsilon$ (-)
25	0.32
25	0.88
56	0.60
87	0.32
87	0.88

### *Experiment 1: Chlamydomonas reinhardtii*

#### *Organism and medium*

A *Chlamydomonas reinhardtii* wild type strain, coded 21 gr, was kindly provided by Dr. C. Vilchez from the University of Huelva (Spain). The organism was cultivated in a Sueoka high salt (HS) medium as described by Harris (1989). The medium has the following composition (amounts in  $\text{g L}^{-1}$ ):  $\text{NH}_4\text{Cl}$ , 0.5;  $\text{MgSO}_4 \cdot 7\text{H}_2\text{O}$ , 0.02;  $\text{CaCl}_2 \cdot 2\text{H}_2\text{O}$ , 0.01;  $\text{K}_2\text{HPO}_4$ , 1.44;  $\text{KH}_2\text{PO}_4$ , 0.72 and 5 mL of Hütner's trace elements solution (Harris, 1989). Pure cultures were maintained on agar slants containing Sueoka medium +  $0.84 \text{ g L}^{-1} \text{NaHCO}_3$  + 1.75 % w/v agar. The cultures were exposed to very mild daylight at room temperature.

### Light intensity

We used  $2\text{-}\pi$  PAR (Photosynthetic Active Radiation, 400-700 nm) sensors made by IMAG-DLO (Wageningen, The Netherlands) to measure the photon flux density in  $\mu\text{mol m}^{-2} \text{s}^{-1}$ . The photon flux density is used to calculate the average light intensity as is explained later.

### Reactor

*Chlamydomonas* was cultivated under non-aseptic conditions in two glass 0.6 L air-lift loop reactors (Figure 2.1). The reactors were equipped with a water jacket connected to a temperature-controlled water bath (25 °C). The pH was maintained at 7.0 by automatic addition of 1 N sodium-hydroxide solution. The applied gas-flow rate was  $30.9 \text{ L h}^{-1}$ ; the gas was a mixture of air and carbon dioxide (3% v/v  $\text{CO}_2$ ). The downcomer of one reactor was sealed with aluminum foil to create a dark part and the algal suspension circulated between this dark part and the illuminated part. The circulation time ( $t_c$ ) through the loop and the residence time in the downcomer ( $t_d$ ) of the reactor liquid were determined by following the movement of a small colored  $\kappa$ -carrageenan gel bead (2.6 % w/v):  $t_c$  was 12.9 s and  $t_d$  was 4.4 s leading to a light fraction ( $\epsilon$ ) of 0.66 ( $= \{t_c - t_d\} / t_c$ ).

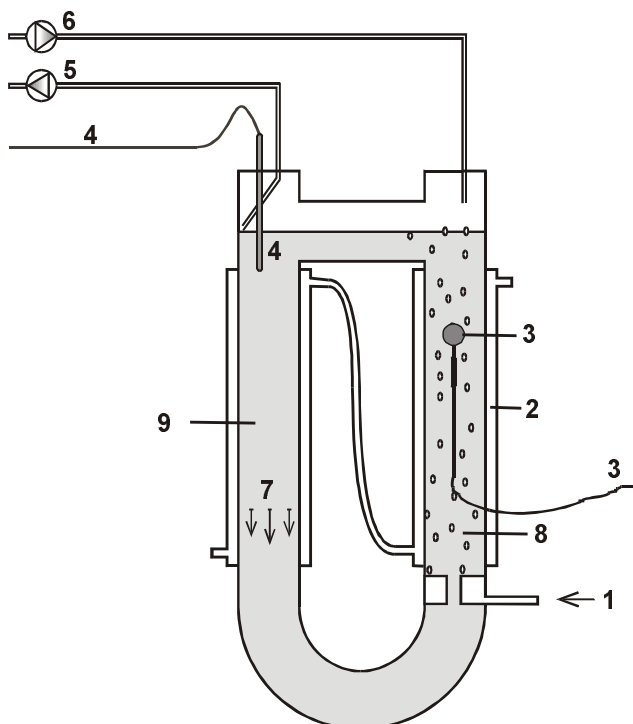


Figure 2.1. Air-lift loop reactor used for cultivation of *Chlamydomonas reinhardtii* (front view), (1) gas inlet, (2) water jacket, (3) quantum sensor, (4) pH electrode, (5) suspension outlet, (6) medium inlet, (7) direction of suspension flow, (8) riser, (9) downcomer.



The reactors were placed in a closed cabinet with 7 fluorescent light tubes placed horizontally at one side (Philips TLD HF, 32W, color 94). Both reactors were placed close to the tubes. One fluorescent tube (Pope FTD, 18W, color 94) was placed vertically at the opposite side of each ALR. The photon flux impinging at a certain height on the surface of the riser of one of the reactors was measured in 4 directions. The sum of these fluxes was divided by 2 to obtain an estimate of the average flux crossing a flat surface from both sides, called the average light intensity (I); I was  $240 \mu\text{mol m}^{-2} \text{s}^{-1}$ . The reactors were illuminated 24 h a day; no day/night cycle was applied.

The reactors were operated as turbidostats. Each reactor was therefore equipped with a quantum sensor positioned behind the riser (Figure 2.1) and this sensor was facing the wall with the horizontal fluorescent tubes. When the biomass density increased the photon flux impinging on the sensors decreased. On the moment the photon flux was lower than the set point, 70% of the maximal flux measured when the reactor contained medium without algae, the reactors were automatically diluted until the set point was reached again. This set point was chosen arbitrarily and it is a compromise between a low level of mutual shading and a cell density sufficient for measurements of biomass characteristics and accurate turbidostat control. All these operations were monitored by a datalogger (CR10, Campbell Scientific Ltd., UK).

### ***Specific growth rate***

The reactors were inoculated with pure *C. reinhardtii* cultures, maintained on agar slants and they were operated as turbidostats for 66 days. The dilution rates of the reactors were determined by daily measurement of the diluted culture volumes. Since the reactors were operated as turbidostats the biomass density in each reactor was constant and the specific growth rate was equal to the measured dilution rate.

### ***Photosynthetic activity***

Photosynthetic activity ( $P_{O_2}$ ) was measured in a small reaction vessel with a water jacket connected to a temperature-controlled water bath (25 °C). The vessel was placed in a closed cabinet. The reaction vessel was equipped with a Clark-type oxygen electrode (YSI 5331, Yellow Springs Instruments Co., USA), connected to a read-out unit (YSI 5300) which in turn was connected to a pen-recorder.

The reaction vessel was surrounded by 4 halogen lamps (Osram 44875 MFL Natura, 12V, 35 - 50W, 30°) which were connected to a power supply equipped with two timers to turn on

and off the lamps alternately to apply a light/dark cycle. The light intensity in the vessel could be adjusted by means of neutral density filters (Schott NG-filters, Schott Glaswerke, Germany). The photon flux in the vessel was measured by placing a quantum sensor in the vessel. The photon flux was measured in 8 directions. The sum of these fluxes was divided by 4 to obtain an estimate of the average flux crossing a flat surface from both sides, called the average light intensity (I).

For each measurement at one light intensity a fresh 6 mL sample was used consisting of 4 mL 75 mM phosphate buffer of pH 6.8 and 2 mL (diluted) culture suspension from the turbidostats; the oxygen activity in the sample was lowered by purging nitrogen gas; extra carbon dioxide was added as sodium bicarbonate (25  $\mu$ L, 0.56 M). First, the oxygen evolution rate was measured under illumination. Following, dark respiration was recorded after it had reached a constant rate. The photosynthetic activity was calculated by adding the measured dark respiration rate to the oxygen evolution rate.

### ***Chlorophyll-a***

A known volume of the algal suspension (containing 24 - 98  $\mu$ g of chlorophyll-*a*) was filtered through a glass-fiber filter (Whatman GF/F) coated with a thin layer of CaCO<sub>3</sub>. The filter was put in a glass tube with screw-cap. The extraction was done with 10 mL of 90 % v/v ethanol and was facilitated by heating the solution for three minutes (78 °C) in closed tubes. The tubes were stored in the dark at 4 °C to complete extraction overnight. After centrifugation the chlorophyll-*a* concentration was determined according to Nusch (1980).

### ***Dry weight***

A known volume (20 - 50 mL) of the algal suspension was filtered through a pre-dried and pre-weighed glass-fiber filter (Whatman GF/F). The biomass on top of the filter was washed filtering de-mineralized water. The filter with biomass was dried at 105 °C and allowed to cool in a desiccator. After this the filter was weighed again.

## ***Experiments 2 and 3: Chlorella sorokiniana***

### ***Organism and medium***

The chlorophyt *Chlorella sorokiniana* (CCAP 211/8k) was obtained from the Culture Collection of Algae and Protozoa (Ambleside, UK). This organism was also used by Lee and Pirt (1981) and was called *Chlorella vulgaris* (Sorokin strain). We used the same A9 medium as described by Lee and Pirt (1981). Since this medium was developed for high-density

cultures we decided to half the concentration of most components. Only the buffer concentration was maintained at 19.5 mM during the experiments in the bubble column. During the experiments in the flat panel reactor the phosphate buffer was decreased to 4.85 mM and the urea concentration was also decreased from 33 mM in the bubble column to 10 mM in the flat panel. The medium was not autoclaved but was stored in the dark as 4 separate solutions. Prior to an experiment the solutions were combined to obtain medium for one week. Growth of contaminant organisms in the medium did not occur in this period.

### **Reactor**

*C. sorokiniana* was cultivated in two types of reactors with different light sources. The first type was a glass bubble column with 380 mL liquid volume with a gas inlet of sintered glass in the bottom. This bubble column was illuminated from two opposite sites by a series of 6 halogen lamps (Osram Decostar Titan, 12V, 50W, 60°) placed on top of each other to illuminate the whole of the column length. This reactor was illuminated 24 hours a day; again no day/night cycle was applied. A 2- $\pi$  PAR sensor was continuously placed in the center of the bubble column containing the growing culture suspension. The signal of this diode was used to apply a turbidostat control. The photon flux in the center of the column was allowed to drop to 70 % of the value measured when the reactor contained medium without algae. The average light intensity in the bubble column was measured in an empty column without liquid. The photon flux density was measured on 5 different heights and at each height in four directions. The sum of these 20 measurements was divided by 10 to obtain an estimate of the average flux crossing a flat surface from both sides and this was called the average light intensity (I).

The second type of reactor was a plexiglass flat panel of 225 mL liquid volume and a depth (= light path) of 1 cm. The height and width of the rectangular panel was 28 cm and 10 cm, respectively. At the bottom gas was injected via an inlet of sintered glass. The complete reactor surface was illuminated by a screen (9 x 28 cm) of 578 light emitting diodes (LEDs). The emission wavelength of the LEDs (Kingbright, type L 53 SRC E) was 660 nm. Matthijs et al. (1996) concluded there was no need for an additional supply of blue light when using these red LEDs for cultivation of *Chlorella pyrenoidosa*. The photon flux density leaving the reactor at the opposite side was continuously measured by a 2- $\pi$  PAR sensor (LI-COR, type LI-190 SA) and this sensor was used to apply turbidostat control. The photon flux leaving the reactor was allowed to drop to 50 % of the value measured when the reactor **OOOOO** contained medium without algae. The average light intensity in the reactor was measured as

the photon flux leaving the reactor, which contained medium without algae. In this flat panel reactor *C. sorokiniana* was illuminated according to a 14/10 hours day/night cycle.

Both reactors were equipped with a water jacket connected to a temperature-controlled water bath (35.5 - 37.5 °C). Carbon dioxide was added bubbling the reactors with a carbon dioxide/air mixture, 3 - 5 % v/v CO<sub>2</sub>. The pH was controlled between 6.5 - 7.2 by automatic addition of 1 N sodium hydroxide or hydrochloric acid. The light sources of both reactors were connected to power supplies each equipped with two timers to turn on and off the lamps alternately to apply a light/dark cycle.

### *Specific growth rate*

Batch cultures (50 mL) were inoculated from pure cultures maintained on agar slants. The batches were cultivated under low light (< 100 μmol m<sup>-2</sup> s<sup>-1</sup>) and used to inoculate the turbidostat reactors. The turbidostats were operated non-aseptically for one or two weeks under a certain light regime. During this period the specific growth rate was determined on three to five days by daily measurement of the diluted culture volume. Since the reactors were operated as turbidostats the biomass density in each reactor was constant and the specific growth rate was equal to the measured dilution rate. The growth rate measurements on the different days were used to calculate the 95 % confidence interval. After each experimental run at a certain light regime the reactors were emptied, cleaned and inoculated for a new run at another light regime.

## **Results and discussion**

### *Experiment 1: Chlamydomonas reinhardtii*

The air-lift loop reactors were inoculated and three days later, denoted as day 0, the biomass density had reached the set point at which the reactors were automatically diluted. From day 0 until day 66 the reactors were operated as turbidostats and the dilution rate was followed. After about a week a considerable amount of algae attached to the reactor surface. The PAR-sensors controlling the dilution rates were placed behind the riser. In the riser attachment of algae and concomitant biofilm growth were negligible due to the rising gas bubbles. As a consequence, the biomass density in the suspension was maintained constant. Attached algae were detached once or twice a day resulting in a temporal increase of biomass density and, consequently, optical density. After detachment the dilution rate increased until the

turbidostat set point was reached again. The extra volume diluted in the hour following detachment was estimated and subtracted from the volume diluted daily. Detachment was done by scraping the inner surface with a magnet or with a rubber ring connected to a stick. The magnet was moved around by another magnet outside of the reactor.

The specific growth rate of both cultures was measured almost continuously by following the dilution rate. The average specific growth rate of the intermittently illuminated culture,  $0.11 \text{ h}^{-1}$ , was 69 % of the average growth rate of the continuously illuminated culture,  $0.16 \text{ h}^{-1}$  (Table 2.2). The specific growth rate of  $0.16 \text{ h}^{-1}$  is higher than to maximal growth rate we measured in another experiment (not shown) with *C. reinhardtii*,  $0.14 \text{ h}^{-1}$ . The light intensity of  $240 \mu\text{mol m}^{-2} \text{ s}^{-1}$  obviously is sufficient for maximal growth and this is said to be saturating. The intermittently illuminated culture was exposed to light 66 % of the time. Hence the specific growth rate was proportional to the fraction of time the algae were exposed to light.

Table 2.2. Average specific growth rate ( $\mu$ ) and dry weight concentration ( $C_x$ ) in the continuously and intermittently illuminated cultures during days 0 to 66. STD represents the estimated standard deviation.

	$\mu \text{ (h}^{-1}\text{)}$	$C_x \text{ (g L}^{-1}\text{)}$	
		average (n)	STD
continuous	0.16	0.22 (6)	0.02
intermittent	0.11	0.16 (6)	0.02

Although the specific growth rate of both cultures is measured, we do not know whether the biomass yield on light energy has changed without information about the amount of light energy that is absorbed by the biomass. The overall biomass yield on light energy ( $Y_{x,E}$ ) in dry weight per amount of photons absorbed ( $\text{g } \mu\text{mol}^{-1}$ ) is calculated according to Eq. 2.1.

$$\text{Eq. 2.1} \quad Y_{x,E} = \frac{C_x \cdot \mu}{E \cdot \varepsilon} \quad [\text{g } \mu\text{mol}^{-1}]$$

$Y_{x,E}$  represents the ratio of biomass production over energy consumption, including maintenance requirements. The volumetric light absorption rate of the algal suspension,  $E$  in  $\mu\text{mol L}^{-1} \text{ h}^{-1}$ , is not known. But  $E$  will be the same under continuous and intermittent illumination because the optical density of the cultures in both turbidostats was equal. The biomass densities ( $C_x$ ) of both cultures were determined several times as dry weight per

volume during the 66 days experimental period and are presented in table 2. The densities of the continuously and intermittently illuminated cultures were  $0.22$  and  $0.16 \text{ g L}^{-1}$ , respectively. The ratio of the yield under continuous and intermittent illumination now can be calculated and was  $1 : 0.76$ .  $Y_{x,E}$  decreased under intermittent illumination in comparison to continuous illumination.

The specific light absorption of the intermittently illuminated culture obviously is higher because the biomass density is lower in comparison to continuous illumination. This is caused by a difference in the chlorophyll-*a* content of both cultures. The chl-*a* content of the continuously illuminated culture was twice as low as the chl-*a* content of the intermittently illuminated culture,  $0.51 \pm 0.057$  (95 % confidence interval). This ratio was determined several times during the experimental period and is presented in Figure 2.2.

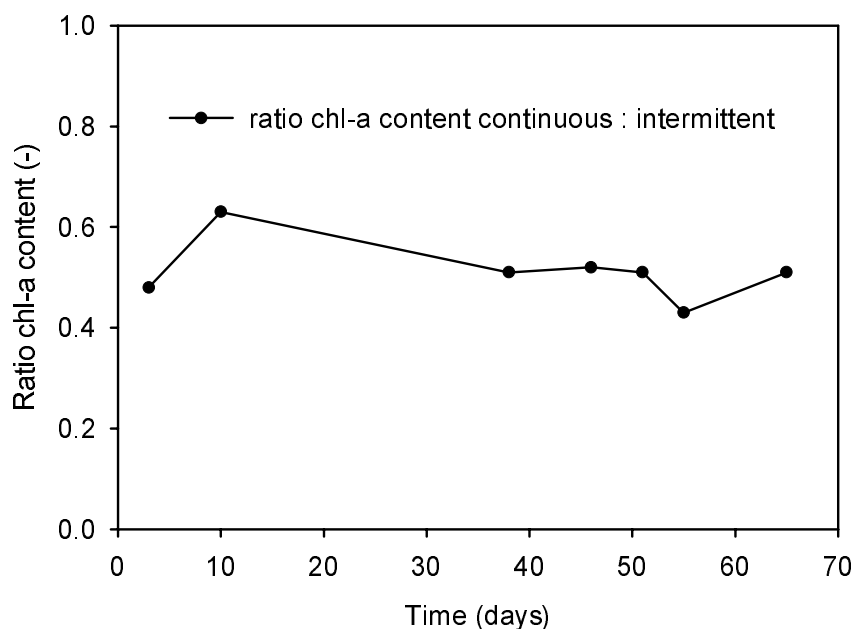


Figure 2.2. Ratio of the chlorophyll-*a* (chl-*a*) content of algal biomass from the continuously and intermittently illuminated cultures during the period of operation (●).

The intermittently illuminated culture acclimated to this light regime by increasing its chl-*a* content, enabling the algal cells to intercept a larger part of the photon flux. This was also reported in other investigations (Quéguiner and Legendre, 1986; Shin, et al., 1987). The higher chl-*a* content, however, could not prevent the decrease of the specific growth rate of *C. reinhardtii* under intermittent illumination in comparison to continuous illumination and consequently also  $Y_{x,E}$  decreased.

Increased pigmentation is also found during the process of acclimation to low light intensities, which is called photoacclimation (Falkowski and LaRoche, 1991). Grobbelaar et al. (1996) already concluded that one of the most important factors influencing photosynthetic rates under continuous or intermittent illumination was whether algae were low or high light acclimated. Low light/dark frequencies (20 s period) were perceived as low light conditions and high light/dark frequencies (20 ms period) as high light conditions. Our results are in agreement with these findings since we applied medium frequency light/dark cycles and *C. reinhardtii* showed low light acclimation.

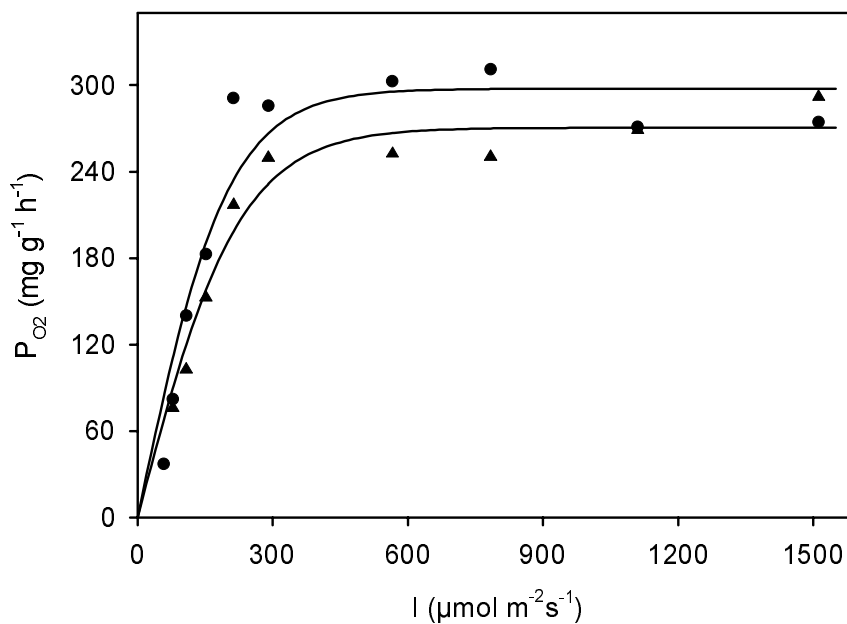


Figure 2.3. Photosynthetic activity ( $P_{O_2}$ ), oxygen production per dry weight, versus light intensity ( $I$ ) for the continuously (●) and intermittently (▲) illuminated cultures under continuous and intermittent illumination (8.5/4.4 s light/dark cycle), respectively. Samples from the turbidostats were analyzed on days 64 and 66, respectively. The light intensity ( $I$ ) on the x-axis represents the intensity in the light period.; the solid lines represent a curve fit with the hyperbolic tangent model (Eq. 2.2).

Next to the specific growth rate also the photosynthetic activity ( $P_{O_2}$ ), oxygen production per dry weight, was measured for both *C. reinhardtii* cultures. This was done at several light intensities to obtain a so-called photosynthesis-irradiance (PI) curve.  $P_{O_2}$  of the intermittently illuminated culture was determined under intermittent illumination and  $P_{O_2}$  of the continuously illuminated culture was determined under continuous illumination. The results

are graphically represented in Figure 2.3. The data were fitted with the hyperbolic tangent model (Chalker, 1980), see Eq. 2.2.

$$\text{Eq. 2.2} \quad P_{O_2} = P_{O_2, \max} * \tanh\left(\frac{\alpha}{P_{O_2, \max}} * I\right) \quad [\text{mg g}^{-1} \text{ h}^{-1}]$$

In this model,  $I$  is the light intensity during the light period in case of intermittent illumination. At increasing light intensities the slope decreases and the activity increases until the maximal activity ( $P_{O_2, \max}$ ) is reached. The fitted constants  $\alpha$ , the initial slope of the PI-curve, and  $P_{O_2, \max}$  are presented in Table 2.3. These constants were used to calculate the specific oxygen production rates in the turbidostats on a dry weight basis.

Table 2.3. PI parameters  $\alpha$  and  $P_{O_2, \max}$  as determined from the data presented in Figure 2.3 by a curve fit of the hyperbolic tangent model, including 95 % confidence intervals. The chl-*a* content on dry weight basis of the continuously and intermittently illuminated cultures was 10.3 and 20.2 mg g<sup>-1</sup>, respectively.

	$\alpha$ (mg g <sup>-1</sup> (μmol m <sup>-2</sup> s <sup>-1</sup> ) <sup>-1</sup> )	$P_{O_2, \max}$ (mg g <sup>-1</sup> h <sup>-1</sup> )
continuous	1.49 ± 0.43	297 ± 37
intermittent	1.19 ± 0.22	270 ± 21

The light intensity in the turbidostats is 240 μmol m<sup>-2</sup> s<sup>-1</sup> or lower. At this light intensity the  $P_{O_2}$  is 248 and 212 mg O<sub>2</sub> g<sup>-1</sup> h<sup>-1</sup> for the continuously and intermittently illuminated cultures under continuous and intermittent illumination, respectively. The lower photosynthetic activity per dry weight of the intermittently illuminated culture under intermittent illumination corresponds to the lower specific growth rate of this culture. The decrease of the photosynthetic activity under intermittent illumination, however, is not proportional to the decrease in specific growth rate under intermittent illumination compared to continuous illumination. Under these circumstances specific growth rate and oxygen production do not seem to be linearly correlated.

### **Experiments 2 and 3: *Chlorella sorokiniana***

The specific growth rate of *C. sorokiniana* was measured under continuous illumination at four different light intensities in the bubble column. The results of these measurements are shown in Figure 2.4. As expected the specific growth rate increased with an increasing light intensity. At 630 μmol m<sup>-2</sup> s<sup>-1</sup> a specific growth rate of 0.27 h<sup>-1</sup> was measured. Lee and Pirt



(1981) measured a maximal specific growth rate of  $0.235 \text{ h}^{-1}$  for *C. sorokiniana* and  $630 \mu\text{mol m}^{-2} \text{ s}^{-1}$  obviously is saturating.

At  $630 \mu\text{mol m}^{-2} \text{ s}^{-1}$  *C. sorokiniana* was cultivated under a 30/10 s light/dark cycle and the average specific growth rate was  $0.18 \text{ h}^{-1}$  (Figure 2.4). This corresponds to a decrease of 33 % in comparison to continuous illumination. Lee and Pirt (1981) and Pirt (1986) suggested that under this light/dark cycle *C. sorokiniana* would be able to maintain the maximal growth rate. We were not able to confirm their conclusion and we found a reduction of the specific growth rate proportional to the fraction of time the culture was exposed to light. Unfortunately the variation of the measured growth rates was considerable. This was caused by attachment of algae to the reactor surface and concomitant biofilm growth.

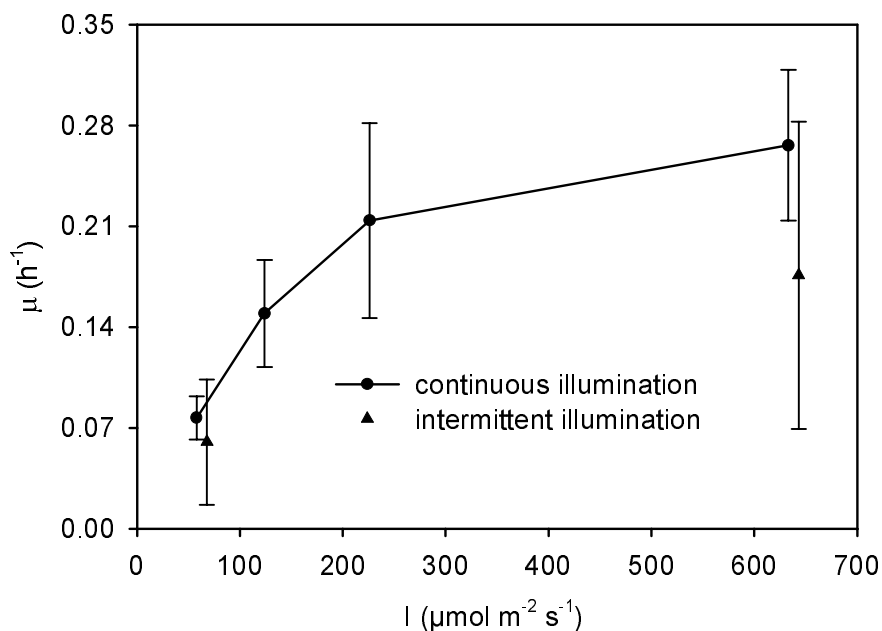


Figure 2.4. Specific growth rate ( $\mu$ ) of *Chlorella sorokiniana* under continuous illumination (●) and intermittent illumination (▲), 30/10 s light/dark cycle. Error bars represent the 95% confidence intervals. The light intensity ( $I$ ) on the x-axis represents the intensity in the light period; the intensity during intermittent illumination was 'increased' by  $10 \mu\text{mol m}^{-2} \text{ s}^{-1}$  in this graph to allow better comparison of the intervals.

*C. sorokiniana* was also cultivated under intermittent illumination at a low light intensity of  $58 \mu\text{mol m}^{-2} \text{ s}^{-1}$ . Again a 30/10 s light/dark cycle was applied and the average specific growth rate was  $0.060 \text{ h}^{-1}$  in comparison to  $0.077 \text{ h}^{-1}$  under continuous illumination. Although the confidence intervals are big, the average specific growth rate decreased by 22 % under intermittent illumination in comparison to continuous illumination.

Similar experiments were done in the other turbidostat, the flat panel illuminated with the LED screen, at 250 to 290  $\mu\text{mol m}^{-2} \text{s}^{-1}$ . The results of these experiments are shown in Figure 2.5. The specific growth rate under a large light fraction of 0.88 was 0.15  $\text{h}^{-1}$  and this is low in comparison to the growth rates measured in the bubble column. The introduction of a 10 hours night period caused a reduction in the specific growth rate. Furthermore, the light intensity could be just too low to support the maximal growth rate and maybe is sub-saturating.

In Figure 2.5 the specific growth rate is plotted as a function of the light fraction ( $\epsilon$ ). The dotted line represents the specific growth rate when it would be proportional to  $\epsilon$ . We assumed that the maximal growth rate could be obtained by extrapolating the line from the origin to the point corresponding to the highest growth rate at a light fraction of 0.88 and cycle duration of 25 s. All measured growth rates are on top or below the dotted line. At a low light fraction of 0.32 the growth rate decreased even more than proportional to  $\epsilon$ .

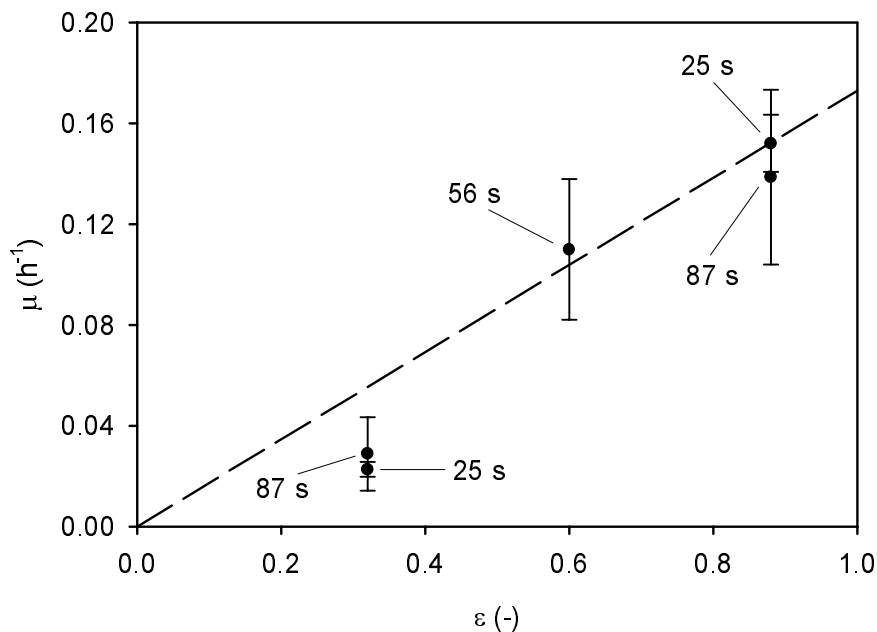


Figure 2.5. Specific growth rate ( $\mu$ ) of *Chlorella sorokiniana* under intermittent illumination of different cycle duration ( $t_c$ ) and light fraction ( $\epsilon$ ) at 250 - 290  $\mu\text{mol m}^{-2} \text{s}^{-1}$ , presented as a function of  $\epsilon$  (●).  $t_c$  is given in seconds inside the graph. The error bars represent the 95 % confidence intervals.

Although large variations were observed in the growth rate measurements all three experiments using *C. reinhardtii* and *C. sorokiniana* showed that the specific growth rate under intermittent illumination decreased proportional, or more than proportional, to the

fraction of time the algae were exposed to light in comparison to continuous illumination. We conclude that these algae are not able to store light energy during the light period to sustain growth in the dark period at the same level as under continuous illumination, as was suggested by Lee and Pirt (1981) and Pirt (1986). At higher light intensities leading to photoinhibition ( $> 600 \mu\text{mol m}^{-2} \text{s}^{-1}$ ), algae could react quite differently to intermittent illumination. Under these intensities the dark period could provide time to recover from photoinhibitory damage as was suggested by Merchuk et al. (1998).

In this study accurate determination of growth rates in dilute culture suspensions was negatively affected by attachment of algae to glass or other surfaces in the reactor. This is an important aspect, which should be kept in mind when designing experiments. Wall growth itself and also the influence of wall growth on measurements should be minimized.

To finalize, we found that the overall biomass yield (specific growth rate over specific light absorption rate) can vary significantly under different light regimes. The overall biomass yield of *C. reinhardtii* under an 8.5/4.4 s light/dark cycle was considerably lower than the yield under continuous illumination. As a result, the dark period will have to be shorter than 4.4 s for optimal light utilization efficiency. Moreover, it is not possible to increase the efficiency of *C. reinhardtii* by applying light/dark cycles of medium duration, 10 – 100 s, at a saturating light intensity of  $240 \mu\text{mol m}^{-2} \text{s}^{-1}$ .

## Nomenclature

PAR	photosynthetic active radiation, 400 - 700 nm	
$\varepsilon$	duration light period as a fraction of full cycle duration	[-]
$\alpha$	initial slope of PI-curve	$[\text{mg g}^{-1} \text{h}^{-1} (\mu\text{mol m}^{-2} \text{s}^{-1})^{-1}]$
$\mu$	specific growth rate	$[\text{h}^{-1}]$
$C_x$	biomass density, dry weight basis	$[\text{g L}^{-1}]$
E	volumetric light absorption rate	$[\mu\text{mol L}^{-1} \text{h}^{-1}]$
I	light intensity in PAR range	$[\mu\text{mol m}^{-2} \text{s}^{-1}]$
$P_{\text{O}_2}$	specific photosynthetic activity	$[\text{mg g}^{-1} \text{h}^{-1}]$
$P_{\text{O}_2, \text{max}}$	maximal specific photosynthetic activity in PI-curve	$[\text{mg g}^{-1} \text{h}^{-1}]$
$Y_{x,E}$	yield of biomass on light energy, dry weight basis	$[\text{g } \mu\text{mol}^{-1}]$

### 3. Efficiency of light utilization of *Chlamydomonas reinhardtii* under medium-duration light/dark cycles: 6 – 25 s

#### Abstract

The light regime inside a photobioreactor is characterized by a light gradient with full (sun)light at the light-exposed surface and darkness in the interior of the bioreactor. Consequently, depending on the mixing characteristics, algae will be exposed to certain light/dark cycles. In this study the green alga *Chlamydomonas reinhardtii* was cultivated under five different light regimes: 1) continuous illumination; 2) a square-wave light/dark cycle with a light fraction ( $\epsilon$ ) of 0.5 and a duration ( $t_c$ ) of 6.1 s; 3)  $\epsilon = 0.5$ ,  $t_c = 14.5$  s; 4)  $\epsilon = 0.5$ ,  $t_c = 24.3$  s and 5)  $\epsilon = 0.8$ ,  $t_c = 15.2$  s.

The biomass yield on light energy, protein per photons, decreased under light/dark cycles ( $\epsilon = 0.5$ ) in comparison to continuous light (CL), from 0.307 to 0.178 - 0.231 g mol<sup>-1</sup>. Concomitantly, the maximal specific photosynthetic activity, oxygen production per protein, decreased from 0.94 (CL) to 0.64 - 0.66 g g<sup>-1</sup> h<sup>-1</sup> ( $\epsilon = 0.5$ ). Also the quantum yield of photochemistry, yield of the conversion of light energy into chemical energy, decreased from 0.47 (CL) to 0.23 ( $\epsilon = 0.5$ ,  $t_c = 24.3$  s). Apparently, *C. reinhardtii* is not able to maintain a high photosynthetic capacity under medium-duration light/dark cycles and since specific light absorption did not change, light utilization efficiency decreased in comparison to continuous illumination.

This chapter has been published as: Janssen M, Janssen M, de Winter M, Tramper J, Mur LR, Snel J and Wijffels RH. Efficiency of light utilization of *Chlamydomonas reinhardtii* under medium duration light/dark cycles. Journal of Biotechnology, Vol. 78, p. 123-137, 2000.

## Introduction

The possibility of using microalgae for various purposes has been recognized in biotechnology. For many of these applications it is necessary to use monocultures which have to be cultivated in closed photobioreactors. The design of photobioreactors, however, is complicated because the surface/volume ratio should be high to reach high biomass densities. A low surface/volume ratio results in more voluminous reactors, low biomass densities and therefore high processing costs of the dilute suspensions. As a result, large-scale cultivation is still limited by economics of reactor design and downstream processing. Improvement of photobioreactor design and productivity is a necessity.

Usually biomass density and light path length are such that photobioreactors can be divided into two zones. In the so-called photic zone algae are exposed to light well in excess of that what is needed to saturate photosynthesis; algae outside the photic zone receive little or no light. Mixing of the culture results in movement of the algae through these zones and, as such, they are exposed to certain light/dark cycles. These light/dark cycles can range from 0.2 seconds in flat-panel reactors (Richmond and Qiang, 1997) to tens of seconds in air-lift loop reactors (Chisti, 1989). The degree of mixing already has been shown to influence reactor productivity significantly (Grobbelaar, 1994; Richmond and Qiang, 1997) and the effect of light/dark fluctuations on algal growth, oxygen production or carbon dioxide fixation has been studied to some extent.

The effect of fast light/dark fluctuations ( $> 0.25$  Hz) on algae is often discussed with help of the term 'light integration' (Terry, 1986). In continuous light the specific growth rate or oxygen production rate can be written as a saturating function of the photon flux density:  $\mu = f(\text{PFD})$ ; both rates initially are nearly proportional to PFD, thereafter both approach a horizontal asymptote which is defined as the maximum rate. On the other hand, if algal cells are placed in an intermittent light environment, then, with full integration of light intensity:  $\mu = f(\epsilon \cdot \text{PFD})$ . With no integration of light:  $\mu = \epsilon \cdot f(\text{PFD})$ , where  $\epsilon$  is equal to the fraction of time cells are subjected to light during a light/dark cycle. Since the specific growth or specific oxygen production rate was a saturating function of PFD it is clear that:  $f(\epsilon \cdot \text{PFD}) \geq \epsilon \cdot f(\text{PFD})$ .

A considerable amount of work has been done on the effect of high-frequency light/dark fluctuations ( $>100$  Hz) on the specific growth rate or oxygen production rate. The Chlorophyt *Chlorella* is able to use light flashes of 1 ms, or less, as efficiently as continuous light of the same time-averaged PFD. These light flashes were followed by dark periods 5 to 40 times as

long. This effect is called the flashing-light effect (Kok, 1953; Phillips and Myers, 1954; Matthijs, et al., 1996; Nedbal, et al., 1996) and is the same as complete light integration. In other words, algal growth or oxygen production only depends on the total amount of photons supplied.

At frequencies decreasing from 100 Hz to 0.25 Hz a decreasing level of light integration was observed (Phillips and Myers, 1954; Terry, 1986; Mouget, et al., 1995; Nedbal, et al., 1996). Light/dark fluctuations in tubular photobioreactors, flat-panel reactors and bubble columns are in this range. In these systems faster mixing of high-density cultures, resulting in light/dark cycles of 0.2 to 1 s (5 to 1 Hz), increased the yield of biomass on light energy at high PFDs (Laws, et al., 1983; Richmond and Qiang, 1997).

The influence of medium-frequency fluctuating light (0.25 - 0.01 Hz) on algal growth, oxygen production or carbon dioxide fixation is not well known. These light/dark fluctuations are encountered in air-lift systems and algal ponds. In short-term experiments with *Chlorella* and *Scenedesmus* no influence of fluctuating light, in the range 1 to 0.0038 Hz, was found on specific oxygen production and carbon dioxide fixation under equal time-averaged PFD (Grobbelaar, 1989 and 1991; Grobbelaar, et al., 1992). Others observed a decrease of the specific growth rate of the chlorophyta *Chlamydomonas*, *Oocystis*, *Dunaliella*, *Chlorella* and *Scenedesmus* at frequencies of 0.1 - 0.2 Hz in comparison to continuous illumination of the same time-averaged PFD (Walsh and Legendre, 1982; Quéguiner and Legendre, 1986; Nedbal, et al., 1996). In other words, light integration was not complete.

On the contrary, Pirt (1986) and Merchuk et al. (1998) concluded that the chlorophyt *Chlorella sorokiniana* and the red microalga *Porphyridium* sp. could sustain their maximal growth rate during light/dark cycles with a dark period of 9 and 6 s, respectively (complete light integration). In addition, Bosca et al. (1991) found that carbon dioxide fixation was higher (up to 2.5 times) under 4 s light/dark fluctuations in comparison to continuous light under equal time-averaged PFD. Also, it is suggested that photosynthesis in green plants is ultimately limited by sucrose synthesis under saturating light and that short dark periods (30 to 60 s) can result in enhanced carbon dioxide fixation (Stitt, 1986).

It is not clear how medium-duration light/dark cycles could affect photobioreactor productivity. In the present study we therefore determined the efficiency of light utilization of the green alga (chlorophyt) *Chlamydomonas reinhardtii* under medium-duration (6 - 24 s) light/dark cycles. The photon flux density during the light period of the cycles was constant and over-saturating, that is to say more than sufficient to sustain the maximal specific growth rate under continuous illumination. Specific growth rate and specific light absorption rate

were measured under 5 different light/dark cycles. These rates were used to calculate the biomass yield on light energy. Also the specific photosynthetic activity and the quantum yield of photochemistry were determined. These two parameters provided information about acclimation of *C. reinhardtii*. The quantum yield of photochemistry was determined by measuring chlorophyll fluorescence and is equal to the efficiency of the first steps of photosynthesis, i.e. light capture and charge separation in the photosystems as is explained in the following Theory section.

### **Theory: Analysis of algal photochemical efficiency by chlorophyll fluorescence**

The chloroplast of a green alga contains thylakoid membranes in which the photosystems are fixed. There are two types of photosystems (PSI and PSII) connected by an electron transport chain and working in series to transfer electrons from water to oxidized nicotinamide adenine dinucleotide phosphate (NADP<sup>+</sup>). This linear electron transport additionally results in pumping of protons across the thylakoid membrane; a trans-thylakoidal proton gradient develops and this is used for adenosine triphosphate (ATP) production.

In Figure 3.1 the processes involved in PSII photochemistry are explained in more detail. Photons are intercepted by the antenna complex and the resulting excitation energy is delivered to the so-called reaction center. In the reaction center the excitation energy is used to increase the energy of an electron which is transferred to an acceptor (charge separation or photochemistry). Additionally, a part of the excitation energy is lost by a number of non-radiative decay processes, predominantly heat dissipation in the antenna complex (Horton, et al., 1994). This heat dissipation is dependent on the energization of the thylakoid membranes, the magnitude of the trans-thylakoidal proton gradient (Briantais, et al., 1980), and serves to protect the photosystems for over-excitation.

A small amount of the excitation energy is also lost as fluorescence. The fluorescence of PSII can be measured and used to calculate two parameters: the quantum yield of photochemistry ( $\phi_p$ ) and non-photochemical quenching (NPQ). The parameter  $\phi_p$  is derived to be equal to the fraction of photons absorbed by the PSII antenna used for charge separation (Genty, et al., 1989). NPQ is defined as the relative decrease (quenching) of PSII fluorescence due to the induction of heat dissipation or other processes except photochemistry. First the actual fluorescence measurement will be covered and following the derivation of  $\phi_p$  and NPQ.

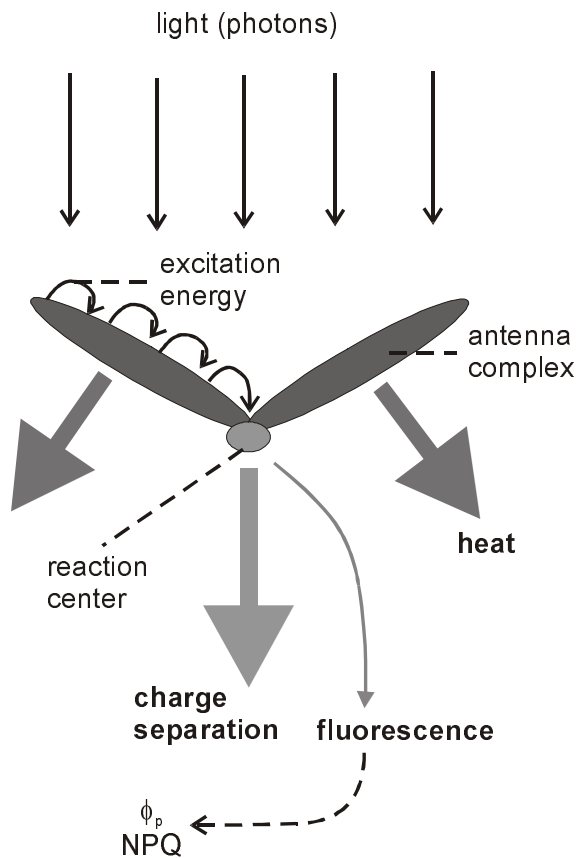


Figure 3.1. Schematic representation of photosystem II, see Theory.

The fluorescence yield is measured by pulse-amplitude-modulation (PAM) fluorometry in combination with the saturating-pulse technique (Schreiber, et al., 1986). Fluorescence is induced with modulated light pulses of 650 nm, low intensity and short duration (1  $\mu$ s). This light is called the measuring light and is too weak to influence photochemistry. The fluorescence intensity or yield (> 700 nm) is measured by a detector, de-modulated and recorded. A typical recorder trace is shown in Figure 2. First the algal sample is placed in the dark for 15 to 30 minutes to reach the situation that all reaction centers are opened (electron transport chain between PSII and PSI is fully oxidized) and the thylakoid membranes are not energized. As a result, the yield of photochemistry is maximal and heat dissipation minimal. The measuring light (ML) is turned on and the fluorescence yield is detected. Because the photochemical yield is maximal, the fluorescence yield is minimal and this level is called  $F_0$  after van Kooten and Snel (1990). Now, a saturating light pulse (SP), 0.6 to 0.8 s, can be given to saturate all photochemistry. All reaction centers are occupied during this pulse and the electron transport chain between PSII and PSI is fully reduced. Heat dissipation is still minimal and consequently the fluorescence yield quickly rises to a maximum,  $F_m$ .



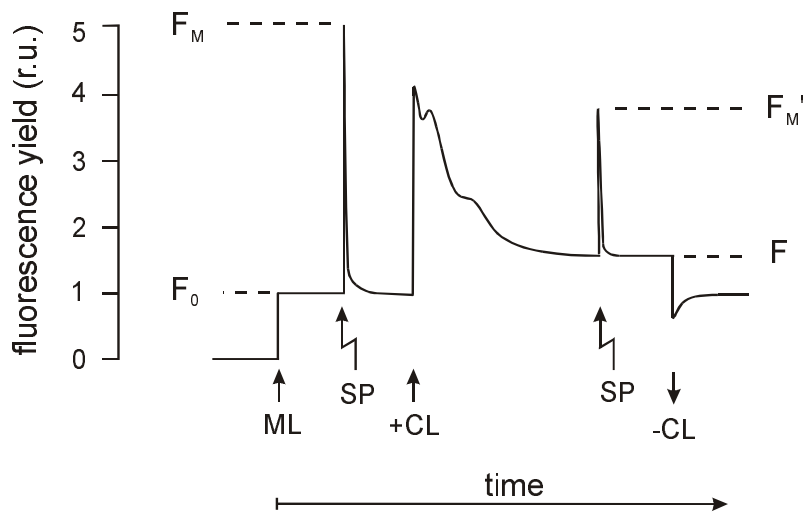


Figure 3.2. Schematic representation of the saturating-pulse fluorescence method, adapted from van Kooten and Snel (1990). Arrows indicate the activation of different light sources: ML, measuring light; SP, saturating-pulse lamp; CL, cultivation light. Four different states with different fluorescence yields are distinguished:  $F_0$ , minimal fluorescence yield in dark-adapted state;  $F_m$ , maximal fluorescence in dark adapted state;  $F$ , fluorescence yield under cultivation light;  $F_m'$ , maximal fluorescence under cultivation light.

After dark-adaptation, cultivation light (CL) is turned on and the fluorescence yield quickly rises because of closing reaction centers. But then the yield starts to decrease to a constant level,  $F$ , because heat dissipation increases. This heat dissipation is induced by the energization of the thylakoid membranes after switching to CL. Also in the light-adapted state a saturating pulse can be given and a maximum,  $F_m'$ , is reached.  $F_m'$  is lower than  $F_m$  because in the light-adapted state more excitation energy is dissipated as heat in the PSII antennae.

The quantum yield of PSII photochemistry ( $\phi_p$ ) can be calculated from  $F$  and  $F_m'$  (Genty, et al., 1989). We will follow the simplified way of Schreiber et al. (1995) to visualize the calculation. In Figure 3.1 it was shown that the excitation energy of an absorbed photon (quantum) can leave PSII by three different ways, photochemistry (charge separation), heat dissipation or fluorescence. It is assumed that: 1) the sum of quantum yields of photochemistry ( $\phi_p$ ), fluorescence ( $\phi_F$ ) and heat dissipation ( $\phi_D$ ) is unity:  $\phi_p + \phi_F + \phi_D = 1$ ; 2) with the application of a saturating pulse  $\phi_p$  becomes zero:  $(\phi_F)_S + (\phi_D)_S = 1$ ; 3) during the saturating pulse there is no change in the ratio between heat dissipation and fluorescence:  $(\phi_F)_S / (\phi_D)_S = \phi_F / \phi_D$ . Based on the above assumptions it is possible to express  $\phi_p$  by fluorescence parameters alone:  $\phi_p = \{(\phi_F)_S - \phi_F\} / (\phi_F)_S$ . Finally,  $(\phi_F)_S$  and  $\phi_F$  are linearly

correlated to the measured fluorescence intensities  $F_m'$  and  $F$  (Figure 3.2), respectively, and therefore  $\phi_p$  can be calculated as  $(F_m' - F)/F_m'$ .

Non-photochemical quenching (NPQ), is calculated as  $(F_m - F_m')/F_m'$  (Gilmore and Yamamoto, 1991). It is clear that the difference between  $F_m$  and  $F_m'$  is correlated to the level of heat dissipation; the difference is larger at higher levels of heat dissipation. The name NPQ, non-photochemical quenching of fluorescence, results from the fact that the quenching of  $F_m$  to  $F_m'$  is caused by other processes than photochemistry.

## Materials and methods

### *Experimental set-up*

*Chlamydomonas reinhardtii* was cultivated under different light regimes, separated into two periods. During the first period, period I, *C. reinhardtii* was cultivated under continuous illumination of varying photon flux densities (PFDs) and only the specific growth rate was determined. These experiments were done without applying a day/night cycle.

During the second period, period II, *C. reinhardtii* was cultivated under five different light regimes: 1) continuous illumination; 2) a square-wave light/dark cycle with a light fraction ( $\epsilon$ ) of 0.5 and a duration ( $t_c$ ) of 6.1 s; 3)  $\epsilon = 0.5$  and  $t_c = 14.5$  s; 4)  $\epsilon = 0.5$  and  $t_c = 24.3$  s; 5)  $\epsilon = 0.8$  and  $t_c = 15.2$  s. Under these circumstances specific growth rate, specific photosynthetic activity, spectrally averaged absorption coefficient and fluorescence parameters were determined. The period II experiments were done at a PFD of 600 - 700  $\mu\text{mol m}^{-2} \text{s}^{-1}$  during the light period. Furthermore, a 16/8 h day/night cycle was applied to control cell-cycle events. It has been shown that the cell-division cycle of *Chlamydomonas* can be controlled by a 24 hours day/night cycle (Goto and Johnson, 1995). Daily samples for the specific absorption coefficient or photosynthetic activity were always taken at the same time, 8 hours after onset of illumination, to obtain cells in the same phase of the cell cycle.

### *Organism and medium*

*Chlamydomonas reinhardtii* CC 1690 wild type 21 gr mt+ was kindly provided by Elizabeth Harris from the Chlamydomonas Genetics Center (Duke University, Durham, NC, USA). The organism was cultivated in a Sueoka high salts (HS) medium as described by Harris (1989), it is composed of (amounts in  $\text{g L}^{-1}$ ):  $\text{NH}_4\text{Cl}$ , 0.5;  $\text{MgSO}_4 \cdot 7\text{H}_2\text{O}$ , 0.06;  $\text{CaCl}_2 \cdot 2\text{H}_2\text{O}$ , 0.02;  $\text{K}_2\text{HPO}_4$ , 1.44;  $\text{KH}_2\text{PO}_4$ , 0.72;  $\text{NaHCO}_3$ , 0.84 and 5  $\text{mL L}^{-1}$  of Hütner's trace-elements

solution. Pure cultures were maintained on agar slants at 15 – 25 °C, 50 - 70  $\mu\text{mol m}^{-2} \text{s}^{-1}$  and a 16/8 h day/night cycle. Before being used as an inoculum, algae from the slants were allowed to grow under the same conditions in 50 mL of liquid medium for several days.

### Culture conditions

A turbidostat-type reactor was used for cultivation of *C. reinhardtii* for one or two weeks under a certain light regime. The turbidostat is shown in Figure 3.3, the suspension volume was 70 mL and the height of the suspension was 3 cm. Illumination of the turbidostat was provided by a halogen lamp (20, 35 or 50 W). The lamp could be dimmed with only minor effects on the spectral distribution. The lamp was connected to a timer to apply a 16/8 h day/night cycle. Two other timers, determining on- and off-time, were used to impose different light/dark cycles during the 16 h day period.

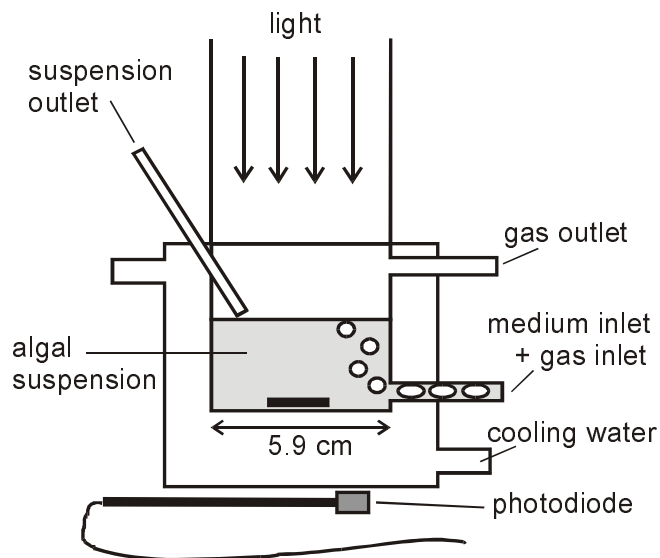


Figure 3.3. Set-up of turbidostat reactor used for cultivation of *C. reinhardtii* under different light regimes.

The optical density in the turbidostat was monitored by means of a 2- $\pi$  PAR-sensor (IMAG-DLO, the Netherlands) placed under the bottom of the reactor (Figure 3.3) to measure the outgoing PFD. This PFD was continuously compared to a setpoint and when it was lower the suspension was temporarily diluted. In this way the optical density at 680 nm ( $\text{OD}_{680}$ ) of the algal culture was maintained between 0.17 and 0.25. The turbidostat was also equipped with a water jacket connected to a temperature-controlled water bath, 24 - 26.5 °C. The suspension was gently bubbled with an air/carbon dioxide mixture, 11 L h<sup>-1</sup>, and mixed with a magnetic stirring bar. The pH of the culture was maintained between 6.6 and 6.9 by setting the carbon

dioxide concentration, 3 - 10% v/v. Carbon dioxide was never limiting under these conditions. The turbidostat was operated under non-aseptic conditions. Cultures were checked regularly under a microscope but contamination was never observed.

### ***Specific growth rate***

The specific growth rate ( $\mu$ ) was measured in three separate batch reactors equal to the turbidostat shown in Figure 3.3. These reactors were inoculated with a known volume of suspension ( $V_s$ ) from the turbidostat and diluted with a known volume of medium ( $V_m$ ). Suspensions from the turbidostat were always taken three or more days after inoculation of the turbidostat itself to allow *C. reinhardtii* to acclimate. The  $OD_{680}$  of the undiluted turbidostat inoculum ( $OD_{start}$ ) was measured. After transfer to the batch reactors growth was allowed to continue for 24 hours and after these 24 hours  $OD_{680}$  was measured again ( $OD_{end}$ ). The specific growth rate now could be calculated according to Eq. 3.1. By choosing the proper dilution of the turbidostat inoculum,  $OD_{end}$  was always maintained below 0.25 in order to minimize self-shading of algae.

$$\text{Eq. 3.1} \quad \mu = \frac{\ln \left\{ OD_{end} / \left[ \frac{OD_{start} \cdot V_s}{V_s + V_m} \right] \right\}}{24} \quad (\text{h}^{-1})$$

At each light regime, corresponding to a 1 or 2-weeks turbidostat run, growth rate was measured on two or three days. On these days we used two or three batch reactors. All these separate determinations at one light regime were pooled to calculate the 95 % confidence interval.

### ***Photon flux density***

The photon flux density (PFD) was measured in the PAR-range (Photosynthetic active radiation, 400 - 700 nm). The PFDs at the bottom of the turbidostat and the batch reactors were measured regularly. The different lamps and lampholders used for the different reactors were placed above a 'dummy' reactor with an open bottom. The photodiode, 190SA 2- $\pi$  PAR-sensor (LI-COR, NE, USA), was placed on different positions spread over the fictional bottom surface and the PFD was measured and averaged.

### ***Spectrally averaged absorption coefficient***

Following the growth rate determinations, biomass from the batch reactors was also used for the determination of the specific absorption coefficient. The suspensions from the batch reactors were collected and centrifuged separately, 5 min at 5000 g and 4 °C. The pellets were

gently resuspended in 8 - 16 mL 25 mM potassium-phosphate buffer of pH 7 to obtain a protein concentration of 60 - 270 mg L<sup>-1</sup>. Absorbance was measured in a Beckman DU-640 spectrophotometer equipped with an RSA-BE-65 integrating sphere (Labsphere, UK) placed behind the sample cuvette (5 mm light path). Forward-scattered light was collected with this set-up. The absorbance was measured in duplicate from 400 to 700 nm with a 0.5 nm interval. Absorbance at 750 nm was also measured and subtracted from the absorbance between 400 and 700 nm assuming this was residual scattering.

The spectrally averaged absorption coefficient ( $a_{\text{prot}}^*$ ), light-absorbing surface per protein, now could be calculated according to Dubinsky et al. (1986). The relative spectral distribution of the halogen lamps was needed for these calculations and was measured from 400 to 700 nm with a 0.5 nm interval on a SR9910 spectroradiometer (Macam, UK).

### ***Photosynthetic activity***

The photosynthetic activity ( $P_{O_2}$ ), measured as oxygen evolution rate per protein, was determined in a small cylindrical stirred vial with a water jacket connected to a temperature-controlled water bath (25° C). The vial was equipped with a YSI 5331 Clark-type oxygen electrode (Yellow Springs Instruments, Co, USA). The vial was illuminated with a slide projector equipped with a halogen lamp. The PFD in the vial was set using NG neutral density filters (Schott Glaswerke, Germany). After each experiment the PFD in the empty vial was measured in the direction of the light beam with a 2- $\pi$  PAR-sensor (IMAG-DLO, The Netherlands).

For each measurement fresh suspension was taken out of the turbidostat and 2 mL was diluted with 4 mL 68 mM phosphate buffer, pH 6.8. After 10 min dark adaptation, the oxygen concentration in the sample was lowered by purging an air/nitrogen mixture, 80 % v/v. Extra carbon dioxide was added as sodium bicarbonate (25  $\mu$ L, 0.56 M) and dark respiration was measured. The projector lamp was turned on and the oxygen evolution rate was followed until air saturation. In this period (20 min) the sample was exposed to ten increasing PFDs. Finally, photosynthetic activity was calculated by adding the dark respiration to the measured oxygen evolution rate.

### ***Optical density***

The optical density of algal suspensions ( $OD_{680}$ ) was measured as absorbance at 680 nm on an Ultrospec 2000 spectrophotometer (Pharmacia Biotech, UK) against a reference of Sueoka medium.

### ***Protein determination***

Algal suspensions (0.7 - 2.0 mg protein) were filtrated over Whatman GF/F glass-fiber filters and washed by additional filtration of 10 mL 25 mM potassium-phosphate buffer of pH 7. The filters with cakes were resuspended in 10 mL buffer containing 1 % w/v sodium dodecyl sulphate (SDS) and sonicated on ice water (Branson Sonifier 250 with microtip) (Meijer and Wijffels, 1998). The suspensions were centrifuged and samples from each supernatant were stored at  $-80\text{ }^{\circ}\text{C}$ . Protein was quantified later with bicinchoninic acid (BCA) (Smith, et al., 1985) using a commercially available kit (Pierce).

### ***Fluorescence measurements***

The algal sample was put into a 10 mm light-path cuvette, which was placed in an emitter-detector-cuvette assembly, ED 101US (Heinz Walz GmbH, Germany). Two light-guiding perspex rods were placed against two sides of the cuvette. One rod was connected to the fluorescence-inducing measuring light and the other to a photodiode. The measuring light and detector were operated by means of the PAM 101 control unit (Heinz Walz GmbH). Another side of the cuvette could be illuminated by a KL1500 saturation pulse lamp controlled by the PAM 103 accessory unit. The clear bottom of the quartz cuvette could be illuminated by a slide projector, which simulated the cultivation light in the turbidostat. Algae were cultivated under light/dark cycles in the turbidostat. In order to simulate this intermittent light regime in the cuvette, a VSR25 shutter (Uniblitz, NY, USA) was used to cut off the projector light beam. The shutter was controlled with a CR 10 datalogger (Campbell Scientific Ltd., UK) programmed for the specific intermittent light regime.

In this study 2 mL samples were taken from the turbidostat and diluted with 4 mL 68 mM phosphate buffer of pH 6.8. Sodium bicarbonate (25  $\mu\text{L}$ , 0.56 M) and ammonium chloride (25  $\mu\text{L}$ , 0.45 M) were added. The cuvette was filled with 2 mL of suspension and dark adapted for 15 - 20 minutes before measuring  $F_0$  and  $F_m$ . After dark adaptation the cultivation light (CL) was turned on and  $F$  and  $F_m'$  were measured. During measurements the samples in the cuvette were mixed with a small stirrer.

## Results and discussion

### *Period I: specific growth rate*

During period I the specific growth rate of *C. reinhardtii* was measured under continuous illumination of varying PFDs. The results are presented in Figure 3.4. Nine turbidostat runs were carried out, corresponding to nine PFDs. Each solid dot is the result of one growth-rate determination in one of the batch reactors. Since the intensity of the three lamps was not exactly the same, the results are grouped around different PFDs. We deduced from Figure 3.4 that *C. reinhardtii* was light-limited up to  $300 \mu\text{mol m}^{-2} \text{s}^{-1}$  and light-saturated at a PFD of  $400 \mu\text{mol m}^{-2} \text{s}^{-1}$ . The Aiba model,  $\mu = f(\text{PFD})$  (Aiba, 1982), was fitted to the measured specific growth rates and is represented as the solid line in Figure 3.4. In this model photoinhibition at high PFDs is included by means of an inhibition constant. But in Figure 3.4 it can be seen that inhibition is negligible at PFDs lower than  $700 \mu\text{mol m}^{-2} \text{s}^{-1}$ .

In addition, a turbidostat run was done under a light/dark cycle of 13 s duration and a light fraction of 0.66 at a PFD of  $200 \mu\text{mol m}^{-2} \text{s}^{-1}$  in the light period (solid squares in Figure 3.4). For comparison, the dashed line in Figure 3.4 represents complete light integration under this light/dark cycle, as explained in the introduction,  $\mu = f(\text{PFD} \cdot \varepsilon)$ . This means that the algae would be able to use intermittent light as efficiently as continuous light of the same time-averaged PFD. It seems that light integration did not take place. Moreover, it is more likely that light integration is completely absent under this light/dark cycle because the specific growth rate decreased proportional to the light fraction in comparison to continuous illumination,  $\mu = \varepsilon \cdot f(\text{PFD})$  (dotted line in Figure 3.4). We did already observe this in previous work (Janssen, et al., 1999).

The period I experiments were done under 24 hours of light per day; no day/night cycle was applied. But we found that without a night period cell division of *Chlamydomonas* still follows a 24 hours periodicity. This was also reported by Goto and Johnson (1995). However, this period was not exactly 24 hours but a little bit longer. Samples taken at the same time on different days could consist of cells in different physiological states. Therefore we applied a 16/8 h day/night cycle during period II to force the cell cycle into a 24-hours rhythm.

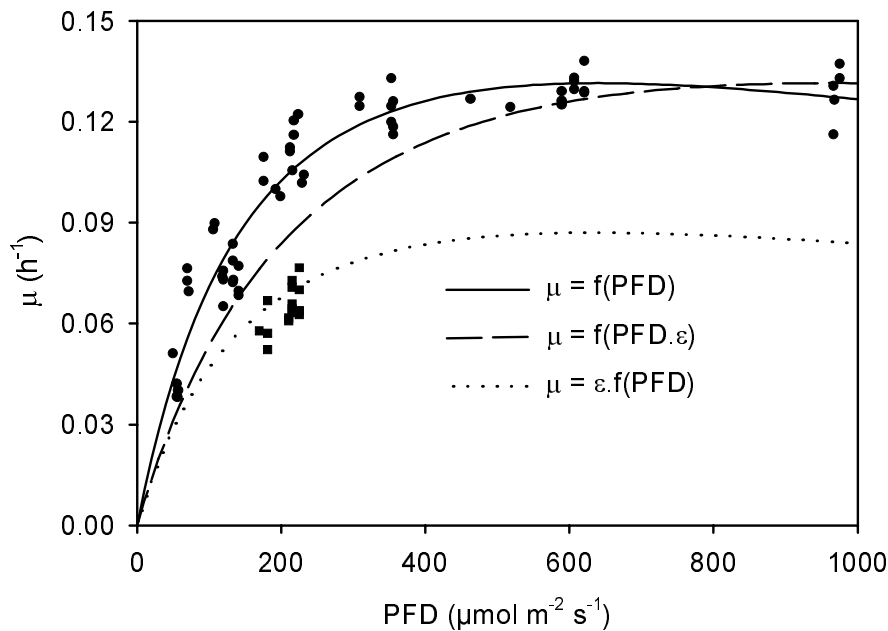


Figure 3.4. Specific growth rate ( $\mu$ ) of *C. reinhardtii* as function of continuous illumination of different PFDs (●). The solid line gives a fit of the Aiba model,  $\mu = f(\text{PFD})$ . The dashed line represents complete light integration at a 13 s light/dark cycle with a light fraction ( $\varepsilon$ ) of 0.66:  $\mu = f(\text{PFD} \cdot \varepsilon)$ . The dotted line represents the absence of any light integration effects:  $\mu = \varepsilon \cdot f(\text{PFD})$ . The closed squares (■) are measured growth rates under this cycle. The x-axis gives the PFD during the light period.

### ***Period II: specific growth and light absorption rate and biomass yield on light energy***

During the second experimental period, period II, *C. reinhardtii* was cultivated under a 16/8 h day/night cycle in contrast to 24 hours of light per day during period I. During the day period four medium-duration light/dark cycles were applied. As a reference, the algae were also cultivated under continuous illumination during the day period. The light intensity during illumination was over-saturating, 600 - 700  $\mu\text{mol m}^{-2} \text{s}^{-1}$ . The results of the measurements of the specific growth rate are shown in Figure 3.5. Under continuous illumination the specific growth rate ( $\mu$ ) was 0.116  $\text{h}^{-1}$ . In Figure 3.4 already could be seen that under 24 hours of continuous illumination  $\mu$  was 0.132  $\text{h}^{-1}$ . Although the daily light supply decreased by 33%,  $\mu$  is only lower by 12% under the 16/8 hours day/night cycle in comparison to 24 hours of saturating light.



All specific growth rates presented in Figure 3.5 are normalized to the rate measured under continuous illumination,  $0.116 \text{ h}^{-1}$ , and plotted against the light fraction ( $\epsilon$ ). For each normalized specific growth rate ( $\mu_n$ ) the corresponding duration of the light/dark cycle is also shown. The normalized rate was 0.85, at a light fraction ( $\epsilon$ ) of 0.8. On the contrary,  $\mu_n$  was lower than  $\epsilon$  at a light fraction of 0.5, i.e. 0.29 - 0.39. Obviously, light integration was completely absent at a 0.5 light fraction since the growth rate decreased even more than proportional to  $\epsilon$ . In a number of studies several Chlorophyta showed a decrease in specific growth rate under fluctuating light, 0.1 - 0.2 Hz, in comparison to continuous light of equal time-averaged PFD (Walsh and Legendre, 1982; Quéguiner and Legendre, 1986; Nedbal, et al., 1996). Also in these studies complete light integration did not occur.

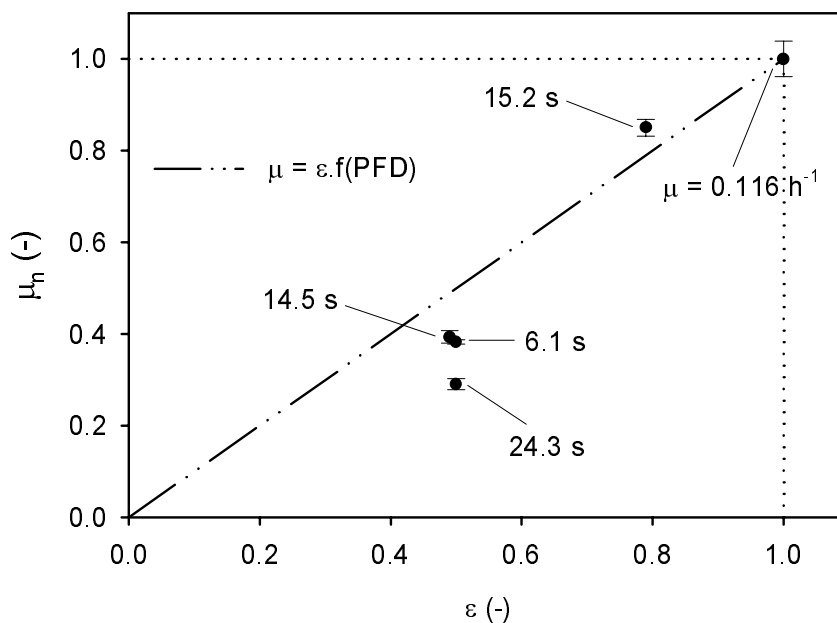


Figure 3.5. Normalized specific growth rate ( $\mu_n$ , ●) as function of light fraction ( $\epsilon$ ) for *C. reinhardtii* cultivated under continuous illumination and under intermittent illumination of variable cycle duration ( $t_c$ ) and light fraction ( $\epsilon$ ). The growth rates were normalized to the rate measured under continuous illumination,  $0.116 \text{ h}^{-1}$ .  $t_c$  is presented as the numbers connected to the data points. The dashed/dotted line represents the absence of any light integration effects:  $\mu = \epsilon \cdot f(\text{PFD})$ . PFDs during the light period varied between 600 and 700  $\mu\text{mol m}^{-2} \text{ s}^{-1}$ . Error bars represent 95 % confidence intervals.

The degree of light integration alone is not a good parameter to compare the efficiency of light utilization under different light regimes because it is only based on specific growth rates. To calculate the efficiency also the specific rate of light absorption should be known.

Therefore the spectrally averaged absorption coefficient was determined on protein basis,  $a^*_{\text{prot}}$  in  $\text{m}^2 \text{g}^{-1}$ . Protein was used as a measure for biomass because the protein fraction is the most constant factor in the cell (Post, et al., 1985 and 1986). The protein fraction consists predominantly of bioactive or structural molecules, and protein does not serve as a major energy storage compound. On the other hand, cellular concentrations of carbohydrates, lipids and chlorophyll can vary strongly during the day and under different light regimes and this will also affect dry weight measurements.

The results of the absorption measurements are shown in Figure 3.5. Remarkably,  $a^*_{\text{prot}}$  was similar for all cultures,  $0.25 \text{ m}^2 \text{g}^{-1}$ . Under continuous illumination specific light absorption generally increases when algae acclimate to lower PFDs (Falkowski and LaRoche, 1991). In our study the time-averaged PFD under intermittent illumination ( $\varepsilon = 0.5$ ) was reduced by a factor of two in comparison to continuous illumination. But this reduction did not lead yet to an increase of specific light absorption by *C. reinhardtii* on protein basis.

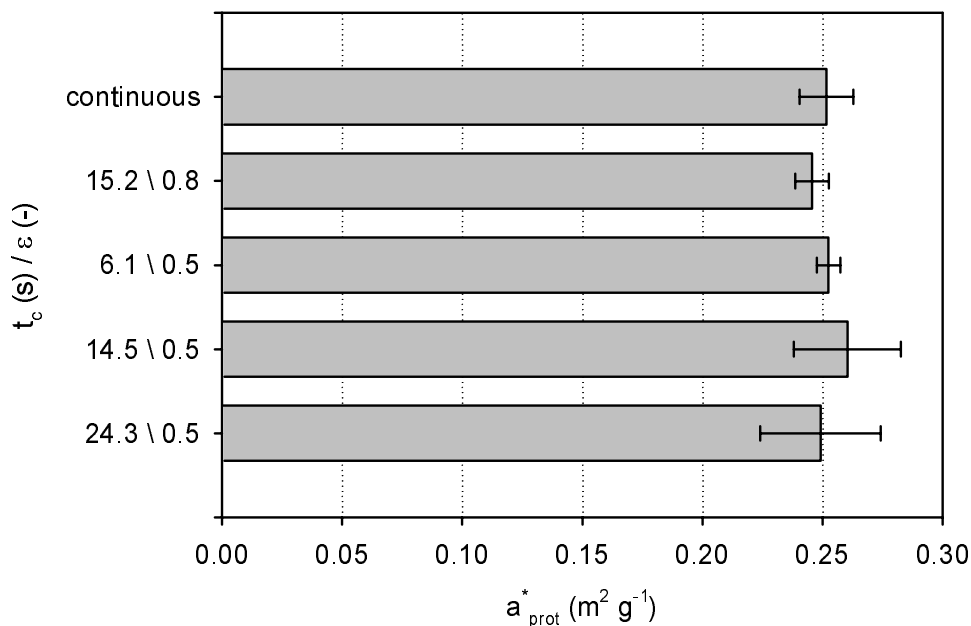


Figure 3.6. Average spectral absorption coefficients ( $a^*_{\text{prot}}$ ) of *C. reinhardtii*. Circumstances as described in Figure 3.5.

The specific growth rate, spectrally averaged absorption coefficient, cultivation PFD ( $\text{PFD}_{\text{cult}}$ ) and the light fraction were combined to obtain the yield of biomass on light energy,  $Y_{x,E}$  in protein per photons (Eq. 3.2). The factors 24, 16 and  $3.6 \cdot 10^{-3}$  in Eq. 3.2 are needed to convert  $\mu\text{mol s}^{-1}$  into  $\text{mol d}^{-1}$  including the 16/8 h day/night cycle. This equation can only be used if the PFD is the same everywhere in the culture. However, in our reactors there was a vertical

light gradient. Nevertheless, the yields were comparable with each other because the light gradients were small and about equal during all the experimental runs.

$$\text{Eq. 3.2} \quad Y_{x,E} = \frac{\mu \cdot 24}{\varepsilon \cdot PFD_{cult} \cdot a_{prot}^* \cdot 3.6 \cdot 10^{-3} \cdot 16} \quad [\text{g mol}^{-1}]$$

The results of the calculations are shown in Figure 7.  $Y_{x,E}$  was highest under continuous illumination and intermittent illumination with a high light fraction of 0.8. But the yields were considerably lower under light fractions of 0.5. These results show that the efficiency of light utilization by *C. reinhardtii* decreases during acclimation to medium-duration light/dark cycles ( $\varepsilon = 0.5$ ) in comparison to continuous illumination.

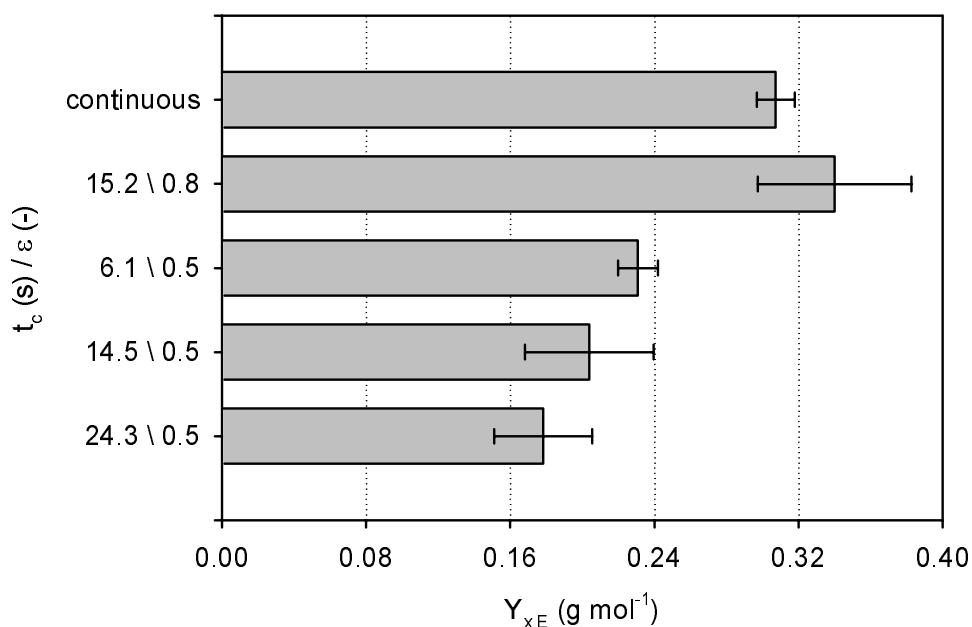


Figure 3.7. Yield of biomass on light energy ( $Y_{x,E}$ ) in gram protein per mol photons of *C. reinhardtii*. Circumstances as described in Figure 3.5.

### ***Period II: specific photosynthetic activity***

More insight in the acclimation of *C. reinhardtii* to the light/dark cycles applied during period II was obtained by measuring the photosynthetic activity ( $P_{O_2}$ ), in oxygen per protein per hour ( $\text{g g}^{-1} \text{h}^{-1}$ ), under a wide range of PFDs. This was done on two or three days during a turbidostat run under a certain light regime. The data of these measurements were pooled and fitted by the hyperbolic tangent model (Chalker, 1980) and a photosynthesis-irradiance (PI) curve was obtained. The model contains two fit parameters: the initial slope of the curve,  $\alpha$ ,

and the maximal photosynthetic activity,  $P_{O_2,max}$ . The fitted parameters for all five light regimes are presented in Table 3.1.

The parameter  $\alpha$  can be combined with  $a^*_{prot}$  to obtain the photosynthetic efficiency at limiting PFDs,  $\alpha/a^*_{prot}$  in oxygen per photons ( $g \mu mol^{-1}$ ). The difference in the initial slope ( $\alpha$ ) of the PI-curves was rather small. Only the 24 s period culture had a significantly lower  $\alpha$ . Since  $a^*_{prot}$  remained unchanged under all light regimes, only the efficiency for the 24 s period culture is significantly smaller. Differences in  $\alpha/a^*_{prot}$  therefore can only partly explain the differences found in  $Y_{x,E}$ . On the other hand, the differences in  $P_{O_2,max}$  correlate very well to  $Y_{x,E}$ .  $P_{O_2,max}$  is a measure of the maximal capacity of the photosynthetic apparatus. The  $P_{O_2,max}$  of the continuously illuminated culture was the highest of all cultures,  $0.94 g g^{-1} h^{-1}$ . The maximal activity of the 0.8 light fraction culture was a bit smaller, but the activities of the other cultures ( $\varepsilon = 0.5$ ) were all significantly lower,  $0.64 - 0.66 g g^{-1} h^{-1}$ .

Table 3.1 Maximal photosynthetic activity ( $P_{O_2,max}$ ) and initial slope of PI-curve ( $\alpha$ ) of *Chlamydomonas reinhardtii* on protein basis. *C. reinhardtii* was cultivated under continuous light and intermittent illumination of variable cycle length ( $t_c$ ) and light fraction ( $\varepsilon$ ).

$t_c$ (s)	$\varepsilon$ (-)	$P_{O_2,max}$ ( $g g^{-1} h^{-1}$ )	95 % interval	$\alpha$ ( $g g^{-1} h^{-1} (\mu mol m^{-2} s^{-1})^{-1}$ )	95 % interval
15.2	0.8	0.862	0.844 - 0.879	2.17	2.08 - 2.26
24.3	0.5	0.661	0.628 - 0.693	1.58	1.42 - 1.75
14.5	0.5	0.635	0.617 - 0.654	2.06	1.93 - 2.19
6.1	0.5	0.642	0.606 - 0.679	1.93	1.70 - 2.17
Continuous light		0.943	0.921 - 0.965	2.12	2.03 - 2.22

***Period II: quantum yield of photochemistry ( $\phi_p$ ) and non-photochemical quenching of fluorescence (NPQ).***

Also the fluorescence parameters  $\phi_p$  and NPQ provide more insight in the acclimation of *C. reinhardtii* to medium-duration light/dark cycles. The quantum yield of photochemistry,  $\phi_p$ , gives the fraction of photons captured by the photosystems which are actually used for charge separation. In addition, non-photochemical quenching of fluorescence, NPQ, is a measure of heat dissipation in the photosystems. The derivation and measurement of both parameters is explained in the Theory section.

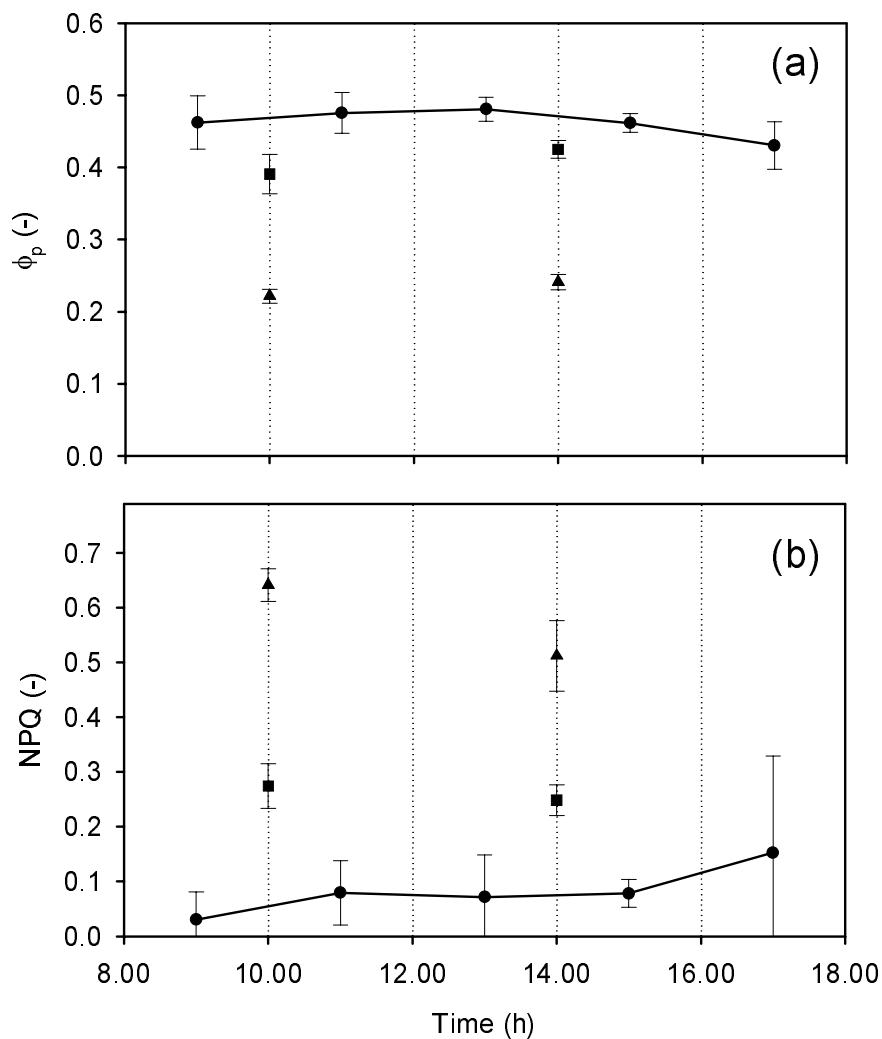


Figure 3.8 Quantum yield of photochemistry (a),  $\phi_p$ , and non-photochemical quenching of fluorescence (b), NPQ, of *C. reinhardtii* cultures acclimated to: continuous illumination (●); intermittent illumination with a 6 s (■) and 24 s (▲) light/dark cycle,  $\varepsilon = 0.5$ . Both parameters were determined under the cultivation light regime and the PFD of the simulated cultivation light was  $580 \mu\text{mol m}^{-2} \text{s}^{-1}$ . The day period of the day/night cycle started at 6.00 h and ended at 22.00 h. Error bars represent 95 % confidence intervals calculated from three independent measurements, each on a different day.

The parameters  $\phi_p$  and NPQ were determined during three of the five turbidostat runs: continuous light and two intermittent light regimes with a light fraction of 0.5 and a cycle duration of 6 and 24 s, respectively. Physiological parameters of algae change during the day and therefore  $\phi_p$  was followed during a part of the day, from 9.00 h to 17.00 h. The day began at 6.00 h and ended at 22.00 h. This was done for the continuously illuminated culture only (Figure 3.8). Between 9.00 h and 15.00 h  $\phi_p$  did not change significantly and was 0.46. This

means that about half of the photons absorbed by the photosystems are used for photochemistry.

The fluorescence parameters of the cultures acclimated to intermittent illumination were determined at two hours, 10.00 h and 14.00 h, during the day. In Figure 3.8 can be seen that  $\phi_p$  under the 24 s light/dark cycle is twice as low as the yield under continuous illumination. Also under the 6 s light/dark cycle  $\phi_p$  seems to be lower than under continuous illumination. We conclude that the quantum yield of photochemistry decreases during acclimation to medium-duration light/dark cycles in comparison to continuous light. This is in agreement with the observed decrease of the biomass yield on light energy,  $Y_{x,E}$ , and the decrease of the specific photosynthetic activity,  $P_{O_2}$ . Under the same circumstances non-photochemical quenching of fluorescence, NPQ, was determined and the results are shown in Figure 3.8. The parameter NPQ was considerably higher under the 24 s light/dark cycle than under continuous illumination and also under the 6 s cycle NPQ appears to be higher. In comparison to continuous illumination, under intermittent illumination a larger part of the excitation energy is dissipated as heat.

Before going further into the details of the results of the fluorescence measurements we can already conclude that changes take place in the photosynthetic apparatus and/or carbon fixation metabolism of *C. reinhardtii* as a result of long exposure to medium-duration light/dark cycles. *C. reinhardtii* is not able to maintain a photosynthetic capacity under light/dark cycles ( $\epsilon = 0.5$ ) as high as under continuous illumination. This is concluded from the observations that the specific photosynthetic activity,  $P_{O_2}$ , and the quantum yield of photochemistry,  $\phi_p$ , decreased under light/dark cycles while specific light absorption,  $a_{\text{prot}}^*$ , did not change. In addition, we found that non-photochemical quenching of fluorescence, NPQ, increased under light/dark cycles reflecting increased thermal dissipation of absorbed light energy. As a result, the biomass yield on light energy,  $Y_{x,E}$ , decreased under medium-duration light/dark cycles in comparison to continuous illumination.

The conclusions above can be specified with respect to the length of the light/dark cycle and the magnitude of the light fraction.  $\phi_p$  was considerably lower under the 24 s light/dark cycle than under the 6 s cycle (Figure 3.8) and also  $Y_{x,E}$  was lower (Figure 3.7). Apparently the length of the dark period is an important variable. Furthermore,  $Y_{x,E}$  and  $P_{O_2}$  did not decrease at a light fraction of 0.8 (15 s cycle duration) in comparison to continuous light (Figure 3.7 and Table 3.1). The relatively short dark period of this light regime did not have a big influence.

In many studies it is already shown that the light utilization efficiency is strongly dependent on the light/dark cycles to which algal cultures are subjected (Laws, et al., 1983; Ogbonna, et al., 1995; Richmond and Qiang, 1997). In this study this is demonstrated again, but now for medium-duration light/dark cycles using the chlorophyt *C. reinhardtii*. However, our results cannot be translated in design rules for practical (air-lift) systems easily because we simplified the light regime. We used square-wave light/dark cycles with a constant and saturating intensity during the light period of 600 - 700  $\mu\text{mol m}^{-2} \text{s}^{-1}$ . This PFD could be equal to the average PFD in the photic zone of an outdoor reactor. But in the photic zone of such a reactor a light gradient will exist, going from more than 2000  $\mu\text{mol m}^{-2} \text{s}^{-1}$  at the surface to almost zero at the dark side. It remains to be investigated whether this simplification of the light regime is allowed.

If our approximation of reality with square-wave light/dark cycles is allowed, we could conclude that the relative size of the dark zone in a photobioreactor should be as small as possible. The dark fraction should not be much larger than 0.2 for *Chlamydomonas* at cycle times of 15 s. Consequently, the biomass density and surface/volume ratio of the photobioreactor need to be in balance. The biomass density preferably should be high and as a result the surface/volume ratio has to be high preventing the creation of a large dark zone. A second possibility is to allow the existence of a considerable dark zone ( $\varepsilon = 0.5$ ), but then the circulation time between light-exposed surface and dark zone should be as short as possible; it should even be considerably shorter than 6 s in the case of *Chlamydomonas*.

***Period II: quantum yield of photochemistry ( $\phi_p$ ) and non-photochemical quenching of fluorescence (NPQ): kinetics during light/dark cycle.***

The fluorescence intensity  $F$  was not constant during a light/dark cycle. The change of  $F$  during a number of cycles is shown in Figure 3.9.  $F$  is higher during a light period than during a dark period. During a light period a considerable part of the PSII reaction centers is occupied and not ready to execute photochemistry. In the following dark period the electron transport chain between PSII and PSI is quickly reoxidized and PSII reaction centers are reopened. Consequently, during a light period a larger part of the excitation energy, coming from the weak and modulated measuring light, will be dissipated as heat or lost as fluorescence than during the dark period.

During long light/dark cycles, like the 24 s cycle,  $F$  also changes significantly within a light or a dark period (Figure 3.9). During a light period,  $F$  shows a very sharp increase immediately after switching from darkness to light. Following the sharp peak,  $F$  decreases. On the other

hand,  $F$  drops to a minimum after switching to darkness. Following this minimum,  $F$  increases again. These fluorescence changes are probably related to changes in the proton gradient across the thylakoid membranes. The time scales of these changes are on the level of seconds to minutes (Dau, 1994). The proton gradient will increase in the light due to photochemistry and will decrease again under darkness. Build-up of a proton gradient during a light period induces an increase of the heat dissipation in the PSII antenna complex and as a result  $F$  decreases. Exactly the opposite process occurs during the following dark period.

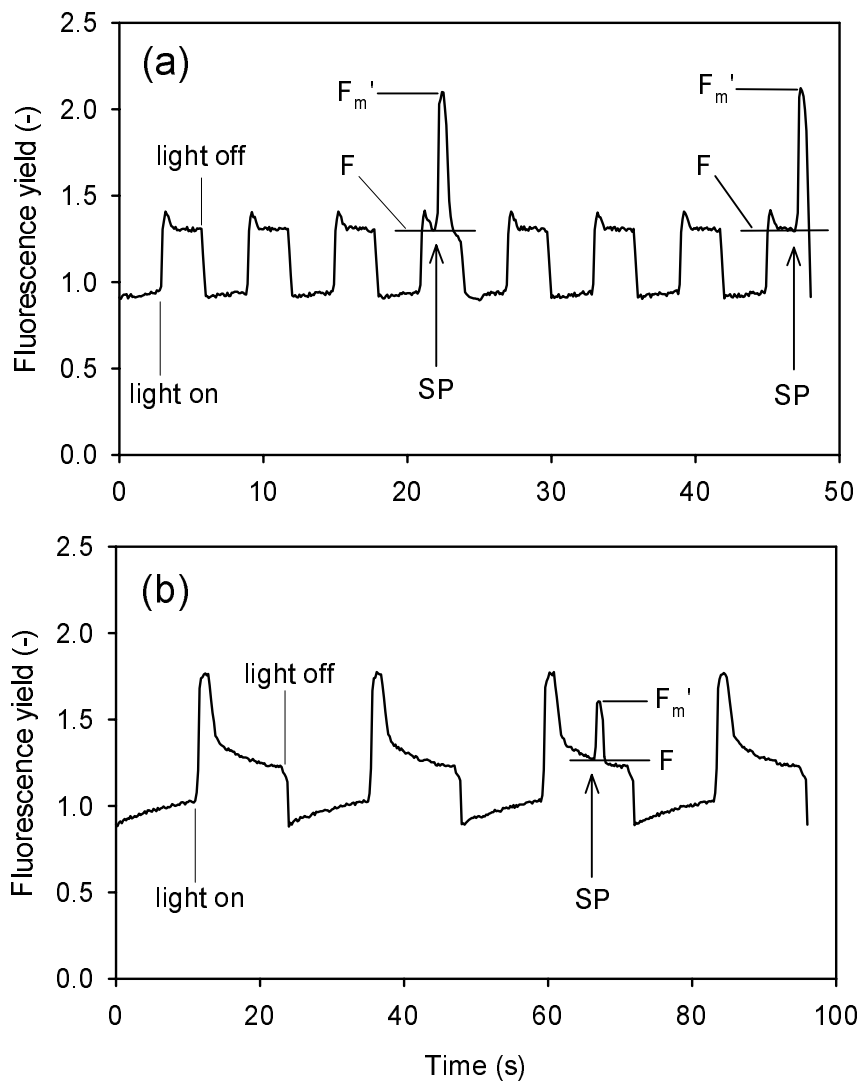


Figure 3.9 Fluorescence intensity in relative units of *C. reinhardtii* cultures during a 6 s (a) and 24 s (b) light/dark cycle,  $\varepsilon = 0.5$ . The cultures were acclimated to these light regimes. Saturating pulses, for determining  $F_m'$ , are indicated by SP and these were given on certain moments within a light/dark cycle, see text. Also the corresponding levels of  $F$  and  $F_m'$  are indicated. These figures were redrawn from the original chart recorder readings.



In order to determine the photochemical quantum yield ( $\phi_p$ ) and the non-photochemical quenching parameter (NPQ) during the light period of a light/dark cycle, saturating pulses (SP) were applied to reach  $F_m'$ . This is also illustrated in Figure 3.9. Since the energization of the thylakoid membranes is continuously changing during a cycle, see above, the pulses have to be given at different moments within the light period. The average  $\phi_p$  and NPQ during the light period can be calculated and those were already presented in Figure 3.8. During the measurements under the 6 s cycle saturating pulses were given on 0, 1 and 2 s within the 3-seconds light period. During the 24 s cycle pulses were given on 1, 6 and 11 s within the 12-seconds light period. Under the 6 s cycle it was not possible to calculate  $\phi_p$  on 0 s within the light period and also under the 24 s cycle it was not possible to calculate  $\phi_p$  on 1 s within the light period. Immediately after switching from the dark period to the light period the F-level changed very quickly (Figure 3.9) and therefore it was not possible to choose the correct F-level for the calculation of  $\phi_p$ ,  $(F_m' - F)/F_m'$ . The average  $\phi_p$  presented in Figure 3.8 therefore was based on the measurements on 1, 2 and 6, 11 s within the light period for the 6 s and 24 s cycle cultures, respectively.

Using the  $F_m'$ -level measured on different moments within the light and dark period we were able to calculate NPQ,  $(F_m - F_m')/F_m'$ , on these moments. In Figure 3.10 the results are shown for the 24 s cycle culture. The parameter NPQ increased during the light period and decreased again during the dark period. These changes are probably related to the changes of the F-level within this cycle (Figure 3.9), discussed above. During the 24 s cycle NPQ was significantly lower after 1 s than after 6 and 11 s in the light period (Figure 3.10). This measurement, however, was not included in the average NPQ presented in Figure 3.8. This was done to be able to present a 95 % confidence interval. However, if the measurement after 1 s is taken into account the average NPQ still is significantly higher than the NPQ levels of the two other cultures.

From the transients in the F-level and NPQ discussed above it is clear that the processes in the photosystems are changing periodically under light/dark cycles of 24 s (Figure 3.9 and Figure 3.10). We already concluded that the transients in NPQ are most likely caused by changes in the energization of the thylakoid membranes (Dau, 1994) during a cycle. Periodicity in this energization (trans-thylakoid proton gradient) could lead to a periodicity in thermal dissipation of absorbed light energy (Briantais, et al., 1980). Furthermore, the differences in the average NPQ between the two light/dark cycles, 6 s and 24 s period, and continuous illumination (Figure 3.8) are most likely caused by differences in the total capacity of thermal

dissipation. The capacity of heat dissipation in *Chlamydomonas reinhardtii* is determined by the concentration of xanthophyll pigments and the magnitude of the trans-thylakoid proton gradient (Niyogi, et al., 1997a and 1997b). Xanthophylls in the antenna complex are able to dissipate excess excitation energy quickly as heat. The capacity of this mechanism is higher when the proton gradient or the cellular concentration of these pigments is higher.

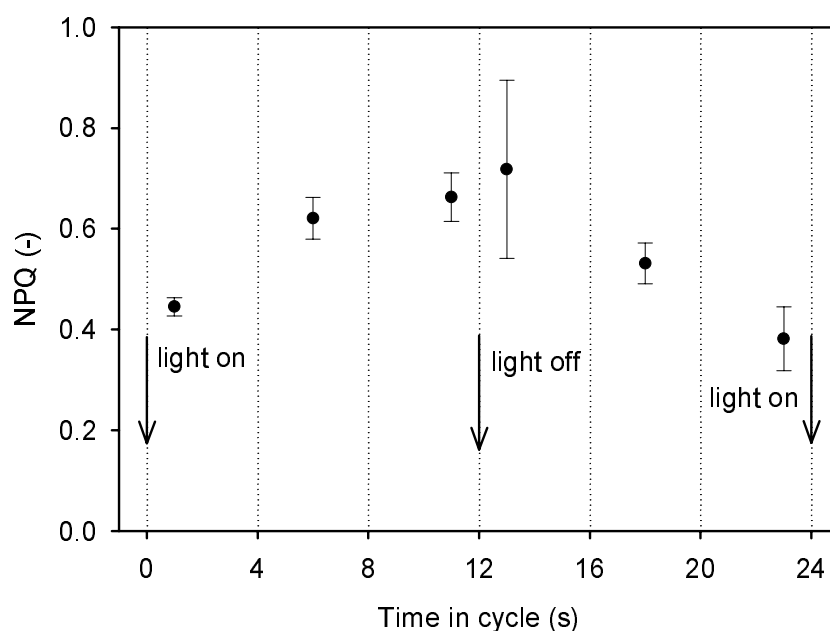


Figure 3.10. NPQ of *C. reinhardtii* culture during the 24 s light/dark cycle,  $\varepsilon = 0.5$ ; the culture was acclimated to this cycle. Circumstances as described in Figure 3.8.

## Conclusions

The green alga *Chlamydomonas reinhardtii* was cultivated under continuous illumination and under light/dark cycles, which will also be encountered when algae are cultivated in air-lift loop reactors. This study was done under over-saturating photon flux densities during the light period,  $600 - 700 \mu\text{mol m}^{-2} \text{s}^{-1}$ , to simulate the situation in the photic zone of such photobioreactors. The biomass (protein) yield on light energy ( $Y_{x,E}$ ) was lower under light/dark cycles with a light fraction of 0.5,  $0.178 - 0.231 \text{ g mol}^{-1}$ , than under continuous illumination,  $0.307 \text{ g mol}^{-1}$ .

Similar results were obtained by measurement of chlorophyll fluorescence. The quantum yield of photochemistry ( $\phi_p$ ) decreased from 0.47 under continuous illumination to 0.23 under intermittent illumination with a light fraction of 0.5 and 24 s duration. The quantum yield is a

measure for the efficiency of the conversion of light energy into chemical energy. This study showed there is a good correlation between the quantum yield of photochemistry and the biomass (protein) yield on light energy. In addition, the high time-resolution of the measurements allowed the determination of changes in heat dissipation within a light/dark cycle.

## Nomenclature

PAR	photosynthetic active radiation, 400 - 700 nm	
PSI	photosystem I	
PSII	photosystem II	
$\alpha$	initial slope of PI-curve	$[g\ g^{-1}\ h^{-1}\ (\mu\text{mol}\ m^{-2}\ s^{-1})^{-1}]$
$\varepsilon$	duration light period as a fraction of full cycle duration	[-]
$\mu$	specific growth rate	$[h^{-1}]$
$\mu_n$	normalized specific growth rate	[-]
$\phi_p$	quantum yield of PSII photochemistry	[-]
$a_{\text{prot}}^*$	spectrally averaged absorption coefficient, protein basis	$[m^2\ g^{-1}]$
F	fluorescence yield under cultivation light regime	[-]
$F_0$	minimal fluorescence yield in dark-adapted state	[-]
$F_m$	maximal fluorescence yield in dark-adapted state	[-]
$F_m'$	maximal fluorescence yield under cultivation light regime	[-]
NPQ	non-photochemical quenching of fluorescence	[-]
$OD_{680}$	optical density at 680 nm	[-]
PFD	photon flux density in PAR range	$[\mu\text{mol}\ m^{-2}\ s^{-1}]$
$P_{O_2}$	photosynthetic activity, oxygen production per protein	$[g\ g^{-1}\ h^{-1}]$
$P_{O_2, \text{max}}$	maximal photosynthetic activity in PI-curve	$[g\ g^{-1}\ h^{-1}]$
$Y_{x,E}$	biomass yield on light energy, protein per photons	$[g\ mol^{-1}]$

Subscripts: cult, cultivation; prot, protein.

#### 4. Efficiency of light utilization of *Chlamydomonas reinhardtii* and *Dunaliella tertiolecta* under medium-duration light/dark cycles: 15 s

##### Abstract

The green micro-algae *Chlamydomonas reinhardtii* and *Dunaliella tertiolecta* were cultivated under medium-duration square-wave light/dark cycles with a cycle time of 15 s. These cycles were used to simulate the light regime experienced by micro-algae in externally-illuminated (sunlight) air-lift loop bioreactors with internal draft tube. Biomass yield in relation to light energy was determined as grams of protein per mol of photons (400 - 700 nm). Between 600 and 1200  $\mu\text{mol m}^{-2} \text{s}^{-1}$  the yield at a 10/5 s light/dark cycle was equal to the yield at continuous illumination. Consequently, provided that the liquid circulation time is 15 s, a considerable dark zone seems to be allowed in the interior of air-lift loop photobioreactors (33 % v/v) without loss of light utilization efficiency. However, at a 5/10 s light/dark cycle, corresponding to a 67 % v/v dark zone, biomass yield decreased. Furthermore, both algae, *C. reinhardtii* and *D. tertiolecta*, responded similarly to these cycles with respect to biomass yield. This was interesting because they were reported to exhibit a different photoacclimation strategy. Finally, it was demonstrated that *D. tertiolecta* was much more efficient at low (average) photon flux densities (57 - 370  $\mu\text{mol m}^{-2} \text{s}^{-1}$ ) than at high PFDs (> 600  $\mu\text{mol m}^{-2} \text{s}^{-1}$ ) and it was shown that *D. tertiolecta* was cultivated at a sub-optimal temperature (20 °C).

This chapter has been published as: Janssen M, de Bresser L, Baijens B., Tramper J, Mur LR, Snel JFH and Wijffels RH. Scale-up aspects of photobioreactors: effects of mixing-induced light/dark cycles. Journal of Applied Phycology, Vol. 12, p. 225-237, 2000.

## Introduction

Although microalgae produce commercially interesting compounds, large-scale cultivation has been hampered so far because production costs are too high. Cultivation of a small number of species in shallow open ponds has developed into a considerable economic activity. Many other interesting applications depend on monocultures susceptible to contamination by other algae or bacteria and cannot be maintained in open systems. Many processes also need to be operated under controlled conditions with respect to temperature, pH, salinity or other environmental factors. Clearly, closed photobioreactors are a necessity but they are expensive and require considerable improvement of reactor productivity (Pulz and Scheibenbogen, 1998).

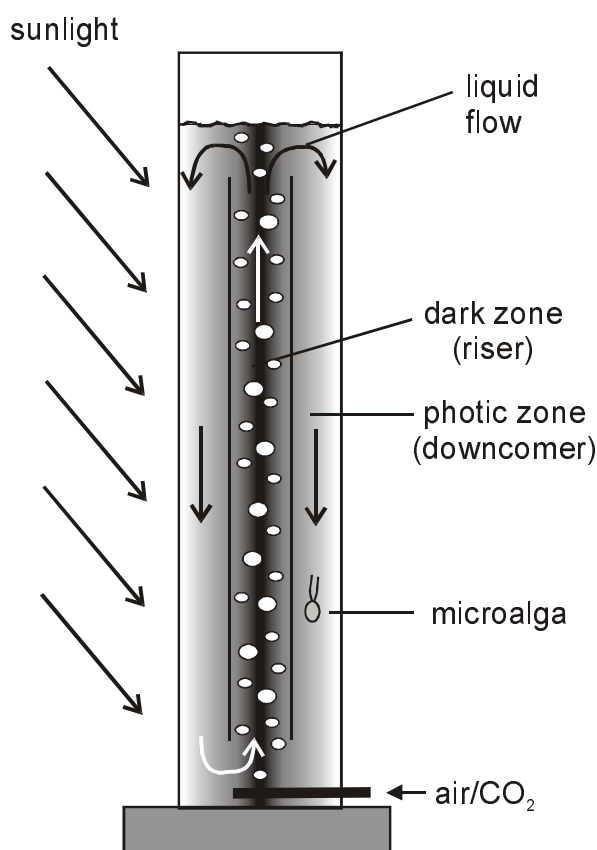


Figure 4.1. Liquid flow and resulting light/dark cycles in a concentric tube air-lift loop photobioreactor.

Air-lift loop bioreactors can be applied as photobioreactors for cultivation of microalgal monocultures (Figure 4.1). In air-lift reactors efficient mixing is combined with a controlled

liquid flow. In such a system carbon-dioxide supply and oxygen removal will not limit reactor productivity, the availability of light, however, will. Depending on the biomass concentration a dark zone will exist in the interior of the reactor (Figure 4.1). A concentric-tube air-lift reactor could be designed in such a way that the riser comprises the dark zone. Consequently, the time algae spend in the dark and the photic zone is determined by the liquid circulation time (10 - 100 s), which depends on the superficial gas flow rate (Chisti, 1998).

In a previous study it was found that light/dark cycles inside the range of 10 - 100 s could have a considerable influence on the efficiency of light utilization. *Chlamydomonas reinhardtii* was cultivated under square-wave light/dark cycles (6 - 24 s) with a saturating photon flux density (PFD) of 600 - 700  $\mu\text{mol m}^{-2} \text{s}^{-1}$  during the light period. The dark period should be limited to about 20 % of the cycle time to maintain a biomass yield on light energy as high as under continuous illumination of this PFD. The efficiency was found to decrease when longer dark periods, 50 % of the cycle time, were applied (Janssen, et al., 2000b).

At PFDs higher than 700  $\mu\text{mol m}^{-2} \text{s}^{-1}$  the probability of photodamage will increase and photodamage will result in a reduction of the photosynthetic capacity (Melis, 1999). This was clearly demonstrated in cyanobacterium cultures (Jensen and Knutsen, 1993; Vonshak, et al., 1994; Torzillo, et al., 1996) and also green algae are susceptible to photoinhibition (Falk, et al., 1992; Sanchez, et al., 1996; Grima, et al., 1996). The introduction of a dark zone could reduce this effect by avoiding long exposure to high PFDs and providing 'dark' time for the algae to repair photo-induced damage (Merchuk, et al., 1998).

The influence of photoacclimation on the response of algae to light/dark cycles could be important as well. In general microalgae show one of two different acclimation strategies (Falkowski and LaRoche, 1991). Considering a shift from high to low light:

- 1) the antenna size is increased while the number of photosystems per cell remains unchanged, as is done by *Chlamydomonas reinhardtii* (Neale and Melis, 1986);
- 2) the number of photosystems is increased while the average antenna size remains unchanged, as is done by *Dunaliella tertiolecta* (Falkowski and Owens, 1980; Falkowski, et al., 1981).

The introduction of a dark zone in a photobioreactor, by increasing the biomass density, will lead to a lower average PFD. This will result in a lower time-averaged reduction state of the electron transport chain between PSII and PSI. This reduction state is suggested to be the signal controlling photoacclimation (Escoubas, et al., 1995; Durnford and Falkowski, 1997). It is likely that the introduction of a dark zone will lead to photoacclimation, i.e. an increase of the specific light-absorbing surface. If photoacclimation takes place, the second

acclimation strategy might be better with respect to bioreactor productivity. An increase of the number of photosystems could give an algal cell the possibility to fix more light energy at the reactor surface where the PFD is high. As a result, light energy could be used more efficiently and reactor productivity could rise.

The effect of the photoacclimation strategy on the efficiency of light utilization of the Chlorophyta *Chlamydomonas reinhardtii* and *Dunaliella tertiolecta* under light/dark cycles were studied. The algae were cultivated at high photon flux densities of 1100 - 1200  $\mu\text{mol m}^{-2} \text{s}^{-1}$  to study the effect of photoinhibition too. For comparison, the average PFD in the photic zone of a cylindrical photobioreactor ( $d = 0.2 \text{ m}$ ) in full sunlight will be in the range of 550 - 800  $\mu\text{mol m}^{-2} \text{s}^{-1}$ . These values were calculated by means of the model presented by Evers (1991). In this model we used different attenuation coefficients to obtain different light/dark ratios at incident PFDs of 1250 - 2500  $\mu\text{mol m}^{-2} \text{s}^{-1}$  ('dark' < 50  $\mu\text{mol m}^{-2} \text{s}^{-1}$ ). Because of these calculations *D. tertiolecta* was also cultivated at 600 - 700  $\mu\text{mol m}^{-2} \text{s}^{-1}$ ; in our previous study *C. reinhardtii* was already cultivated at 600 - 700  $\mu\text{mol m}^{-2} \text{s}^{-1}$  (Janssen, et al., 2000b). The light/dark cycles applied were 15 s and this is within the range of liquid circulation times in air-lift loop reactors.

Under these light regimes the biomass yield on light energy ( $Y_{x,E}$ ) was determined and compared to the yield determined under continuous illumination. In addition, the quantum yield of PSII photochemistry and the photochemical quantum yield of open PSII reaction centers,  $\phi_p$  and  $\phi_{po}$  (Genty, et al., 1989), were determined. The parameter  $\phi_{po}$  was used as an indicator of photoinhibition (Vonshak, et al., 1994; Torzillo, et al., 1996). Finally, as a comparison, the biomass yield of *D. tertiolecta* was also determined at low (average) PFDs (57 - 370  $\mu\text{mol m}^{-2} \text{s}^{-1}$ ) and at 25 °C instead of 20 °C. The biomass yield will be higher at low PFDs and at temperatures closer to the optimum growth temperature.

## **Materials and Methods**

### ***Organism and culture medium***

*Chlamydomonas reinhardtii* CC 1690 wild type 21 gr mt+ was kindly provided by Elizabeth Harris from the Chlamydomonas Genetics Center (Duke University, Durham, NC, USA). The organism was cultivated in a Sueoka high-salts (HS) medium as described by Harris (1989). The medium is composed of (quantities in mmol L<sup>-1</sup>): NH<sub>4</sub>Cl, 9.35; MgSO<sub>4</sub>·7H<sub>2</sub>O, 0.0811; CaCl<sub>2</sub>·2H<sub>2</sub>O, 0.0680; K<sub>2</sub>HPO<sub>4</sub>, 8.27; KH<sub>2</sub>PO<sub>4</sub>, 5.29; NaHCO<sub>3</sub>, 10; 5 mL L<sup>-1</sup> of Hütner's trace-

elements solution (Harris, 1989). Pure cultures were maintained on agar slants at 20 °C, 50 - 70  $\mu\text{mol m}^{-2} \text{s}^{-1}$  and a 16/8 h day/night cycle. Before inoculating a reactor, algae were transferred from the slants to a 100 mL Erlenmeyer flask containing 50 mL of medium. This suspended culture was stirred and maintained under the same conditions as the slants. In the exponential growth phase the suspended culture was used as an inoculum for the bioreactor.

*Dunaliella tertiolecta* CCAP 19/6B was obtained from the Culture Collection of Algae and Protozoa (Oban, UK). *D. tertiolecta* was cultivated in artificial seawater medium composed of (quantities in  $\text{g L}^{-1}$ ): NaCl, 24.5;  $\text{MgCl}_2 \cdot 6\text{H}_2\text{O}$ , 9.80;  $\text{CaCl}_2 \cdot 2\text{H}_2\text{O}$ , 0.53;  $\text{Na}_2\text{SO}_4$ , 3.20;  $\text{K}_2\text{SO}_4$ , 0.85. The following nutrients were added (quantities in  $\text{mmol L}^{-1}$ ):  $\text{KNO}_3$ , 5.00;  $\text{NaH}_2\text{PO}_4 \cdot \text{H}_2\text{O}$ , 0.50;  $\text{NaHCO}_3$ , 5.00. Also the following trace-elements were added (quantities in  $\mu\text{mol L}^{-1}$ ):  $\text{Na}_2\text{EDTA} \cdot 2\text{H}_2\text{O}$ , 61.6;  $\text{FeCl}_3 \cdot 6\text{H}_2\text{O}$ , 23.3;  $\text{CuSO}_4 \cdot 7\text{H}_2\text{O}$ , 0.210;  $\text{ZnSO}_4 \cdot 7\text{H}_2\text{O}$ , 0.303;  $\text{CoCl}_2 \cdot 6\text{H}_2\text{O}$ , 0.085;  $\text{MnCl}_2 \cdot 4\text{H}_2\text{O}$ , 1.83;  $\text{Na}_2\text{MoO}_4$ , 0.052. Finally the following vitamins were added (quantities in  $\mu\text{g L}^{-1}$ ): biotin, 1; thiamine-HCl, 20; cyanocobalamine (B12), 1. *Dunaliella* was maintained as pure suspended culture in 100 mL Erlenmeyer flasks containing 50 mL of medium. The cultures were not stirred and they were placed at 20 °C, 50 - 70  $\mu\text{mol m}^{-2} \text{s}^{-1}$  under a 16/8 h day/night cycle. Every three weeks 0.5 mL of a culture was transferred to a new flask containing fresh medium. The reactor was inoculated directly with the culture of one flask.

### **Description of the reactors**

*Chlamydomonas* and *Dunaliella* both were cultivated in rectangular bioreactors with a short light path. The reactors were placed in an aquarium filled with water. The water was maintained at 25 °C for *Chlamydomonas* and at 20 °C for *Dunaliella*. The front side of the reactor was illuminated by a series of 12 halogen lamps (Decostar Titan, 50 W, 35 W or 20 W, Osram) placed outside the aquarium. Always a 16/8 hours day/night cycle was applied. During the day period the lamps could be alternately turned on and off to create square-wave light/dark cycles of 15 s duration.

Figure 4.2a represents a front view of the *Chlamydomonas* reactor, with a 525 mL liquid volume and an optical depth (= reactor depth) of 1.45 cm. Gas was sparged at the bottom, i.e. 2.5 % v/v carbon dioxide in air at a rate of 20  $\text{L h}^{-1}$ . The gas flow provided mixing, carbon dioxide and a constant pH (6.6 - 6.9). *Dunaliella* was cultivated in a different type of bioreactor (Figure 4.2b), with a 1000 mL liquid volume and a 3 cm light path. Again, the liquid was mixed by air sparged at a rate of 21.5  $\text{L h}^{-1}$ . The pH was maintained in the range



7.85 - 8.05. This was done by pulsed addition of carbon dioxide to the air flow. As a result, also the carbon-dioxide concentration was maintained constant.

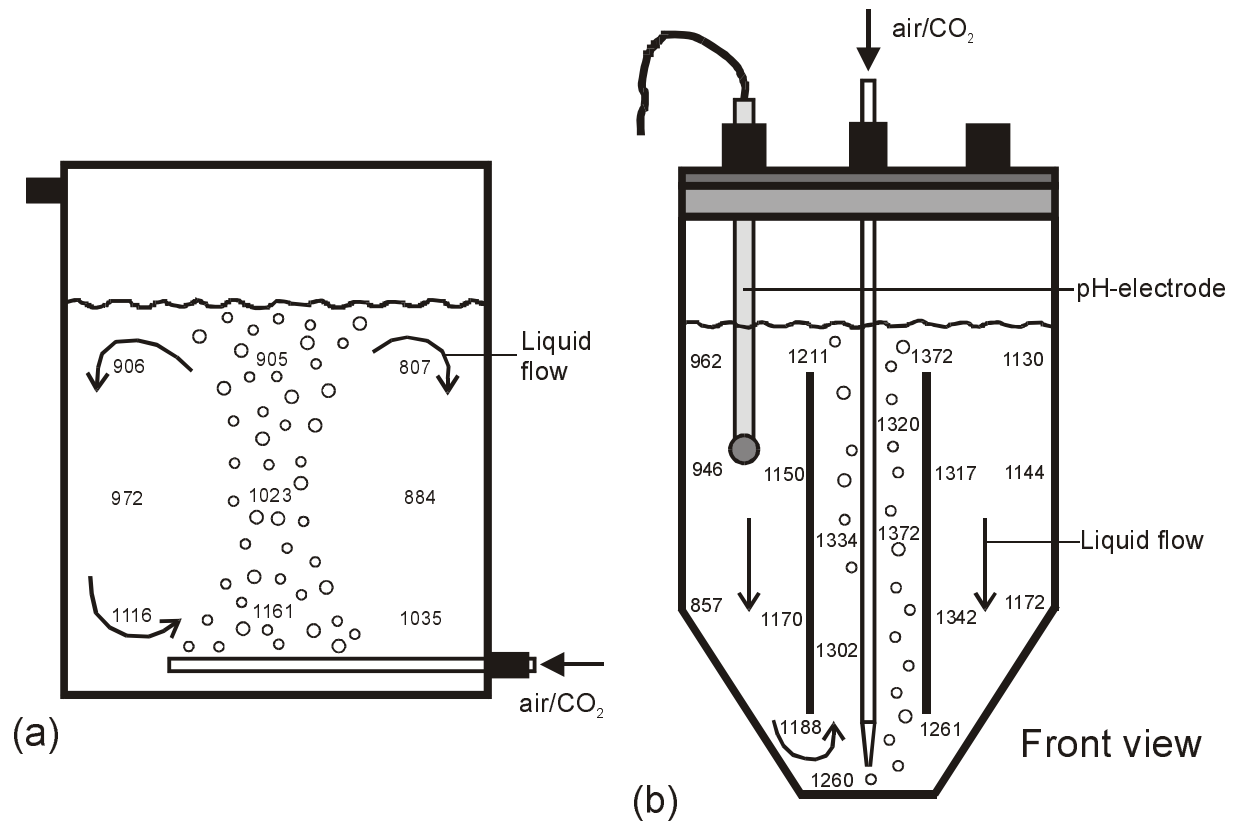


Figure 4.2. Set-up of the *Chlamydomonas* reactor (a) and *Dunaliella* reactor (b). The numbers represent the PFD distribution in the *Chlamydomonas* reactor and the absolute PFD incident on the *Dunaliella* reactor surface in  $\mu\text{mol m}^{-2} \text{s}^{-1}$  during one of the experiments.

The algal cultures in both types of bioreactors were maintained under a specific light regime for one or two weeks and they were diluted daily. In other words, the reactors were operated semi-continuously. Under one light regime only, the *Dunaliella* reactor was also operated as a turbidostat in order to achieve a steep light gradient alongside the reactor light path. For this experiment a quantum sensor was placed behind the reactor and the photon flux passing through the reactor was measured continuously. When the flux dropped below a certain value the reactor was automatically diluted until this set point was reached again. The continuous dilution in this turbidostat was stopped during the 8 hours night period.

## **Analytical procedures and measurements**

### **Specific growth rate**

After three or four days of acclimation, the specific growth rate ( $\mu$ ) was followed daily. The reactors were emptied completely every 24 hours, always at the middle of the 16 hours day period. A known volume of suspension ( $V_s$ ) was diluted with a known volume of medium ( $V_m$ ). The diluted algal suspension was put into a new and clean reactor and the reactor was quickly placed in the aquarium again. The optical density of the undiluted algae suspension was measured at 680 nm ( $OD_{680}$ ) and is called  $OD_{start}$ . In the reactor exponential growth was allowed to continue for 24 hours again and after this  $OD_{680}$  was measured for the second time,  $OD_{end}$ . The specific growth rate was calculated according to Eq. 4.1. By choosing an appropriate dilution,  $OD_{end}$  was maintained between 0.15 and 0.30 in order to minimize self-shading of the algae.

$$\text{Eq. 4.1} \quad \mu = \frac{\text{Ln} \left\{ OD_{end} / \left[ \frac{OD_{start} \cdot V_s}{V_s + V_m} \right] \right\}}{24} \quad [\text{h}^{-1}]$$

At each light regime, corresponding to a 1 or 2-weeks run, the growth rate was measured on three or more days. These separate determinations at a certain light regime were used to calculate the 95 % confidence interval. As already stated the *Dunaliella* reactor was also operated as a turbidostat at one light regime and in this experiment the specific growth rate was taken equal to the measured dilution rate.

### **Photon flux density**

The photon flux density was always measured as PAR (Photosynthetic Active Radiation, 400-700 nm). We used a  $2\text{-}\pi$  PAR-sensor, LI-190SA (LI-COR, Lincoln, NE, USA). This sensor could be placed directly in the empty *Dunaliella* reactor (Figure 4.2b). The PFD was measured at 19 positions facing the light, see the numbers in Figure 4.2b, and these values were averaged. The average PFD was measured before starting and after ending an experiment at a specific light regime. The resulting values were averaged again. The light intensities were measured at different places inside the *Chlamydomonas* reactor as well, as is shown in Figure 4.2a.

### **Spectrally averaged absorption coefficient**

After daily dilution of the semi-continuous reactor the algae suspension was centrifuged (5 min, 5000 g and 4 °C). The supernatant was centrifuged again. Both pellets were gently

resuspended in 8 - 16 mL 25 mM potassium-phosphate buffer of pH 7 in the case of *Chlamydomonas*. *Dunaliella* pellets were resuspended in growth medium of pH 7.8 - 8.0. After this, OD<sub>680</sub> of the suspension was 1.4 or lower. The absorbance of these suspensions was measured from 400 to 700 nm in a spectrophotometer equipped with an integrating sphere as described in Janssen et al. (2000b). The absorbance at the concentrations used was linear with biomass concentration. Afterwards, the protein concentration of the suspensions was determined.

From the absorbance scans the spectrally averaged absorption coefficient,  $a_{\text{prot}}^*$  or  $a_{\text{chl-a}}^*$ , was calculated according to Dubinsky et al. (1986). This coefficient is equal to the light-absorbing surface in terms of protein or chlorophyll-*a*, respectively, in  $\text{m}^2 \text{g}^{-1}$ . The relative spectral distribution of the halogen lamps was needed for these calculations and was measured from 400 to 700 nm on a SR9910 spectroradiometer (Macam, UK).

### ***Protein concentration***

Algal suspensions were filtrated and after this the filters with cakes were washed, resuspended in buffer containing sodium dodecyl sulphate and sonicated before protein was determined (Janssen, et al., 2000b). Bovine serum albumine (fraction V, crystallized, A-4378, Sigma) was used as a standard. Protein in *Dunaliella* suspensions was determined in a similar way only growth medium was used for washing the filter cake and the filter was cut in small strips before sonication. Also we changed from filtration to centrifugation (5 min, 5000 g and 4 °C) during the experiments. The determination was always done in triplicate.

### ***Biomass yield on light energy***

The biomass yield ( $Y_{x,E}$ ) was determined and expressed in terms of protein in  $\text{g mol}^{-1}$ . The yield could be calculated by dividing the specific growth rate by the specific light absorption rate according to Eq. 4.2. The factors 24, 16 and  $3.6 \cdot 10^{-3}$  in Eq. 4.2 are needed to convert  $\mu\text{mol s}^{-1}$  into  $\text{mol d}^{-1}$  including the 16/8 h day/night cycle. For this calculation we needed the specific spectrally averaged absorption coefficient ( $a_{\text{prot}}^*$ ) and this coefficient was determined together with the specific growth rate ( $\mu$ ). The calculation of the specific light absorption is not possible at high algal densities because the PFD is not constant along the light path but will decrease sharply. This was the reason we used short light-path reactors and maintained a low culture density. As a result we could assume a constant PFD during the measurement of the specific growth rate.

$$\text{Eq. 4.2} \quad Y_{x,E} = \frac{\mu \cdot 24}{\varepsilon \cdot \text{PFD} \cdot a_{\text{prot}}^* \cdot 3.6 \cdot 10^{-3} \cdot 16} \quad [\text{g mol}^{-1}]$$

During the experiment with *D. tertiolecta* in the turbidostat  $Y_{x,E}$  was calculated differently because a steep light gradient was allowed alongside the reactor light path. The quantity of algal biomass (protein) diluted in a day was measured and divided by the quantity of light absorbed. The light absorbed was equal to the incident PFD minus the PFD passing through the reactor multiplied by the illuminated surface and the daily illumination time.

### ***Chlorophyll-a***

The chlorophyll-*a* concentration in algal suspensions was determined according to the method of Nusch (1980). Also this determination was done in triplicate.

### ***Fluorescence measurements***

The fluorescence yield was determined by pulse-amplitude-modulation (PAM) fluorometry in combination with the saturating-pulse technique (Schreiber, et al., 1986). The quantum yield of PSII photochemistry ( $\phi_p$ ) was calculated according to Genty et al. (1989). The measurement apparatus was already described in Janssen et al. (2000b).

*Chlamydomonas* samples were diluted with phosphate buffer, pH 6.8, and *Dunaliella* samples with growth medium containing Hepes buffer, pH 7.9, resulting in chlorophyll-*a* concentrations between 0.2 and 1.3  $\mu\text{g mL}^{-1}$ . Extra sodium bicarbonate was added and the *Chlamydomonas* samples also received extra ammonium chloride. After this, two cuvettes were filled with 1.00 - 1.55 mL of the same suspension. One cuvette was placed immediately in the cuvette assembly to determine the photochemical quantum yield ( $\phi_p$ ) under the cultivation light regime. In the case of light/dark cycles the quantum yield was determined during the light period as was shown in Janssen et al. (2000b). The second cuvette was placed in the dark to determine the maximal photochemical quantum yield or the photochemical yield of open PSII reaction centers ( $\phi_{po}$ ). This was done after the measurements under cultivation light. The algal samples in the cuvette were mixed by a small stirrer (*Chlamydomonas*) or by a small glass pipette used to suck and release the sample regularly (*Dunaliella*).

## Results

*Chlamydomonas reinhardtii* and *Dunaliella tertiolecta* were cultivated under 3 and 9 different light regimes, respectively. As an example Figure 4.3a shows the optical density ( $OD_{680}$ ) and the daily-calculated specific growth rate ( $\mu$ ) during the cultivation of *D. tertiolecta* under continuous illumination of  $58 \mu\text{mol m}^{-2} \text{s}^{-1}$ . The algal suspension in the reactor was diluted every day at the middle of the 16 hours day period. Before dilution the optical density ( $OD_{680}$ ) was measured and the specific growth rate ( $\mu$ ) calculated.

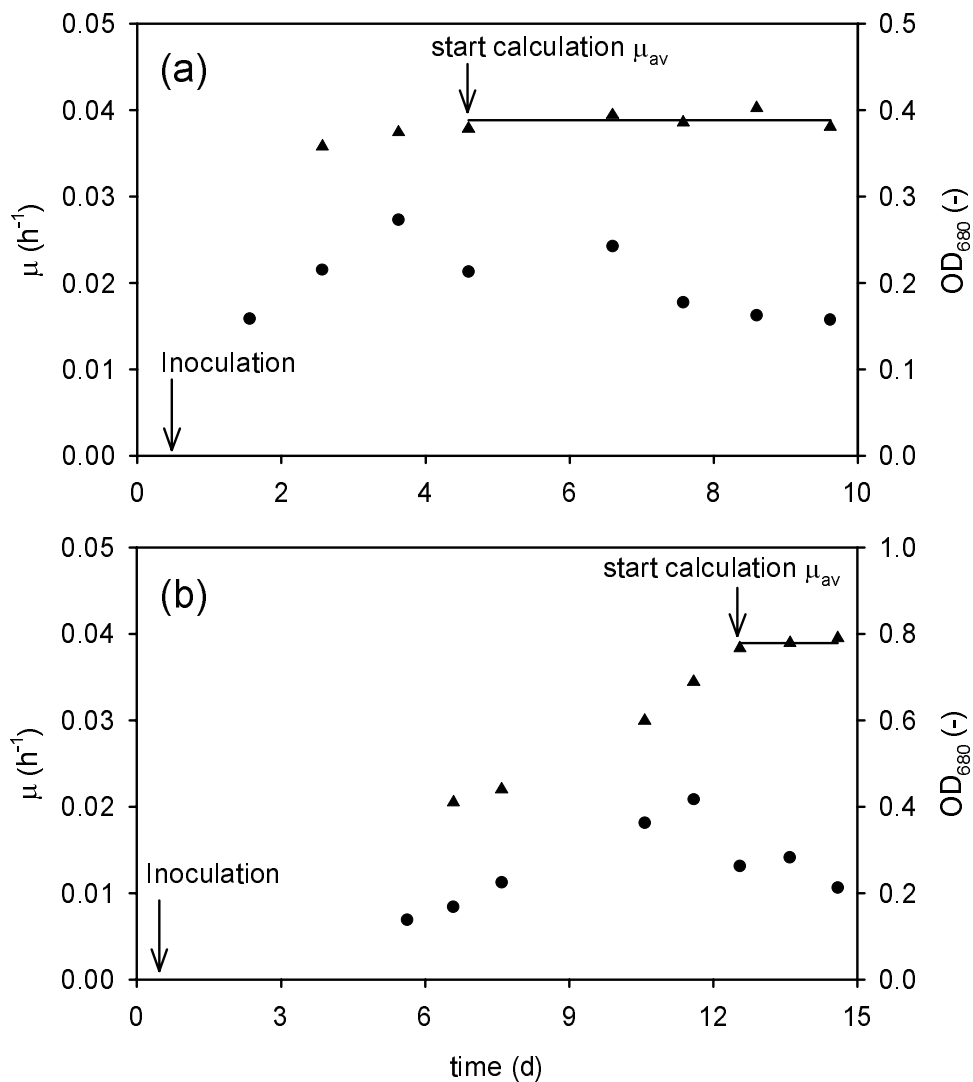


Figure 4.3. Specific growth rate ( $\mu$ ,  $\blacktriangle$ ) of *Dunaliella tertiolecta* when exposed to continuous illumination of  $58 \mu\text{mol m}^{-2} \text{s}^{-1}$  (a) and  $1215 \mu\text{mol m}^{-2} \text{s}^{-1}$  (b). The calculated average specific growth rate is given by  $\mu_{av}$  ( $\blacktriangle$ ) and  $OD_{680}$  ( $\bullet$ ) is the optical density of the cultures at the end of every 24 hours batch period.

Three or four days after inoculation the specific growth rate did not change anymore, and an average growth rate could be calculated ( $\mu_{av}$ ). Only under continuous illumination of 1215  $\mu\text{mol m}^{-2} \text{s}^{-1}$  the acclimation took longer. It took almost 12 days before the specific growth of *D. tertiolecta* seemed to reach a constant rate (Figure 4.3b).

Algal suspensions became available each day because daily a part of the algal suspension was replaced by fresh medium. After three or four days of acclimation time these suspensions were used to determine several parameters: the spectrally averaged absorption coefficient based on protein ( $a_{\text{prot}}^*$ ); the spectrally averaged absorption coefficient based on chlorophyll-*a* ( $a_{\text{chl-a}}^*$ ), for *D. tertiolecta* only; the biomass yield on light energy in terms of protein ( $Y_{x,E}$ ); the chlorophyll-*a* content expressed on protein basis ( $[\text{chl-a}]$ ), for *D. tertiolecta* only. Finally, the actual photochemical quantum yield ( $\phi_p$ ) and the maximal quantum yield ( $\phi_{po}$ ) were determined using samples taken directly from the bioreactors. These samples were taken 1 to 3 hours before the middle of the day period.

Table 4.1. Specific growth rate ( $\mu$ ) and spectrally averaged absorption coefficient ( $a_{\text{prot}}^*$ ) on protein basis of *Chlamydomonas reinhardtii* under light/dark (L/D) cycles and continuous light (CL). STD is the estimated standard deviation of 'n' independent determinations.

Light Regime	PFD ( $\mu\text{mol m}^{-2} \text{s}^{-1}$ )	$\mu$ ( $\text{h}^{-1}$ )	STD (n)	$a_{\text{prot}}^*$ ( $\text{m}^2 \text{g}^{-1}$ )	STD (n)
CL	1153	0.110	0.008 (6)	0.163	0.006 (3)
10/5 s L/D	1153	0.085	0.004 (5)	0.187	0.019 (6)
5/10 s L/D	1203	0.033	0.003 (4)	0.233	0.013 (4)

In Table 4.1 the specific growth rates ( $\mu$ ) of *C. reinhardtii* are presented. These rates were divided by the rate under continuous illumination of 627  $\mu\text{mol m}^{-2} \text{s}^{-1}$  measured by Janssen et al. (2000b), which was 0.116  $\text{h}^{-1}$ . This was the highest rate measured in that study and is a good estimate of the maximal specific growth rate of *Chlamydomonas reinhardtii* at 25 °C and a 16/8 h day/night rhythm. The resulting normalized growth rates ( $\mu_n$ ) are presented in Figure 4.4a and for comparison also two other points from that previous study are shown. The light fraction,  $\varepsilon$ , on the x-axis of Figure 4.4 is equal to the fraction of time the algae are exposed to light. The 10/5 s light/dark (L/D) cycle corresponds to an  $\varepsilon$  of 0.67 and the 5/10 s L/D cycle corresponds to an  $\varepsilon$  of 0.33. The specific growth rates ( $\mu$ ) of *Dunaliella tertiolecta* are shown in Table 4.2 and they were divided by the growth rate under continuous

illumination of  $660 \mu\text{mol m}^{-2} \text{s}^{-1}$ . Also this rate is a good estimate of the maximal specific growth rate of *D. tertiolecta* under the cultivation parameters, 20 °C and a 16/8 h day/night rhythm. The resulting normalized rates ( $\mu_n$ ) are shown in Figure 4.4b.

Table 4.2. Specific growth rate ( $\mu$ ), spectrally averaged absorption coefficient ( $a_{\text{prot}}^*$  and  $a_{\text{chl-a}}^*$ ) and chlorophyll-*a* content ([chl-*a*]) on protein basis of *Dunaliella tertiolecta* under light/dark (L/D) cycles and continuous light (CL). STD is the estimated standard deviation of 'n' independent determinations.

Light Regime	PFD ( $\mu\text{mol m}^{-2} \text{s}^{-1}$ )	$\mu$ ( $\text{h}^{-1}$ )	STD (n)	$a_{\text{prot}}^*$ ( $\text{m}^2 \text{g}^{-1}$ )	STD (n)	$a_{\text{chl-a}}^*$ ( $\text{m}^2 \text{g}^{-1}$ )	STD (n)	[chl- <i>a</i> ] ( $\text{mg g}^{-1}$ )	STD (n)
CL	1215	0.0389	0.0006 (3)	---	---	---	---	---	---
10/5 s L/D	1199	0.0324	0.0010 (8)	0.198	0.004 (3)	7.84	0.06 (3)	25.2	0.4 (3)
5/10 s L/D	1163	0.0162	0.0007 (8)	0.242	0.006 (3)	7.10	0.09 (3)	34.1	1.0 (3)
CL	660	0.0440	0.0006 (7)	0.156	0.010 (4)	8.29	0.37 (4)	18.9	1.3 (4)
10/5 s L/D	634	0.0356	0.0009 (4)	0.192	0.009 (4)	7.22	0.09 (4)	26.9	1.3 (3)
5/10 s L/D	633	0.0154	0.0013 (5)	0.227	0.006 (4)	6.55	0.09 (4)	34.7	0.6 (4)
CL	58	0.0388	0.0010 (5)	0.233	0.019 (4)	6.04	0.26 (4)	38.5	1.5 (4)

Specific light absorption was measured as the spectrally averaged absorption coefficient ( $a_{\text{prot}}^*$  in Table 4.1 and Table 4.2). The absorption coefficient is expressed on a protein basis but can also be presented based on other cellular compounds, e.g. chlorophyll-*a*. The chlorophyll-*a* content ([chl-*a*]) of *D. tertiolecta* was determined and is presented in Table 4.2. This value is therefore used to express the spectrally averaged absorption coefficient in terms of chlorophyll-*a* ( $a_{\text{chl-a}}^*$ , in Table 4.2).

The biomass yield on light energy ( $Y_{x,E}$ ) was calculated under each light regime using the specific growth rate ( $\mu$ ), photon flux density (PFD), spectrally averaged absorption coefficient ( $a_{\text{prot}}^*$ ) and Eq. 4.2. The values of these parameters are shown in Table 4.1 and Table 4.2. The biomass yields resulting from these calculations are expressed in g protein per mol of photons (400 - 700 nm) and are shown in Figure 4.5; Figure 4.5a for *C. reinhardtii* and Figure 4.5b for *D. tertiolecta*. The yield of *D. tertiolecta* at low PFD ( $58 \mu\text{mol m}^{-2} \text{s}^{-1}$ ) is  $1.20 \pm 0.151 \text{ g mol}^{-1}$  which is not shown in Figure 4.5b.

The quantum yield of PSII photochemistry ( $\phi_p$ ) was also determined under different cultivation light regimes and is presented in Figure 4.6. In addition, the maximal quantum yield was determined after dark incubation ( $\geq 45$  minutes) to obtain the quantum yield of open PSII reaction centers ( $\phi_{po}$ ). These results are presented in Figure 4.6a for *C. reinhardtii* and in

Figure 4.6b for *D. tertiolecta*. Due to technical problems we were not able to measure the quantum yield ( $\phi_p$ ) of *D. tertiolecta* in the range of 1100 - 1200  $\mu\text{mol m}^{-2} \text{s}^{-1}$ .

*Dunaliella tertiolecta* was always cultivated at 20 °C. But at one light regime, the 10/5 s L/D cycle at 1200  $\mu\text{mol m}^{-2} \text{s}^{-1}$ , *D. tertiolecta* was also cultivated at 25 °C. The results are presented in the second column of Table 4.3. The data in the first column of Table 4.3 were already presented in Table 4.2, but added again to allow easy comparison between the two cultivation temperatures.

Table 4.3. Physiological parameters of *Dunaliella tertiolecta* cultivated at 1200  $\mu\text{mol m}^{-2} \text{s}^{-1}$  under a 10/5 s light/dark cycle at 20 and 25 °C in a dilute suspension without light gradient, and under a 10/5 s cycle at 25 °C with a light gradient in the reactor. The experiment under the light gradient was done in a turbidostat mode. STD is the estimated standard deviation of 'n' independent determinations.

Parameter	No light gradient	No light gradient	Light gradient
	20 °C	25 °C	25 °C
PFD ( $\mu\text{mol m}^{-2} \text{s}^{-1}$ )	1199	1203	1184 → 57
$\mu$ ( $\text{h}^{-1}$ )	0.0324	0.0495	0.0393
STD (n)	0.0010 (8)	0.0011 (6)	0.0010 (4)
$a_{\text{prot}}^*$ ( $\text{m}^2 \text{g}^{-1}$ )	0.198	0.183 / 0.170	0.226 / 0.234
STD (n)	0.004 (3)	--- (2)	--- (2)
$Y_{x,E}$ ( $\text{g mol}^{-1}$ )	0.085	0.138 / 0.148	0.265 / 0.257
STD (n)	0.003 (3)	--- (2)	--- (2)
$\phi_p$ (-) PFD:			
	1210 – 1230 →	→	0.254 / 0.256
	610 – 630 →	→	0.415 / 0.419
	56 – 59 →	→	0.649 / 0.643
[chl-a] ( $\text{mg g}^{-1}$ )	25.2	26.2 / 24.2	33.8 / 36.5
STD (n)	0.4 (3)	--- (2)	--- (2)

Furthermore, the algae were always cultivated under a constant PFD during the light period. In practice a light gradient will exist in the photic zone of a photobioreactor. This is the reason *D. tertiolecta* was also cultivated under a light gradient during the light period. This was done at one light regime again, the 10/5 s L/D cycle at 1200  $\mu\text{mol m}^{-2} \text{s}^{-1}$  and 25 °C. For this, the *Dunaliella* reactor was operated as a turbidostat at high biomass density. The PFD passing through the reactor was controlled at 57  $\mu\text{mol m}^{-2} \text{s}^{-1}$ , resulting in a biomass density, protein concentration, of 417  $\text{mg L}^{-1}$  ( $\text{OD}_{680} = 2.42$ ). Because standing biomass concentration was



higher than during the other experiments nitrogen and phosphorus in the medium were increased to 1 and 16 mM, respectively. The results are shown in the third column of Table 4.3. Because the PFD during the 10 s light period was not constant due to the light gradient, the photochemical quantum yield ( $\phi_p$ ) was measured at three different PFDs (Table 4.3).

## Discussion

The efficiency of light utilization of *Chlamydomonas reinhardtii* and *Dunaliella tertiolecta* under medium-duration light/dark cycles was determined in comparison to the efficiency at continuous illumination. Light/dark cycles of 15 s were applied: a 10/5 s light/dark (L/D) cycle, corresponding to  $\varepsilon = 0.67$ , and a 5/10 s L/D cycle, corresponding to  $\varepsilon = 0.33$ , were used. Figure 4.4 shows that the specific growth rates of *C. reinhardtii* and *D. tertiolecta* increased with the light fraction as was found in previous studies (Janssen, et al., 1999; Janssen, et al., 2000b). The diagonal lines in Figure 4.4 represent this proportionality. At light fractions of 0.67 and higher, the average specific growth rate of both *C. reinhardtii* and *D. tertiolecta* are above the proportionality line. At light fractions of 0.5 and lower the average specific growth rates of *C. reinhardtii* are below the line. The specific growth seems to depend on the light fraction in a non-linear way.

Photoinhibition at high photon flux densities (PFDs) should result in lower specific growth rates in comparison to lower PFDs. In Figure 4.4a it is shown that the average specific growth of *C. reinhardtii* at continuous illumination of  $1153 \mu\text{mol m}^{-2} \text{s}^{-1}$  is approximately the same as at  $627 \mu\text{mol m}^{-2} \text{s}^{-1}$ . *D. tertiolecta* was more sensitive to photo inhibition as the specific growth rate at  $1215 \mu\text{mol m}^{-2} \text{s}^{-1}$  was slightly lower than at  $660 \mu\text{mol m}^{-2} \text{s}^{-1}$  (Figure 4.4b). In Figure 4.3b it could already be seen that *D. tertiolecta* needs a long time to acclimate to  $1215 \mu\text{mol m}^{-2} \text{s}^{-1}$  but eventually specific growth is almost as fast as at  $660 \mu\text{mol m}^{-2} \text{s}^{-1}$ .

Energy for algal growth originates from light captured by the antennae of the photosystems. Acclimation to a different light regime will lead to a change in photosystem number or antenna size resulting in a change in specific light absorption (Falkowski, et al., 1981; Neale and Melis, 1986). In this study we determined the spectrally averaged absorption coefficient in terms of protein ( $a_{\text{prot}}^*$ ). In the case of *C. reinhardtii*,  $a_{\text{prot}}^*$  increased from  $0.163 \text{ m}^2 \text{ g}^{-1}$  under continuous illumination ( $1100 - 1200 \mu\text{mol m}^{-2} \text{s}^{-1}$ ) to  $0.187 \text{ m}^2 \text{ g}^{-1}$  under the 10/5 s L/D cycle, and even further to  $0.233 \text{ m}^2 \text{ g}^{-1}$  under the 5/10 cycle (Table 4.1). *D. tertiolecta* showed an increase of  $0.156 \text{ m}^2 \text{ g}^{-1}$  under continuous illumination ( $600 - 700 \mu\text{mol m}^{-2} \text{s}^{-1}$ ) to  $0.227$

$\text{m}^2 \text{g}^{-1}$  under the 5/10 cycle. Also at 1100 - 1200  $\mu\text{mol m}^{-2} \text{s}^{-1}$ ,  $a^*_{\text{prot}}$  of *D. tertiolecta* increased from 0.198  $\text{m}^2 \text{g}^{-1}$  under the 10/5 s L/D cycle to 0.242  $\text{m}^2 \text{g}^{-1}$  under the 5/10 cycle (Table 4.2).

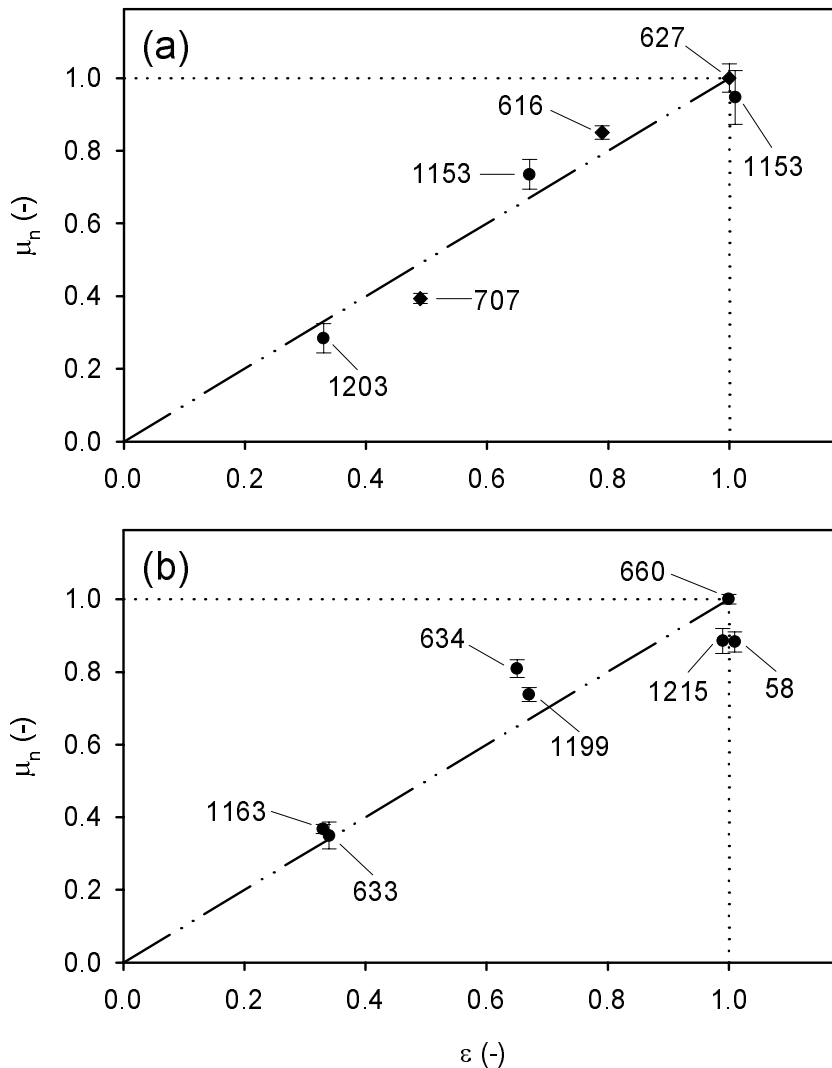


Figure 4.4. Normalized specific growth rate ( $\mu_n$ ) of *Chlamydomonas reinhardtii* (a): •, results this study, ♦, results previous study (Janssen, et al., 2000b). And the normalized specific growth rate ( $\mu_n$ ) of *Dunaliella tertiolecta* (b). The cycle time of the light/dark cycles was 15 s, the numbers give the PFD during the light period in  $\mu\text{mol m}^{-2} \text{s}^{-1}$  and error bars represent 95 % confidence intervals.

The photosystem antennae consist of several hundred chlorophyll molecules, predominantly chlorophyll-*a*. The chlorophyll-*a* content ( $[\text{chl-}a]$ ) of *D. tertiolecta* was measured and expressed in terms of protein. The chlorophyll-*a* content was positively correlated to  $a^*_{\text{prot}}$ ;  $[\text{chl-}a]$  was highest under the 5/10 s L/D cycles when also  $a^*_{\text{prot}}$  was highest too (Table 4.2). This correlation is not linear, which can be deduced from the spectrally averaged absorption

coefficient on chlorophyll-*a* basis ( $a_{\text{chl-a}}^*$ , Table 4.2). If  $a_{\text{prot}}^*$  and  $[\text{chl-a}]$  were linearly correlated  $a_{\text{chl-a}}^*$  should be a constant. However,  $a_{\text{chl-a}}^*$  decreases as  $[\text{chl-a}]$  increases. This can be explained by the fact that at high chlorophyll-*a* concentrations a considerable amount of chlorophyll molecules are in the shade of others (Duysens, 1956). To conclude, the changes in  $[\text{chl-a}]$  and  $a_{\text{prot}}^*$  show that acclimation occurs when *D. tertiolecta* and *C. reinhardtii* are subjected to different light/dark cycles in comparison to continuous light.

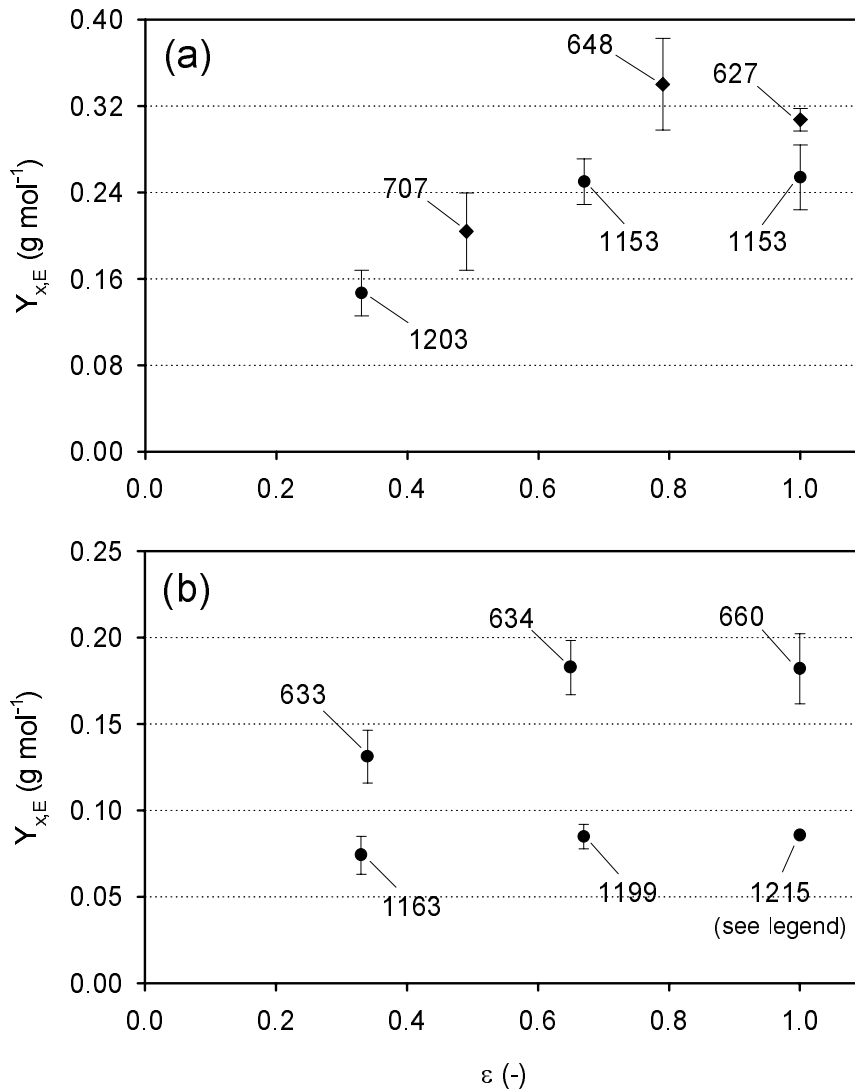


Figure 4.5. Biomass yield on light energy ( $Y_{x,E}$ ) of *Chlamydomonas reinhardtii* (a) on protein basis: •, results this study, ♦, results previous study (Janssen, et al., 2000b). And biomass yield on light energy ( $Y_{x,E}$ ) of *Dunaliella tertiolecta* (b). The cycle time of the light/dark cycles was 15 s, the numbers give the PFD during the light period in  $\mu\text{mol m}^{-2} \text{s}^{-1}$  and error bars represent 95 % confidence intervals.  $Y_{x,E}$  at 1215  $\mu\text{mol m}^{-2} \text{s}^{-1}$  and  $\epsilon = 1$  was estimated using the  $a_{\text{prot}}^*$  of 0.156  $\text{m}^2 \text{g}^{-1}$  determined at 660  $\mu\text{mol m}^{-2} \text{s}^{-1}$  and  $\epsilon = 1$  (Table 4.2).

For development of photobioreactors one of the most important factors is the yield of biomass on light energy ( $Y_{x,E}$ ). If light is limiting bioreactor productivity it is of crucial importance to use light energy as efficiently as possible. The biomass yield is expressed in terms of protein because the protein fraction is the most constant factor in the cell (Post, et al., 1985 and 1986). The protein fraction consists predominantly of bioactive and structural molecules and protein does not serve as a major energy storage compound. On the other hand, cellular concentrations of carbohydrates, lipids and chlorophyll can vary strongly during the day and under different light regimes and this will also affect dry weight measurements.

At 1100 - 1200  $\mu\text{mol m}^{-2} \text{s}^{-1}$  the biomass yield of *C. reinhardtii* under continuous light is equal to the yield under a 10/5 s L/D cycle. However, under a 5/10 cycle,  $Y_{x,E}$  is significantly lower (Figure 4.5a). In a previous study we found a similar trend for *C. reinhardtii* cultivated under 600 - 700  $\mu\text{mol m}^{-2} \text{s}^{-1}$  (Janssen, et al., 2000b). In order to allow easy comparison, these data are also presented in Figure 4.5a. The biomass yields of *D. tertiolecta* under 600 - 700  $\mu\text{mol m}^{-2} \text{s}^{-1}$  were higher than the yields determined under 1100 - 1200  $\mu\text{mol m}^{-2} \text{s}^{-1}$  (Figure 4.5b). Also for *Dunaliella*  $Y_{x,E}$  is lower at the 5/10 s L/D cycle than at the 10/5 cycle. Furthermore, it can be seen that *D. tertiolecta* utilizes intermittent light with a 10/5 s L/D cycle as efficiently as continuous light. Because the specific absorption coefficient was not determined under continuous light of 1215  $\mu\text{mol m}^{-2} \text{s}^{-1}$  the biomass yield was estimated using the  $a_{\text{prot}}^*$  of 0.156  $\text{m}^2 \text{g}^{-1}$  determined under continuous light of 660  $\mu\text{mol m}^{-2} \text{s}^{-1}$  (Table 4.2).

Provided the liquid circulation time is 15 s we could extrapolate our results to large-scale (air-lift loop) photobioreactors. If the efficiency of light utilization is not affected by a 5 s dark period within a 15 s cycle this means that a dark zone of at least 33% v/v is allowed in photobioreactors. This relative dark-zone volume can be used to set a limit to biomass density or column diameter.

In addition to the biomass yield we were able to measure the photochemical quantum yield ( $\phi_p$ ) under several of the light regimes applied. In the case of light/dark cycles, the parameter  $\phi_p$  was measured within the light period. The quantum yield is equal to the probability a photon absorbed by PSII is used for charge separation in the PSII reaction center and concomitant electron transport. The quantum yield of *C. reinhardtii* is significantly lower under the 5/10 s L/D cycle than under the 10/5 cycle and continuous light (Figure 4.6a). Under the 10/5 s L/D cycle, on the other hand, the quantum yield is not significantly different from that under continuous light. If Figure 4.5a and Figure 4.6a are compared it can be seen

that  $\phi_p$  shows a similar trend as  $Y_{x,E}$ . Neale and Melis (1986) showed that the cellular number of PSII units and cytochrome f did not change in *C. reinhardtii* during photoacclimation, only the PSII antenna size changed. The low yield in the process of charge separation and electron transport ( $\phi_p$ ) therefore could have resulted in the low biomass yield on light energy ( $Y_{x,E}$ ) under the 5/10 s L/D cycle.

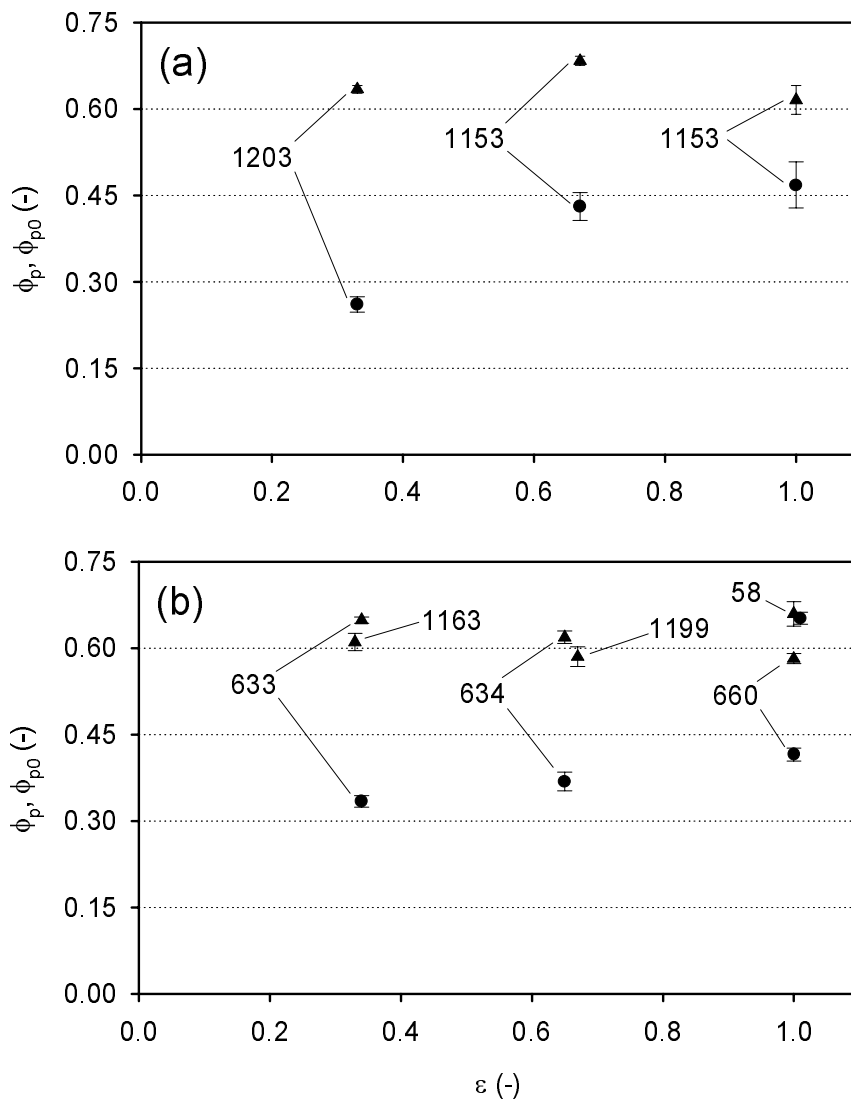


Figure 4.6. Photochemical quantum yields ( $\phi_p$ , ● and  $\phi_{po}$ , ▲) of *Chlamydomonas reinhardtii* (a) and *Dunaliella tertiolecta* (b);  $\phi_p$  is the quantum yield determined during the light period of the simulated cultivation light regime and  $\phi_{po}$  is the photochemical quantum yield of open PSII reaction centers. The cycle time of the light/dark cycles was 15 s, the numbers give the PFD during the light period in  $\mu\text{mol m}^{-2} \text{s}^{-1}$  and error bars represent 95 % confidence intervals.

Also the photochemical quantum yield of *D. tertiolecta* was lowest under the 5/10 s L/D cycle at 600 - 700  $\mu\text{mol m}^{-2} \text{s}^{-1}$  (Figure 4.6b). The difference with the quantum yield under the 10/5 cycle and continuous light, however, is rather small. In other studies it was shown that *D. tertiolecta* increases the cellular number of photosystems during photoacclimation to low light (Falkowski and Owens, 1980; Falkowski, et al., 1981). In addition, we determined that the average spectral light absorption coefficient and the chlorophyll-*a* content were highest under the 5/10 cycle (Table 4.2). Provided the high specific absorption coefficient reflects a high number of photosystems per cell or cellular protein it could be deduced that the absolute electron flow is highest during the light period of the 5/10 cycle. The biomass yield on light energy, however, was lowest under the 5/10 cycle. A considerable part of the electron transport maybe is used for other processes than protein production and could be wasted in over-flow processes like Mehler reactions or photorespiration (Vacha, 1995) or is used for accumulation/excretion of metabolites.

Fluorescence measurements are also a tool to investigate photoinhibition. A decrease of the maximal photochemical quantum yield or the quantum yield of open PSII reaction centers ( $\phi_{\text{po}}$ ) is an indication of photoinhibitory damage (Vonshak, et al., 1994; Torzillo, et al., 1996). At higher PFDs the possibility of photodamage will increase and the introduction of a dark period could give algae time to recover (Merchuk, et al., 1998). Indeed, in Figure 4.6a it can be seen that  $\phi_{\text{po}}$  is lowest when *C. reinhardtii* is exposed to continuous light ( $\varepsilon = 1$ ). The difference with the 10/5 s L/D cycle, however, is rather small and when the dark period increases from 5 to 10 s,  $\phi_{\text{po}}$  decreases again.

Also in the case of *D. tertiolecta*, the maximum quantum yield is lowest under continuous illumination of 660  $\mu\text{mol m}^{-2} \text{s}^{-1}$  and increases if a 5 s dark period is introduced. In contrast to *C. reinhardtii*,  $\phi_{\text{po}}$  increases further if the dark period is increased to 10 s (Figure 4.6b). The maximum quantum yield was found to be lower at higher PFDs of 1100 to 1200  $\mu\text{mol m}^{-2} \text{s}^{-1}$ . The difference between the 10/5 and 5/10 s L/D cycle, however, was not significant in this range. *D. tertiolecta* was also cultivated at a PFD of 58  $\mu\text{mol m}^{-2} \text{s}^{-1}$  yielding the highest  $\phi_{\text{po}}$ . This was expected because photoinhibition will not occur at these low PFDs.

Based on the maximum quantum yields and specific growth rates (Figure 4.6 and Figure 4.4) we think that photoinhibition was not important under our experimental conditions with PFDs of 1200  $\mu\text{mol m}^{-2} \text{s}^{-1}$  or less. In bioreactors, though, algae can be subjected to peak PFDs much higher than 1200  $\mu\text{mol m}^{-2} \text{s}^{-1}$ . Such PFDs could result in considerable inhibition after prolonged exposure. But, if the photic zone is well mixed, exposure time to high PFDs is

short and, as a result, photoinhibition probably will be low. This assumption is based on other studies. It was found that the effect of photoinhibition on biomass productivity was low in well-mixed photobioreactors operated at high biomass densities, i.e. a large dark zone (Hu and Richmond, 1994; Vonshak, et al., 1994; Torzillo, et al., 1996; Grima, et al., 1996; Hu, et al., 1996b).

Although *C. reinhardtii* and *D. tertiolecta* differ, as discussed above, these differences are not reflected in the relation between specific growth rate ( $\mu$ ) and light regime (Figure 4.4) and in the relation between biomass yield ( $Y_{x,E}$ ) and light regime (Figure 4.5). If the capacity of the photosystems and the photosynthetic electron transport chain were limiting algal growth, it would be expected to observe a different relation between biomass yield or specific growth rate and the light regime. This was not observed and it seems that the capacity of the photosystems and electron transport chain is not limiting, but metabolic processes following the light reactions. Sukenik et al. (1987) already found strong evidence that the absolute rate of light-saturated photosynthesis of *D. tertiolecta* is limited in carbon fixation rather than electron transport.

Photosynthetic organisms are most efficient with respect to light utilization at low photon flux densities. For this reason *D. tertiolecta* was cultivated under continuous illumination of low PFD,  $58 \mu\text{mol m}^{-2} \text{s}^{-1}$ ) to have a good estimate of the maximal biomass yield on light energy. The specific growth rate ( $\mu$ ) at  $58 \mu\text{mol m}^{-2} \text{s}^{-1}$  is slightly smaller than at  $660 \mu\text{mol m}^{-2} \text{s}^{-1}$  and the specific spectrally averaged absorption coefficient ( $a_{\text{prot}}^*$ ) is  $0.233 \text{ m}^2 \text{ g}^{-1}$  (Table 4.2). As a result the biomass yield on light energy ( $Y_{x,E}$ ) is high,  $1.20 \pm 0.151 \text{ g mol}^{-1}$ . Also the photochemical quantum yield ( $\phi_p$ ) is highest at  $58 \mu\text{mol m}^{-2} \text{s}^{-1}$  (Figure 4.6b). Much more light energy is wasted under continuous illumination at  $660 \mu\text{mol m}^{-2} \text{s}^{-1}$  than at  $58 \mu\text{mol m}^{-2} \text{s}^{-1}$ . A considerable part of the absorbed light energy is lost as heat in the antennae or is used for processes other than protein production, probably waste-metabolism as there are Mehler reactions and photorespiration (Vacha, 1995) or accumulation/excretion of metabolites.

The difference between the biomass yield on light energy determined at  $58 \mu\text{mol m}^{-2} \text{s}^{-1}$  and PFDs higher than or equal to  $600 \mu\text{mol m}^{-2} \text{s}^{-1}$  is very large. The question rose whether our experimental conditions were close enough to practical systems. In other studies was found that the optimum temperature of *D. tertiolecta* is closer to  $30 \text{ }^\circ\text{C}$  than to  $20 \text{ }^\circ\text{C}$  (Eppley and Sloan, 1966). However, we cultivated *D. tertiolecta* at  $20 \text{ }^\circ\text{C}$  because this was the most common temperature in lab-scale experiments (Eppley and Coatsworth, 1966; Falkowski and

Owens, 1980; Sukenik, et al., 1987) and it is also an economic cultivation temperature in countries with a moderate climate. Probably *D. tertiolecta* is limited in temperature-dependent processes at PFDs equal to or higher than  $600 \mu\text{mol m}^{-2} \text{s}^{-1}$ . Because of this we also cultivated *D. tertiolecta* at  $25 \text{ }^\circ\text{C}$  under a 10/5 s L/D cycle and  $1200 \mu\text{mol m}^{-2} \text{s}^{-1}$ . The results are presented in Table 4.3 together with the results obtained at  $20 \text{ }^\circ\text{C}$ . Specific growth rate was considerably larger at  $25 \text{ }^\circ\text{C}$  in comparison to  $20 \text{ }^\circ\text{C}$ ,  $a_{\text{prot}}^*$  was lower, and [chl-*a*] content did not change. Consequently, going from  $20$  to  $25 \text{ }^\circ\text{C}$ , the biomass yield increased from  $0.085$  to  $0.142 \text{ g mol}^{-1}$  and it is clear that  $20 \text{ }^\circ\text{C}$  is a sub-optimal growth temperature for *D. tertiolecta*. The light regime in the photic zone is different in practical systems in comparison to our experiments. The PFD in the photic zone was assumed to be constant. In reality a light gradient will exist in the downcomer of the air-lift reactor with full (sun)light at the surface and a low PFD at the riser tube wall (Figure 4.1). Because the biomass yield is much higher under low PFDs, the yield under such a light gradient was measured as well; the PFD decreased from  $1184$  at the front surface of the reactor (Figure 4.2b) to  $57 \mu\text{mol m}^{-2} \text{s}^{-1}$  at the back. Again a 10/5 s light/dark cycle was applied at  $25 \text{ }^\circ\text{C}$ .

The specific growth rate is lower under the light gradient in comparison to constant light during the light period, but  $a_{\text{prot}}^*$  and [chl-*a*] are considerably higher (Table 4.3). The average PFD under the light gradient is  $370 \mu\text{mol m}^{-2} \text{s}^{-1}$  and apparently this decrease in PFD induced an acclimation to collect more light energy. The  $Y_{\text{x,E}}$  is much higher under the light gradient;  $0.261 \text{ g mol}^{-1}$  in comparison to  $0.142 \text{ g mol}^{-1}$  without light gradient. A similar increase with a factor 2.1 was observed when *D. tertiolecta* was cultivated under  $634 \mu\text{mol m}^{-2} \text{s}^{-1}$  instead of  $1199 \mu\text{mol m}^{-2} \text{s}^{-1}$  at a 10/5 cycle without light gradient (Figure 4.5b). The difference between the biomass yield under a light gradient and no light gradient can very well be explained by the difference in the average PFD alone. Also photochemical quantum yields were determined at three different PFDs. As the PFD decreases from  $1230$  to  $56 \mu\text{mol m}^{-2} \text{s}^{-1}$ ,  $\phi_p$  increases from  $0.255$  to  $0.646$  (Table 4.3). Depending on the distance to the illuminated surface the photosynthetic efficiency of *D. tertiolecta* in the turbidostat will differ considerably.

It can be concluded that the biomass yield in outdoor air-lift systems will be considerably lower than the yield obtained under low photon flux densities in the lab. Higher yields could be reached in other reactor types, like well-aerated flat panels or bubble columns, with shorter light path and/or faster circulation patterns (Richmond, 1996; Richmond and Qiang, 1997; Pulz and Scheibenbogen, 1998). Also tubular bioreactors with a turbulent flow could give rise to higher yields (Pulz and Scheibenbogen, 1998). Circulation times between the light-exposed



surface and the dark zone are less than one second in these systems. Other aspects such as oxygen removal, biofilm formation, complexity of design and scalability should be taken into account as well. Performance of air-lift reactors in this respect is very good and therefore knowledge about the relation between medium-duration light/dark cycles and biomass yield will still be valuable.

## **Nomenclature**

PAR	photosynthetic active radiation, 400-700 nm	
PSI	photosystem I	
PSII	photosystem II	
chl- <i>a</i>	chlorophyll- <i>a</i>	
$\varepsilon$	duration light period as a fraction of full cycle duration	[-]
$\mu$	specific growth rate	[h <sup>-1</sup> ]
$\mu_n$	normalized specific growth rate	[-]
$\phi_p$	quantum yield of PSII photochemistry	[-]
$\phi_{po}$	quantum yield of open PSII reaction centers	[-]
[chl- <i>a</i> ]	chl- <i>a</i> content, protein basis	[mg g <sup>-1</sup> ]
$a_{chl-a}^*$	spectrally averaged absorption coefficient, chl- <i>a</i> basis	[m <sup>2</sup> g <sup>-1</sup> ]
$a_{prot}^*$	spectrally averaged absorption coefficient, protein basis	[m <sup>2</sup> g <sup>-1</sup> ]
OD <sub>680</sub>	optical density at 680 nm	[-]
PFD	photon flux density in PAR range	[ $\mu\text{mol m}^{-2} \text{s}^{-1}$ ]
$Y_{x,E}$	biomass yield on light energy, protein per photons	[g mol <sup>-1</sup> ]

## 5. Microalgae cultivation: modeling biomass yield on light energy as a function of light-gradient/dark cycles: 10 - 100 s

### Abstract

The slow development of microalgal biotechnology stems from the failure in the design of large-scale photobioreactors where light energy is efficiently utilized. Due to the light gradient inside the reactor and depending on the mixing properties, algae are subjected to certain light/dark cycles where the light period is characterized by a light gradient. These light-gradient/dark cycles will determine productivity and biomass yield on light energy.

Air-lift reactors can be used for microalgae cultivation and medium-frequency light/dark cycles will be found in these systems. Light/dark cycles are associated with two basic parameters: first, the light fraction, i.e. the ratio between the light period and the cycle time and secondly, the frequency of the cycle. In the present work, light/dark cycles found in air-lift reactors were simulated taking into account the light gradient during the light period. The effect of medium-duration cycle time (10 - 100 s) and the effect of the light fraction (0.1 - 1.0) on the biomass yield on light energy of *Dunaliella tertiolecta* was studied. The biomass yield was mainly affected by the light fraction, whereas cycle time had little influence. Response surface methodology was used and a statistical model, describing the effect of light fraction and cycle time on the biomass yield on light energy, was developed. The use of the model as a reactor design criterion is discussed.

This chapter is a modified version of the manuscript submitted for publication as: Barbosa MJ, Janssen M, Ham N, Tramper J and Wijffels RH. Microalgae cultivation in air-lift reactors: modeling biomass yield and growth rate as a function of light gradient / dark cycles.

## **Introduction**

Algal biotechnology has progressed relatively slowly in spite of its recognized utility as a potential source of high-value compounds for the pharmaceutical and food industry (Apt and Behrens, 1999). A constraining factor is the lack of efficient large-scale cultivation techniques. Several of the microalgae applications demand the use of monocultures and controlled cultivation systems. This requirement has led to increased emphasis on the development of closed photobioreactors. Many engineering problems still need to be worked out in order to develop cost-effective production systems. For this reason it is important to build up general knowledge in this field, with emphasis on the most critical scaling up parameters.

One of the major subjects on which efforts in microalgal biotechnology should be focused is the efficient utilization of high light intensities, with the aim of increasing the biomass yield on light energy. In dense microalgal cultures light intensity decreases with distance from the irradiated surface due to self-shading and light absorption. As a result of this light gradient across the reactor, algae are exposed to mixing-induced light/dark cycles where the light period is characterised by a gradient. For this reason these cycles, which are commonly found in photobioreactors, will be referred to as light-gradient/dark cycles (Figure 5.1). Cells of mass cultures therefore receive light intermittently, which is the most practical mode to dilute strong light and could result in an effective use of light by the culture (Richmond, 2000). Light intermittence is associated with two basic parameters: first, the light fraction, i.e. the ratio between the light period and the cycle time ( $\epsilon$ ), and second, the length of the light/dark cycle ( $t_c$ ).

In photobioreactors, the reactor design, light-path length, cell concentration, extent of culture turbulence and light intensity, will determine the frequency and light fraction of the cycles.

The degree of mixing is known to significantly affect the reactor productivity and the yield of biomass on light energy due to the resultant light/dark cycles (Hu, et al., 1996a; Hu and Richmond, 1996). High frequency fluctuating light ( $t_c \leq 100$  ms) has been reported to lead to higher growth rates and higher photosynthesis rates in comparison to continuous light (Kok, 1953; Matthijs, et al., 1996; Nedbal, et al., 1996). In some of these experiments the light intensity during the light period was chosen equal to the intensity of the continuous light. In other experiments the time-averaged intensity was equal under intermittent and continuous light.

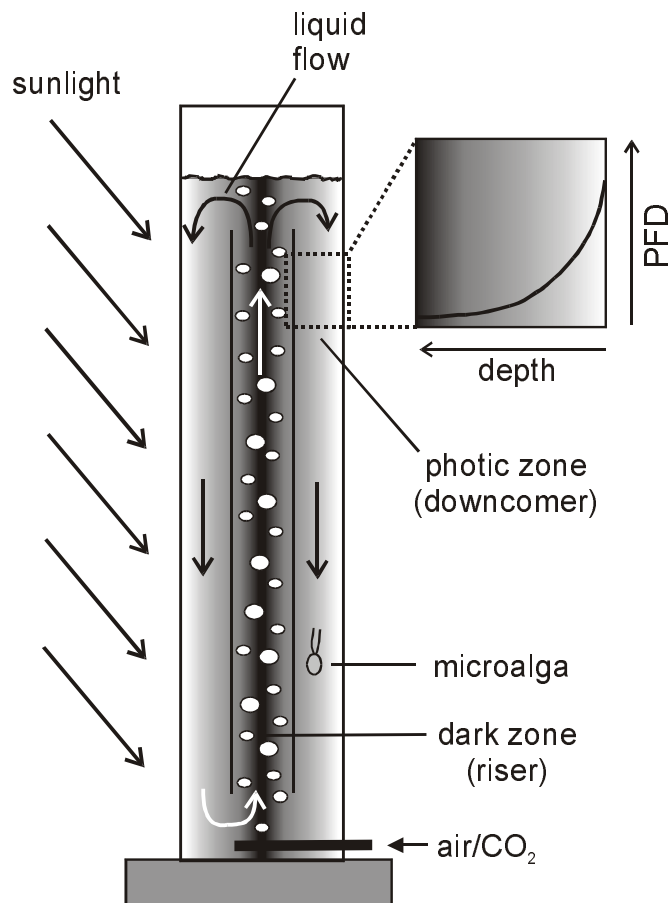


Figure 5.1. Air-lift loop reactor: liquid flow, light regime and resulting light-gradient / dark cycles. PFD is the photon flux density.

However, these short cycles are not found in photobioreactors, where medium-frequency fluctuations prevail. The behavior seems to be different for medium-frequency fluctuations. Light/dark cycles in the range of 6 to 87 s lead to similar or lower growth rates and biomass yields on light energy in comparison to the ones obtained under continuous light of the same light intensity as during the light period of the light/dark cycles (Janssen, et al., 1999, 2000a and 2000b). No influence of light/dark cycles in the range 1-263 s was found on the volumetric productivity, specific oxygen production or carbon dioxide fixation rate (Grobbelaar, 1989 and 1991).

In contradiction to the findings above, Lee and Pirt (1981) and Merchuk et al. (1998) observed maximal growth rates under light/dark cycles with a dark period of 9 and 6 s, respectively. Bosca et al. (1991) reported a higher carbon dioxide fixation under 4 s light/dark fluctuations in comparison to continuous light. The effect of medium-frequency light/dark cycles is thus to be clarified further. Moreover, most of the earlier studies mentioned above have the drawback of being done with diluted cultures in order to avoid a light gradient. As a

result (high) light periods were followed by periods of total darkness. However, the reality in photobioreactors with dense cultures is different. The cells move randomly with the flow from light-saturated to light-limited zones. The light intensity never cycles sharply from total darkness to homogeneous light; instead, there is a continuous change in the light intensity from high to light-limited levels as illustrated in Figure 5.1.

Janssen et al. (2000a) showed that a light gradient during the light period strongly influences the biomass yield on light energy. As a consequence the light/dark cycle data obtained in the past can not be used to accurately estimate the performance of photobioreactors. Clarifying and modeling the effect of medium-duration light-gradient/dark cycles on microalgal productivity still needs to be done as it is an important design tool for photobioreactors.

Air-lift reactors can be used for microalgae cultivation. A concentric draught-tube internal loop air-lift reactor could be designed in such a way that the riser comprises the dark zone and the downcomer the photic zone (Figure 5.1). Consequently the time algae spend in the dark and photic zone is determined by liquid circulation time (10 - 100 s), which depends on the superficial gas velocity and reactor design (Chisti, 1989).

In the present work the effect of cycle time (10 - 100 s) and light fraction (0.1 – 1.0) on biomass yield on light energy was studied. The biomass yield was mainly affected by the light fraction. Cycle time had a small influence on the yield. A statistical model describing the effect of light fraction and cycle time is proposed. An empirical model was preferred to a theoretical model because it allows the study of a wide range of light-gradient/dark cycles and it is an established method to study main effects and two-factor interactions with relatively few experimental trials (Hwang and Hansen, 1996; El-Helow, et al., 2000). The development of a theoretical model would require extensive knowledge on the metabolic response to different light-gradient/dark cycles, which is not available yet. The use of the model as a reactor design criterion is discussed.

## **Materials and Methods**

### ***Experimental design***

The 11 different runs (Table 5.1) were done according to a central composite design (Haaland, 1989). The observations obtained in the experiments were fitted to the following model:

$$\text{Eq. 5.1} \quad Y = b_0 + b_1 \cdot X_1 + b_2 \cdot X_2 + b_{11} \cdot X_1^2 + b_{22} \cdot X_2^2 + b_{12} \cdot X_1 \cdot X_2$$

Where Y is the dependent variable, the biomass yield on light energy ( $Y_{x,E}$ );  $X_1$  and  $X_2$  are the independent variables, cycle time ( $t_c$ ) and light fraction ( $\epsilon$ );  $b_0$  is the regression coefficient at the center point;  $b_1$  and  $b_2$  are linear coefficients;  $b_{11}$  and  $b_{22}$  are quadratic coefficients;  $b_{12}$  is a second-order interaction coefficient.

Table 5.1 Experimental design

$t_c$ (s)	$\epsilon$ (-)
23.1	0.231
23.1	0.869
86.9	0.231
86.9	0.869
10.0	0.550
100.0	0.550
55.0	0.100
55.0	1.000
55.0	0.550
55.0	0.550
55.0	0.550

### ***Strain and culture medium***

*Dunaliella tertiolecta* CCAP 19/6B was obtained from the Culture Collection of Algae and Protozoa (Oban, UK). *D. tertiolecta* was cultivated in artificial seawater medium (ASW) composed of (quantities in  $g L^{-1}$ ): NaCl, 24.5;  $MgCl_2 \cdot 6H_2O$ , 9.8;  $CaCl_2 \cdot 2H_2O$ , 0.53;  $Na_2SO_4$ , 3.2;  $K_2SO_4$ , 0.85. The following nutrients were added (quantities in  $mmol L^{-1}$ ):  $KNO_3$ , 16.0;  $NaH_2PO_4 \cdot 2H_2O$ , 1.0;  $NaHCO_3$ , 5.0. Also the following trace elements were added (quantities in  $\mu mol L^{-1}$ ):  $Na_2EDTA \cdot 2H_2O$ , 61.6;  $FeCl_3 \cdot 6H_2O$ , 23.3;  $CuSO_4 \cdot 7H_2O$ , 0.210;  $ZnSO_4 \cdot 7H_2O$ , 0.303;  $CoCl_2 \cdot 6H_2O$ , 0.085;  $MnCl_2 \cdot 4H_2O$ , 1.83;  $Na_2MoO_4$ , 0.052.

*D. tertiolecta* was maintained as pure suspended culture in 250 mL-Erlenmeyer flasks containing 50 mL of medium. The cultures were kept at 20 °C, under a light intensity of 50 - 70  $\mu mol m^{-2} s^{-1}$  and a 16/8 h day/night cycle. Every three weeks 0.5 mL of a culture was transferred to a new flask containing fresh medium. The reactor was inoculated directly with the 3 weeks old culture of one flask.

### **Cultivation system**

A turbidostat-type reactor was used for cultivation of *D. tertiolecta* for 2 weeks under each light regime. The reactor is shown in Figure 5.2, the suspension volume was about 100 mL and the light path was 3 cm. The turbidostat was equipped with a water jacket connected to a temperature-controlled water bath operated at the cultivation temperature, 30 °C. The pH was maintained between 7.70 - 7.85 by adding pulses of carbon dioxide to the air or nitrogen flow. During the 16 h day period the culture was bubbled with nitrogen and during the 8 h night period air was used, both at a flow rate of 2.3 L h<sup>-1</sup>.

Light was provided by a slide projector equipped with a halogen lamp (150 W) and connected to a timer to apply a 16/8 h day/night cycle. A shutter placed between the reactor and the light simulated the light/dark cycles by cutting off the projector light beam. The biomass concentration in the turbidostat was maintained constant by continuously measuring the outgoing photon flux density (PFD<sub>out</sub>) with a 2π PAR sensor (IMAG-DLO, The Netherlands), see Figure 5.2. A CR 10 datalogger (Campbell Scientific, UK) was programmed to control the VSR25 shutters (Uniblitz, NY, USA) and to measure and register PFD<sub>out</sub> and dilute the reactors whenever PFD<sub>out</sub> was below the set point (PFD<sub>set</sub>). The continuous dilution in the turbidostat was stopped during the 8 h night period.

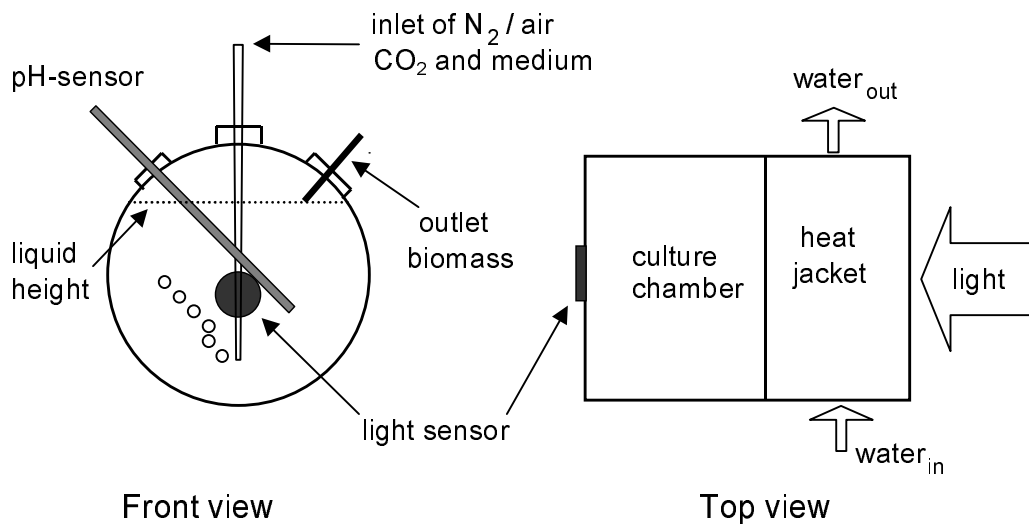


Figure 5.2. Reactor set-up: front and top view.

### ***Photon flux density (PFD)***

The photon flux density was always measured as PAR, photosynthetic active radiation (400 - 700 nm).

***PFD<sub>in</sub>*** The in-going PFD was measured with a LI-190SA 2π PAR-sensor, (LI-COR, Lincoln, NE, USA) behind a dummy reactor filled with water simulating the heat jacket of the reactor. The PFD was measured on 7 different spots of the illuminated area. The average of these values will be referred to as PFD<sub>in</sub>.

***PFD<sub>0</sub>*** Before inoculation, the outgoing PFD was continuously measured for 2 hours with a 2π PAR sensor as is shown in Figure 5.2. In this situation the reactor was filled with medium only. The average PFD during this time will be referred to as PFD<sub>0</sub>.

***PFD<sub>out</sub>*** During the experiments, the outgoing PFD was continuously measured with the PAR sensor as is shown in Figure 5.2. In this situation the reactor was filled with medium and also algae. The PFD<sub>out</sub> was set in order to keep the transmittance constant for all the experiments. The transmittance (T) was kept at 4.2 %.

The set point (PFD<sub>set</sub>) for each experiment was calculated according to Eq. 5.2.

$$\text{Eq. 5.2} \quad PFD_{set} = \frac{T}{100} \cdot PFD_0 \quad [\mu\text{mol m}^{-2} \text{s}^{-1}]$$

### ***Photoacclimation***

In order to avoid photoinhibition and to assure the same initial culture conditions for all the experiments the cultures were initially grown under the same conditions before imposing the experimental light-gradient/dark cycles. During this period (one week) the light intensity was gradually increased as follows:

- 1) Low light intensity (PFD<sub>in</sub> = 200 - 400 μmol m<sup>-2</sup> s<sup>-1</sup>) and continuous light
- 2) High light intensity (PFD<sub>in</sub> = 900 - 1200 μmol m<sup>-2</sup> s<sup>-1</sup>) and continuous light
- 3) High light Intensity (PFD<sub>in</sub> = 900 - 1200 μmol m<sup>-2</sup> s<sup>-1</sup>) and experimental light/dark cycles

The specific growth rate of the algal cultures at the end of phase 2 was almost equal in all experiments. The average, ± 95 % confidence interval, was 0.056 ± 0.004 h<sup>-1</sup>. It can be concluded the experiments started under the same initial conditions, i.e. ‘physiological state’ of the algae. All measurements were done for 4 consecutive days after this week of acclimation.



### ***Specific growth rate***

As the reactor was operated as a turbidostat the specific growth rate ( $\mu$ ) corresponds to the dilution rate which was followed by daily measurement of the diluted volume. The dilution rate was calculated by dividing the volume collected, with the reactor liquid volume, and with 16 hour, which corresponds to the day period.

### ***Suspension collection***

The suspension collected from the reactor was centrifuged at 5000 *g* and 4 °C for 5 min. The supernatant was centrifuged again. Both pellets were re-suspended in ASW to a final OD<sub>680</sub> of 1.4. This concentrated suspension was used for the determination of the protein concentration in the original suspension.

### ***Protein determination***

The concentrated suspension (5.5 mL, see above) was centrifuged at 5000 *g* and 4 °C for 5 min. The supernatant was centrifuged again. Both pellets were re-suspended in sodium-phosphate buffer (10 ml) containing 1 % w/v sodium dodecyl sulphate (SDS) and sonicated on ice water (Meijer and Wijffels, 1998). The suspensions were centrifuged and samples from each supernatant were stored at -80 °C until analysis. Protein was quantified with bicinchoninic acid (BCA) (Smith, et al., 1985) using a commercially available kit (Pierce).

### ***Light absorption***

The light absorbed ( $E_{abs}$ ) by the culture was calculated as mmol photons per day according to Eq. 5.3:

$$\text{Eq. 5.3} \quad E_{abs} = PFD_{in} \cdot \left(1 - \frac{T}{100}\right) \cdot (\varepsilon \cdot 16 \cdot 3.6) \cdot A \quad [\text{mmol d}^{-1}]$$

The parameter  $T$  is the transmittance, which was set at 4.2 %. The parameter  $A$  is the illuminated area in  $\text{m}^2$ . The factors 3.6 and 16 are needed to convert  $\mu\text{mol s}^{-1}$  into  $\text{mmol d}^{-1}$  including the 16/8 h day/night cycle.

### ***Biomass yield on light energy***

The biomass yield on light energy ( $Y_{x,E}$ ) was calculated as gram protein produced per mol photons absorbed according to Eq. 5.4.

$$\text{Eq. 5.4} \quad Y_{x,E} = \frac{P_x}{E_{abs}} \quad [\text{g mol}^{-1}]$$

The parameter  $P_x$  is the productivity, i.e. the amount of protein produced per day ( $\text{mg d}^{-1}$ ). The daily productivity ( $P_x$ ) was calculated multiplying the volume of culture suspension diluted during one day with the protein concentration of that suspension.

## Results and Discussion

The efficiency of light utilization by the microalga *Dunaliella tertiolecta* under medium-duration light-gradient/dark cycles was investigated. During all experiments a light gradient was maintained in the light period, going from 1066 - 1331  $\mu\text{mol m}^{-2} \text{s}^{-1}$  ( $\text{PFD}_{\text{in}}$ , Table 5.2) to 4.2 % of this range (45 - 56  $\mu\text{mol m}^{-2} \text{s}^{-1}$ ).

Table 5.2. Productivity ( $P_x$ ,  $\text{mg protein d}^{-1}$ ) and light absorption ( $E_{\text{abs}}$ ,  $\text{mmol photons d}^{-1}$ ) inside the turbidostat (Figure 5.2) as a function of light fraction ( $\epsilon$ ) and cycle time ( $t_c$ ) of light-gradient/dark cycles. Also  $\text{PFD}_{\text{in}}$  is presented; the transmittance of the culture was maintained at 4.2 %.  $P_x$  and  $E_{\text{abs}}$  are averages of four independent determinations on consecutive days.

$t_c$ (s)	$\epsilon$ (-)	$\text{PFD}_{\text{in}}$ ( $\mu\text{mol m}^{-2} \text{s}^{-1}$ )	$E_{\text{abs}}$ ( $\text{mmol d}^{-1}$ )	$P_x$ ( $\text{mg d}^{-1}$ )
23.1	0.231	1168	44.2	3.79 <sup>(1)</sup>
23.1	0.869	1331	202	47.1
86.9	0.231	1091	---	0.00 <sup>(2)</sup>
86.9	0.869	1066	174	47.1
10.0	0.550	1154	111	24.3
100.0	0.550	1248	117	17.5
55.0	0.100	1103	---	0.00 <sup>(2)</sup>
55.0	1.000	1247	237	64.7
55.0	0.550	1219	123	19.8
55.0	0.550	1237	129	19.5
55.0	0.550	1172	123	17.6

(1) value based on first two days after acclimation,  $P_x$  dropped and on day 3 production was too low to be measured

(2) algae did not grow under these cycles

In Table 5.2 the turbidostat productivity ( $P_x$ ) and light absorption ( $E_{\text{abs}}$ ) during all the 11 experimental runs are presented. As was expected a correlation was found between  $P_x$  and  $E_{\text{abs}}$ ;  $P_x$  is high when  $E_{\text{abs}}$  is high and vice versa. The exact ratio between  $P_x$  and  $E_{\text{abs}}$  gives the biomass yield on light energy ( $Y_{x,E}$ ) in (m)gram protein per (m)mol photons (Eq. 5.4). For all

the 11 experiments of the design, the biomass yield is presented in Figure 5.3 as a function of the light fraction,  $\epsilon$ , and the cycle time,  $t_c$ .

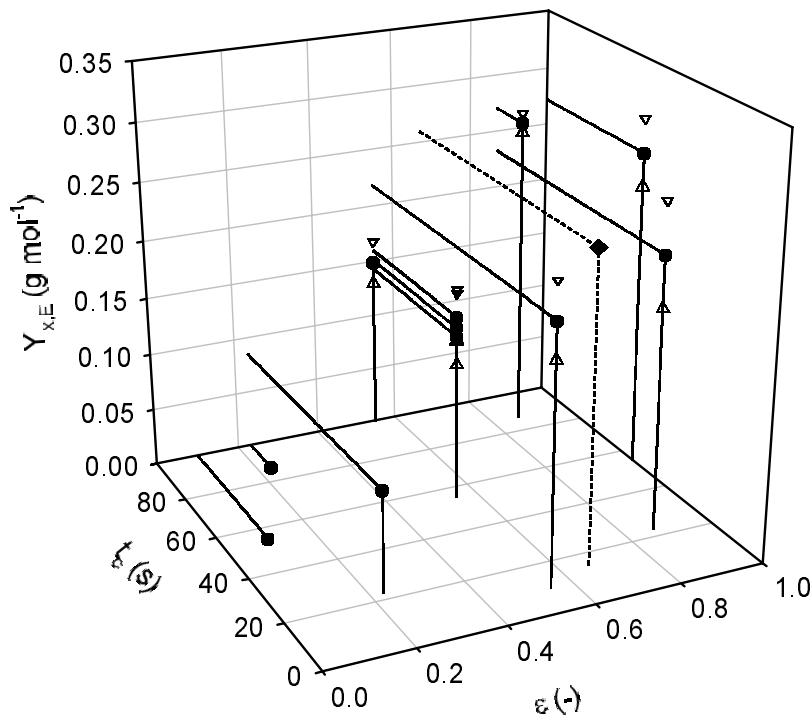


Figure 5.3. Cultivation of *Dunaliella tertiolecta* under light-gradient/dark cycles. Effect of light fraction ( $\epsilon$ ) and cycle time ( $t_c$ ) on the biomass yield on light energy ( $Y_{x,E}$ ) in gram protein per mol photons. Non-filled triangles represent 95 % confidence intervals. One data point ( $\blacklozenge$ , with dashed drop lines) originates from previous work described in Chapter 4 (Janssen, et al., 2000a).

The effect of the two main parameters associated to light-gradient/dark cycles, i.e. light fraction ( $\epsilon$ ) and cycle time ( $t_c$ ), on the biomass yield on light energy ( $Y_{x,E}$ ) can be deduced from Figure 5.3. An increase in the light fraction leads to a significant increase in the biomass yield as was previously reported in Chapters 3 and 4 (Janssen, et al., 2000a and 2000b). Biomass production was found not to be possible at  $\epsilon$  smaller than 0.231. But, under a light fraction of 0.869,  $Y_{x,E}$  was almost as high as under continuous illumination ( $\epsilon = 1$ ). Furthermore, it can be observed that under light fractions smaller than or equal to 0.55, short cycle times resulted in higher biomass yields than longer cycles. At  $\epsilon$  equal to 0.869, on the other hand, longer cycle times seemed to be more beneficial with respect to the biomass yield (Figure 5.3). This was not expected and will be discussed later. All these results show the

importance of well defining each parameter (cycle time and light fraction) to study the effect of medium-duration light-gradient/dark cycles in microalgae cultivation.

The biomass yield on light energy under continuous illumination agrees with previous work, described in Chapter 4, in a 1-L turbidostat with a light path of 3 cm (Janssen, et al., 2000a). In that study a yield of  $0.261 \text{ g mol}^{-1}$  was found in a 15 s light-gradient/dark cycle with  $\epsilon$  equal to 0.67 and the same light gradient in the light period. That value is close to the maximal yield of  $0.272 \text{ g mol}^{-1}$  found under continuous illumination in this study (Figure 5.3). But, it must be noted that a yield of  $0.272 \text{ g mol}^{-1}$  still is significantly lower than the yield of  $1.20 \text{ g mol}^{-1}$  determined under a constant PFD of only  $58 \mu\text{mol m}^{-2} \text{ s}^{-1}$  (Chapter 4). The yield under low photon flux densities is a good measure for the maximal efficiency of light utilization.

In chapter 4 it was also described that *Dunaliella tertiolecta* increased its specific light absorbing surface ( $a^*_{\text{prot}}$ ) under light/dark cycles with decreasing light fraction, i.e. decreasing light supply (Janssen, et al., 2000a). The same was observed again during this study, but these data are not presented.

It was already mentioned that it was not expected that the biomass yield would be higher at longer cycle times. But this was observed at the light fraction of 0.869 (Figure 5.3). At  $t_c$  equal to 86.9 s the yield was higher than at 23.1 s. Moreover,  $Y_{x,E}$  under the 86.9 s cycle was almost equal to the yield determined under continuous light,  $0.271 \text{ g mol}^{-1}$  as opposed to  $0.272 \text{ g mol}^{-1}$ . This result possibly is related to the fact that  $\text{PFD}_{\text{in}}$  was higher under the 23.1 s cycle in comparison to the 86.9 s cycle, 1331 as opposed to  $1066 \mu\text{mol m}^{-2} \text{ s}^{-1}$  (Table 5.2). The ‘additional’ PFD of  $275 \mu\text{mol m}^{-2} \text{ s}^{-1}$  under the 23.1 s cycle possibly cannot be utilized as efficiently as the ‘original’  $\text{PFD}_{\text{in}}$  of  $1066 \mu\text{mol m}^{-2} \text{ s}^{-1}$  applied under the 86.9 s cycle.

A similar effect was found by coincidence. Two experiments out of the 11-experiment design were also done at a  $\text{PFD}_{\text{in}}$  of approximately  $1600 \mu\text{mol m}^{-2} \text{ s}^{-1}$ . Comparing these extra experiments with the corresponding experiments from the experimental design, carried out under  $\text{PFD}_{\text{in}}$  of  $1240 \mu\text{mol m}^{-2} \text{ s}^{-1}$ , shows that the biomass yield drops considerably under higher  $\text{PFD}_{\text{in}}$  (Figure 5.4b). It appears that ‘additional’ PFD added to  $\text{PFD}_{\text{in}}$  cannot be utilized as efficiently as the original photon flux supplied to the microalgae. Moreover, it seems that photoinhibition occurs under  $1600 \mu\text{mol m}^{-2} \text{ s}^{-1}$ . Photoinhibition is characterized by a decrease in the photosynthetic capacity (Melis, 1999). In Figure 5.4a can be seen that the specific growth rate is significantly lower at  $1600 \mu\text{mol m}^{-2} \text{ s}^{-1}$  in comparison to  $1240$

$\mu\text{mol m}^{-2} \text{s}^{-1}$ . The photoinhibition effect is also more pronounced under the 100 s cycle than under the 55 s cycle.

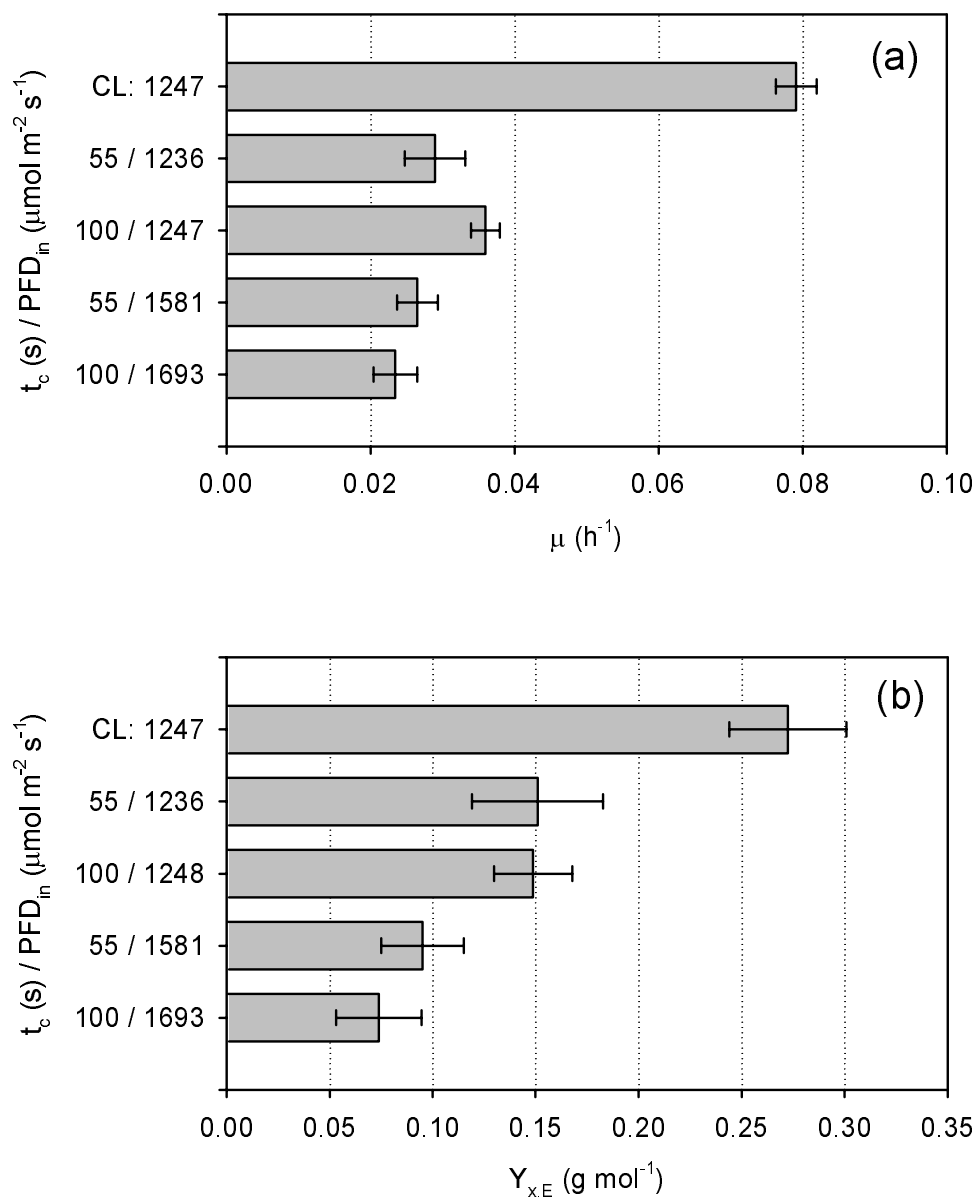


Figure 5.4. Cultivation of *Dunaliella tertiolecta* under light-gradient/dark cycles, effect of  $\text{PDF}_{in}$  on: (a) specific growth rate ( $\mu$ ); (b) biomass yield on light energy ( $Y_{X,E}$ ) in gram protein per mol photons. All 4 light/dark cycle experiments were done at  $\epsilon$  equal to 0.55; CL is continuous light ( $\epsilon = 1$ ). Error bars represent 95 % confidence intervals.

Although photoinhibition was demonstrated this does not mean that light/dark cycling might be better than continuous light as was suggested by Merchuk et al. (1998). It can be safely concluded that, up to in-coming photon flux densities of at least  $1200 \mu\text{mol m}^{-2} \text{s}^{-1}$ , the process of photoinhibition did not lead to more efficient light utilization under medium-

duration light-gradient/dark cycles in comparison to continuous light. On the contrary, it seems more likely that introduction of significant dark zones will lead to a higher vulnerability to light-induced damage. Due to the process of photoacclimation observed in this and previous work, Chapter 4 (Janssen, et al., 2000a), the specific light absorbing surface of the microalgae increases under light(-gradient)/dark cycles. As a result, the algae will intercept even more light in the high light zone possibly leading to more photodamage.

At photon flux densities higher than  $1200 \mu\text{mol m}^{-2} \text{s}^{-1}$  the role of photoinhibition could become more pronounced as can be seen in Figure 5.4. In this situation light-gradient/dark cycling might be more attractive with respect to the efficiency of light utilization than a continuous light-gradient. However, the negative effect of photoinhibition on the biomass yield on light energy can be reduced with an increased rate of cycling between light and dark zones in a photobioreactor. This was demonstrated by others (Vonshak, et al., 1994; Torzillo, et al., 1996; Grima, et al., 1996) and this effect can also be seen in Figure 5.4 comparing the 55 s and 100 s cycles.

To summarize, the effect of medium-duration light/dark cycles on microalgal productivity has been shown to have a strong influence on the biomass yield on light energy. Modeling this dependency would thus be an important design tool for photobioreactors.

### *Statistical model*

Response surface methodology is an empirical modeling technique devoted to the evaluation of the relationship of a set of controlled experimental factors and observed results (Annadurai, 2000). An empirical model was preferred here to a theoretical model because the first one is an established method to study main effects and two factor interactions with relatively few experimental trials (Hwang and Hansen, 1996; El-Helow, et al., 2000). The development of a theoretical model would require extensive knowledge on the metabolic response to different light-gradient/dark cycles, which would severely limit the range and number of combinations of the two variables. A statistical model overcomes this limitation.

This is the first study on the demonstration of the response surface method to optimize biomass yield on light energy as a function of light-gradient/dark cycles in microalgae cultivation. As already discussed, 11 runs were done according to a central composite design (Haaland, 1989). It was pointed out that the two experiments done at  $\varepsilon$  equal to 0.869 could be affected by a considerable difference in  $\text{PFD}_{\text{in}}$ . This is the reason the yield, determined in previous work under a 15 s cycle at  $\varepsilon$  equal to 0.67 (Figure 5.3), was added to the other 11

data points. A second-order polynomial function (Eq. 5.1) was fitted to the experimental results of the biomass yield on light energy,  $Y_{x,E}$ :

$$Y_{x,E} = 0.111 - 4.01 \cdot 10^{-3} \cdot t_c + 0.308 \cdot \varepsilon + 1.64 \cdot 10^{-5} \cdot t_c^2 - 0.124 \cdot \varepsilon^2 + 2.70 \cdot 10^{-3} \cdot t_c \cdot \varepsilon$$

The fit of the model is expressed by the coefficient of determination,  $r^2$ , which was calculated to be 0.978. The closer the  $r^2$  value to 1.00, the stronger the model is and the better it predicts responses. Accordingly, our calculated  $r^2$  value indicates that the model could explain 97.8 % of the variability in the response. The contour for the biomass yield adjusted to the model are shown in Figure 5.5.

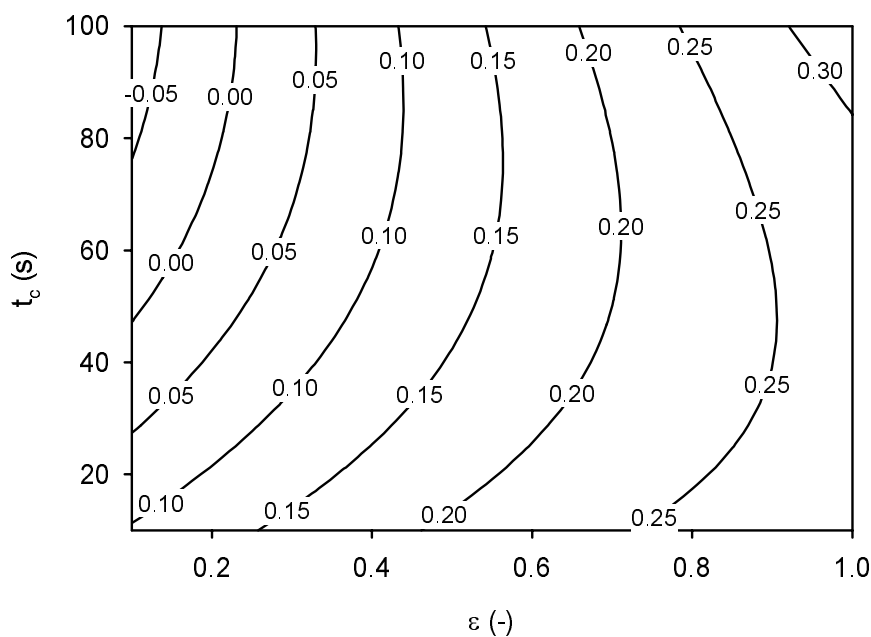


Figure 5.5. Cultivation of *Dunaliella tertiolecta* under light-gradient/dark cycles. Contour plots illustrating the effect of light fraction ( $\varepsilon$ ) and cycle time ( $t_c$ ) on the biomass yield on light energy ( $Y_{x,E}$ ) in gram protein per mol photons.

According to the results obtained from the model, an increase of light fraction, for a constant cycle time, always leads to an increase of the biomass yield. The rate of increase slows down significantly at higher  $\varepsilon$  (Figure 5.5). The influence of the cycle duration on the biomass yield is less pronounced and depends on the light fraction. In general it can be said that shorter cycle duration leads to higher efficiencies, i.e. biomass yields on light energy. Only at high light fraction ( $\varepsilon \geq 0.8$ ) the efficiency is highest at short, but also at long cycle times. However, as discussed, this effect may be due to experimental variability of which the variation in  $PFD_{in}$  probably is the most important.

The statistical model developed in this study can be used as a tool for photobioreactor design. Air-lift reactors could be used for microalgae cultivation. A concentric draught-tube internal loop air-lift reactor can be designed in such a way that the riser comprises the dark zone ( $\text{PFD} \leq 50 \mu\text{mol m}^{-2} \text{s}^{-1}$ ) and the downcomer equals the photic zone (Figure 5.1). Consequently, the time algae spend in the dark and photic zone is dependent on reactor design and the liquid circulation velocity. The liquid circulation velocity on its turn depends on the superficial gas velocity and also reactor design.

The superficial liquid velocity in the riser, cycle time ( $t_c$ ) and the light fraction ( $\epsilon$ ) can be calculated for each specific reactor design using relations as described by Chisti (1989). Knowing the parameters  $t_c$  and  $\epsilon$ , the biomass yield on light energy ( $Y_{x,E}$ ) can be estimated using the statistical model. This can be done only under the assumption that  $\text{PFD}_{\text{in}}$  is approximately equal to  $1200 \mu\text{mol m}^{-2} \text{s}^{-1}$ . The effect of parameters such as reactor height, superficial gas velocity and downcomer to riser cross-sectional area on photobioreactor productivity can be evaluated.

It can be concluded already that air-lift reactors are inefficient for microalgae cultivation due to presence of medium-duration light/dark cycles (10 – 100 s) associated with these reactors. The existence of such a dark period will always lead to a decrease of biomass yield on light energy in comparison to continuous light. Only at high light fractions ( $\epsilon \geq 0.67$ ) biomass yield will be comparable to the yield under a continuous light gradient. At this point it should be noted again that the biomass yield under a light gradient ( $1200 \rightarrow 50 \mu\text{mol m}^{-2} \text{s}^{-1}$ ) without a dark period ( $\epsilon = 1$ ) is lower than the yield obtained under low PFDs:  $0.27 \text{ g mol}^{-1}$  (Figure 5.3) as opposed to  $1.20 \text{ g mol}^{-1}$  (Chapter 4). The yield under low photon flux densities is a good measure for the maximal efficiency of light utilization, which should be the target for photobioreactor design.

## Nomenclature

PAR	photosynthetic active radiation, 400-700 nm	
$\epsilon$	duration light period as a fraction of full cycle duration	[-]
$\mu$	specific growth rate	[h <sup>-1</sup> ]
A	illuminated area turbidostat	[m <sup>2</sup> ]
$a_{\text{prot}}^*$	spectrally averaged absorption coefficient, protein basis	[m <sup>2</sup> g <sup>-1</sup> ]
$E_{\text{abs}}$	light absorbed in turbidostat	[mmol d <sup>-1</sup> ]



PFD	photon flux density in PAR range	$[\mu\text{mol m}^{-2} \text{s}^{-1}]$
PFD <sub>in</sub>	PFD on light-exposed surface turbidostat (Figure 5.2)	$[\mu\text{mol m}^{-2} \text{s}^{-1}]$
P <sub>x</sub>	productivity of turbidostat, protein basis	$[\text{mg d}^{-1}]$
T	transmittance turbidostat culture	$[\%]$
t <sub>c</sub>	duration light-gradient/dark cycle	$[\text{s}]$
Y <sub>x,E</sub>	biomass yield on light energy, protein per photons	$[\text{g mol}^{-1}]$

## 6. Efficiency of light utilization of *Dunaliella tertiolecta* under short light/dark cycles: 0.19 - 6 s

### Abstract

Inside photobioreactors algae are exposed to light/dark fluctuations. In this study the marine green alga *Dunaliella tertiolecta* was cultivated under short light/dark cycles of 3/3 s, 94/94 ms and 31/156 ms as found in medium and short light-path reactors. The photon flux density (PFD) during the light period was 440 - 455  $\mu\text{mol m}^{-2} \text{s}^{-1}$  and, under the 31/156 ms cycle only, 1025  $\mu\text{mol m}^{-2} \text{s}^{-1}$ . Artificial illumination was used: 'red' light emitting diodes (LEDs) with a peak wavelength at 666 nm. The photosynthetic efficiency was determined and expressed as the biomass yield on light energy in gram protein produced per mol of photons absorbed. The yield under the 94/94 ms cycle was higher than the yield under continuous light of 440 - 455  $\mu\text{mol m}^{-2} \text{s}^{-1}$ . Apparently a light integration effect occurs under the 94/94 ms cycle together with an increase of the photosynthetic efficiency. On the contrary, at the 3/3 s cycle the efficiency decreased. Also under the 31/156 ms cycle, with 1025  $\mu\text{mol m}^{-2} \text{s}^{-1}$  in the light period, the yield was lower than under continuous light. The results obtained under the 31/156 ms light/dark cycle are discussed with respect to the performance of short light-path flat panel photobioreactors operated at high biomass densities.

This chapter has been published as: Janssen M, Slenders P, Tramper J, Mur LR and Wijffels RH. Photosynthetic efficiency of *Dunaliella tertiolecta* under short light/dark cycles. *Enzyme and Microbial Technology*, Vol. 29, p. 298-305, 2001.

## Introduction

Large-scale cultivation of algal monocultures is still limited to a small number of species cultivated in open raceway ponds. The constraining factor is that many species need controlled and aseptic conditions and therefore need to be cultivated in closed photobioreactors. Several types of closed photobioreactors have been developed and studied but either the productivity is low or scale-up is problematic. Because light energy is the limiting substrate in such systems it is important to focus on the photosynthetic efficiency or the biomass yield on light energy. The light regime inside photobioreactors is complicated: algae are exposed to high-intensity sunlight in the so-called photic zone close to the reactor surface and complete darkness in the interior. As a result, algae are exposed to certain light/dark cycles, which could have a considerable effect on the photosynthetic efficiency.

Short light/dark cycles of several seconds to tenths of a second are found in well-mixed medium light-path (40 - 300 mm) or short light-path (< 40 mm) reactors like bubble columns, tubular reactors or flat panels. It has already been demonstrated that short cycles can have a strong influence on photosynthetic activity and specific growth rate (Terry, 1986; Nedbal, et al., 1996; Merchuk, et al., 1998). The term light integration is often used in this respect. In continuous light the specific growth rate or oxygen production rate can be written as a saturating function of the photon flux density (PFD):  $\mu = f(\text{PFD})$ . The initial rate is nearly proportional to PFD and approaches a horizontal asymptote at higher PFDs defined as the maximum rate. On the other hand, under light/dark cycles algae are exposed to a certain PFD during the light period and no photon flux at all in the dark zone. The fraction of time the cells are illuminated during a cycle ( $\epsilon$ ) can be used to predict the growth rate: with full integration of light:  $\mu = f(\epsilon \cdot \text{PFD})$ , and with no integration of light:  $\mu = \epsilon \cdot f(\text{PFD})$ . Since the growth rate or oxygen production rate is a saturating function of PFD it is clear that under saturating PFDs:  $f(\epsilon \cdot \text{PFD}) \geq \epsilon \cdot f(\text{PFD})$ . In other words, due to light integration the rate will decrease less than proportional to a decrease of the light fraction ( $\epsilon$ ).

In several studies light integration under short light/dark cycles was demonstrated during oxygen production measurements with the green alga *Chlorella* and the diatom *Phaeodactylum* (Kok, 1953; Phillips and Myers, 1954; Terry, 1986). Also in more recent studies light integration was observed for other green algae and cyanobacteria with respect to

specific oxygen production and specific growth rate (Matthijs, et al., 1996; Grobbelaar, et al., 1996; Nedbal, et al., 1996).

The occurrence of light integration can be explained with the fact light energy can be utilized more efficiently by the photosynthetic apparatus if it is delivered in small pulses, separated in time, in comparison to a constant flux. This could lead to the partial re-oxidation of the plastoquinone pool in the photosynthetic membrane during dark periods giving rise to an increased capacity to convert light energy into chemical energy during the light pulse (Nedbal, et al., 1996). In addition, changes in the oxidation/reduction state could influence the antenna size of the photosynthetic apparatus (Escoubas, et al., 1995). In that situation specific light absorption could increase and the efficiency increase due to light/dark cycling could be lower. Because of this, also specific light absorption should be considered when evaluating the effect of light/dark fluctuations. Nevertheless, intense mixing of algal cultures, leading to short light/dark cycles, could lead to higher photosynthetic efficiencies.

Strong evidence for this mixing-induced increase of the photosynthetic efficiency is provided by the studies done in short light-path (1.3 - 2.6 cm) flat panel reactors (Hu and Richmond, 1996; Hu, et al., 1996a). In these studies photosynthetic efficiencies of 15% were found for the cyanobacterium *Spirulina platensis*. The photosynthetic efficiency was based on the energy content of the biomass produced and photons absorbed. The PFD at the reactor surface was  $1800 \mu\text{mol m}^{-2} \text{s}^{-1}$  which resembles intense sunlight. Probably the PFD can be increased further to  $2500 \mu\text{mol m}^{-2} \text{s}^{-1}$  without affecting the efficiency (Hu, et al., 1998c). For comparison, the highest photosynthetic efficiencies reported in other studies range from 10% to 18% and a theoretical limit was calculated at 29% (Pulz and Scheibenbogen, 1998). These laboratory studies were carried out under light-limiting conditions and, usually, at a low PFD yielding the highest efficiency (Pirt, et al., 1980). On the other hand, the PFD on the flat panel surface was very high, but the light/dark cycles were very short ( $< 200 \text{ ms}$ ) (Hu and Richmond, 1996; Hu, et al., 1996a). Therefore it was suggested that light energy was integrated in time and very efficiently directed to growth.

The photosynthetic efficiency in these pilot-scale systems could be determined easily (Hu and Richmond, 1996; Hu, et al., 1996a). The actual light/dark cycles inside the reactor, however, could not be clearly determined or calculated by the authors. On the other hand, in lab-scale experiments the light/dark cycle could be controlled very well but the specific rate of light absorption was never determined. Although light integration was demonstrated, it was not possible to draw conclusions concerning the photosynthetic efficiency without accurate knowledge of specific light absorption (Terry, 1986; Nedbal, et al., 1996). In addition, in most

studies algae were not allowed to acclimate (> 3 generation times) to the light/dark cycles studied (Kok, 1953; Phillips and Myers, 1954; Terry, 1986; Grobbelaar, et al., 1996).

In the present study the photosynthetic efficiency was directly measured as the biomass yield on light energy. This is done in lab-scale reactors after acclimation to precisely defined light/dark cycles of several seconds to tenths of a second. The green alga *Dunaliella tertiolecta* was cultivated under light/dark (L/D) cycles of 3/3 s, 94/94 ms and 31/156 ms. For comparison the alga was also cultivated under continuous light of low and high light intensity. It was demonstrated that under the 94/94 ms cycle a light integration effect takes place and that photosynthetic efficiency increases in comparison to continuous illumination. This confirms the expectations from other studies that light integration can take place in short light-path reactors together with an increase of the photosynthetic efficiency. Under the 3/3 s and the 31/156 ms L/D cycles the efficiency was lower in comparison to continuous illumination. The results obtained under the 31/156 ms L/D cycle are discussed with respect to the performance of short light-path flat panel photobioreactors operated at high biomass densities.

## Materials and Methods

### *Organism and medium*

*Dunaliella tertiolecta* CCAP 19/6B was obtained from the Culture Collection of Algae and Protozoa (Oban, UK). *D. tertiolecta* was cultivated in artificial seawater medium as described previously (Janssen, et al., 2000a). *Dunaliella* was maintained as pure suspended culture in 100 mL erlenmeyer flasks containing 50 mL of medium. The cultures were not stirred and placed at 20 °C, at a photon flux density (PFD) of 50 - 70  $\mu\text{mol m}^{-2} \text{s}^{-1}$  under a 16/8 h day/night cycle. Every three weeks 0.5 mL of a culture was transferred to a new flask containing fresh medium. The reactor was inoculated directly with the culture of one flask.

### *Reactor set-up*

*Dunaliella* was cultivated in a flat bioreactor placed in an aquarium filled with water as described previously (Janssen, et al., 2000a). The water was maintained at the cultivation temperature, 30 °C. The reactor had a 1000 mL liquid volume and a 3 cm light path. The liquid was mixed by air bubbled at a rate of 21.5 L h<sup>-1</sup>. The pH was maintained between 7.85

and 8.05 by pulsed addition of carbon dioxide to the air flow. As a result, also the carbon-dioxide concentration was maintained constant.

The front side of the reactor as a whole was illuminated with a panel (width x height = 20 x 30 cm) of 1452 light emitting diodes (LEDs) which was placed outside the aquarium. During cultivation always a 16/8 hours day/night cycle was applied comparable to day/night cycles in outdoor photobioreactors. In addition, the lamps could be alternately turned on and off to create short light/dark cycles with variable cycle length (188 ms and 6 s) and light fractions (0.5 and 0.167) during the day, see below. The algal cultures in the bioreactors were maintained for one week under a certain light regime and were diluted daily.

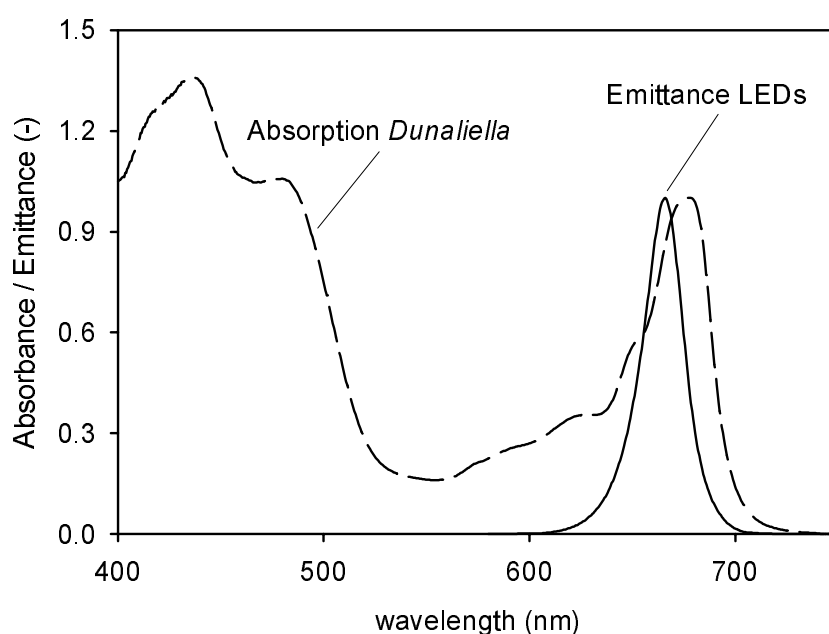


Figure 6.1. Characteristic absorption spectrum of *Dunaliella tertiolecta* and emission spectrum (in  $\mu\text{mol } \mu\text{mol}^{-1}$ ) of the Kingbright L-53SRC-F light emitting diode (LED). The absorption spectrum is normalized to the absorption at 680 nm. The emission spectrum is normalized to the peak irradiance at 666 nm.

The LED type used was a Kingbright L-53SRC-F (Kingbright, UK) and the emission spectrum is shown in Figure 6.1 together with a characteristic absorption spectrum of *Dunaliella*. The PFD inside the reactor was measured before starting and after ending each one-week experiment and if necessary the panels were moved closer to the reactors in order to maintain a constant PFD. The LEDs were connected in series of 22 LEDs. The voltage applied per LED was 1.8 V and the lamps could be turned on or off via a TIP 141 Darlington transistor connected to a pulse generator via an opto-coupler. The pulse generator used was a

Campbell CR10 datalogger (Campbell, UK) which could be programmed to deliver 5V pulses in intervals of 1/32 s (31.25 ms) or a multiple of this.

### ***Specific growth rate***

After 3 or 4 days of acclimation time, the specific growth rate ( $\mu$ ) was followed daily by measuring the dilution. The reactors were emptied completely, always at the middle of the 16 hours day period. A known volume of suspension ( $V_s$ ) was diluted with a known volume of medium ( $V_m$ ). The optical density of the undiluted algal suspension ( $OD_{start}$ ) was measured and the diluted algal suspension was put into a clean reactor. Exponential growth continued for 24 hours and after this the OD was measured again ( $OD_{end}$ ). The specific growth rate could be calculated according to Eq. 6.1.

$$\text{Eq. 6.1} \quad \mu = \frac{\ln \left\{ OD_{end} / \left[ \frac{OD_{start} * V_s}{V_s + V_m} \right] \right\}}{24} \quad [\text{h}^{-1}]$$

In order to minimize mutual shading of algal cells, biomass concentrations at the end of a 24 hours growth cycle were maintained at a low level ( $< 30 \text{ mg protein L}^{-1}$ ). The accuracy of the optical density (OD) determination, however, decreases with biomass concentration and therefore the OD was measured at 680 nm corresponding to the chlorophyll-*a* absorption maximum. It is known the cellular chlorophyll-*a* content will change during day/night cycles and it will also depend on the cultivation light regime. But, these factors did not interfere because the OD was always measured on the same moment within the day/night cycle and it was only used to calculate the growth rate using the ratio  $OD_{end} : OD_{start}$ .

At each light regime the growth rate was measured on 3, 4 or 5 days after a 3 or 4 days acclimation period. These separate determinations were used to calculate the 95%-confidence interval using a t-test.

### ***Photon flux density***

The photon flux density (PFD) was measured in the PAR-range (Photosynthetic Active Radiation, 400-700 nm). We used a  $2\text{-}\pi$  PAR-sensor, LI-190SA (LI-COR, NE, USA), which could be placed directly in the empty reactor. The PFD inside the reactor was measured before starting and after ending each one-week experiment. This was done on positions spread across the reactor surface and the corresponding values were averaged as described in a previous study (Janssen, et al., 2000a).

### ***Spectrally averaged absorption coefficient***

After the daily dilution of a reactor the remaining algal suspension was collected and used to determine the spectrally averaged absorption coefficient. The method is described more extensively in previous studies (Janssen, et al., 2000a and 2000b). Biomass was concentrated and the absorbance of the suspensions was measured in a spectrophotometer equipped with an integrating sphere. Forward-scattered light was collected with this set-up. Absorbance was measured from 400 to 700 nm. Average absorbance between 740 and 750 nm was measured too and subtracted from the absorbance between 400 and 700 nm because the pigments do not absorb in this range and the absorbance must be caused by residual scattering (Duysens, 1956). Afterwards, the protein content of the suspensions was determined.

From the absorbance scans the spectrally averaged specific absorption coefficient, light-absorbing surface per amount of protein ( $a_{\text{prot}}^*$ ), was calculated according to Dubinsky et al. (1986). The relative spectral distribution of the light emitting diodes (Figure 6.1) was needed for these calculations and was measured from 400 to 700 nm with a spectroradiometer (SR 9910, Macam, UK). Similar to optical density measurements the average absorption between 740 and 750 nm ( $SCA_{750}$ ) was caused by scattering and could be used as a measure of cell number. Therefore the spectrally averaged absorption coefficient was expressed on this value too and was designated as  $a_{750}^*$  in  $\text{m}^{-1} SCA_{750}^{-1}$ .

### ***Protein concentration***

Protein concentration in the samples used for the measurement of the spectrally averaged absorption coefficient was determined immediately after the absorbance measurement. Each sample was diluted to a protein concentration of 50 - 100  $\text{mg L}^{-1}$  using fresh medium and 1 mL samples were stored at  $-80\text{ }^{\circ}\text{C}$ . After thawing the cells were broken and at the same time protein was precipitated with 0.1 ml 20 % w/v trichloroacetic acid. The suspensions were centrifuged (9100 RCF, 10 min,  $4\text{ }^{\circ}\text{C}$ ) and the pellets were re-suspended in 1 N sodium hydroxide. Following, the samples were heated for 5 min at  $70\text{ }^{\circ}\text{C}$  to dissolve the protein. After this pretreatment protein was determined following the Bradford method (Bradford, 1976) using a commercially available kit (Coomassie Protein Assay Reagent, Pierce, USA). Bovine serum albumine (fraction V, crystallized, A-4378, Sigma) was used as a standard.

### ***Biomass yield on light energy***

The biomass yield on light energy ( $Y_{x,E}$ ) was determined on protein basis: gram protein produced per mol of photons absorbed. The yield was calculated by dividing the specific



growth rate by the specific light absorption rate according to Eq. 6.2. In this equation  $\varepsilon$  is the fraction of time the algae are illuminated within a light/dark cycle. The PFD is the average value measured inside the empty reactor and was assumed to be constant. This assumption was allowed because we used bioreactors with a small light path and the culture was maintained at low density ( $< 30 \text{ mg protein L}^{-1}$ ).

$$\text{Eq. 6.2} \quad Y_{x,E} = \frac{\mu \cdot 24}{\varepsilon \cdot \text{PFD} \cdot a_{\text{prot}}^* \cdot 3.6 \cdot 10^{-3} \cdot 16} \quad [\text{g mol}^{-1}]$$

The factors 24, 16 and  $3.6 \cdot 10^{-3}$  in Eq. 6.2 are needed to convert  $\mu\text{mol s}^{-1}$  into  $\text{mol d}^{-1}$  including the 16/8 h day/night cycle.

## Results and Discussion

### *Specific growth rate*

The specific growth rate of *Dunaliella tertiolecta* was determined under 5 different light regimes as is shown in Figure 6.2. In Figure 6.2 the photon flux density (PFD) is given on the x-axis as the time-averaged photon flux density ( $\text{PFD}_{\text{av}}$ ) in  $\text{mol m}^{-2} \text{d}^{-1}$ . Under the light/dark regimes applied, the actual PFD during the light period was higher and usually this PFD is given in the paragraphs below in  $\mu\text{mol m}^{-2} \text{s}^{-1}$ . In Figure 6.2 it can be seen that the specific growth rate was highest under continuous illumination of  $24.9 \text{ mol m}^{-2} \text{d}^{-1}$  ( $433 \mu\text{mol m}^{-2} \text{s}^{-1}$ ) and was equal to  $0.077 \pm 0.0016 \text{ h}^{-1}$ . At a lower  $\text{PFD}_{\text{av}}$  of  $4.62 \text{ mol m}^{-2} \text{d}^{-1}$  ( $80 \mu\text{mol m}^{-2} \text{s}^{-1}$ ) the specific growth rate was lower,  $0.054 \pm 0.0019 \text{ h}^{-1}$ . At a PFD of zero the specific growth rate also will be zero and therefore it is clear that the relationship between specific growth rate and PFD is not linear. The growth rate is best described as a saturating function of the photon flux density.

The time-averaged photon flux density ( $\text{PFD}_{\text{av}}$ ) will also decrease after introduction of light/dark cycles, while the PFD in the light period remains equal, as will occur in photobioreactors. Under the 3/3 s light/dark (L/D) cycle,  $\text{PFD}_{\text{av}}$  was  $12.9 \text{ mol m}^{-2} \text{d}^{-1}$  and the PFD during the light period was  $448 \mu\text{mol m}^{-2} \text{s}^{-1}$ . The specific growth rate under this cycle was considerably lower than the rate under continuous illumination of  $433 \mu\text{mol m}^{-2} \text{s}^{-1}$ . On the other hand, under the 94/94 ms L/D cycle the specific growth was considerably higher again than under the 3/3 s L/D cycle,  $0.060 \pm 0.0008 \text{ h}^{-1}$  as opposed to  $0.042 \pm 0.0015 \text{ h}^{-1}$  (Figure 6.2). This result shows that under light/dark cycles of several seconds the specific

growth rate decreases almost proportional to the light fraction at an equal PFD during the light period (dotted line in Figure 6.2). This was already shown for *Dunaliella*, *Chlamydomonas* and *Chlorella* in previous studies (Janssen, et al., 1999, 2000a and 2000b). But, under a 94/94 ms L/D cycle specific growth is considerably faster than under the 3/3 s cycle. This is clear evidence that considerable light integration occurs when the cycle time is sufficiently small.

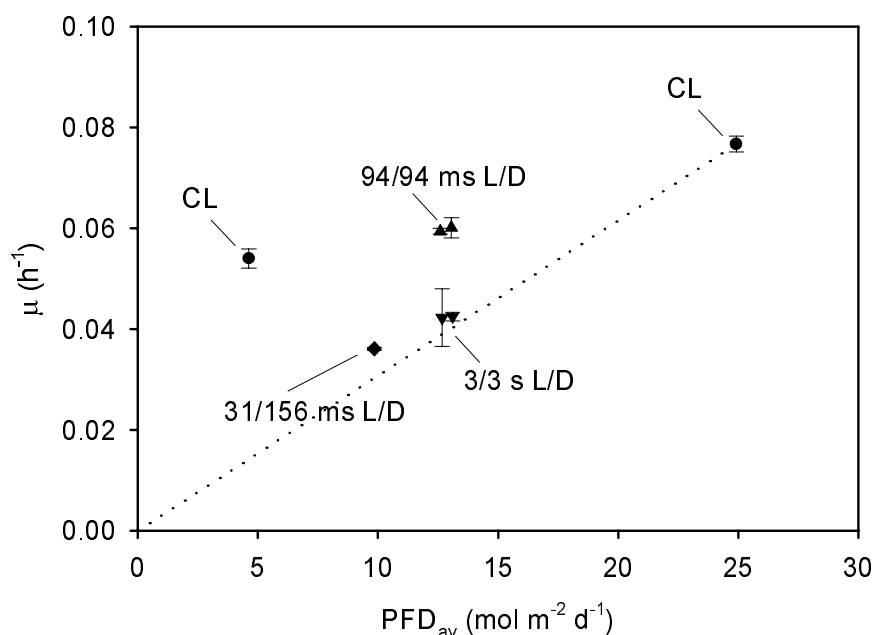


Figure 6.2. Specific growth rate ( $\mu$ ) of *Dunaliella tertiolecta* under continuous illumination (CL), a 3/3 s light/dark (L/D) cycle, a 94/94 ms L/D cycle and under a 31/156 ms L/D cycle as a function of PFD<sub>av</sub>. The error bars give the 95 % confidence interval.

Besides cycle time also the PFD in the light period and the relative size of the light period have a big influence. The specific growth rate was lowest under the 31/156 ms light/dark cycle. The PFD during the light period was increased from 430 - 455 to 1025  $\mu\text{mol m}^{-2} \text{s}^{-1}$  to approach the situation in photobioreactors with a steep light gradient and a high PFD at the surface. Although the cycle time was only 188 ms the light integration effect almost disappeared (Figure 6.2).

### ***Specific light absorption***

The spectrally averaged absorption coefficient ( $a_{\text{prol}}^*$ ) can be used to calculate specific light absorption and this parameter is presented in Figure 6.3. The light absorbing surface per amount of protein is lowest under continuous illumination of the highest intensity,  $0.46 \pm$

$0.017 \text{ m}^2 \text{ g}^{-1}$ . On the other hand, under low intensity continuous light  $a_{\text{prot}}^*$  is significantly higher,  $0.72 \pm 0.016 \text{ m}^2 \text{ g}^{-1}$ . The values for  $a_{\text{prot}}^*$  under the 3/3 s and 94/94 ms L/D cycles are in between these two values. More specifically, the specific light absorbing surface of *Dunaliella* is lower after acclimation to the 188 ms cycle than after acclimation to the 6 s cycle.

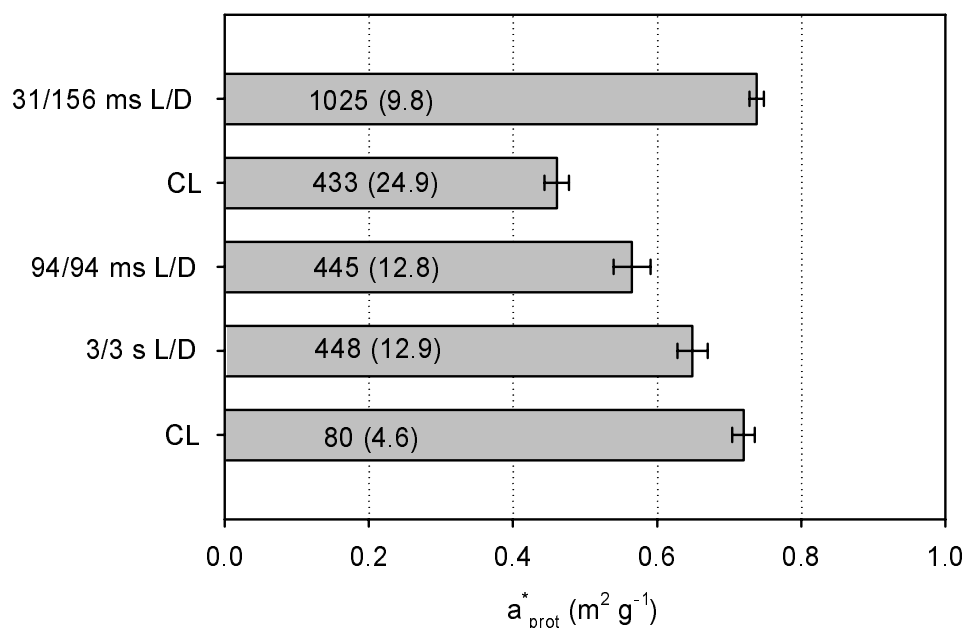


Figure 6.3. Spectrally averaged absorption coefficient ( $a_{\text{prot}}^*$ ) in square meter per gram protein as a function of light regime: L/D = light/dark cycle and CL = continuous light. The numbers within the bars give the PFD in  $\mu\text{mol m}^{-2} \text{ s}^{-1}$  in the light period and, in between brackets,  $\text{PFD}_{\text{av}}$  in  $\text{mol m}^{-2} \text{ d}^{-1}$ . The error bars give the 95 % confidence interval.

From the results presented in Figure 6.3 it appears that the spectrally averaged absorption coefficient is higher at lower time-averaged PFDs. This was expected because in situations of decreasing light availability algae generally respond by increasing their light absorbing surface (Falkowski and LaRoche, 1991). The parameter  $\text{PFD}_{\text{av}}$ , however, is not the only factor determining specific absorption. At equal  $\text{PFD}_{\text{av}}$ ,  $12.9 \text{ mol m}^{-2} \text{ d}^{-1}$ , the specific surface was higher under the 3/3 s than under the 94/94 ms L/D cycle. Moreover, the specific surface was highest under the 31/156 ms L/D cycle although  $\text{PFD}_{\text{av}}$  is still considerable,  $9.8 \text{ mol m}^{-2} \text{ d}^{-1}$  (Figure 6.3). Apparently, also longer light/dark cycles or longer dark fractions within a cycle lead to an increase in the content of antenna pigments. The signal inducing the cellular production of antenna pigments is suggested to be the reduction state of the plastoquinone pool located in the photosynthetic membranes (Escoubas, et al., 1995). It seems that the signal

evolving from this redox state or the redox state itself does not only depend on  $\text{PFD}_{\text{av}}$  but also depends on the nature of the light/dark fluctuations.

The protein based wavelength-dependent specific absorption coefficients determined during the measurement of  $a_{\text{prot}}^*$  can be used to calculate the light gradient during a 24 hours growth cycle. In Figure 6.4 this is illustrated for the experiment under continuous light of  $433 \mu\text{mol m}^{-2} \text{s}^{-1}$ . The light gradient across the 3 cm reactor light path is smallest at the start of the 24 hours cycle (0 h in Figure 6.4). Even after 24 hours the gradient is small. The biomass concentration in the reactor after 24 h corresponds to only  $26 \text{ mg protein L}^{-1}$ . Based on these calculations we think it is justified to neglect mutual shading of algal cells in our experiments. Furthermore, the small error introduced applying this simplification is comparable in all experiments.

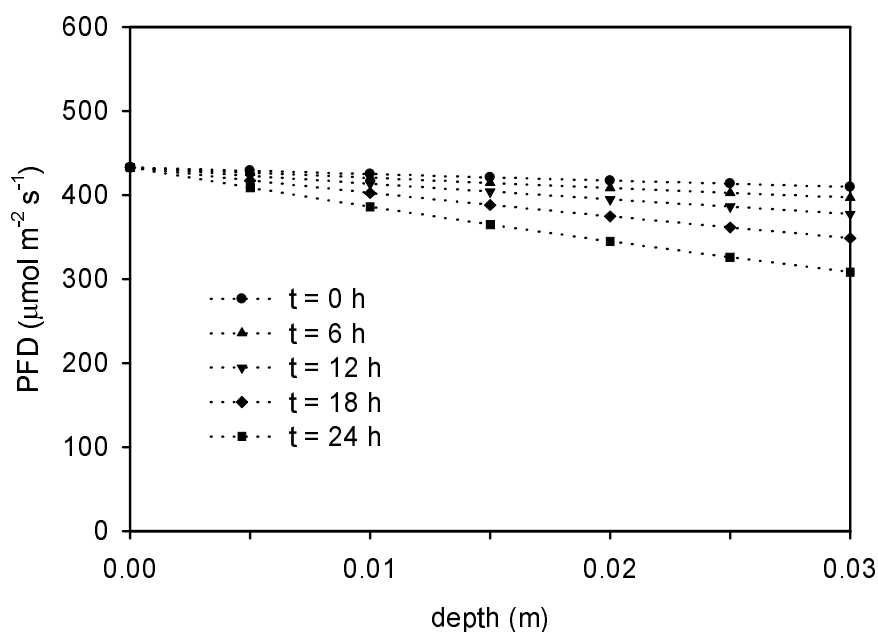


Figure 6.4. PAR as a function of reactor depth and time during a 24 hours growth cycle under continuous illumination of  $433 \mu\text{mol m}^{-2} \text{s}^{-1}$ . The PAR was calculated using Beer's Law, the in-coming PAR measured as PAR, the protein based wavelength-dependent specific absorption coefficients and the spectral distribution of the LED light source.

The spectrally averaged absorption coefficient ( $a_{\text{prot}}^*$ ) was expressed per amount of protein. Protein was chosen because the cellular protein fraction represents predominantly structural and bioactive molecules. Besides protein also cell number could be chosen as a basis for the specific light absorption. Light scattering by algal suspensions could be used as a measure of cell number. During the absorbance measurements the average absorbance between 740 and

750 nm,  $SCA_{750}$ , was determined. This absorbance actually was residual scattering, which was not corrected for by the integrating sphere because the scattering angle was too high. This value was subtracted from the absorbance between 400 and 700 nm to obtain the real absorbance. In addition, we used  $SCA_{750}$  as a measure of cell number and expressed the specific absorption coefficient on basis of  $SCA_{750}$  ( $a_{750}^*$ ).

The results of these calculations are shown in Figure 6.5. Although there are some differences between  $a_{750}^*$  and  $a_{prot}^*$  (Figure 6.3) the trends are the same. The differences probably could be caused by differences in cell size and cell composition under different light regimes resulting in different scattering properties (Stramski and Morel, 1990). As a result the relationship between scattering and protein content may not be linear. For the calculation of the biomass yield we therefore chose for the protein basis.

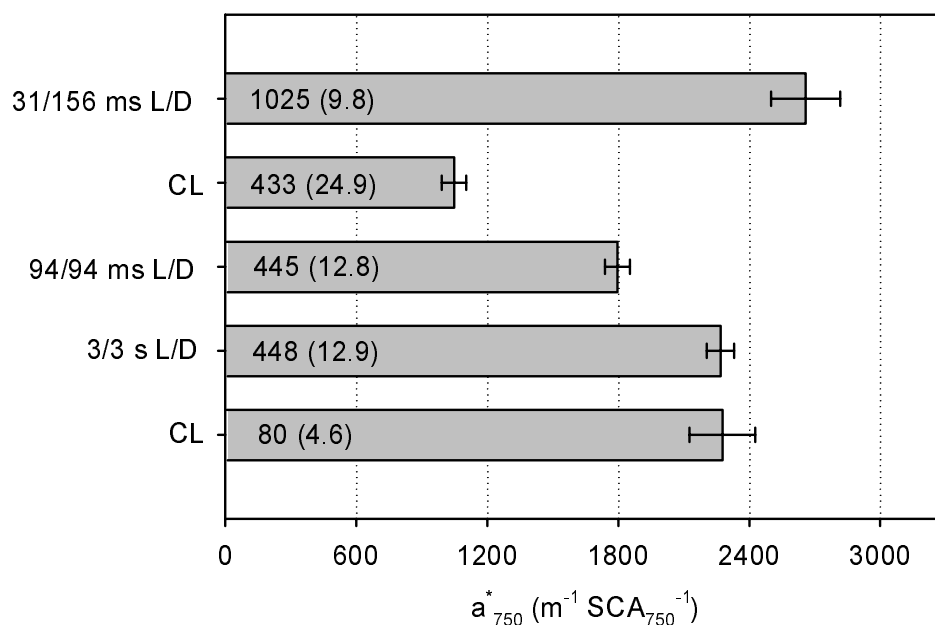


Figure 6.5. Spectrally averaged absorption coefficient ( $a_{750}^*$ ) in square meter per  $SCA_{750}$  unit as a function of light regime, see Figure 6.3.

### ***Biomass yield on light energy***

The biomass yield on light energy,  $Y_{x,E}$  in gram protein per mol of photons absorbed, is shown in Figure 6.6. The yield was calculated according to Eq. 6.2 in which the specific growth rate is divided by the specific rate of light absorption. The specific rate of light absorption was calculated from the average PFD in the empty reactor, the light fraction ( $\epsilon$ ) and the specific spectrally averaged absorption coefficient ( $a_{prot}^*$ ). As expected the yield was

highest under continuous light of the lowest intensity,  $80 \mu\text{mol m}^{-2} \text{s}^{-1}$ . Under these circumstances  $0.389 \pm 0.017 \text{ g}$  of protein is produced per mol of photons absorbed (Figure 6.6). At a PFD of  $433 \mu\text{mol m}^{-2} \text{s}^{-1}$  the yield was much lower,  $0.160 \pm 0.0035 \text{ g mol}^{-1}$ . It can be concluded that under high light intensities the algae are not able to use all the light energy absorbed and a considerable part is lost, probably via heat dissipation and fluorescence.

In the situation *Dunaliella* is exposed to light/dark cycles the yield was highest under the shortest cycle. Although the PFD during illumination is high,  $445 \mu\text{mol m}^{-2} \text{s}^{-1}$ , the alga is able to utilize this photon flux more efficiently than during continuous illumination with the same PFD. At longer L/D cycles (3/3 s L/D), however, the effect is opposite and the biomass yield on light energy is lower than under continuous light. Light/dark cycles in medium light-path reactors will be in the second range and this is apparently not very efficient with respect to light utilization.

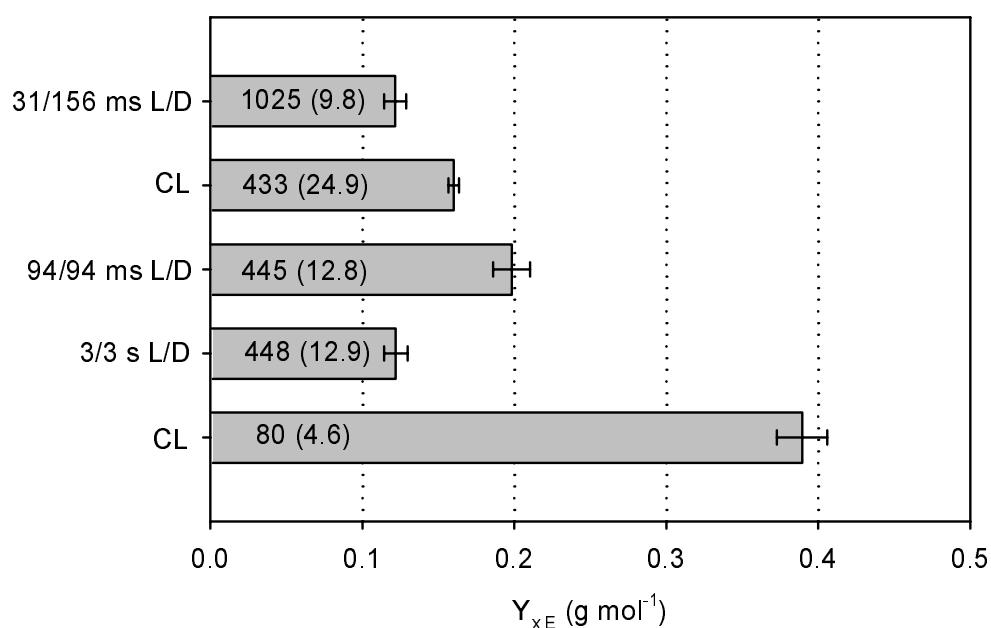


Figure 6.6. Biomass yield on light energy ( $Y_{x,E}$ ) in gram protein per mol photons as a function of light regime, see Figure 6.3.

Apparently, short L/D cycles are beneficial with respect to the photosynthetic efficiency. However, when the light fraction ( $\varepsilon$ ) within a 188 ms cycle was decreased from 0.5 to 0.167 the biomass yield was lowest (Figure 6). Only  $0.122 \pm 0.0072 \text{ gram protein}$  is produced per mol of photons absorbed. But it needs to be considered the PFD during the light period was increased from 430 - 455 to  $1025 \mu\text{mol m}^{-2} \text{s}^{-1}$ . This light regime was chosen because it

resembles the practical situation in photobioreactors with over-saturating PFD in the photic zone and a large dark zone in the interior. It seems that the PFD cannot be increased without affecting the efficiency even at these short cycles. This was not expected because studies done with short light-path flat-panel reactors showed a high photosynthetic efficiency at similar cycle lengths and high PFDs at the reactor surface,  $2500 \mu\text{mol m}^{-2} \text{s}^{-1}$  (Hu and Richmond, 1996; Hu, et al., 1996a). Therefore we return to these studies to characterize the light regime in these reactors more accurately and compare this with the light regime applied in our present study.

The photobioreactor volume can be divided into a photic zone and a dark zone. Gitelson et al. (1996) defined the photic zone as the culture depth at which 90 % of the incoming light was absorbed. The average PFD in the photic zone then is 39 % of the incoming PFD using Beer's law. The maximal light intensity falling on one side of the reactor at maximal photosynthetic efficiency was  $2500 \mu\text{mol m}^{-2} \text{s}^{-1}$  and in that case the average intensity in the photic zone can be calculated at  $975 \mu\text{mol m}^{-2} \text{s}^{-1}$ .

Gitelson et al. (1996) stated the penetration depth for blue and red light is less than 1 mm at  $100 \text{ mg L}^{-1}$  of chlorophyll-*a* for *Spirulina platensis*. At maximal photosynthetic efficiency, the biomass concentration in short light-path reactors is around  $10 \text{ g L}^{-1}$  (Hu and Richmond, 1996; Hu, et al., 1996a, 1996b and 1998b). This corresponds to  $125 \text{ g chl-}a \text{ m}^{-3}$  using a chl-*a* content of 1.25 % (Hu, et al., 1996b). Using Beer's law we can calculate a penetration depth of 0.8 mm for red light. This corresponds to a light fraction ( $\epsilon$ ) of 0.062 or 0.031 for a light path of 1.3 or 2.6 cm, respectively.

The frequency of the light/dark cycles was estimated based on the liquid flow, which was measured as the rate of dispersion of a dye inside the reactor (Hu and Richmond, 1996; Hu, et al., 1996a). The liquid flow was in the range of 20 to 30  $\text{cm s}^{-1}$ . Richmond assumed that the liquid moves with the same velocity alongside the light-path axis (Richmond, 1996). In that situation the length of a cycle would be 87 - 130 ms and 173 - 260 ms in a 1.3 and 2.6 cm light path reactor, respectively. The absolute length of the light and dark periods now can be calculated by multiplying the relative size of the dark or light zone and the estimated cycle length, the results are shown in Table 1.

Table 6.1. Estimated light/dark cycles in short light-path flat-panel photobioreactors (Hu and Richmond, 1996; Hu, et al., 1996a; Hu, et al., 1998b); calculations are explained in the text.

light-path (cm)	cycle duration (ms)	light fraction ( $\epsilon$ ) (%)	light period (L) (ms)	dark period (D) (ms)
1.3	87	6.2	5.4	81.6
1.3	130	6.2	8.0	122.0
2.6	173	3.1	5.3	167.7
2.6	260	3.1	8.0	252.0

The difference between the estimated cycles in the pilot-scale flat panel reactors and the light/dark cycles applied in the present study is obvious. The total cycle length of 188 ms is comparable and also the average PFD in the light period or photic zone is comparable. However, due to the high biomass density, the light fraction and therefore the absolute time in the photic zone in the pilot-scale systems (Table 6.1) is much smaller than the light periods in our experiments. Apparently the absolute time in the photic zone must be very short at high PFDs. A light period of 31 ms is too long, and probably needs to be reduced to less than 10 ms to obtain higher photosynthetic efficiencies.

A minor difference between the different studies is the organism used. In this study we used *Dunaliella tertiolecta*, which is a marine green alga. The pilot-scale experiments in the flat-panel reactors were done with *Spirulina*, a cyanobacterium, and also with *Monodos*, a freshwater green alga, and with *Chlorococcum*, a marine green alga. All these photoautotrophs yielded similar results: high photosynthetic efficiencies in turbulently mixed short light-path reactors operated at high cell densities (Hu and Richmond, 1996; Hu, et al., 1996a and 1998a). The type of organism probably does not have a big influence on the general effect of light/dark cycles and this is not strange because the photosynthetic pathway and the carbon fixation cycle is similar in all oxygenic phototrophic micro-organisms.

## Conclusions

Despite the differences between the lab-scale experiments of the present study and pilot-scale experiments with short light-path reactors, the present results clearly show that under the 94/94 ms cycle light energy is integrated and the photosynthetic efficiency is higher than under continuous light. Maybe the efficiency will be as good or even better at smaller light



fractions and/or higher photon flux densities. But in the latter case the absolute length of the light period must be very short, probably less than 10 ms. A light exposure time of 31 ms at a PFD of  $1025 \mu\text{mol m}^{-2} \text{s}^{-1}$  was proven to be too long in the present study. With respect to photobioreactor design it is clear that very short light/dark cycles ( $< 200$  ms) are a necessity to reach high photosynthetic efficiencies in systems with an over-saturating PFD in the photic zone. In that case it is probably essential to reduce the light exposure time to 10 ms or less. On the other hand, if it is possible to reduce the PFD in the photic zone to levels just below light saturation, together with an increase of the relative size of the photic zone, light/dark cycling could become less important. This can be deduced from the high biomass yield under continuous light of low PFD.

## Nomenclature

PAR	photosynthetic active radiation, 400-700 nm	
$\varepsilon$	duration light period as a fraction of full cycle duration	[-]
$\mu$	specific growth rate	[h <sup>-1</sup> ]
$a_{750}^*$	spectrally averaged absorption coefficient, SCA <sub>750</sub> basis	[m <sup>-1</sup> SCA <sub>750</sub> <sup>-1</sup> ]
$a_{\text{prot}}^*$	spectrally averaged absorption coefficient, protein basis	[m <sup>2</sup> g <sup>-1</sup> ]
OD <sub>680</sub>	optical density at 680 nm	[-]
PFD	photon flux density in PAR-range	[ $\mu\text{mol m}^{-2} \text{s}^{-1}$ ]
PFD <sub>av</sub>	time-averaged PFD	[mol m <sup>-2</sup> d <sup>-1</sup> ]
SCA <sub>750</sub>	scattering at 750 nm measured with integrating sphere	[-]
Y <sub>x,E</sub>	biomass yield on light energy, protein per photons	[g mol <sup>-1</sup> ]

## **7. Enclosed outdoor photobioreactors: light regime, photosynthetic efficiency, scale-up and future prospects**

### **Abstract**

Enclosed outdoor photobioreactors need to be developed and designed for large-scale production of phototrophic microorganisms. The light regime and the photosynthetic efficiency in characteristic examples of state-of-the-art pilot-scale photobioreactors were analyzed. It is shown that productivity of photobioreactors is determined by the light regime inside the bioreactors. In addition to light regime, only oxygen accumulation and shear stress limit productivity in certain designs. In short light-path systems, high efficiencies, 10 to 20 % based on photosynthetic active radiation (PAR: 400 - 700 nm), can be reached at high biomass concentrations ( $> 5 \text{ kg dw m}^{-3}$ ). But is demonstrated that these and other photobioreactor designs are poorly scalable (maximal unit size of 0.1 to  $10 \text{ m}^3$ ) and/or not applicable for cultivation of monocultures. This is the reason new photobioreactor designs are proposed in which light capture is physically separated from photoautotrophic cultivation. These systems possibly can be scaled to larger unit sizes,  $10 \text{ m}^3$  to more than  $100 \text{ m}^3$ , and the reactor liquid as a whole is mixed and aerated. It is deduced that high photosynthetic efficiencies, 10 to 15 % on PAR-basis, can be achieved. Old and new designs from optical engineers should be used to collect, concentrate and transport sunlight followed by re-distribution in an efficient large-scale photobioreactor.

This chapter has been submitted for publication as: Janssen M, Tramper J, Mur LR and Wijffels RH. Enclosed outdoor photobioreactors: light regime, photosynthetic efficiency, scale-up and future prospects.

## **Introduction**

Phototrophic microorganisms such as microalgae and cyanobacteria could provide valuable compounds: as pigments, vitamins or other food supplements (Apt and Behrens, 1999). Microalgae are also considered to be a promising source of new secondary metabolites demonstrating highly selective pharmacological activity (Shimizu, 2000). In addition, photosynthesis provides the only way of producing biomass as an energy source from sunlight and carbon dioxide. Although production of microalgae and cyanobacteria as a biofuel does not seem to be very attractive at the moment, this possibility could become important in the future. Unicellular phototrophic organisms are able to use sunlight much more efficiently than higher plants. Also genetic engineering could provide microalgae or cyanobacteria with smaller pigment complexes. In that case light energy can be utilized much more efficiently (Melis, et al., 1998; Nakajima, et al., 2001).

For many of these applications it is essential to use enclosed photobioreactors in which monocultures can be maintained for an extended time, preferably with sunlight as the energy source. A large variety of enclosed photobioreactors has been developed (Pulz and Scheibenbogen, 1998). In this review three of the most interesting designs have been selected: pneumatically agitated vertical column reactors, tubular reactors and flat panel reactors. The following aspects will be compared: light gradients and mixing-induced light/dark (L/D) cycles; photosynthetic efficiency; scalability. At the end new photobioreactor designs will be proposed and these will be analyzed with respect to the same aspects. But, first the general relationship between light regime and photosynthetic efficiency will be discussed.

## **Photosynthetic efficiency and light regime**

Light supply plays a key role in photobioreactor design. All other nutrients are cheap inorganic salts and can be supplied at a fast rate. In order to intercept sufficient sunlight a high surface to volume ratio is a pre-requisite for photobioreactors. Light energy falling on the light-exposed surface, however, is not always utilized efficiently. Even under low-intensity sunlight most photosynthetic organisms intercept too much light at the light-exposed surface. The excitation energy is only partly utilized in the photosynthetic apparatus and residual energy is lost as heat or fluorescence (Gruszecki, et al., 1994). Even worse, an overdose of excitation energy could damage the photosynthetic apparatus in a process called

photoinhibition (Melis, 1999). Following exposure to light, liquid movements will bring the same organisms also into the interior of the reactor where light availability is low.

Phototrophic micro-organisms cultivated under a certain constant photon flux density (PFD) will exhibit a corresponding specific growth rate. Also the size of the cellular light-absorbing surface, consisting of pigment molecules arranged in antenna complexes, will adapt to this PFD. The specific surface decreases if the PFD increases and this process is called photoacclimation (Falkowski and LaRoche, 1991).

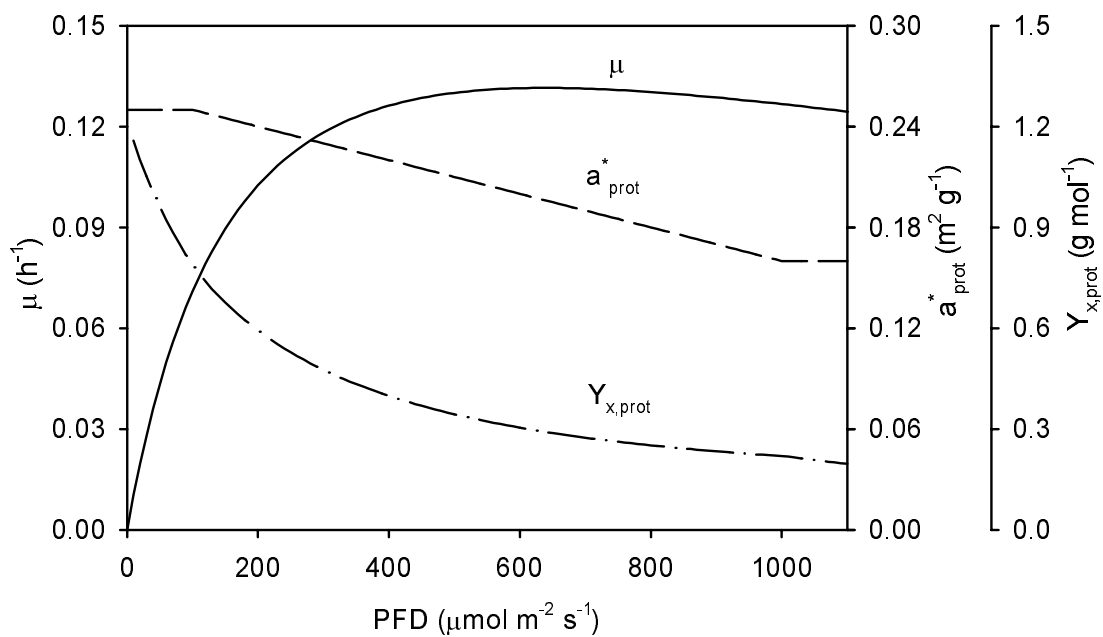


Figure 7.1 Specific growth rate ( $\mu$ ), protein based spectrally averaged absorption coefficient ( $a_{\text{prot}}^*$ ) and protein based biomass yield on light energy ( $Y_{\text{prot}E}$ ) of *Chlamydomonas reinhardtii* as functions of the photon flux density (PFD) (Janssen, et al., 2000a and 2000b). In this simulation no light/dark cycles and day/night cycles were taken into account (Eq. 7.1).

In Figure 7.1 the specific growth rate ( $\mu$ ) of the green alga *Chlamydomonas reinhardtii* is plotted as a function of the PFD (Janssen, et al., 2000b). Also an estimated relationship between the protein based spectrally averaged absorption coefficient ( $a_{\text{prot}}^*$ ) and PFD is shown. It was assumed that  $a_{\text{prot}}^*$  is  $0.25 \text{ m}^2 \text{ g}^{-1}$  at PFDs lower than  $100 \text{ } \mu\text{mol m}^{-2} \text{ s}^{-1}$  and  $0.16 \text{ m}^2 \text{ g}^{-1}$  at PFDs higher than  $1000 \text{ } \mu\text{mol m}^{-2} \text{ s}^{-1}$ . These were the highest and lowest values for *C. reinhardtii* determined in previous studies (Janssen, et al., 2000a and 2000b). In addition, a linear decrease of  $a_{\text{prot}}^*$  was assumed going from 100 to  $1000 \text{ } \mu\text{mol m}^{-2} \text{ s}^{-1}$ .

The specific growth rate, the specific absorption coefficient and the photon flux density can be combined to obtain the biomass yield on light energy ( $Y_{\text{prot,E}}$ ) in gram protein per mol of photons in the range of photosynthetic active radiation (PAR: 400 - 700 nm) as illustrated in Eq. 7.1. This parameter is a good measure for the photosynthetic efficiency of phototrophic growth. But, instead of protein also dry weight (dw) could be used as was done by Pulz and Scheibenbogen,  $Y_{\text{dw,E}}$  (Pulz and Scheibenbogen, 1998). In addition, the photosynthetic efficiency of phototrophic growth can be defined as the energy stored as new biomass per unit of light energy absorbed and is usually abbreviated as PE (Hu and Richmond, 1996). All these parameters will have a similar dependency on the PFD and in Figure 7.1 the relation between  $Y_{\text{prot,E}}$  and the PFD is presented. It can be seen that  $Y_{\text{prot,E}}$  is highest at low PFDs but decreases when the PFD increases.

$$\text{Eq. 7.1} \quad Y_{\text{prot,E}} = \frac{\mu}{a_{\text{prot}}^* \cdot \text{PFD} \cdot 3.6 \cdot 10^{-3}} \quad [\text{g mol}^{-1}]$$

Microorganisms are not exposed to a constant PFD in photobioreactors due to mutual shading of the cells and mixing-induced liquid movements. It is often suggested that circulation between dark and light zones could lead to photosynthetic efficiencies higher than the efficiency determined under continuous illumination of a PFD equal to the PFD in the light zone. Indeed, very fast fluctuations on a  $\mu\text{s}$  - ms scale have been shown to give rise to considerable higher photosynthetic efficiency (Kok, 1953; Phillips and Myers, 1954; Matthijs, et al., 1996; Nedbal, et al., 1996). The photosynthetic efficiency in these studies was defined as the specific oxygen production rate or specific growth rate per unit of light energy supplied. The dark periods in these studies were significantly larger than the light periods. Also when going from 1 ms to cycles of 1 - 4 s this effect has been demonstrated (Phillips and Myers, 1954; Terry, 1986; Nedbal, et al., 1996; Janssen, et al., 2001). However, the efficiency improvement was low at the longest cycles in this range.

The influence of light/dark cycles of several seconds to tens of seconds does not appear to result in an improvement of the photosynthetic efficiency. It was even found that these long cycles could lead to a decrease in the photosynthetic efficiency in comparison to the efficiency under continuous light (Janssen, et al., 2000a, 2000b and 2001; Barbosa, et al., 2002). This could be explained by the fact that specific light absorption increases due to photoacclimation. The cells will acclimate to an average PFD sensed as the average redox state of the plastoquinone pool of the photosynthetic electron transport chain (Durnford and Falkowski, 1997; Kana, et al., 1997). Plastoquinone is a mobile electron carrier in the

photosynthetic membranes. The average PFD will be lower than the PFD at the sunlight-exposed reactor surface. As a result, the specific surface,  $a_{\text{prot}}^*$ , will be relatively large (Janssen, et al., 2000a) and the amount of light energy wasted at the light-exposed surface will be higher than under continuous illumination of a PFD equal to the PFD in the light zone as was illustrated in Figure 7.1.

In addition, it is suggested that photodamage during long high-light periods leads to a decrease of the photosynthetic efficiency (Merchuk, et al., 1998). Strong evidence for such an effect is given by Molina Grima et al. (1996). Long dark periods, on the other hand, give rise to increased maintenance requirements as reported by Lee and Pirt (1981). But, their results can also be interpreted as a decrease in the capability to utilize the light energy absorbed, which is expressed in the parameters  $Y_{\text{dw,E}}$  and PE already introduced. Clearly, mixing-induced light/dark cycles can be very important with respect to the photosynthetic efficiency of phototrophic growth in photobioreactors. In the next part the light regime in pilot-scale enclosed photobioreactors will be analyzed first.

### **Light regime in enclosed outdoor photobioreactors**

The light regime inside a photobioreactor can be characterized with a photic zone of intense sunlight at the reactor surface and a dark zone in the interior of the reactor. In this study the photic zone is arbitrarily defined with the depth at which 90 % of the incoming photon flux is absorbed and this will be called the light penetration depth ( $d_p$ ). As an example, for a one-dimensional system, a flat panel with light entering at one side, the average PFD in the photic zone is 39 % of the PFD at the surface ( $\text{PFD}_{\text{in}}$ ) according to Beer's law. In this paragraph we will only discuss the light gradient in state-of-the-art pilot-scale photobioreactors and also the mixing-induced L/D cycles resulting from this gradient. The absolute value of the incident PFD ( $\text{PFD}_{\text{in}}$ ) is dependent on many factors: geographical, seasonal and climate factors. In this section we will not discuss the absolute value. The influence of  $\text{PFD}_{\text{in}}$  on the photosynthetic efficiency (PE) of photobioreactors will be considered later in the section on the efficiency.

#### ***Vertical column reactors***

Vertical bubble column and air-lift reactors are considered to be attractive for outdoor cultivation of phototrophic micro-organisms. Only columns with diameters higher than 0.1 m are considered. Light will enter the reactor through the transparent wall and depending on biomass concentration and column diameter a part of the reactor center will be dark. Using a

modified model of Evers (1991), see Figure 7.2, Eq. 7.2 and Eq. 7.3, and wavelength-dependent chlorophyll-*a*-specific absorption coefficients ( $a_{chl-a}$ ), the penetration depth of light of different wavelengths was calculated. The values for  $a_{chl-a}$  were obtained from the green alga *Dunaliella tertiolecta* cultivated under a low PFD,  $58 \mu\text{mol m}^{-2} \text{s}^{-1}$  (Janssen, et al., 2000a).

$$\text{Eq. 7.2} \quad PFD(s) = \frac{PFD_{in}}{\int_{0.5\pi}^{1.5\pi} \cos(\Theta + \pi) \cdot d\Theta} \cdot \left[ \int_{0.5\pi}^{1.5\pi} \cos(\Theta + \pi) \cdot \exp[-a_{chl-a} \cdot [chl-a] \cdot b] \cdot d\Theta \right]$$

$$\text{Eq. 7.3} \quad b = (r - s) \cdot \cos \Theta + \left[ r^2 - (r - s)^2 \cdot \sin^2 \Theta \right]^{0.5}$$

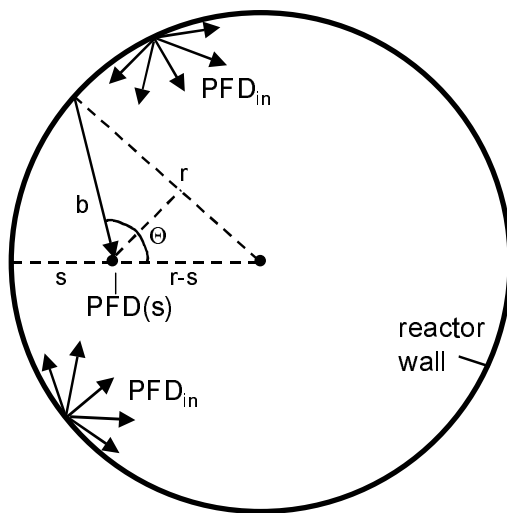


Figure 7.2. Illustration of the calculation of the light gradient in vertical column reactors or tubular reactors; the gradient is calculated according to a modified model of Evers (1991). This model can be represented with Eq. 7.2 and Eq. 7.3.

Although the model does not describe reality completely because light scattering by the microalgae cells is neglected it is suitable to estimate light penetration. Especially when it is taken into account that in outdoor conditions half of the irradiance is mono-directional and light is scattered predominantly under small forward angles by microalgae (Stramski and Morel, 1990). In the original model the light absorbing surface was taken as a cylindrical surface. In our modified version we take the light exposed surface as a flat surface facing the reactor wall, using the cosine law. Only light beams with an angle of incidence of  $90^\circ$  to  $-90^\circ$  with the normal of the flat surface were taken into account. This modification was done to

allow a better comparison of light gradients in curved reactors, vertical columns and horizontal tubes, with gradients in flat panel photobioreactors.

The relative photic volume ( $\varepsilon$ ), ratio of the volume of the photic zone over reactor volume, is calculated separately for three wavelengths as a function of chl-*a* concentration. Three wavelengths were used: 440 nm, representing light absorption by carotenoids and chlorophylls in the ‘blue’ region (400 - 500 nm); 678 nm, representing chlorophyll absorption in the ‘red’ region (600 - 700 nm); 550 nm, representing ‘green’ light (500 - 600 nm) poorly absorbed by green algal carotenoids and chlorophylls.

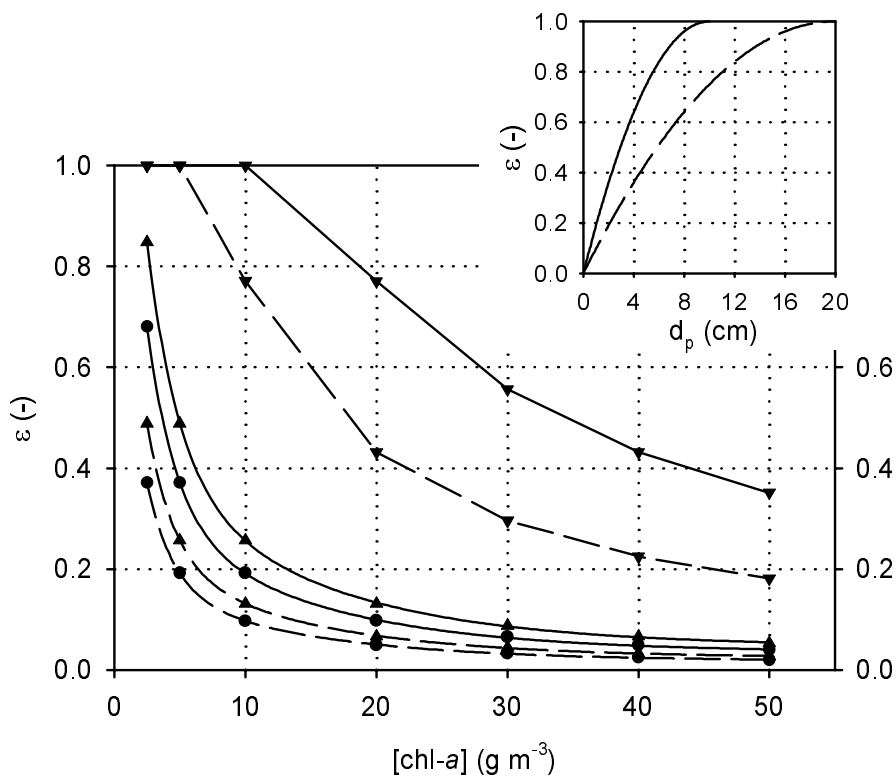


Figure 7.3. Light fraction ( $\varepsilon$ ) as function of the chlorophyll-*a* (chl-*a*) concentration in vertical column reactors with diameter of 0.2 m (solid lines) and 0.4 m (dashed lines) for blue (440 nm; ●), green (550 nm; ▼) and red (678 nm; ▲) light. In the small Figure  $\varepsilon$  is given as a function of the penetration depth ( $d_p$ ). Specific absorption coefficients of *Dunaliella tertiolecta* cultivated under  $58 \mu\text{mol m}^{-2} \text{s}^{-1}$  (Janssen, et al., 2000a) were used in combination with a modified model of Evers (Figure 7.2, Eq. 7.2 and Eq. 7.3).

The results are presented in Figure 7.3 for two column diameters (0.2 and 0.4 m) and also the relation between penetration depth ( $d_p$ ) and photic volume ( $\varepsilon$ ) is shown. For each wavelength another chl-*a* specific absorption coefficient is used. It can be seen that the penetration depth for blue (440 nm) and red light (678 nm) is only reasonable for  $5 \text{ g chl-}a \text{ m}^{-3}$  in the 0.2 m



diameter column:  $d_p = 2 - 3$  cm and  $\varepsilon = 0.4 - 0.5$  (Figure 7.3). At a chl-*a* concentration of  $20 \text{ g m}^{-3}$ ,  $\varepsilon$  already has dropped to 0.1. For a 0.4 m diameter column it is even worse and  $\varepsilon$  is 0.05 for blue and red light at  $20 \text{ g chl-}a \text{ m}^{-3}$ . Only ‘green’ light (550 nm) is able to penetrate far into the interior of the reactor.

The model of Evers is a simplification of reality. In Figure 7.3 it seems that at high chl-*a* concentrations ( $20 \text{ g m}^{-3}$  or more) the relative photic volume decreases very slowly with the chl-*a* concentration. It was assumed light is only absorbed and therefore ‘pure’ absorption coefficients were used. However, light is also scattered by the microalgal cells (Bricaud, et al., 1983). Especially at high biomass concentrations scattering will increase the light path and, as a result, the probability of absorption will increase. In reality the penetration depth and relative photic volume at high chl-*a* concentrations will be smaller than those presented in Figure 7.3.

On a pilot-plant scale level not many experiments have been done with vertical column reactors. In outdoor vertical column reactors of 0.193 m diameter, Mirón et al. (2000a) found biomass dry weight (dw) concentrations between  $1.25$  and  $2.75 \text{ g L}^{-1}$  ( $\approx 19 - 41 \text{ g chl-}a/c \text{ m}^{-3}$  at an estimated 1.5 % of dw, Fernandez, et al., 2000) in the linear growth phase of batch cultures of *Phaeodactylum tricornutum*. Also in our laboratory we carried out experiments with a 0.2 m diameter bubble column. An optimal biomass density of  $0.49 \text{ g l}^{-1}$  ( $= 22.3 \text{ g chl-}a \text{ m}^{-3}$ , 4.6 % of dw) was found yielding the highest productivity for *Dunaliella tertiolecta* (unpublished data). This experiment was done indoors with continuous artificial illumination of moderate PFD,  $367 \mu\text{mol m}^{-2} \text{ s}^{-1}$  at the reactor surface. Because the optimal chl-*a* concentration seems to be in the range of  $20 - 40 \text{ g m}^{-3}$  it is clear that 90 % of the blue and red light is absorbed in the outer 5 to 15 % of the culture volume. Green light, however, will penetrate much further and between 40 and 75 % of the volume will be exposed to more than 10 % of the ‘green’ PFD entering the reactor (Figure 7.3).

#### **Vertical-column reactors: air-lift loop reactors**

Only air-lift reactors with internal draught tube are considered. Air is injected into the draught tube. As a result of a difference in density, the reactor liquid rises in the draught tube, the riser, and comes down again in the space between draught tube and reactor wall, the downcomer. The liquid flow in the downcomer resembles plug flow (Merchuk, et al., 1996). Also the flow regime in the riser is close to plug flow with only small differences in lateral velocity (Merchuk, 1986; Merchuk, et al., 1996). Adjusting reactor design and/or biomass concentration the dark zone can be made to overlap with the riser and the downcomer

becomes the photic volume (Figure 5.1). In that situation the liquid circulation velocity will determine the frequency of L/D fluctuations.

The liquid circulation velocity depends on reactor design and superficial gas velocity. Chisti (1989) developed a procedure to calculate the superficial liquid velocity in the riser ( $v_{lsr}$ ). Using this velocity the liquid circulation time ( $t_c$ ) can be calculated as a function of reactor design as is explained in Appendix I. Such calculations were done for two reactor sizes: 5 m height and 0.2 m diameter ( $T_v$ ), 10 m height and 0.4 m diameter. The results are presented in Table 7.1 and Table 7.2, respectively. For each reactor size the circulation time was calculated for three different draught tube diameters corresponding to downcomer/reactor cross-sectional ratios ( $A_d/A_R$ ) of one third, half and two thirds. Also the influence of the superficial gas flow rate in the riser ( $v_{gsr}$ ) was considered. It can be seen that the circulation time does not vary much and it will be in the range of 25 to 50 s. Apparently, the influence of superficial gas flow rate and  $A_d/A_R$ -ratio is rather small.

Table 7.1. Liquid circulation time ( $t_c$ ) in air-lift loop reactors,  $T_v = 0.2$  m;  $h_l = 5$  m and  $C_b = 0.118$  m. Water at 30 °C is taken as the liquid phase (Appendix I).

$A_d / A_R (-) \rightarrow$	0.33	0.50	0.67
$v_{gsr} (m s^{-1}) \downarrow$	$t_c (s) \downarrow$	$t_c (s) \downarrow$	$t_c (s) \downarrow$
0.025	39.4	35.6	36.1
0.050	31.8	28.6	28.8

Table 7.2. Liquid circulation time ( $t_c$ ) in air-lift loop reactors,  $T_v = 0.4$  m;  $h_l = 10$  m and  $C_b = 0.472$  m. Water at 30 °C is taken as the liquid phase (Appendix I).

$A_d / A_R (-) \rightarrow$	0.33	0.50	0.67
$v_{gsr} (m s^{-1}) \downarrow$	$t_c (s) \downarrow$	$t_c (s) \downarrow$	$t_c (s) \downarrow$
0.025	47.6	43.8	44.9
0.050	38.2	35.0	35.8

### **Vertical-column reactors: bubble columns**

Liquid flow in bubble columns in the heterogeneous flow regime is characterized by large circulatory flows. The circulation arises from higher gas hold-up values in the center of the column leading to an upward velocity in the center and a downward velocity close to the reactor wall (Merchuk, 1986). The circulatory flows do not cover the whole length of the

column but appear to be of the order of the column diameter ( $T_v$ ) (Merchuk, et al., 1994). The circulatory movements of different liquid elements differ considerably. Nevertheless, we will characterize the L/D cycles to which cells, present in different liquid elements, are subjected with a single average cycle time. For this, we used a liquid-flow model for bubble columns developed by Joshi and Sharma (1979); the procedure is explained in Appendix II.

The liquid circulation model was developed for heterogeneous flow. For column diameters of 0.2 m or more, the transition from the homogeneous regime to the heterogeneous regime takes place at superficial gas velocities between 0.04 and 0.07  $\text{m s}^{-1}$  (Merchuk, et al., 1994). Joshi and Sharma (1979) showed that their model was still able to predict liquid velocities at superficial gas velocities of 0.05  $\text{m s}^{-1}$ . In addition, Menzel et al. (1990) and Lefèbre and Guy (1999) demonstrated the existence of a considerable radial gradient in the axial liquid velocity at superficial gas flows of 0.05  $\text{m s}^{-1}$  with upward liquid flow in the center and a downward flow close to the reactor wall.

In algal biotechnology only a few studies have been done in bubble columns and usually gas flow rates of 0.01  $\text{m s}^{-1}$  or smaller were applied. Circulation cells do not really exist at these gas velocities as was seen in visual observation (Merchuk, 1986). In that situation the circulation model cannot be used and Merchuk et al. (1998) used a different approach to estimate the L/D regime in bubble columns. The analogy between heat and mass transfer was used as a tool to calculate the mass transfer coefficient followed by the calculation of the liquid film renewal rate at the reactor surface (Appendix II).

The results of the calculations described above are shown in Table 7.3. At high superficial gas velocities, 0.05  $\text{m s}^{-1}$  or higher, the average liquid circulation time is between 0.5 and 2 s according to the model of Joshi and Sharma. At a superficial gas flow rate of 0.0066  $\text{m s}^{-1}$  the Merchuk approach was used and a surface contact time of 1.28 s was calculated and this value is independent of column diameter. The surface contact time is strongly dependent on the superficial gas flow. At a flow of 0.05  $\text{m s}^{-1}$  the contact time decreases to 0.46 s. The depth of the liquid film renewed at the reactor wall has to be estimated arbitrarily. Merchuk et al. (1998) estimated 1 cm for a column diameter of 18 cm. Accordingly, the circulation time is 11.8 s assuming the photic zone overlaps with the liquid film renewed. A liquid film layer of 1 cm, however, is big and this approach does not seem to be suitable. Moreover, we recalculated the surface contact time and our value of 1.28 s (Table 7.3) is more than two times smaller than the value of 2.7 s originally calculated by Merchuk et al. (1998).

Table 7.3. Liquid circulation time ( $t_c$ ) and surface contact time ( $t_{sc}$ ) in bubble column reactors. Water at 30 °C is taken as the liquid phase (Appendix II).

$T_v$ (m) →	-	0.2	0.4
$v_{gs}$ (m.s <sup>-1</sup> ) ↓	$t_{sc}$ (s) <sup>(1)</sup> ↓	$t_c$ (s) <sup>(2)</sup> ↓	$t_c$ (s) <sup>(2)</sup> ↓
0.0066	1.28	-	-
0.0500	0.46	0.96	1.53

(1) calculations according to Merchuk et al. (1998)

(2) calculations according to Joshi and Sharma (1979)

As a consequence, without more elaborate research or study on liquid circulation in bubble column reactors we can only make a rough estimation of the average circulation time. These probably are in the range of 0.5 to 15 s. Only at high superficial gas flow rates ( $\geq 0.05$  m s<sup>-1</sup>) we can conclude that the average cycle time will be shorter than 2 s. Such gas flows have not been used for microalgae cultivation in pilot-scale studies. The reason for this could be non-published observations of decreased productivity due to shear stress imposed on microalgae at high aeration rates. This has been observed in air-lift reactors during batch cultivation of *Phaeodactylum* and *Porhyridium* (Gomez, et al., 1998; Merchuk, et al., 2000). On the other hand, it seems it has not been tried yet to cultivate a wide range of microalgae in bubble column reactors at high superficial gas velocities ( $\geq 0.05$  m s<sup>-1</sup>).

### **Flat panel reactors**

Flat panel reactors consist of a rectangular transparent box with a depth of only 1 to 5 cm. Height and width can be varied to some extent but in practice only panels with a height and width both smaller than 1 m have been studied. Also these photobioreactors are mixed with air introduced via a perforated tube at the bottom of the reactor. In order to create a high degree of turbulence 2.8 to 4.2 liter of air per liter of reactor volume per minute has to be provided corresponding to superficial gas velocities between of 0.030 to 0.035 m s<sup>-1</sup> (Hu, et al., 1996a; Hu and Richmond, 1996; Hu, et al., 1998b). Usually the panels are illuminated from one side by direct sunlight and the panels are placed vertically or inclined facing the sun. In flat panel reactors biomass concentrations are in the range of 5 to 17.5 g L<sup>-1</sup> at maximal productivity of the cyanobacterium *Spirulina platensis* (Hu and Richmond, 1996; Hu, et al., 1998b). This corresponds to 62.5 to 219 g m<sup>-3</sup> chl-*a* using a chl-*a* content of 1.25 % (Hu, et al., 1996b). Gitelson et al. (1996) showed that the penetration depth for blue and red light is less than 1 mm at 100 g m<sup>-3</sup> of chl-*a* for *Spirulina platensis*. As an average for flat panel

reactors, a biomass concentration of  $10 \text{ g L}^{-1}$  can be used (Hu, et al., 1996a, 1996b and 1998b), corresponding to  $125 \text{ g chl-}a \text{ m}^{-3}$ . Using Beer's law we calculated a penetration depth of 0.8 mm for 'red' light (678 nm) and this is equal to a photic zone ( $\epsilon$ ) of 0.062 or 0.031 for a light path of 1.3 or 2.6 cm, respectively.

The frequency of the light/dark cycles was estimated based on the liquid flow, which was measured as the rate of dispersion of a dye inside the reactor (Hu, et al., 1996a; Hu and Richmond, 1996). The liquid flow was in the range of 20 to 30  $\text{cm s}^{-1}$ . Richmond (1996) assumed that the liquid moves with the same velocity alongside the light-path axis. In that situation the length of a cycle would be 87 - 130 ms and 173 - 260 ms in a 1.3 and 2.6 cm light path reactor, respectively. The absolute length of the light and dark periods can be calculated by multiplying the relative size of the dark or light zone and the estimated cycle duration, the results are shown in Table 7.4. The absolute length of the light period for red light is only 5 to 10 ms.

Table 7.4. Estimated light/dark (L/D) cycles for 'red' light (678 nm) in short light-path flat panel reactors (Richmond, 1996; Hu, et al., 1996a; Hu and Richmond, 1996); calculations are explained in the text.

light-path (cm)	cycle duration (ms)	light faction ( $\epsilon$ ) (%)	light period (L) (ms)	dark period (D) (ms)
1.3	87	6.2	5.4	81.6
1.3	130	6.2	8.0	122.0
2.6	173	3.1	5.3	167.7
2.6	260	3.1	8.0	252.0

### ***Tubular reactors***

Tubular photobioreactors consist of long transparent tubes with diameters ranging from 3 to 6 cm and lengths ranging from 10 to 100 m. The culture liquid is pumped through these tubes by means of mechanical or air-lift pumps. The tubes can be positioned on many different ways: in a horizontal plane as straight tubes with a small or large number of U-bends; vertical, coiled as a cylinder or a cone; in a vertical plane, positioned in a fence-like structure using U-bends or connected by manifolds; horizontal or inclined, parallel tubes connected by manifolds; in addition, horizontal tubes can be placed on different reflective surfaces with a certain distance between the tubes. Although tubular reactor design is very diverse, the predominant effect of the specific designs on the light regime is a diversity in the photon flux

density incident on the reactor surface ( $\text{PFD}_{\text{in}}$ ). The shape of the light gradient in the tubes is similar in most designs. Also with respect to liquid mixing, i.e. L/D cycling, the circumstances in most designs are similar.

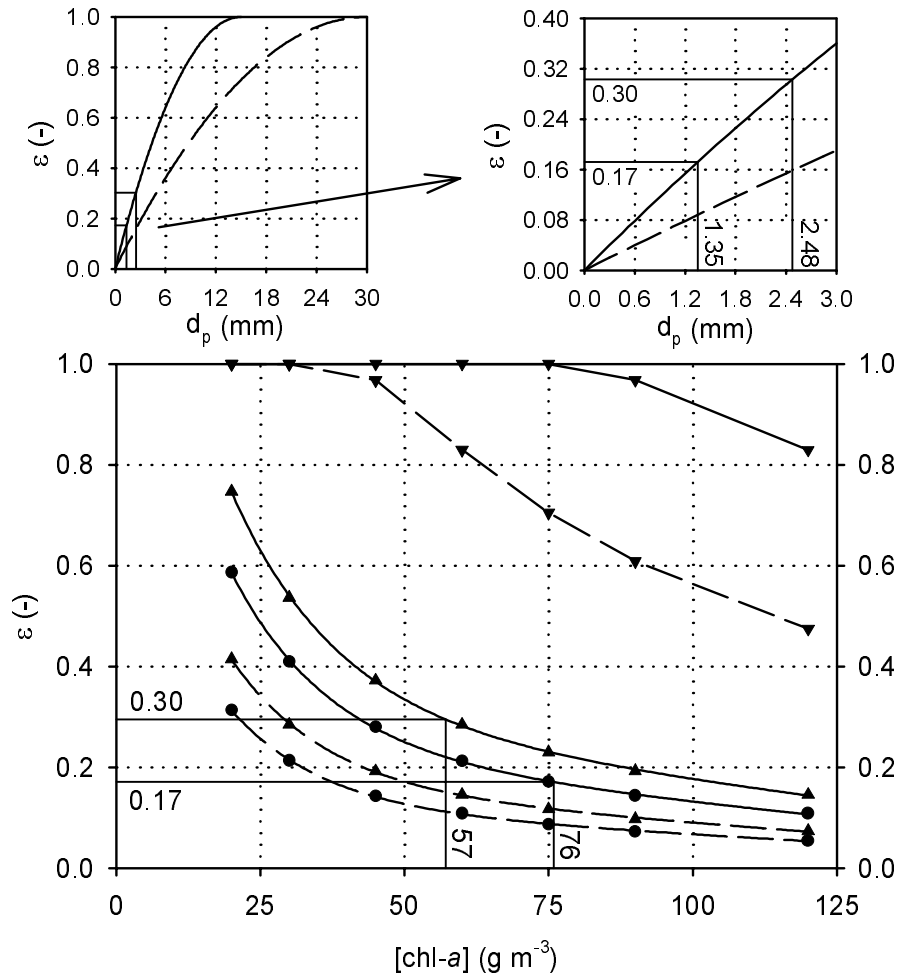


Figure 7.4. Light fraction ( $\epsilon$ ) as function of the chlorophyll-*a* (*chl-a*) concentration in tubular reactors with diameter of 3 cm (solid lines) and 6 cm (dashed lines) for blue (440 nm, ●), green (550 nm, ▼) and red (678 nm, ▲) light. In the small Figure  $\epsilon$  is given as a function of the penetration depth ( $d_p$ ). Specific absorption coefficients of *Dunaliella tertiolecta* cultivated under  $58 \mu\text{mol m}^{-2} \text{s}^{-1}$  (Janssen, et al., 2000a) were used in combination with a modified model of Evers (Figure 7.2, Eq. 7.2 and Eq. 7.3).

The diameter of the tube and the biomass density in the culture liquid are the predominant factors determining the light gradient. Again we will use the modified version of the model of Evers (1991) to estimate the penetration depth of blue (440 nm), green (550 nm) and red light (678 nm), using *chl-a* specific absorption coefficients determined for *Dunaliella tertiolecta*. The only difference is the diameter used for the calculations. These were smaller than those

used for the vertical column reactors: 3 and 6 cm. The results are presented in Figure 7.4. Comparing Figure 7.4 with Figure 7.3 it can be seen that biomass density in tubular systems theoretically can be higher with a factor 5 in order to maintain the same light fraction ( $\epsilon$ ) as in larger diameter (0.2 - 0.4 m) vertical column reactors.

Torzillo et al. (1993) used a culture density of 3.5 and 6.3 g dw L<sup>-1</sup> for *Spirulina* in a horizontal tubular system of 2.6 cm diameter. For *Spirulina* a chl-*a* content of 1.59 % on dw basis was measured in a similar system by Tredici and Zitelli (1998). Tredici and Zitelli used culture densities of 3.6 and 4.0 g L<sup>-1</sup> in horizontal tubular systems with internal diameters of 3.4 and 3.0 cm. It appears therefore that in horizontal tubular systems of 3 cm diameter chl-*a* concentration will be between 57 to 76 g m<sup>-3</sup> and this corresponds to an  $\epsilon$  between 0.17 and 0.30 for blue and red light (Figure 7.4). At these chl-*a* concentrations we would find a penetration depth of about 2 mm in a flat panel according to Gitelson et al. (1996). This also corresponds with our calculations, as is shown in Figure 7.4. Photic volumes of 0.17 and 0.30 correspond to a penetration depth of 1.4 and 2.5 mm, respectively. In addition, Grima et al. (2000) compared horizontal tubular reactors of 3 cm and 6 cm diameter. The highest productivities of the microalga *Phaeodactylum tricornutum* were reached at biomass densities between 4 and 7 g L<sup>-1</sup> ( $\approx$  40 - 105 g chl-*a/c* m<sup>-3</sup> at 1.0 - 1.5 % of dw, Fernandez, et al., 2000).

Table 7.5. Liquid circulation time ( $t_c$ ) and surface contact time ( $t_{sc}$ ) in tubular photobioreactors. Water at 30 °C is taken as the liquid phase (Appendix II and Appendix III).

d (cm) →	3		6	
$v_{ls}$ (m s <sup>-1</sup> ) ↓	$t_c$ (s) <sup>(1)</sup> ↓	$t_{sc}$ (s) <sup>(2)</sup> ↓	$t_c$ (s) <sup>(1)</sup> ↓	$t_{sc}$ (s) <sup>(2)</sup> ↓
0.2	1.41	7.94	3.07	11.4
0.4	0.77	2.86	1.68	3.77
0.6	0.54	1.49	1.18	1.97

(1) calculations according to Fernandez et al. (2000)

(2) calculations according to Merchuk et al. (1998)

Fernandez et al. (2000) used the characteristic turbulence velocity (Davies, 1972) to estimate the average cycle time in tubular photobioreactors. This procedure is elucidated in Appendix III and the results are presented in Table 7.5. According to these calculations the average cycle time ( $t_c$ ) is between 0.5 and 3 seconds depending on tube diameter ( $d$ ) and superficial axial liquid velocity ( $v_{ls}$ ). The average surface contact time ( $t_{sc}$ ) was also calculated following the procedure of Merchuk et al. (1998) (Appendix II). The internal heat transfer coefficients

for (turbulent) pipe flow were calculated using the Sieder-Tate and Hausen's equations (Perry and Greene, 1984). The surface contact times were found to be higher than the cycle times calculated using the Davies equation. An explanation for this discrepancy will be given in the next paragraph.

### ***Residence time distribution in photic and dark zones***

In the preceding paragraphs estimations of the average length of L/D cycles in different photobioreactors are given together with an analysis of the light gradient during cultivation of phototrophic microorganisms. In reality a distribution in cycle times will exist. Powell et al. (1965) used a probability model calibrated with a diffusion model to calculate this distribution for turbulent flow in small channels. This system is comparable to horizontal tubular photobioreactors. Their calculations showed that the residence time distribution in photic and dark zones was very wide and they concluded that the actual light regime experienced by an alga will deviate considerably from the calculated average L/D cycle.

Another complicating factor is the fact that the mixing intensity is not uniform across the cross section of a tubular reactor. Even in turbulent flow a laminar sub-layer develops at the reactor surface. The depth of this layer can be calculated using Deisslers empirical formula (Bird, et al., 1960). In a tube with a diameter of 6 cm and a superficial liquid flow of  $0.6 \text{ m s}^{-1}$  the depth of the laminar sublayer is 0.13 mm. Turbulent flow is only fully developed at a depth of 0.67 mm. This is also in agreement with the relatively long surface contact time calculated for this system. In Table 7.5 can be seen that the surface contact time ( $t_{cs}$ ) equals 1.97 s, but the average duration of a light/dark cycle ( $t_c$ ) is only 1.18 s. It is very likely that liquid elements close to the reactor surface ( $< 0.67 \text{ mm}$ , see above) are relatively slowly replaced with elements coming from the interior. Algae suspended in the surface liquid film could be exposed to high photon flux densities much longer than estimated from the average light exposure time ( $t_l = t_c \times \varepsilon$ ). Also in bubble column and air-lift reactors the liquid close to the reactor surface will be mixed more slowly. In short light-path aerated flat panel reactors this effect could be reduced by gas bubbles regularly shearing the surface.

### **Photosynthetic efficiency in enclosed outdoor photobioreactors**

Productivity of photobioreactors is light limited as explained in the section on photosynthetic efficiency and light regime. The light regime inside the reactor, therefore, has a predominant effect on the productivity. In the preceding section the light regime was analyzed with respect



to the light gradient and mixing-induced L/D cycles. The photosynthetic efficiency of phototrophic growth in pilot-scale photobioreactors is covered in this section and is related to the light regime. Reactors are compared with respect to the photosynthetic efficiency (PE): energy stored as biomass produced per unit of light energy absorbed in the PAR range (400-700 nm). The maximum PE under ideal conditions is 20 % (Radmer and Kok, 1977; Kirk, 1994), or 9 % based on full solar irradiance (all wavelengths included). Next to the PE also the dry weight (dw) biomass yield on light energy ( $Y_{dw,E}$ ) is used: dry weight produced per mol of photons absorbed in the PAR range.

In Table 7.6 the reactor types discussed before are compared using representative examples from literature. Only a few studies have been published on bubble column and air-lift reactors for phototrophic cultivation under high-PFD outdoor conditions. Combining productivity data of Camacho et al. (1999) and Mirón et al. (2000a) and solar irradiance data from the European Database of Daylight and Solar Radiation (Fontoynt, et al., 1998) we were able to calculate biomass yields ( $Y_{dw,E}$ ) for the diatom *Phaeodactylum*. These were considerable, a yield of  $0.82 \text{ g dw mol}^{-1}$  was found for a 0.096 diameter draft-tube air-lift reactor. In larger diameter (0.193 m) bubble column and also air-lift reactors (internal draught tube and split-cylinder) a similar yield was obtained,  $0.84 \text{ g dw mol}^{-1}$ . In addition, Merchuk et al. (1998) did not find a difference between a bubble column reactor and a draft-tube air-lift reactor (diameter: 0.18 m; reactor height: 2 m) under indoor conditions ( $\text{PFD}_{in} = 300 \mu\text{mol m}^{-2} \text{ s}^{-1}$ ).

It may seem surprising that bubble column and air-lift reactors show a similar yield because L/D cycles in these systems were shown to be quite different in the previous paragraph. The superficial gas flow rates in these comparative studies, however, were low,  $0.0065$  and  $0.011 \text{ m s}^{-1}$  respectively (Merchuk, et al., 1998; Miron, et al., 2000a). This is the reason the average cycle times inside the bubble column reactors are difficult to estimate. But, as mentioned in the second paragraph, the average L/D cycle could be close to 15 s. In addition, the height of the reactors was only 2 m and the circulation time in an air-lift is proportional to the square root of the liquid dispersion height ( $h_d$ ). It can be calculated that the circulation time in the air-lift reactors will be approximately 20 s. These facts combined lead to the conclusion that the light regime in the bubble columns and air-lift reactors studied resemble each other as does their productivity.

It is possible that the performance of bubble columns will improve when operated under higher superficial gas velocities because cycle times will become much shorter and will be 1.5 s or less in the heterogeneous flow regime (Table 7.3). Terry et al. (1986) demonstrated that the photosynthetic efficiency of *Phaeodactylum* under high PFDs was higher under light/dark

cycles (0.13 - 4 s) in comparison to continuous light. In addition, the performance of bubble columns compared to air-lift reactors might be better at increased column height. Cycle times in 10 m air-lift columns are 40 s (Table 7.2) in comparison to 20 s in 2 m columns. In Chapter 5 (Barbosa, et al., 2002) was demonstrated that the photosynthetic efficiency of *Dunaliella tertiolecta* decreased slightly when the cycle time was increased. As opposed to air-lift reactors, circulation times in bubble columns are not dependent on column height (Appendix II).

The biomass density of *Phaeodactylum* in the vertical column reactors was such that the photic zone comprised only 5 to 10 % of the culture volume for blue and red light. In Chapters 3, 4 and 5 was concluded that the photosynthetic efficiency of the green algae *Chlamydomonas reinhardtii* and *Dunaliella tertiolecta* under medium-duration L/D cycles (10 - 100 s) were highest at high relative photic volumes (Janssen, et al., 2000a and 2000b; Barbosa, et al., 2002). Extrapolating these results would result in low biomass densities corresponding to a photic zone of more than 0.66 ( $\epsilon$ ). Apparently these results cannot be extrapolated directly. One discrepancy is the fact that different organisms were used. The Chl-*a* content on a dw basis of *Dunaliella*, for example, is twice as high that of *Phaeodactylum*. This will reflect on the light gradient and possibly also on the photosynthetic efficiency. More important could be the set-up of the lab-scale experiments. In the laboratory well-defined light/dark cycles were applied in low-density cultures using alternating light sources. As a result, dark periods were completely dark and no photosynthesis was possible. In the pilot-scale reactors the interior is not completely dark because the dark zone still receives 10 % of the total photon flux. In addition, green light is able to penetrate much further inside the culture than blue and red light (Figure 7.3), and can be utilized as efficiently by many microalgae (Emerson and Lewis, 1943; Tanada, 1951).

Tubular photobioreactors are as efficient or less efficient than bubble column or air-lift reactors (Table 7.6). The biomass yield,  $Y_{dw,E}$ , ranges from 0.48 to 0.95 g dw mol<sup>-1</sup> for *Phaeodactylum* in an extensive study done by Fernandez et al. (1998). These yields were based on the photon flux entering the tubes because the positioning of the tubes themselves on the available ground surface was not optimized yet. This was done later and an aerial productivity of 19.5 g dw m<sup>-2</sup> d<sup>-1</sup> was found in the spring time in Southern Spain without affecting the photosynthetic efficiency of the culture (Fernandez, et al., 2001). Torzillo et al. (1993) found 25.4 g dw m<sup>-2</sup> d<sup>-1</sup> for *Spirulina* in summer time in northern Italy. This last value was recalculated by them and corresponded to a  $Y_{dw,E}$  of 0.60 g mol<sup>-1</sup> and a PE of 6.5 % (Table 7.6).

Table 7.6. Enclosed photobioreactors; biomass density ( $C_x$ ), photon flux density incident on reactor wall ( $PFD_{in}$ ), Photosynthetic efficiency (PE) and biomass yield on light energy ( $Y_{dw,E}$ ).

photobioreactor type	dimensions	$C_x$ (g dw L <sup>-1</sup> )	$PFD_{in}$ <sup>(1)</sup> ( $\mu\text{mol m}^{-2} \text{s}^{-1}$ )	PE or $Y_{dw,E}$ <sup>(1)</sup> (% or g dw mol <sup>-1</sup> )	Reference
bubble column and air-lift column reactors:	d: 19.3 cm height: 2.17 - 2.32 m	1.25 - 2.75	sunlight: 651 <sup>(2)</sup>	0.84 ( $Y_{dw,E}$ ) <sup>(3)</sup>	Miron et al. (2000a) ( <i>Phaeodactylum tricornutum</i> )
- internal draught tube	$A_d/A_R = 1.24$ (draught tube)				
- split cilinder	$A_d/A_R = 1$ (split cylinder)				
air-lift column	d: 9.6 height: 2 m; $A_d/A_R = 0.5$	3.3	sunlight: 643 <sup>(2)</sup>	0.82 ( $Y_{dw,E}$ )	Camacho et al. (1999) ( <i>Phaeodactylum tricornutum</i> )
flat panel	a) vertical, width: 2.6 cm b) tilted: 10 - 90°, facing south, width: 2.8 cm	a) 15 - 17.5 b) 5 - 8	a) artificial light: 1800 b) sunlight: 229 - 1259	a) 1.48 ( $Y_{dw,E}$ ) $\approx$ 16 (PE) b) 10 - 20 (PE)	a) Hu and Richmond (1996) b) Hu et al. (1998b) ( <i>Spirulina platensis</i> )
tubular reactor	length: 2 x 122.5 m; $d_{int}$ : 2.6 cm	3.5	sunlight: 1152 <sup>(4)</sup>	0.60 ( $Y_{dw,E}$ ); 6.5 (PE) <sup>(5)</sup>	Torzillo et al. (1993) ( <i>Spirulina platensis</i> )
tubular reactor	length: 90 m: a) $d_{int}$ : 2.5 cm b) $d_{int}$ : 5.3 cm	a) 3.3 - 6.9 b) 2.5 - 5.1	a) sunlight: 327 - 738 b) sunlight: 328 - 910	a) 0.48 - 0.63 ( $Y_{dw,E}$ ) <sup>(6)</sup> b) 0.68 - 0.95 ( $Y_{dw,E}$ ) <sup>(6)</sup>	Fernandez et al. (1998) ( <i>Phaeodactylum tricornutum</i> )

(1) daily irradiance values in MJ m<sup>-2</sup> d<sup>-1</sup> were divided by 12 x 3600 s, assuming a day length of 12 h, multiplied with 0.429, the fraction PAR in the solar spectrum (Thimijan and Heins, 1983), and multiplied with 4.57 mol photons MJ<sup>-1</sup> (Thimijan and Heins, 1983)

(2) monthly averages of daily solar irradiance on a vertical cylindrical surface in the same period of the year were obtained from the European Database of Daylight and Solar Radiation, [www.satel-light.com](http://www.satel-light.com) (Fontoynt, et al., 1998); this database is based on measured (1996 and 1997) and modeled data

(3) based on a linear growth phase with a productivity of about 0.49 g L<sup>-1</sup> d<sup>-1</sup> observed in an outdoor batch culture in three different reactor types

(4) irradiance on ground surface instead of reactor wall

(5) before calculating PE and  $Y_{dw,E}$ , irradiance data were corrected for transmittivity tubes (Torzillo, et al., 1993)

(6) see Appendix V

Although the biomass yield in tubular reactors is lower than or comparable to the yield in vertical column reactors, the biomass density is twice as high (Table 7.6). With respect to the light regime, tubular photobioreactors should be better because the average L/D cycles are shorter than in the vertical column reactors (Table 7.5). It seems, therefore, that other factors limit the photosynthetic efficiency, for example accumulation of photosynthetically produced oxygen in the non-aerated tubes (Weissman, et al., 1988). This is supported by the fact the efficiency is lower in tubes with smaller diameter and higher volumetric productivity (Table 7.6). Oxygen competes with carbon dioxide for the carbon dioxide fixing enzyme Rubisco in a process called photorespiration. But, maybe more important is the high peak irradiance close to the reactor wall in tubular photobioreactors (Camacho, et al., 1999). Microalgae could be exposed to this peak irradiance for a few seconds (Table 7.5) because the laminar sublayer is poorly mixed. Combined with the elevated oxygen partial pressure (Vacha, 1995) this could lead to considerable photoinhibition.

Fernandez et al. (1998) developed a model to predict productivity in tubular photobioreactors. They only found a good fit of their experiments if they included photoinhibition in their growth equation. In addition, Torzillo et al. (1996) directly showed photoinhibition in an outdoor tubular photobioreactor. In vertical column reactors, on the other hand, photoinhibition will be much less severe because the irradiance is more evenly distributed across the reactor wall (Camacho, et al., 1999). Also oxygen accumulation will not be a problem in well-aerated column and flat panel photobioreactors.

Flat panel reactors appear to be superior to the other reactor types with respect to the photosynthetic efficiency or biomass yield on light energy. Moreover, biomass density is highest in these systems (Table 7.6). Using high-PFD illumination a photosynthetic efficiency of 16 % was reached corresponding to a biomass yield (dw) on light energy of  $1.48 \text{ g mol}^{-1}$ . Also in outdoor conditions efficiencies of 10 to 20 % were reached. It should be noted that power consumption of aeration is high,  $334 \text{ W m}^{-3}$  (Appendix IV). Although light energy is utilized very efficiently, a considerable amount of energy will be needed to feed the air compressor(s).

The light path in the panels is very small (2.6 cm) and the biomass density was high ranging from 5 to  $17.5 \text{ g L}^{-1}$ . Optimal volumetric productivity was achieved at high biomass densities. In paragraph 2 it was already shown that the average light/dark cycles are very short in these reactors (90 to 260 ms) with a relatively short light period (3 to 6 % for red light). This specific light regime is considered to be the key factor leading to the high photosynthetic efficiency of flat panel photobioreactors (Richmond, 2000). This hypothesis is supported by

the fact that in lab-scale studies under short L/D cycles (1 ms - 4 s) the photosynthetic efficiency was higher than the efficiency determined under continuous illumination of a PFD equal to the PFD in the light zone (Phillips and Myers, 1954; Terry, 1986; Nedbal, et al., 1996; Janssen, et al., 2001).

The analysis of typical examples of microalgal cultivation in enclosed (outdoor) photobioreactors showed that the photosynthetic efficiency and productivity is determined by the light regime inside the reactors. In addition to the light regime, only oxygen accumulation and shear stress limit productivity in certain designs. Knowledge of the light regime inside photobioreactors, including mixing-induced L/D cycles, allows qualitative estimation of the photosynthetic efficiency and volumetric productivity, provided gas exchange is sufficient to prevent oxygen built-up. More accurate modeling of light regime, including scattering, liquid circulation, including residence time distribution, and, most importantly, more knowledge of photosynthesis dynamics under changing light regimes can provide us with a quantitative model to predict photobioreactor productivity.

#### ***Improvement photosynthetic efficiency photobioreactors***

The photosynthetic efficiency (PE) of the photobioreactors described possibly can be increased. Higher gas flow rates in bubble columns could lead to shorter L/D cycles, higher biomass density and a higher PE. But, higher gas flow rates will also lead to increased power consumption (Appendix IV) and shear stress for the microorganisms. Both effects will have to be balanced in the future. With respect to air-lift reactors it is interesting to apply annulus sparging instead of sparging the inner cylinder. In that way turbulence is shifted from the dark zone in the center of the photobioreactor to the photic zone in the outer cylinder and this could lead to higher efficiencies.

Many interesting ideas on the improvement of the photosynthetic efficiency in tubular photobioreactors have been published. Most designs involve a lower PFD incident on the surface of the tubes, for example the cone-shaped helical reactor (Morita, et al., 2001), the  $\alpha$ -shaped tubular reactor (Lee, et al., 1995) or undulating row photobioreactors (Carlozzi, 2000). Lower PFDs will lead to considerably higher efficiencies as explained in the section 'photosynthetic efficiency and light regime' and clearly demonstrated by Grima et al. (1997). The disadvantage of most of these designs is their complexity. In addition, the biomass density at optimal productivity will be lower in comparison to the original horizontal tubes.

In a similar way the efficiency of flat panels is highest when they are placed vertically and/or close to each other (Pulz, et al., 1995; Richmond, 1996; Pulz, et al., 2001). This was

demonstrated by Hu et al. (1998b). In Table 7.6 their data were shown. The PE ranged from 10 to 20 % in the outdoor flat panel reactors inclined at different angles. More specifically, in the reactors inclined at 10° and 30° with the horizontal the PE ranged from 10 to 14 %. In the reactors inclined at 60° PE was about 15 % and in vertical reactors (90°) efficiencies of 20 % were reached (Hu, et al., 1998b). If the panels are placed vertically, and/or close to each other, the irradiance at the surface around solar noon will be lower and, as a consequence, light energy is utilized more efficiently. But again, the optimal biomass density will be considerably lower in vertical systems in comparison to inclined systems.

### Scale-up of photobioreactors

The scalability of vertical air-lift reactors and bubble columns is often used as an advantage of these systems (Miron, et al., 1999). In the same study calculations for a production farm of eicosapentaenoic acid from *Phaeodactylum tricornutum* based on the use of bubble columns were presented. The column volume was only 126 L (0.2 m diameter and 4 m height) and hence a large forest of columns would be necessary for a considerable production capacity. A significant increase of the column volume is not possible. The diameter cannot be increased without a decrease in the biomass density and, correspondingly, volumetric productivity when a similar relative photic volume must be maintained (Figure 7.3). Also column height cannot be increased significantly because the axial mixing rate will decrease and the reactor must be able to resist high wind loads.

The maximal unit size of tubular photobioreactors is limited too (Fernandez, et al., 2001). The tube length is limited because of oxygen accumulation in the non-aerated tubes. Oxygen accumulation also mandates a certain liquid velocity in a tube of fixed length. The diameter is balanced to obtain an optimum for two conflicting parameters: aerial productivity ( $\approx Y_{dw,E}$  or PE) and volumetric productivity ( $\approx$  biomass density). In addition, the liquid flow in the tubes should be turbulent to obtain short L/D cycles. The phototrophs, however, could be subjected to high shear stresses at high liquid flow rates and therefore the flow rate should be limited. Fernandez et al. (2001) found a good balance in a bioreactor with a tubular loop of 80 m and a tube diameter of 6 cm. The reactor volume was only 200 L on a 12 m<sup>2</sup> land area. The only way to scale tubular systems further than this size was described by Richmond et al. (1993) and is also used in the BIOCOIL design (Borowitzka, 1999). In these designs a

number of tubes are connected via manifolds. In this way the reactor volume can be increased without increasing the length of the separate tubes.

This is also the path followed at the IGV (Institut für Getreideverarbeitung GmbH, Germany). After long-term investigation by the IGV the German company Preussag initiated the construction of a 16 million DM photobioreactor system in Klötze (Germany) of 700 m<sup>3</sup> volume and 12000 m<sup>2</sup> surface. This system actually consists of 20 separate 35 m<sup>3</sup> units and 35 m<sup>3</sup> therefore seems to be the maximal scalable size. Each unit consists of 25000 m glass tubes of approximately 4 cm diameter through which the culture is pumped mechanically. To prevent build-up of high oxygen levels in the tubes they are connected in parallel using manifolds and a central degassing unit. Combined with the fact that radiation is diluted strongly (Pulz, et al., 1995), and liquid flow is turbulent this could be an efficient and productive system.

Although, at present, it is the largest enclosed photobioreactor in the world it remains to be seen whether it will answer the production demands. The estimated productivity of 150 ton yr<sup>-1</sup> *Chlorella vulgaris* biomass in the 12000 m<sup>2</sup> photobioreactor system reported by Pulz et al. (2001) must be too high. Assuming a combustion enthalpy of 23.6 kJ g<sup>-1</sup> dw and a yearly irradiance of 3603 MJ m<sup>-2</sup> yr<sup>-1</sup> (European Database of Daylight and Solar Radiation, Fontoynt, et al., 1998) this would imply a PE on PAR basis of 19 %, which is very high in comparison to other (tubular) photobioreactors (Table 7.6). In addition, Pulz and Scheibenbogen (1998) reported an aerial productivity of 24 g m<sup>-2</sup> d<sup>-1</sup> in a similar system at a similar location. Extrapolating these data the production would be only 105 ton yr<sup>-1</sup> on a 12000 m<sup>2</sup> ground surface.

Olaizola (2000) described a 25 m<sup>3</sup> commercial-scale tubular photobioreactor occupying a ground surface of only 100 m<sup>2</sup> in use at Aquasearch Inc. (Hawaii, USA). The soft plastic tubes are very wide, 0.18 to 0.41 m diameter, making the system very voluminous although they are only partly filled with culture suspension. The aerial productivity was 13 g m<sup>-2</sup> d<sup>-1</sup>, which is about half the productivity obtained in horizontal tubular photobioreactors. Although this is a voluminous system it is not very productive and biomass concentration is low, less than 0.4 g L<sup>-1</sup>. It can be considered as an intermediate design between shallow ponds and enclosed tubular photobioreactors.

Finally, the maximal unit size of flat panels is approximately 1000 l. Richmond and Cheng-Wu (2001) reported on a 1000 L system consisting of five 200 L units with a passage between the units. The mixing-rate of the reactor liquid as a whole (1000 L) will be low in this system and 1000 L seems to be the maximum size. In addition, the reactor depth was increased to 10

cm and, as a result, biomass density and volumetric productivity are lower than in the short light-path (2.6 cm) panels (Hu and Richmond, 1996; Hu, et al., 1998b).

The scalability of the photobioreactors described is modest to poor. In general, scale-up of the production of photosynthetic micro-organisms can only be done by increasing the number of units. For every unit separate control devices for pH, temperature, aeration, carbon dioxide supply, nutrients supply and culture dilution are needed. This makes such a production 'farm' labor intensive and costly. In addition, it will be very difficult to maintain monocultures in a large number of small-volume reactors. Although the IGV design has a large volume single unit, 35 m<sup>3</sup>, it is not clear whether it can be sterilized thoroughly and used for cultivation of specific monocultures. Finally, complete temperature control is costly or impractical for all these separate units placed outdoors. Usually only spraying devices are used for evaporative cooling of the reactor wall.

### **Future prospects in photobioreactor design**

Although the photobioreactors described above are not easily scalable, they are useful in small-scale applications as there is the on-site production of aquaculture feed. Also their use for production of a large size monoculture as an inoculum for open raceway systems is without any doubt (Olaizola, 2000). Also the IGV design could open up new possibilities. However, for the future of microalgal biotechnology it is important to develop large-scale photobioreactors which can be operated under fixed and optimal conditions with good possibilities for sterilization, and contamination risks as low as possible.

We think it is very attractive to separate light collection from algal cultivation as was already done by Mori (1985). Solar beam irradiation in 'clear-sky' areas can be collected and concentrated into optical fibers with lenses or parabolic mirrors. Via the fibers light can be guided into a large-scale photobioreactor. This seems a very costly solution, but, as a first step, this could be applied for the production of high-value compounds (Shimizu, 2000). In time, the material and production costs of the lenses, mirrors, solar tracking devices and optical fibers will decrease because of scale-effects. And possibly, in the future, this cultivation technique could be used for other applications too.

Feuermann and Gordon (1998 and 2001) reported on an interesting system consisting of a large number of small parabolic mirrors to collect and concentrate solar beam irradiance into glass fibers. It was estimated 80 % of the sunlight incident on such a 'fiber optic mini-dish' could be transported to a central receiver via the glass fibers. A considerable fraction of the



losses is caused by attenuation in the fibers (Feuermann and Gordon, 1998; Jaramillo, et al., 1998).

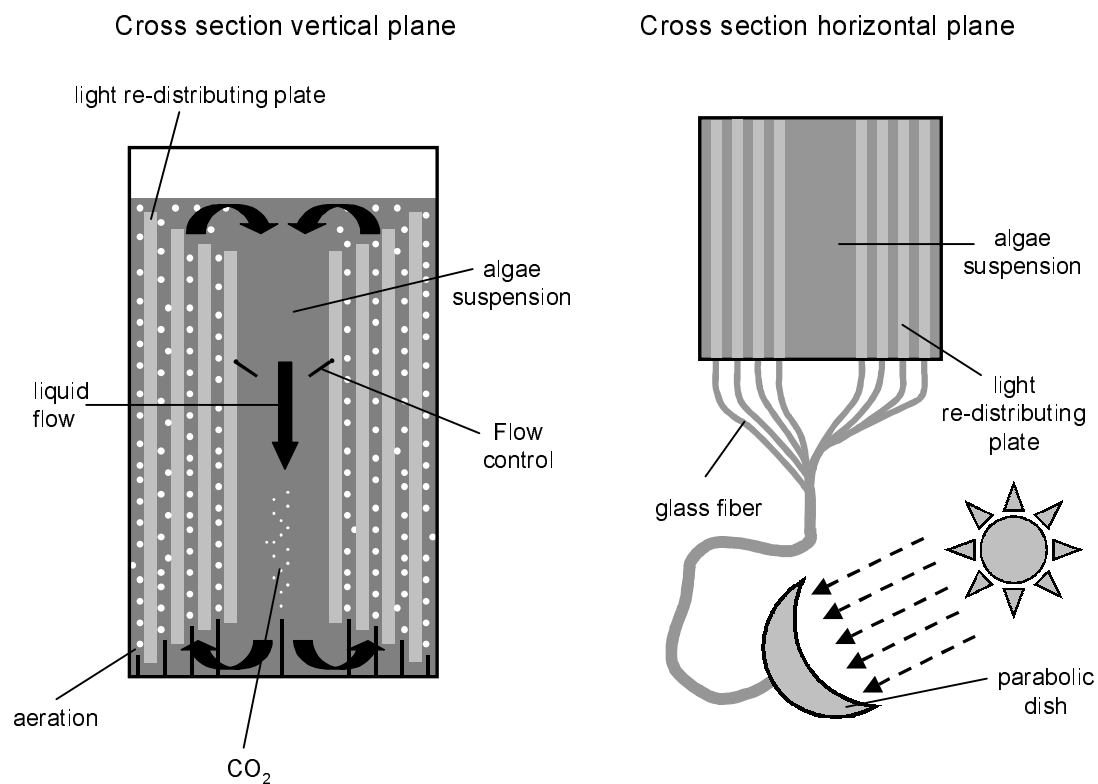


Figure 7.5. Design of a rectangular air-lift photobioreactor with light re-distributing plates and external light collection.

The design of a photobioreactor with a light re-distributing system will be a great challenge for process engineers. Mori (1985) used a vertical (bubble) column with a large number of glass fibers fixed axially. Ogbonna et al. (1999) replaced the fibers with a few solid transparent bars (glass or quartz) and used a stirred tank reactor. Both systems are not scalable since you will need an incredible amount of fibers or bars in a large-scale fermentor. We propose a new kind of system illustrated in Figure 7.5. It is a rectangular air-lift photobioreactor with a large number of light re-distributing plates fixed a few centimeters from each other. Mixing will be provided by air injected between adjacent plates and the culture liquid will rise in between. Only the space between the two center plates is not aerated and will act as a downcomer. This reactor concept is similar to systems described by Usui and Ikenouchi (1997) and Javanmardian and Palsson (1991). In our system, however, the culture volume as a whole is mixed.

The rectangular air-lift bioreactor (Figure 7.5) could be made in a cylindrical way too. In a rectangular system, however, it seems easier to connect the glass fibers to the light re-distributing plates. The plates can be connected to the sides of the reactor and the fibers can be connected to the plates at these sides. Ideas already exist for the design of the light re-distributing plates and the connections between the fibers and the plates (Csögör, et al., 2001). This design needs to be done by optical engineers in close collaboration with bioprocess engineers. Dimensional calculations have been done and are presented in Table 7.7. From these dimensions it appears the system can be scaled to more than hundred cubic meters of culture volume. After optimizing the air-lift type of mixing by changing the gas flow rate and the downcomer area, only one regulatory unit for carbon dioxide supply, pH control, nutrients supply, culture dilution and temperature control will suffice. This is a big advantage in comparison to existing systems as explained in the preceding section. In addition, such a system can be sterilized using steam and/or chemicals because the materials used will be only stainless steel and glass. As a result, long-term large-scale cultivation of monocultures of attractive photoautotrophic cultures will become possible.

Table 7.7. Dimensions of conceptual rectangular air-lift reactor with light re-distributing plates.

total volume	252.5 m <sup>3</sup>
width	5.05 m
depth	5 m
height	10 m
thickness plates	0.03 m
distance between plates	0.03 m
# plates	80
surface light re-distributing plates	8000 m <sup>2</sup>
width downcomer	0.25 m
liquid volume	132.5 m <sup>3</sup>
specific light-exposed surface	60.4 m <sup>2</sup> m <sup>3</sup>

Besides parabolic mirrors also a large number of flat mirrors, heliostat field (Kribus, et al., 1998), could be used to increase the PFD falling on a large number of tall vertical reactors. The big advantage of this possibility is that no light is lost during ‘transport’ through air. A conceptual design of such a system is shown in Figure 7.6 and dimensional calculations are presented in Table 7.8. In this set-up it is essential to have an outer surface as large as possible

and therefore it is best to have a large number of small diameter columns. In this design with 255 columns of 10 m height and 0.1 m diameter (Table 7.8) the liquid volume is 22 m<sup>3</sup>. Again via an air-lift system the liquid in all the separate columns can be mixed as a whole. For the mixing it is essential the central downcomer is provided with helical flow promoters (Merchuk, et al., 2000) to create a tangential flow.

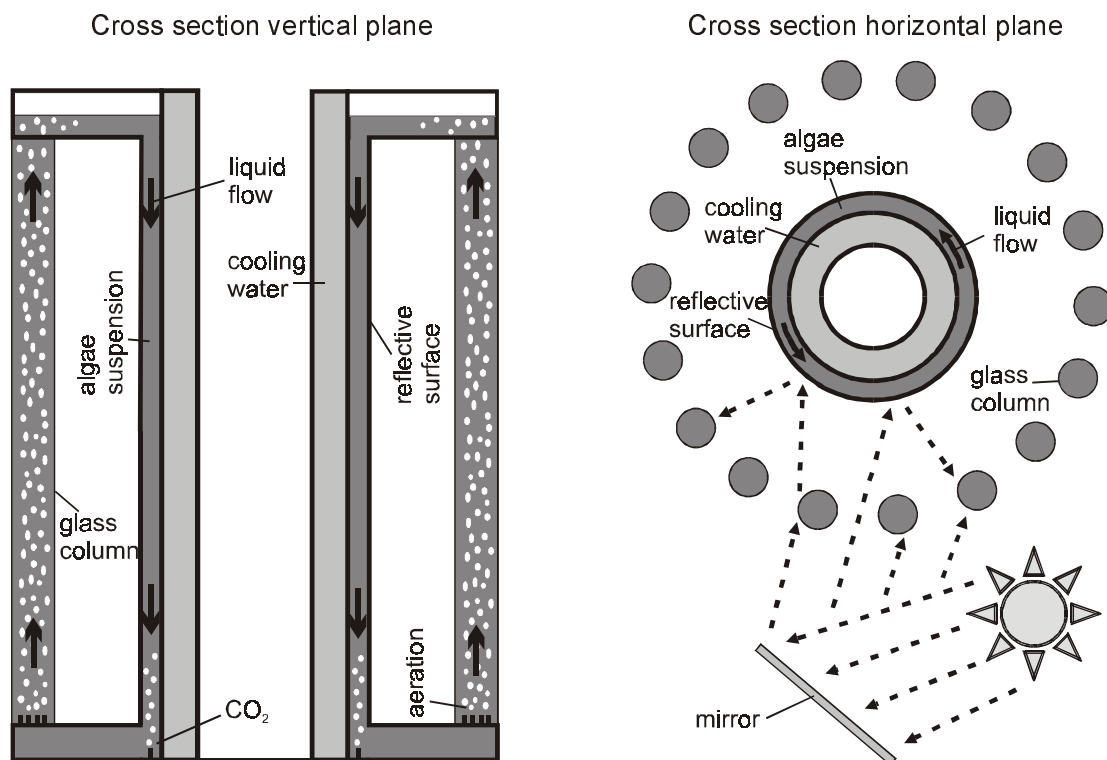


Figure 7.6. Design of a multiple column air-lift photobioreactor with flat mirrors to increase irradiance on reactor surface.

With respect to the L/D cycles, both photobioreactors can be divided into two zones. The downcomers of the reactors are dark zones. The fraction of the downcomer volume to total volume is only 0.095. If the absolute time in this dark zone is not too large, for example 13 s, the biomass yield on light energy will decrease only slightly in comparison to the situation with no dark zone (Barbosa, et al., 2002). Consequently, the liquid velocity in the downcomer should be 0.77 m s<sup>-1</sup> and the upward liquid velocity between the plates (Figure 7.5) or in the columns (Figure 7.6) is 0.08 m s<sup>-1</sup>. As a result, the residence time in the risers is 2 minutes. The second L/D cycle is found inside the risers. Depending on the biomass concentration a light gradient develops and due to the rising air algae move quickly through this gradient. These cycles can be compared to those found in flat panel reactors. The only difference is a

net upward liquid movement of  $0.08 \text{ m s}^{-1}$  in the air-lift bioreactor. Probably this net axial velocity will decrease lateral transport to some extent.

Table 7.8. Dimensions of conceptual air-lift reactor with multiple columns.

total volume (= liquid volume)	22.14 m <sup>3</sup>
height	10 m
diameter columns	0.1 m
# columns	255
surface columns	801 m <sup>2</sup>
outer diameter downcomer	4.058 m
inner diameter downcomer	4.025 m
width downcomer	1.66 cm
specific light-exposed surface	36.2 m <sup>2</sup> m <sup>3</sup>

The similarity with flat panel photobioreactors allows an estimation of reactor productivity. The hydrodynamics of the rectangular air-lift reactor with light re-distributing plates resemble those in flat panels and also the light-path length is similar. Consequently, L/D cycles are very short and a high biomass density, up to  $20 \text{ g dw L}^{-1}$ , can be maintained together with a high PFD at the light re-distributing plates. Under these operational parameters a photosynthetic yield of 15 % can be reached with PFDs of  $2000 \mu\text{mol m}^{-2} \text{ s}^{-1}$  (Richmond, 2000) at the reactor surface. In order to estimate the productivity we aimed at a daily average PFD of  $1200 \mu\text{mol m}^{-2} \text{ s}^{-1}$  at the surface of the light re-distributing plates. Together with other data (Appendix VI) a productivity of  $193.5 \text{ ton dw yr}^{-1}$  of *Spirulina* biomass was estimated.

The high-tech design of the air-lift photobioreactor with light re-distributing plates and solar collectors seems to be very expensive. To produce  $193.5 \text{ ton yr}^{-1}$  direct solar beam radiation from a ground surface of  $22678 \text{ m}^2$  (= 85 m radius circular field) needs to be collected (Appendix VI). At the moment, cost of optical fiber is  $1 \text{ US\$ m}^{-1}$ , which implies fiber costs of  $1699 \text{ US\$ m}^{-2}$  for a light collection field with 85 m radius (Feuermann and Gordon, 1998). Costs of optical fiber are expected to decrease with a factor 10 to 100 at sufficiently large-volume production and this would reduce total costs to 3.85 to 0.385 million US\$ for the 85 m radius field. At the moment production costs of *Nannochloropsis*, rich in eicosapentaenoic acid, is estimated at  $50 \text{ kg}^{-1} \text{ dw}$  or more (Cheng-Wu, et al., 2001). This means total investment and production costs of 96.76 million US\$ is allowed for our design during a 10 years lifetime. An investment of 3.85 million US\$ for optical fiber therefore seems

reasonable, especially when it is considered the lifetime of optical fiber could be much longer than 10 years.

In addition to light collection, total power dissipation in this system could be costly. A power dissipation of  $334 \text{ W m}^{-3}$  is needed to provide sufficient turbulence and this adds up to  $0.640 \text{ TJ yr}^{-1}$  for the whole reactor (Appendix IV). This is equal to 14 % of the solar energy fixed inside the biomass produced,  $4.56 \text{ TJ yr}^{-1}$  (Appendix VI). Although these numbers seem to be very high, they are comparable to conventional photobioreactors. Especially, when it is considered that the volumetric productivity in this design is much higher than in conventional reactors. In other words, it would be safer to express the power dissipation per amount of biomass produced,  $3.33 \text{ KJ g}^{-1} \text{ dw}$  in our design.

A similar estimation can be done for the multiple column air-lift design (Table 7.8). Camacho et al. (1999) and Mirón et al. (2000a) provided the only useful data from which yields of  $0.82$  and  $0.84 \text{ g dw mol}^{-1}$  were obtained in  $0.096$  and  $0.193 \text{ m}$  diameter vertical column reactors, respectively (Table 7.6). This corresponds to a PE of approximately 9 % on PAR basis. For our design we took a PE of 10 %. Based on this efficiency we calculated a productivity of  $12.92 \text{ ton dry Spirulina biomass yr}^{-1}$  (Appendix VI) and a  $1817 \text{ m}^2$  ground surface for the heliostat field.

An important advantage of these compact reactor designs is the possibility of efficient temperature control. For the rectangular air-lift design with light re-distributing plates cooling devices will not be necessary because thermal radiation can be removed and possibly used during collection and concentration of sunlight. Furthermore, the contact surface between bioreactor and environment is relatively small. Heating of the culture liquid will be much less costly and heating could be coupled to heat collected in the cooling mode of reactor operation. Temperature control of the multiple-column air-lift reactor will be less efficient because of the large contact surface between bioreactor and environment.

Temperature control allows lowering of the temperature during the night to decrease respiratory activity (Torzillo, et al., 1991). In addition, in the early morning temperature can be quickly increased to optimal values. As a consequence high PFDs can be utilized more efficiently by the algae (Lee, et al., 1985; Davison, 1996) and the solar collectors or flat mirrors can be inclined facing the sun to start the day with a high PFD inside the reactor resulting in a high biomass productivity. This aspect is particularly interesting in areas with big temperature fluctuations between day and night. Also in colder areas or during a cold season temperature control will allow optimal temperatures under high PFDs which would normally result in photoinhibition (Jensen and Knutsen, 1993).

### ***Prospects for artificial illumination***

Sunlight is implicitly assumed to be the only suitable source of light energy in this study. But, it is often suggested to use artificial illumination for the phototrophic production of high-value compounds. In Appendix VII it is calculated what is needed to provide artificial illumination equivalent to the rectangular air-lift design with 8000 m<sup>2</sup> light re-distributing plates. At the moment fluorescent tubes are the most practical light source for such an application and 92492 tubes of 1.2 m (36 W) are needed. The costs of the lamps and their power consumption is estimated at 2.17 million US\$ per year. Also a one-time investment of 1.10 million US\$ is needed for the power supplies. The costs of replacement of the fluorescent tubes twice a year is very labor intensive, but these are not considered yet.

In addition to economic arguments, it is practically almost impossible to install thousands of lamps inside a large-scale photobioreactor while allowing sufficient mixing of the culture liquid. And, from an environmental point of view, a lot of energy is wasted using artificial illumination. Almost 70 % of the electrical power consumed by the lamps is not converted to light. Even worse, electricity production from natural gas or coal leads to more energy wasting and carbon dioxide production. In the future more efficient lamps could become available such as light-emitting diodes (LEDs) or sulfur lamps, which also have a much longer lifetime. In that scenario, applicability of artificial illumination most likely will be limited to the small-scale production of high-value compounds depended on very specific cultivation conditions.

### **Appendix I: Light/dark frequency in air-lift loop reactors**

The liquid circulation velocity in air-lift loop reactors was calculated according to the procedure of Chisti (1989). The superficial liquid velocity in the riser was calculated with Eq. 7.4.

$$\text{Eq. 7.4} \quad v_{lsr} = \left[ \frac{2 \cdot g \cdot h_d \cdot (\varepsilon_{gr} - \varepsilon_{gd})}{K_B \cdot \left(\frac{A_r}{A_d}\right)^2 \cdot \frac{1}{(1 - \varepsilon_{gd})^2}} \right]^{0.5} \quad [\text{m s}^{-1}]$$

The hold-up in the riser and downcomer was estimated with the following equations (Eq. 7.5 and Eq. 7.6):

$$\text{Eq. 7.5} \quad \varepsilon_{gr} = \frac{v_{gsr}}{0.24 + 1.35 \cdot (v_{gsr} + v_{lsr})^{0.93}} \quad [-]$$

$$\text{Eq. 7.6} \quad \varepsilon_{gd} = 0.89 \cdot \varepsilon_{gr} \quad [-]$$

The parameters  $h_d$ , the height of liquid dispersion, and  $K_B$ , the friction loss coefficient for the bottom zone, could be calculated using reactor dimensions (Chisti, 1989) and the hold-up. Since  $v_{lsr}$  appears also in Eq. 7.4 an initial estimation has to be made followed by an iteration procedure. Liquid circulation time finally is calculated with Eq. 7.7.

$$\text{Eq. 7.7} \quad t_c = \frac{V_l}{v_{lsr} \cdot A_r \cdot (1 - \varepsilon_{gr})} \quad [s]$$

## Appendix II: Light/dark frequency in bubble columns

Joshi and Sharma (1979) developed a flow model for bubble columns in the heterogeneous regime and were able to describe the average liquid circulation velocity ( $v_{lc}$ ) fairly well by means of Eq. 7.8.

$$\text{Eq. 7.8} \quad v_{lc} = 1.31 \cdot [g \cdot T_v \cdot (v_{gs} - \varepsilon_g \cdot v_{bs})]^{1/3} \quad [m \cdot s^{-1}]$$

The average liquid circulation time ( $t_c$ ) then is calculated with Eq. 7.9 since the length traveled within a circulation cell is about two times the diameter.

$$\text{Eq. 7.9} \quad t_c \approx \frac{2 \cdot T_v}{v_{lc}} \quad [s]$$

The fractional gas hold-up ( $\varepsilon_g$ ) can be estimated by means of Eq. 7.10 (Chisti, 1989).

$$\text{Eq. 7.10} \quad \varepsilon_g = 2.47 \cdot v_{gs}^{0.97} \quad [-]$$

The slip velocity ( $v_{bs}$ ) of the gas bubbles in the riser is assumed to be equal to the stationary rise velocity (Heijnen and Riet, 1984),  $0.25 \text{ m s}^{-1}$ .

Merchuk et al. (1998) developed a method to calculate the surface renewal rate (Danckwerts, 1951),  $s$ , and the mean residence time,  $t_{sc}$ , at the wall of a bubble column (Eq. 7.11 and Eq. 7.12). This was used as an estimation for the average time an algal cell is exposed to light at the reactor wall.

$$\text{Eq. 7.11} \quad k_l = \sqrt{ID \cdot s} \quad [m \cdot s^{-1}]$$

$$\text{Eq. 7.12} \quad t_{sc} = \frac{1}{s} \quad [s]$$

The diffusion coefficient of water in water (ID) was estimated with the Wilke-Chang technique (Perry and Greene, 1984). The mass transfer coefficient ( $k_l$ ) was calculated by means of the heat transfer coefficient ( $h$ ) using Eq. 7.13, the Colburn analogy (Bird, et al., 1960).

$$\text{Eq. 7.13} \quad \frac{h}{C_p} \cdot \text{Pr}^{2/3} = k_l \cdot \rho \cdot \text{Sc}^{2/3}$$

$$\text{Eq. 7.14} \quad \text{Sc} = \frac{\eta}{\rho \cdot \text{ID}} \quad [-]$$

$$\text{Eq. 7.15} \quad \text{Pr} = \frac{\eta \cdot C_p}{\lambda} \quad [-]$$

The heat transfer coefficient was calculated using a relationship (Eq. 7.16) developed for bubble columns with only the superficial gas velocity as a variable (Deckwer and Field, 1992).

$$\text{Eq. 7.16} \quad \text{St} = 0.1 \cdot (\text{Re} \cdot \text{Fr} \cdot \text{Pr}^2)^{-0.25} \quad [-]$$

$$\text{Eq. 7.17} \quad \text{St} = \frac{h}{v_{gs} \cdot \rho \cdot C_p} \quad [-]$$

$$\text{Eq. 7.18} \quad \text{Re} \cdot \text{Fr} = \frac{v_{gs}^3 \cdot \rho}{g \cdot \eta} \quad [-]$$

### Appendix III: Light/dark frequency in tubular photobioreactors

Following Fernandez et al. (2000) the characteristic turbulence velocity (Davies, 1972) was used to estimate average radial velocity,  $v_{lr}$ , of a fluid element (Eq. 7.19).

$$\text{Eq. 7.19} \quad v_{lr} = \sqrt{\frac{\tau_0}{\rho}} \quad [\text{m s}^{-1}]$$

$$\text{Eq. 7.20} \quad \tau_0 = C_f \cdot \frac{1}{2} \cdot \rho \cdot v_{ls}^2 \quad [\text{N m}^{-2}]$$

The Fanning friction factor,  $C_f$ , is calculated with the Blasius equation (Eq. 7.21).

$$\text{Eq. 7.21} \quad C_f = 0.079 \cdot \text{Re}^{-1/4} \quad [-]$$



$$\text{Eq. 7.22} \quad \text{Re} = \frac{\rho \cdot d \cdot v_{ls}}{\eta} \quad [-]$$

If a dark zone is taken comprising two thirds of the total volume the light/dark interface is a fictional tube of diameter  $d_{2/3}$  (Eq. 7.23).

$$\text{Eq. 7.23} \quad d_{2/3} = \sqrt{\frac{2}{3}} \cdot d \quad [\text{m}]$$

The specific interfacial liquid flow,  $Q_{L/D}'$ , towards the light or dark zone now can be calculated using Eq. 7.24.

$$\text{Eq. 7.24} \quad Q_{L/D}' = 0.5 \cdot \pi \cdot d_{2/3} \cdot v_{lr} \quad [\text{m}^3 \text{ m}^{-1} \text{ s}^{-1}]$$

The factor 0.5 is introduced because half of the liquid flow crossing the light/dark interface is directed towards the tube center and the other half towards the tube wall. Finally we can calculate the liquid circulation time.

$$\text{Eq. 7.25} \quad t_c = \frac{0.25 \cdot \pi \cdot d^2}{Q_{L/D}'} \quad [\text{s}]$$

#### Appendix IV: Power dissipation aeration bubble columns and flat panels

Roels and Heijnen (1980) showed that the power dissipation,  $P_g$  in W, in bubble column reactors can be calculated from the change of entropy of the gas (Eq. 7.26).

$$\text{Eq. 7.26} \quad P_g = F_g \cdot R \cdot T \cdot \ln\left(\frac{p_s}{p_t}\right) \quad [\text{W}]$$

$F_g$  is the molar gas flow rate and  $p_s$  and  $p_t$  are the pressures at the sparger and the top of the reactor liquid, respectively. Usually  $p_t$  is approximately equal to the standard pressure  $p_0$  and  $p_s$  can be calculated using Eq. 7.27.

$$\text{Eq. 7.27} \quad p_s = p_t + g \cdot \rho_l \cdot h_l \quad [\text{Pa}]$$

For a flat panel reactor aerated at  $4.2 \text{ L L}^{-1} \text{ min}^{-1}$  and an estimated non-aerated liquid height,  $h_l$ , of 0.5 m (Hu and Richmond, 1996) we calculated a power dissipation of  $334 \text{ W m}^{-3}$  ( $T = 30 \text{ }^\circ\text{C}$ ). This is almost the same as a dissipation of  $331 \text{ W m}^{-3}$  at an aeration rate of  $3 \text{ L L}^{-1} \text{ min}^{-1}$  at a given height of 0.7 m (Hu, et al., 1996a). Also for the  $132.5 \text{ m}^{-3}$  rectangular air-lift design with light re-distributing plates we anticipated a power consumption of  $334 \text{ W m}^{-3}$  during 12 hours per day for 335 days per year:  $0.640 \text{ TJ yr}^{-1}$ .

## Appendix V: Estimation photosynthetic efficiency tubular photobioreactors

Fernandez et al. (1998) reported extensively on the biomass yield on light energy ( $Y_{dw,E}$ ). Yields higher than  $2 \text{ g mol}^{-1}$  were reported. In comparison with the other data in Table 7.6 this seems too high. We recalculated  $Y_{dw,E}$  differently, as will be explained below. In their work the quantum scalar irradiance  $E_w$  in  $\text{mol m}^{-2} \text{ d}^{-1}$  was measured with a spherical sensor inside the water pool in which the tubes were immersed (Fernandez, et al., 1998). This can be recalculated to  $F_{vol,max}$ , the amount of photons (PAR) absorbed per volume per day, using the tube radius  $R$ :

$$\text{Eq. 7.28} \quad F_{vol,max} = \frac{2 \cdot E_w}{R \cdot \pi} \quad [\text{mol m}^{-3} \text{ d}^{-1}]$$

This equation was deduced by Comez et al. (1998) and Grima et al. (1997) assuming all light is absorbed within the culture. In addition, it was deduced for a diffuse flux in one plane (2-dimensional) (Evers, 1991; Grima, et al., 1997). In practice the light field, originating from the sun, was 3 dimensional and consisted of a monodirectional fraction (direct beams) and a diffuse fraction. As mentioned,  $E_w$  was measured with a spherical sensor (Fernandez, et al., 1998) and Miron et al. (2000b) showed that  $F_{vol,max}$  calculated as such yielded similar results as two different approaches. As a result,  $F_{vol,max}$  and the volumetric productivity,  $P_{dw}$  in  $\text{g m}^{-3} \text{ d}^{-1}$ , can be combined to obtain a good estimate of  $Y_{dw,E}$  (Eq. 7.29).

$$\text{Eq. 7.29} \quad Y_{dw,E} = \frac{P_{dw}}{F_{vol,max}} \quad [\text{g mol}^{-1}]$$

If we compare the new procedure above with the original calculation procedure of Fernandez et al. (1998) it follows that we did not use the estimated average PFD inside the bioreactor, but the total photon flux entering the tubes.

## Appendix VI: estimation productivity air-lift reactor with light re-distributing plates and multiple column air-lift reactor

The light-exposed surface of the air-lift reactor with light re-distributing plates is  $8000 \text{ m}^2$  (Table 7.7). We aimed at a daily average irradiance of  $1200 \text{ } \mu\text{mol m}^{-2} \text{ s}^{-1}$  coming from the plates, corresponding to  $260.9 \text{ W m}^{-2}$  ( $4.57 \text{ } \mu\text{mol J}^{-1}$  for sunlight, Thimijan and Heins, 1983). Taking a 12 hours day period the daily input of PAR radiation becomes  $90.75 \text{ GJ}$ . Furthermore we assumed the reactor will be down from December 16 until January 15 (335

days) and as a result the yearly input is 30.40 TJ. Finally, assuming a PE of 15 % and a caloric value of Spirulina of 23.6 kJ.g<sup>-1</sup> (Torzillo, et al., 1991) we obtain a productivity of 193.5 ton dw yr<sup>-1</sup>.

However, to be able to collect 30.40 TJ PAR per year from January 16 until December 15, ground surface is needed. First, PAR radiation (photosynthetic active radiation, 400 - 700 nm) should be converted to solar radiation. Sunlight consists for 42.9 % of PAR (Thimijan and Heins, 1983) and the yearly PAR input of 30.40 TJ corresponds to 70.86 TJ solar radiation. Next, we used the monthly means of daily direct beam irradiance on a horizontal surface in Sevilla (southern Spain) during the years 1996 and 1997 ([www.Satel-light.com](http://www.Satel-light.com), the European Database of Daylight and Solar Radiation, Fontoynt, et al., 1998), on average 11.66 MJ m<sup>-2</sup> d<sup>-1</sup> between January 16 and December 15. With these values we calculated a horizontal ground surface of 18142 m<sup>2</sup> from which all direct beam irradiance should be collected and transported to the photobioreactor via optical fibers. We anticipated a loss of 20 % of sunlight during collection and transport to the reactor. As a result, the ground surface covered with solar collectors should be increased to 22678 m<sup>2</sup>. This is equal to a circular field with a radius of 84.96 m.

The light-exposed surface of the multiple-column air-lift reactor is 801.1 m<sup>2</sup> (Table 7.8). The same estimations were done as described above, only a PE of 10 % was used. This resulted in a productivity of 12.92 ton dw yr<sup>-1</sup>. For this direct solar beam irradiance on a ground surface of 1817 m<sup>2</sup> should be redirected to the tube surfaces using mirrors, a heliostat field.

## **Appendix VII: Costs artificial illumination**

In order to estimate the costs of artificial illumination a very efficient fluorescent tube was chosen: the Britegro 2023, 1.2 m length and 36 W power consumption (Osram-Sylvania, Germany). This tube converts 28 % of the electrical energy into photosynthetic active radiation (PAR) and delivers 4.10 mol d<sup>-1</sup>. In Appendix VI it is estimated that the rectangular air-lift reactor with light re-distributing plates can distribute 30.40 TJ yr<sup>-1</sup>, corresponding to 13.92 Mmol yr<sup>-1</sup>. Artificial illumination can be used 24 hours a day the whole year round and therefore 92492 tubes are needed to provide a yearly PAR input of 30.40 TJ yr<sup>-1</sup>. The lifetime of the tubes was 300 days at 50 % loss of output. For this reason, it was incorporated the tubes should be replaced twice a year. The price of the lamps was US\$ 5.23 per piece and the cost of electricity was estimated at 0.011 US\$ MJ<sup>-1</sup>.

## Nomenclature

chl	chlorophyll	
dw	dry weight	
L/D	light/dark	
PAR	photosynthetic active radiation, 400 – 700 nm	
PE	photosynthetic efficiency	
$\eta$	dynamic viscosity	[N s m <sup>-2</sup> ]
$\varepsilon$	duration light period as a fraction of full cycle duration	[-]
$\tau_0$	wall shear stress	[N m <sup>-2</sup> ]
$\varepsilon_g$	fractional gas hold-up	[-]
$\varepsilon_{gd}$	fractional gas hold-up downcomer	[-]
$\varepsilon_{gr}$	fractional gas hold-up riser	[-]
$a_{chl-a}$	wavelength-dependent absorption coefficient, chl- <i>a</i> basis	[m <sup>2</sup> g <sup>-1</sup> ]
$a^*_{prot}$	spectrally averaged absorption coefficient, protein basis	[m <sup>2</sup> g <sup>-1</sup> ]
$A_d$	cross sectional area downcomer	[m <sup>2</sup> ]
$A_R$	cross sectional area reactor	[m <sup>2</sup> ]
$A_r$	cross sectional area riser	[m <sup>2</sup> ]
$C_b$	bottom clearance air-lift reactor	[m]
$C_f$	Fanning friction factor	[-]
$d$	tube diameter	[m]
$Fr$	Froude dimensionless group	[-]
$h_d$	liquid dispersion height	[m]
$h_l$	non-aerated liquid height	[m]
$K_B$	friction loss coefficient bottom zone air-lift reactor	[-]
$P_g$	dissipated power gas flow	[W]
$Pr$	Prandtl dimensionless group	[-]
$p_s$	pressure at sparger	[N m <sup>-2</sup> ]
$p_t$	pressure top reactor	[N m <sup>-2</sup> ]
$Re$	Reynolds dimensionless group	[-]
$Sc$	Schmidt dimensionless group	[-]
$St$	Stanton dimensionless group	[-]
$t_{sc}$	average surface contact time	[s]
$T_v$	vessel diameter	[m]
$V_l$	liquid volume reactor	[m <sup>3</sup> ]

$Y_{dw,E}$	biomass yield on light energy, dry weight per photons	$[g\ mol^{-1}]$
$Y_{prot,E}$	biomass yield on light energy, protein per photons	$[g\ mol^{-1}]$
$d_p$	penetration depth light	$[m]$
$t_c$	circulation time = duration L/D cycle	$[s]$
$t_l$	duration light period L/D cycle	$[s]$
$R$	tube radius	$[m]$
$P_{dw}$	volumetric productivity, dry weight basis	$[g\ m^{-3}\ d^{-1}]$
$\rho$	density	$[kg\ m^{-3}]$
$[chl-a]$	chlorophyll- <i>a</i> concentration	$[g\ m^{-3}]$
$h$	heat transfer coefficient	$[W\ m^{-2}\ K^{-1}]$
PFD	photon flux density in PAR range	$[\mu mol\ m^{-2}\ s^{-1}]$
$PFD_{in}$	photon flux density on reactor surface	$[\mu mol\ m^{-2}\ s^{-1}]$
$F_{vol,max}$	time-averaged volumetric photon absorption rate	$[mol\ m^{-3}\ d^{-1}]$
$\lambda$	thermal conductivity	$[W\ m^{-1}\ K^{-1}]$
$C_p$	heat capacity	$[J\ kg^{-1}\ K^{-1}]$
$E_w$	time-averaged PFD as measured with spherical sensor	$[mol\ m^{-2}\ d^{-1}]$
$\mu$	specific growth rate	$[h^{-1}]$
$F_g$	molar gas flow	$[mol\ s^{-1}]$
ID	diffusivity	$[m^2\ s^{-1}]$
$k_l$	mass transfer coefficient	$[m\ s^{-1}]$
$Q_{L/D}'$	specific liquid flow light/dark interface	$[m^2\ s^{-1}]$
$s$	surface renewal rate	$[s^{-1}]$
$v_{bs}$	bubble slip velocity	$[m\ s^{-1}]$
$v_{gs}$	superficial gas velocity	$[m\ s^{-1}]$
$v_{gsr}$	superficial gas velocity in the riser	$[m\ s^{-1}]$
$v_{lc}$	liquid circulation velocity	$[m\ s^{-1}]$
$v_{lr}$	liquid radial velocity	$[m\ s^{-1}]$
$v_{ls}$	superficial liquid velocity	$[m\ s^{-1}]$
$v_{lsr}$	superficial liquid velocity in the riser	$[m\ s^{-1}]$
$C_x$	biomass concentration, dry weight basis	$[g\ L^{-1}]$

## **Summarizing discussion**

In this thesis the efficiency of light utilization of microalgae was studied under light/dark cycles encountered in photobioreactors. Phototrophic microorganisms such as microalgae and cyanobacteria could provide valuable compounds. For many of these applications it is essential to use enclosed photobioreactors in which monocultures can be maintained for an extended time. Because light energy is the growth limiting substrate, light supply plays a key role in photobioreactor design.

The light regime inside photobioreactors is complicated: algae are exposed to high-intensity sunlight in the so-called photic zone close to the reactor surface and complete darkness in the interior. As a result of mixing of the reactor liquid, algae are exposed to light-gradient/dark cycles and this fluctuating light regime could have a considerable influence on the efficiency of light utilization for biomass growth, also referred to as the photosynthetic efficiency.

Even under low-intensity sunlight most photosynthetic microorganisms intercept too much light at the light-exposed surface. The excitation energy is only partly utilized in the photosynthetic apparatus and a considerable amount of light energy is lost as heat or fluorescence. It is often suggested that intermittent illumination, i.e. light/dark cycling, is the most practical mode to dilute strong light and could result in effective light utilization by algal cultures (Richmond, 2000). This effect of 'light integration' has been demonstrated under high-frequency fluctuating light (> 10 Hz) and is also referred to as the 'flashing-light effect' (Kok, 1953). However, such a light regime is very difficult to establish in large-scale photobioreactors (Powell, et al., 1965; Laws, et al., 1983).

The present study therefore was limited to medium-frequency light/dark cycles. These have a duration of a few seconds to 100 s. Only in Chapter 6 experiments were done on the influence of light/dark cycles smaller than 1 s. Medium-duration light/dark cycles will be encountered during scale-up of photobioreactors. For this reason it is essential to understand the relation between medium-duration light/dark cycles and the photosynthetic efficiency. Moreover, it was hoped for that also medium-duration cycles might lead to higher photosynthetic efficiency in the photic zone of photobioreactors in comparison to constant light levels, but clear evidence was still lacking.

In the present study it is clearly shown that medium-duration light/dark cycles do not lead to light integration. The efficiency of light utilization was determined as the yield of biomass, measured as protein, on light energy, measured as 'photosynthetic active radiation' (PAR,

400 - 700 nm). In addition, the quantum yield of photochemistry was determined using pulse-amplitude-modulation (PAM) fluorometry. Both determinations showed that the efficiency of photosynthesis generally is lower during the light period of light/dark cycles in comparison to continuous illumination.

In Chapter 2 it was demonstrated the specific growth rate of two freshwater green algae, *Chlamydomonas reinhardtii* and *Chlorella sorokiniana* decreases after introduction of a dark period in a continuous light regime (square-wave light/dark cycle, Figure 1.13). Moreover, circumstantial evidence was provided that specific light absorption is higher under light/dark cycles. Combining the increase of light absorption with the decrease of growth rate, the photosynthetic efficiency was thought to be lower during the light period of light/dark cycles than during continuous light.

This 'expectation' was confirmed for *Chlamydomonas* by the experiments described in Chapter 3. The biomass yield on light energy, measured as protein per photons, was lowest under light/dark cycles. It was 0.178 - 0.231 g mol<sup>-1</sup> under light/dark cycles with a light period duration half of the cycle duration ( $\epsilon = 0.5$ ), as opposed to 0.307 g mol<sup>-1</sup> under continuous light ( $\epsilon = 1$ ). The decrease in biomass yield was the result of a decrease of the specific growth rate. The specific light absorption coefficient was constant under the light regimes applied.

Additional experiments showed that together with the biomass yield on light energy also the capacity of the photosynthetic apparatus decreased. The photosynthetic capacity was measured as the maximum oxygen production rate. In addition, the quantum yield of photochemistry was found to be lower during the light period of a light/dark cycle in comparison to continuous illumination. Although the decrease in growth rate under light/dark fluctuations could be traced back to the rate of electron transport in the photosynthetic apparatus, it is not known which steps are rate-limiting. Nevertheless, because the light/dark cycles applied were relatively fast it is likely the limitation can be found in the so-called light reactions of photosynthesis, or in pathways immediately following the light reactions, such as carbon dioxide fixation.

In Chapter 2 it was suggested the specific light absorption coefficient of algae cultivated under light/dark cycles is higher than those cultivated under continuous light. This would imply that photoacclimation (Falkowski and LaRoche, 1991) takes place after transfer of algae from a constant photon flux density (PFD) to light/dark cycles. For this reason also the marine green alga *Dunaliella tertiolecta* was investigated together with *Chlamydomonas*. *Dunaliella* has been studied extensively with respect to photoacclimation (Falkowski and

Owens, 1980; Falkowski, et al., 1981) and demonstrated a different strategy of photoacclimation than *Chlamydomonas* (Neale and Melis, 1986). In Chapter 4, however, is described *Dunaliella* behaves similar to *Chlamydomonas*: the biomass yield on light energy is lower under medium-duration light/dark cycles than under cultivation with constant PFD.

These experiments were also extended to higher photon flux densities (PFDs): 600 - 700 → 1100 - 1200  $\mu\text{mol m}^{-2} \text{s}^{-1}$  (Chapter 4). At higher PFDs photoinhibitory damage of algal photosystems could become an important factor. Although photoinhibition was observed this did not have a significant influence on the comparison between continuous and fluctuating light regimes. The biomass yield on light energy and the quantum yield of photochemistry were higher under a constant PFD of 1100 - 1200  $\mu\text{mol m}^{-2} \text{s}^{-1}$  than under light/dark cycles with the same PFD during the light period.

In these experiments it was also demonstrated that the transition from constant PFD to light/dark cycles resulted in a significant increase in the specific absorption coefficient of *Dunaliella* (600 – 1200  $\mu\text{mol m}^{-2} \text{s}^{-1}$ ) and *Chlamydomonas* (1100 – 1200  $\mu\text{mol m}^{-2} \text{s}^{-1}$ ). This acclimation resembles the process of photoacclimation observed after a transition from a high, but constant, photon flux density to a low PFD. It seems likely that a shift from a constant PFD to light/dark cycling leads to a decrease in the (average) reduction state of the photosynthetic apparatus of algae. As a reaction, algae will acclimate increasing their specific light absorbing surface (Durnford and Falkowski, 1997). This could be the reason more light energy is wasted (heat losses) during the light period of light/dark cycles than under constant light.

The efficiency of light utilization was found to be lower under light/dark cycles as is described in Chapters 3 and 4. But it should also be noted that, in the situation the dark period comprises only 20 % (Chapter 3) or 33 % (Chapter 4), the yield was equal to the one determined under continuous illumination. This means a relatively small dark zone can be allowed in photobioreactors without affecting reactor productivity; reactors can be operated at slightly higher biomass densities facilitating downstream processing of the biomass.

The previous observation is related to the fact that the specific growth rate does not decrease linear to a decrease of the ratio between light period and cycle duration ( $\epsilon$ ). At high  $\epsilon$  ( $> 0.67$ ) the specific growth rate decreases less than proportional to  $\epsilon$ . This observation was also described in the regularly cited studies of Lee and Pirt (1981) and Merchuk et al. (1998). They found algae (*Porphyridium* and *Chlorella*) could be in the dark for 6 – 9 s while still exhibiting their maximum growth rate during light/dark cycles of 27 and 40 s duration,



respectively. Nothing was known about the efficiency of light utilization. Based on the work described in this thesis it seems likely that also under their circumstances the biomass yield on light energy under light/dark cycles was not higher, and presumably lower, than obtainable under constant PFD. Moreover, this could be deduced from the inverse proportionality between the maintenance requirement and  $\epsilon$  reported by Lee and Pirt (1981). The increase of the maintenance requirement can be translated into the observation a larger part of the light energy absorbed cannot be utilized for growth. This will lead to a lower yield of biomass on light energy as defined in this thesis.

*Dunaliella tertiolecta* was chosen as a model organism for further research and the effect of cycle duration (10 - 100 s) and light fraction ( $\epsilon$ : 0.1 – 1.0) on the biomass yield was modeled as described in Chapter 5. Light/dark cycles found in air-lift reactors were simulated taking into account the light gradient during the light period (Figure 5.1). This means the light period was characterized by a light gradient going from 1200 to only 50  $\mu\text{mol m}^{-2} \text{s}^{-1}$ . In addition, the cultivation temperature was increased from 20 to 30 °C; 30 °C was found to be the optimum growth temperature for *Dunaliella* (Eppley and Sloan, 1966).

The biomass yield was mainly affected by the light fraction ( $\epsilon$ ), whereas cycle duration only had a small influence (Chapter 5). A statistical model, describing the effect of light fraction and cycle time on the biomass yield was developed. The model predictions correlated well with the more qualitative results described in Chapters 3 and 4. The yield of biomass on light energy was lower under light-gradient/dark cycles ( $\epsilon \leq 0.5$ ) in comparison to a light-gradient only ( $\epsilon = 1$ ). Only in the situation the duration of the light period was relatively short the biomass yield approached the yield under a light gradient without an additional dark period.

The statistical model developed can be used as a tool for the design of photobioreactors. This specific model was particularly suitable for air-lift loop reactors. These can be designed in such a way that the riser comprises the dark zone and the downcomer equals the photic zone or vice versa. Consequently, the time algae spend in the dark and photic zone is dependent on reactor design and the liquid circulation velocity. However, it can be concluded that such designs are inefficient for microalgae cultivation due to presence of medium-duration light/dark cycles (10 – 100 s). Only at high light fractions ( $\epsilon \geq 0.67$ ) biomass yield will be comparable to the yield under a continuous light gradient ( $\epsilon = 1$ ). In addition, the biomass yield under the light gradient (1200  $\rightarrow$  50  $\mu\text{mol m}^{-2} \text{s}^{-1}$ ) without dark period ( $\epsilon = 1$ ) itself is much lower than the yield obtained under a low PFD (58  $\mu\text{mol m}^{-2} \text{s}^{-1}$ ) without dark period: 0.27  $\text{g mol}^{-1}$  as opposed to 1.20  $\text{g mol}^{-1}$  (Chapters 4 and 5). The yield under such low photon

flux densities is a good measure for the maximal efficiency of light utilization, which should be the ultimate target for photobioreactor design.

Because it was clearly shown that light/dark cycles of several seconds to tens of seconds did not result in enhanced photosynthetic activities, short light/dark cycles were studied. In Chapter 6 experiments were presented of *Dunaliella tertiolecta* grown under short (0.19 and 6 s) square-wave light/dark cycles. A significant efficiency increase was observed under 0.19 s cycles in comparison to continuous illumination. These results were discussed with respect to the performance of short light-path photobioreactors operated at high biomass densities. Those reactors are reported to exhibit high photosynthetic efficiencies together with fast liquid circulation (0.2 s) between photic and dark zones inside the photobioreactor (Richmond, 2000). The lab-scale studies described in Chapter 6 therefore are in agreement with these observations.

To summarize, the state-of-the-art of enclosed outdoor photobioreactors was analyzed in Chapter 7. Characteristic examples were selected and studied with respect to the light regime and the photosynthetic efficiency. It is shown that high photosynthetic efficiencies only can be reached at high biomass concentration in short light-path bioreactors. It is demonstrated, however, that these and also the other types of photobioreactors are poorly scalable and/or not applicable for cultivation of monocultures. This is the reason new photobioreactor designs are proposed in which light capture is physically separated from photoautotrophic cultivation. An air-lift type photobioreactor is proposed with many light re-distributing plates connected to solar concentrators via optical fibers. The reactor liquid, up to 100 m<sup>3</sup>, can be mixed as a whole providing many possibilities for controlled cultivation of monocultures of microalgae.



## References

- Aiba S. 1982. Growth kinetics of photosynthetic microorganisms. *Adv Biochem Eng* 23:85-156.
- Akimoto M, Yamada H, Ohtaguchi K, Koide K. 1997. Photoautotrophic cultivation of the green alga *Chlamydomonas reinhardtii* as a method for carbon dioxide fixation and alpha-linolenic acid production. *J Am Oil Chem Soc* 74:181-183.
- Annadurai G. 2000. Design of optimum response surface experiments for adsorption of direct dye on chitosan. *Bioprocess Eng* 23:451-455.
- Apt KE, Behrens PW. 1999. Commercial developments in microalgal biotechnology. *J Phycol* 35:215-226.
- Barber J. 1994. Molecular basis of the vulnerability of photosystem II to damage by light. *Aust J Plant Physiol* 22:201-208.
- Barbosa MJ, Janssen M, Ham N, Tramper J, Wijffels RH. 2002. Microalgae cultivation in air-lift reactors: modeling biomass yield and growth rate as a function of light gradient / dark cycles. Submitted.
- Becker EW. 1994. *Microalgae: biotechnology and microbiology*. Cambridge: Cambridge University Press.
- Benemann JR. 1990. Microalgae products and production: an overview. *J Ind Microbiol* 31:247-256.
- Bird RB, Stewart WE, Lightfoot EN. 1960. *Transport Phenomena*. New York: Wiley. 780 p.
- Borowitzka MA. 1992. Algal biotechnology products and processes- matching science and economics. *J Appl Phycol* 4:267-279.
- Borowitzka MA. 1995. Microalgae as sources of pharmaceuticals and other biologically active compounds. *J Appl Phycol* 7:3-15.
- Borowitzka MA. 1999. Commercial production of microalgae: ponds, tanks, tubes and fermenters. *J Biotechnol* 70:313-321.
- Bosca C, Dauta A, Marvalin O. 1991. Intensive outdoor algal cultures: How mixing enhances the photosynthetic production rate. *Bioresource Technol* 38:185-188.
- Bradford MM. 1976. A rapid and sensitive method for the quantitation of microgram quantities of protein utilizing the principle of protein-dye binding. *Analyt Biochem* 72:248-254.
- Braun AR, Reith JH. 1993. *Algen in de Nederlandse energiehuishouding*. Netherlands Organisation for Energy and the Environment (NOVEM): Report No. 9304.
- Briantais JM, Vernotte C, Picaud M, Krause GH. 1980. Chlorophyll fluorescence as a probe for the determination of the photo-induced proton gradient in isolated chloroplasts. *Biochim Biophys Acta* 591:198-202.
- Bricaud A, Morel A, Prier L. 1983. Optical efficiency factors of some phytoplankters. *Limnol Oceanogr* 28:816-832.
- Camacho FG, Gomez AC, Fernandez FGA, Sevilla JMF, Grima EM. 1999. Use of concentric-tube airlift photobioreactors for microalgal outdoor mass cultures. *Enzyme Microb Tech* 24:164-172.
- Carlozzi P. 2000. Hydrodynamic aspects and *Arthrospira* growth in two outdoor tubular undulating row reactors. *Appl Microbiol Biotechnol* 54:14-22.
- Casadevall E, Dif D, Largeau C, Gudín C, Chaumont D, Desanti O. 1985. Studies on batch and continuous cultures of *Botryococcus braunii*: hydrocarbon production in relation to physiological state, cell ultrastructure, and phosphate nutrition. *Biotechnol Bioeng* 27:286-295.

- Casper-Lindley C, Björkman O. 1998. Fluorescence quenching in four unicellular algae with different light-harvesting and xanthophyll-cycle pigments. *Photosynth Res* 56:277-289.
- Chalker BE. 1980. Modelling light saturation curves for photosynthesis: An exponential function. *J theor Biol* 84:205-215.
- Cheng-Wu Z, Zmora O, Kopel R, Richmond A. 2001. An industrial-size flat plate glass reactor for mass production of *Nannochloropsis* sp. (Eustigmatophyceae). *Aquaculture* 195:35-49.
- Chisti MY. 1989. Airlift bioreactors. London: Elsevier Applied Science. 339 p.
- Chisti MY. 1998. Pneumatically agitated bioreactors in industrial and environmental bioprocessing: Hydrodynamics, hydraulics, and transport phenomena. *Appl Mech Rev* 51:33-112.
- Cohen Z. 1986. Products from microalgae. In: Richmond A, editor. *Handbook of Microalgal Mass Culture*. Boca Raton: CRC. p 421-454.
- Csögör Z, Herrenbauer M, Perner I, Schmidt K, Posten C. 2001. Design of a photo-bioreactor for modelling purposes. *Chem Eng Process* 38:517-523.
- Dankwerts PV. 1951. Significance of liquid-film coefficients in gas absorption. *Ind Eng Chem* 43:1460-1467.
- Dau H. 1994. Short-term adaptation of plants to changing light intensities and its relation to Photosystem II photochemistry and fluorescence emission. *J Photoch Photobio B* 26:3-27.
- Davies JT. 1972. Turbulence phenomena: an introduction to the eddy transfer of momentum, mass and heat, particularly interfaces. New York: Academic Press, 412 p.
- Davison IR. 1996. Minireview: Environmental effects on algal photosynthesis: Temperature. *J Phycol* 27:2-8.
- Deckwer WD, Field RW. 1992. *Bubble Column Reactors*. Chichester: Wiley. 533 p.
- Demmig-Adams B, Adams WW, Logan BA, Verhoeven AS. 1995. Xanthophyll-cycle dependent energy dissipation and flexible photosystem II efficiency in plants acclimated to light stress. *Aust J Plant Physiol* 22:249-260.
- Dubinsky Z, Falkowski PG, Wyman K. 1986. Light harvesting and utilization by phytoplankton. *Plant Cell Physiol* 27:1335-1349.
- Durnford DG, Falkowski PG. 1997. Chloroplast redox regulation of nuclear gene transcription during photoacclimation. *Photosynth Res* 53:229-241.
- Duysens LNM. 1956. The flattening of the absorption spectrum of suspensions, as compared to that of solutions. *Biochim Biophys Acta* 19:1-12.
- Edge R, McGarvey DJ, Truscott TG. 1997. The carotenoids as anti-oxidants - a review. *J Photoch Photobio B* 41:189-200.
- El-Helow ER, Abdel-Fattah YR, Ghanem KM, Mohamad EA. 2000. Application of the response surface methodology for optimizing the activity of an aprE-driven gene expression system in *Bacillus subtilis*. *Appl Microbiol Biotechnol* 54:515-520.
- Emerson R, Lewis CM. 1943. The dependence of the quantum yield of *Chlorella* on wavelength of light. *Am J Bot* 30:165-178.
- Eppley RW, Coatsworth JL. 1966. Culture of the marine phytoplankter, *Dunaliella tertiolecta*, with light-dark cycles. *Arch Mikrob* 55:66-80.
- Eppley RW, Sloan PR. 1966. Growth rates of marine phytoplankton: correlation with light absorption by cell chlorophyll a. *Physiol Plantarum* 19:47-59.
- Escoubas JM, Lomas M, LaRoche J, Falkowski PG. 1995. Light intensity regulation of cab gene transcription is signaled by the redox state of the plastoquinone pool. *Proc Nat Acad Sci (USA)* 92:10237-10241.

- Evers EG. 1991. A model for light-limited continuous cultures: growth, shading, and maintenance. *Biotechnol Bioeng* 38:254-259.
- Falk S, Leverenz JW, Samuelsson G, Oquist G. 1992. Changes in photosystem II fluorescence in *Chlamydomonas reinhardtii* exposed to increasing levels of irradiance in relationship to the photosynthetic response to light. *Photosynth Res* 31:31-40.
- Falkowski PG, Owens TG. 1980. Light-shade adaptation; two strategies in marine phytoplankton. *Plant Physiol* 66:592-595.
- Falkowski PG, Owens TG, Ley AC, Mauzerall D. 1981. Effects of growth irradiance levels on the ratio of reaction centers in two species of marine phytoplankton. *Plant Physiol* 68:969-973.
- Falkowski PG, LaRoche J. 1991. Minireview: Acclimation to spectral irradiance in algae. *J Phycol* 27:8-14.
- Fernandez FGA, Camacho FG, Perez JAS, Sevilla JMF, Grima EM. 1998. Modeling of biomass productivity in tubular photobioreactors for microalgal cultures: Effects of dilution rate, tube diameter, and solar irradiance. *Biotechnol Bioeng* 58:605-616.
- Fernandez FGA, Perez JAS, Sevilla JMF, Camacho FG, Grima EM. 2000. Modeling of eicosapentaenoic acid (EPA) production from *Phaeodactylum tricorutum* cultures in tubular photobioreactors. Effects of dilution rate, tube diameter, and solar irradiance. *Biotechnol Bioeng* 68:173-183.
- Fernandez FGA, Sevilla JMF, Perez JAS, Grima EM, Chisti MY. 2001. Airlift-driven external-loop tubular photobioreactors for outdoor production of microalgae: assesment of design and performance. *Chem Eng Sci* 56:2721-2732.
- Feuermann D, Gordon JM. 1998. Solar fiber-optic mini-dishes: A new approach to the efficient collection of sunlight. *Sol Energy* 65:159-170.
- Feuermann D, Gordon JM. 2001. High-concentration photovoltaic designs based on miniature parabolic dishes. *Sol Energy* 70:423-430.
- Fontoynt M, Dumortier D, Heinemann D, Hammer A, Olseth J, Skartveit A, Ineichen P, Reise Ch, Page J, Roche L, Beyer HG, Wald L. 1998. Satellites: a www server which provides high quality daylight and solar radiation data for western and central Europe. *Proc 9th Conf on Satellite Meteorology and Oceanography* (Paris).
- Genty B, Briantais JM, Baker NR. 1989. The relationship between the quantum yield of photosynthetic electron transport and quenching of chlorophyll fluorescence. *Biochim Biophys Acta* 990:87-92.
- Gilmore AM, Yamamoto HY. 1991. Zeaxanthin formation and energy-dependent fluorescence quenching in pea chloroplasts under artificially mediated linear and cyclic electron transport. *Plant Physiol* 96:635-643.
- Gilmore AM. 1997. Mechanistic aspects of xanthophyll-cycle dependent photoprotection in higher plant chloroplasts and leaves. *Physiol Plantarum* 99:197-209.
- Gitelson A, Qiang H, Richmond A. 1996. Photic volume in photobioreactors supporting ultrahigh population densities of the photoautotroph *Spirulina platensis*. *Appl Environ Microbiol* 62:1570-1573.
- Gomez AC, Camacho FG, Grima EM, Merchuk JC. 1998. Interaction between CO<sub>2</sub>-mass transfer, light availability, and hydrodynamic stress in the growth of *Phaeodactylum tricorutum* in a concentric tube airlift bioreactor. *Biotechnol Bioeng* 60:317-325.
- Goto K, Johnson CH. 1995. Is the cell division cycle gated by a circadian clock? The case of *Chlamydomonas reinhardtii*. *J Cell Biol* 129:1061-1069.

- Grima EM, Sevilla JMF, Perez JAS, Camacho FG. 1996. A study on simultaneous photolimitation and photoinhibition in dense microalgal cultures taking into account incident and averaged irradiances. *J Biotechnol* 45:59-69.
- Grima EM, Camacho FG, Perez JAS, Fernandez FGA, Sevilla JMF. 1997. Evaluation of photosynthetic efficiency in microalgal cultures using averaged irradiance. *Enzyme Microb Tech* 21:375-381.
- Grima EM, Fernandez FGA, Camacho FG, Rubio FC, Chisti MY. 2000. Scale-up of tubular photobioreactors. *J Appl Phycol* 12:355-368.
- Grobbelaar JU. 1989. Do light/dark cycles of medium frequency enhance phytoplankton productivity? *J Appl Phycol* 1:333-340.
- Grobbelaar JU. 1991. The influence of light/dark cycles in mixed algal cultures on their productivity. *Bioresource Technol* 38:189-194.
- Grobbelaar JU, Kroon BMA, Burger-Wiersma T, Mur LR. 1992. Influence of medium frequency light/dark cycles of equal duration on the photosynthesis and respiration of *Chlorella pyrenoidosa*. *Hydrobiologia* 238:53-62.
- Grobbelaar JU. 1994. Turbulence in mass algal cultures and the role of light/dark fluctuations. *J Appl Phycol* 6:331-335.
- Grobbelaar JU, Nedbal L, Tichy V. 1996. Influence of high frequency light/dark fluctuations on photosynthetic characteristics of microalgae photoacclimated to different light intensities and implications for mass algal cultivation. *J Appl Phycol* 8:335-343.
- Gruszecki WI, Wojtowicz K, Krupa Z, Strzalka K. 1994. A direct measurement of thermal energy dissipation in the photosynthetic apparatus during induction of fluorescence. *J Photochem Photobiol B: Biol* 22:23-27.
- Haaland P. 1989. *Experimental design in Biotechnology*. New York and Basel: Marcel Dekker, Inc. 259 p.
- Harris EH. 1989. *The Chlamydomonas sourcebook: a comprehensive guide to biology and laboratory use*. San Diego: Academic Press.
- Heijnen JJ, Riet K. 1984. Mass transfer, mixing and heat transfer phenomena in low viscosity bubble column reactors. *Chem Eng J* 28:B21-B42.
- Horton P, Ruban AV, Walters RG. 1994. Regulation of light harvesting in green plants. *Plant Physiol* 106:415-420.
- Hu Q, Richmond A. 1994. Optimizing the population density in *isochrysis galbana* grown outdoors in a glass column photobioreactor. *J Appl Phycol* 6:391-396.
- Hu Q, Richmond A. 1996. Productivity and photosynthetic efficiency of *Spirulina platensis* as affected by light intensity, algal density and rate of mixing in a flat plate photobioreactor. *J Appl Phycol* 8:139-145.
- Hu Q, Guterman H, Richmond A. 1996a. A flat inclined modular photobioreactor for outdoor mass cultivation of photoautotrophs. *Biotechnol Bioeng* 51:51-60.
- Hu Q, Guterman H, Richmond A. 1996b. Physiological characteristics of *Spirulina platensis* (cyanobacteria) cultured at ultrahigh cell densities. *J Phycol* 32:1066-1073.
- Hu Q, Kurano N, Kawachi M, Iwasaki I, Miyachi S. 1998a. Ultrahigh-cell-density culture of a marine green alga *Chlorococcum littorale* in a flat-plate photobioreactor. *Appl Microbiol Biotechnol* 49:655-662.
- Hu Q, Faiman D, Richmond A. 1998b. Optimal tilt angles of enclosed reactors for growing photoautotrophic microorganisms outdoors. *J Ferment Bioeng* 85:230-236.

- Hu Q, Zarmi Y, Richmond A. 1998c. Combined effects of light intensity, light-path and culture density on output rate of *Spirulina platensis* (Cyanobacteria). *Eur J Phycol* 33:165-171.
- Hwang S, Hansen CL. 1996. Modeling and optimisation in anaerobic bioconversion of complex substrates to acetic and butyric acids. *Biotechnol Bioeng* 54:451-460.
- Janssen M, Kuijpers TC, Veldhoen B, Ternbach MB, Tramper J, Mur LR, Wijffels RH. 1999. Specific growth rate of *Chlamydomonas reinhardtii* and *Chlorella sorokiniana* under medium duration light/dark cycles: 13-87 s. *J Biotechnol* 70:323-333.
- Janssen M, de Bresser L, Baijens T, Tramper J, Mur LR, Snel JFH, Wijffels RH. 2000a. Scale-up aspects of photobioreactors: effects of mixing-induced light/dark cycles. *J Appl Phycol* 12:225-237.
- Janssen M, de Winter M, Tramper J, Mur LR, Snel JFH, Wijffels RH. 2000b. Efficiency of light utilization of *Chlamydomonas reinhardtii* under medium-duration light/dark cycles. *J Biotechnol* 78:123-137.
- Janssen M, Slenders P, Tramper J, Mur LR, Wijffels RH. 2001. Photosynthetic efficiency of *Dunaliella tertiolecta* under short light/dark cycles. *Enzyme Microb Tech* 29:298-305.
- Jaramillo OA, Arriaga LG, Sebastian PJ, Fernandez AM, Del Rio JA. 1998. Application of fiber optics in the hydrogen production by photoelectrolysis. *Int J Hydrogen Energy* 23:985-993.
- Javanmardian M, Palsson BO. 1991. High-density photoautotrophic algal cultures: design, construction and operation of a novel photobioreactor system. *Biotechnol Bioeng* 38:1182-1189.
- Jensen S, Knutsen G. 1993. Influence of light and temperature on photoinhibition of photosynthesis in *Spirulina platensis*. *J Appl Phycol* 5:495-504.
- Joshi B, Sharma MM. 1979. A circulation cell model for bubble column. *Trans IChemE* 57:244-252.
- Kana TM, Geider RJ, Critchley C. 1997. Regulation of photosynthetic pigments in micro-algae by multiple environmental factors: a dynamic balance hypothesis. *New Phytol* 137:629-638.
- Kirk JTO. 1994. Light and photosynthesis in aquatic ecosystems. Cambridge: Cambridge University Press. 509 p.
- Kok B. 1953. Experiments on photosynthesis by *Chlorella* in flashing light. In: Burlew JS, editor. *Algal Culture*. Washington: Carnegie Institution of Washington, Pub 600. p 63-75.
- Kooten van O, Snel JFH. 1990. The use of chlorophyll fluorescence nomenclature in plant stress physiology. *Photosynth Res* 25:147-150.
- Kribus A, Krupkin V, Yogev A, Spirkl W. 1998. Performance limits of heliostat fields. *Transactions of the ASME* 120:240-246.
- Kromkamp J, Limbeek M. 1993. Effect of short-term variation in irradiance on light harvesting and photosynthesis of the marine diatom *Skeletonema costatum*: a laboratory study simulating vertical mixing. *J gen Microbiol* 139:1-8.
- Laws EA, Terry KL, Wickman J, Chalup MS. 1983. A simple algal production system designed to utilize the flashing light effect. *Biotechnol Bioeng* 25:2319-2335.
- Lee YK, Pirt SJ. 1981. Energetics of photosynthetic algal growth: Influence of intermittent illumination in short (40s) cycles. *J gen Microbiol* 124:43-52.
- Lee YK, Tan HM, Hew CS. 1985. The effect of growth temperature on the bioenergetics of photosynthetic algal cultures. *Biotechnol Bioeng* 27:555-561.
- Lee YK, Ding SY, Low C-S, Chang Y-C, Forday WL, Chew P-C. 1995. Design and performance of an  $\alpha$ -type tubular photobioreactor for mass cultivation of microalgae. *J Appl Phycol* 7:47-51.
- Lefebvre S, Guy C. 1999. Characterization of bubble column hydrodynamics with local measurements. *Chem Eng Sci* 54:4895-4902.



- Masojidek J, Torzillo G, Koblížek M, Kopecký J, Bernardini P, Sacchi A, Komenda J. 1999. Photoadaptation of two members of the Chlorophyta (*Scenedesmus* and *Chlorella*) in laboratory and outdoor cultures: changes in chlorophyll fluorescence quenching and the xanthophyll cycle. *Planta* 209:126-135.
- Masojidek J, Torzillo G, Kopecký J, Koblížek M, Nidiaci L, Komenda J, Lukavska A, Sacchi A. 2000. Changes in chlorophyll fluorescence quenching and pigment composition in the green alga *Chlorococcum* sp. grown under nitrogen deficiency and salinity stress. *J Appl Phycol* 12:417-426.
- Matthijs HCP, Balke H, Hes van UM, Kroon BMA, Mur LR, Binot RA. 1996. Application of light-emitting diodes in bioreactors: Flashing light effects and energy economy in algal culture (*Chlorella pyrenoidosa*). *Biotechnol Bioeng* 50:98-107.
- Meijer EA, Wijffels RH. 1998. Development of a fast, reproducible and effective method for the extraction and quantification of proteins of micro-algae. *Biotechnol Tech* 12:353-358.
- Melis A, Neidhardt J, Benemann JR. 1998. *Dunaliella salina* (Chlorophyta) with small chlorophyll antenna sizes exhibit higher photosynthetic productivities and photon use efficiencies than normally pigmented cells. *J Appl Phycol* 10:515-525.
- Melis A. 1999. Photosystem-II damage and repair cycle in chloroplasts: what modulates the rate of photodamage *in vivo*? *Trends Plant Sci* 4:130-135.
- Menzel T, in der Weide T, Staudacher O, Wein O, Onken U. 1990. Reynolds shear stress for modeling of bubble column reactors. *Ind Eng Chem Res* 29:988-994.
- Merchuk JC. 1986. Gas hold-up and liquid velocity in a two-dimensional air lift reactor. *Chem Eng Sci* 41:11-16.
- Merchuk JC, Ben ZS, Niranjana K. 1994. Why use bubble column bioreactors? *Trends Biotechnol* 12:501-511.
- Merchuk JC, Ladwa N, Cameron A, Bulmer M, Berzin I, Pickett AM. 1996. Liquid flow and mixing in concentric tube air-lift reactors. *J Chem Tech Biotechnol* 66:174-182.
- Merchuk JC, Ronen M, Giris S, Arad SM. 1998. Light/dark cycles in the growth of the red microalga *Porphyridium* sp. *Biotechnol Bioeng* 59:705-713.
- Merchuk JC, Gluz M, Mukmenev I. 2000. Comparison of Photobioreactors for cultivation of the red microalga *Porphyridium* sp. *J Chem Tech Biotechnol* 75:1119-1126.
- Miron AS, Gomez AC, Camacho FG, Grima EM, Chisti MY. 1999. Comparative evaluation of compact photobioreactors for large-scale monoculture of microalgae. *J Biotechnol* 70:249-270.
- Miron AS, Camacho FG, Gomez AC, Grima EM, Chisti MY. 2000a. Bubble-column and airlift photobioreactors for algal culture. *AIChE Journal* 46:1872-1887.
- Miron AS, Grima EM, Sevilla JMF, Chisti MY, Camacho FG. 2000b. Assessment of the photosynthetically active radiation in outdoor photobioreactors using oxalic acid/uranyl sulfate chemical actinometer. *J Appl Phycol* 12:385-394.
- Mori K. 1985. Photoautotrophic bioreactor using visible solar rays condensed by Fresnel lenses and transmitted through optical fibers. *Biotechnol Bioeng Symp* 15:331-345.
- Morita M, Watanabe Y, Okawa T, Saiki H. 2001. Photosynthetic productivity of conical helical tubular photobioreactors incorporating *Chlorella* sp. under various culture medium flow conditions. *Biotechnol Bioeng* 74:136-144.
- Mouget J-L, Noue de la J, Legendre L, Jean Y, Viarouge P. 1995. Long-term acclimatization of *Scenedesmus bicellularis* to high-frequency intermittent lighting (100 Hz). I. Growth, photosynthesis and photosystem II activity. *J Plankton Res* 17:859-874.
- Nakajima Y, Tsuzuki M, Ueda R. 2001. Improved productivity by reduction of the content of light-harvesting pigment in *Chlamydomonas perigranulata*. *J Appl Phycol* 13:95-101.

- Neale PJ, Melis A. 1986. Algal photosynthetic membrane complexes and the photosynthesis-irradiance curve: a comparison of light-adaptation responses in *Chlamydomonas reinhardtii* (Chlorophyta). *J Phycol* 22:531-538.
- Nedbal L, Tichy V, Xiong F, Grobbelaar JU. 1996. Microscopic green algae and cyanobacteria in high-frequency intermittent light. *J Appl Phycol* 8:325-333.
- Niyogi KK, Björkman O, Grossman AR. 1997a. *Chlamydomonas* xanthophyll cycle mutants identified by video imaging of chlorophyll fluorescence quenching. *Plant Cell* 9:1369-1380.
- Niyogi KK, Björkman O, Grossman AR. 1997b. The roles of specific xanthophylls in photoprotection. *Proc Nat Acad Sci (USA)* 94:14162-14167.
- Nusch EA. 1980. Comparison of different methods for chlorophyll and phaeopigment determination. *Arch Hydrobiol Beiheft* 14:14-36.
- Ogbonna JC, Yada H, Tanaka H. 1995. Effect of cell movement by random mixing between the surface and the bottom of photobioreactors on algal productivity. *J Ferment Bioeng* 79:152-157.
- Ogbonna JC, Soejima T, Tanaka H. 1999. An integrated solar and artificial light system for internal illumination of photobioreactors. *J Biotechnol* 70:289-297.
- Olaizola M. 2000. Commercial production of astaxanthin from *Haematococcus pluvialis* using 25,000-liter outdoor photobioreactors. *J Appl Phycol* 12:499-506.
- Perry RH, Greene D. 1984. *Perry's Chemical Engineers' Handbook*. New York: McGraw-Hill, Inc.
- Phillips JN, Myers JN. 1954. Growth rate of *Chlorella* in flashing light. *Plant Physiol* 29:152-161.
- Pirt SJ, Lee YK, Richmond A, Watts Pirt M. 1980. The photosynthetic efficiency of *Chlorella* biomass growth with reference to solar energy utilisation. *J Chem Tech Biotechnol* 30:25-34.
- Pirt SJ. 1986. The thermodynamic efficiency (quantum demand) and dynamics of photosynthetic growth. *New Phytol* 102:3-37.
- Post AF, Dubinsky Z, Wyman K, Falkowski PG. 1985. Physiological responses of a marine planktonic diatom to transitions in growth irradiance. *Mar Ecol-Prog Ser* 25:141-149.
- Post AF, Loogman JG, Mur LR. 1986. Photosynthesis, carbon flows and growth of *Oscillatoria agardhii* Gomont in environments with a periodic supply of light. *J gen Microbiol* 132:2129-2136.
- Powell CK, Chaddock JB, Dixon JR. 1965. The motion of algae in turbulent flow. *Biotechnol Bioeng* 7:295-308.
- Pulz O, Gerbsch N, Buchholz R. 1995. Light energy supply in plate-type and light diffusing optical fiber bioreactors. *J Appl Phycol* 7:145-149.
- Pulz O, Scheibenbogen K. 1998. Photobioreactors: Design and performance with respect to light energy input. In: Scheper T, editor. *Advances in Biochemical Engineering/Biotechnology*. Berlin Heidelberg: Springer-Verlag. Vol 59, p 123-152.
- Pulz O, Scheibenbogen K, Grob W. 2001. Biotechnology with cyanobacteria and microalgae. In: Rehm HJ, Reed G, Puhler A, Stadler P, editors. *Biotechnology*. Weinheim: Wiley-VCH. Vol 10, p 107-136.
- Quéguiner B, Legendre L. 1986. Phytoplankton photosynthetic adaptation to high frequency light fluctuations simulating those induced by sea surface waves. *Mar Biol* 90:483-491.
- Radmer R, Kok B. 1977. Photosynthesis: Limited yields, unlimited dreams. *BioScience* 27:599-605.
- Rao KK, Hall DO. 1996. Hydrogen production by cyanobacteria: Potential, problems and prospects. *J Mar Biotechnol* 4:10-15.
- Richmond A, Boussiba S, Vonshak A, Kopel R. 1993. A new tubular reactor for mass production of microalgae outdoors. *J Appl Phycol* 5:327-332.

- Richmond A. 1996. Efficient utilization of high irradiance for production of photoautotrophic cell mass: a survey. *J Appl Phycol* 8:381-387.
- Richmond A, Qiang H. 1997. Principles for efficient utilization of light for mass production of photoautotrophic microorganisms. *Appl Biochem Biotech* 63-65:649-658.
- Richmond A. 2000. Microalgal biotechnology at the turn of the millennium: A personal view. *J Appl Phycol* 12:441-451.
- Richmond A, Cheng-Wu Z. 2001. Optimization of a flat plate glass reactor for mass production of *Nannochloropsis* sp. outdoors. *J Biotechnol* 85:259-269.
- Roels JA, Heijnen JJ. 1980. Power dissipation and heat production in bubble columns: Approach based on nonequilibrium thermodynamics. *Biotechnol Bioeng* 22:2405-2409.
- Sanchez JLG, Perez JAS, Camacho FG, Sevilla JMF, Grima EM. 1996. Optimization of light and temperature for growing *Chlorella* sp. using response surface methodology. *Biotechnol Tech* 10:329-334.
- Schreiber U, Schliwa U, Bilger W. 1986. Continuous recording of photochemical and non-photochemical chlorophyll fluorescence quenching with a new type of modulation fluorometer. *Photosynth Res* 10:51-62.
- Schreiber U, Hormann H, Neubauer C, Klughammer C. 1995. Assessment of photosystem II photochemical quantum yield by chlorophyll fluorescence quenching analysis. *Aust J Plant Physiol* 22:209-220.
- Schulz R. 1996. Hydrogenases and hydrogen production in eukaryotic organisms and cyanobacteria. *J Mar Biotechnol* 4:16-22.
- Sharkey DS, Stitt M, Heineke D, Gerhardt R, Raschke K, Heldt HW. 1986a. Limitation of photosynthesis by carbon metabolism. II. O<sub>2</sub>-insensitive CO<sub>2</sub> uptake results from limitation of triose phosphate utilization. *Plant Physiol* 81:1123-1129.
- Sharkey DS, Seemann JR, Percy RW. 1986b. Contribution of metabolites of photosynthesis to postillumination CO<sub>2</sub> assimilation in response to lightflecks. *Plant Physiol* 82:1063-1068.
- Shimizu Y. 2000. Microalgae as a drug source. In: Fusetani N, editor. *Drugs from the sea*. Basel: Karger. p 30-45.
- Shin CN, Rhee G-Y, Chen J. 1987. Phosphate requirement, photosynthesis, and diel cell cycle of *Scenedesmus obliquus* under fluctuating light. *Can J Fish aquat Sci* 44:1753-1758.
- Smith PK, Krohn RI, Hermanson GT, Mallia AK, Gartner FH, Provenzano MD, Fujimoto EK, Goeke NM, Olson BJ, Klenk DC. 1985. Measurement of protein using bicinchoninic acid. *Analyt Biochem* 150:76-85.
- Stitt M. 1986. Limitation of photosynthesis by carbon metabolism. I. Evidence for excess electron transport capacity in leaves carrying out photosynthesis in saturating light and CO<sub>2</sub>. *Plant Physiol* 81:1115-1122.
- Stramski D, Morel A. 1990. Optical properties of photosynthetic picoplankton in different physiological states as affected by growth irradiance. *Deep-Sea Res Part A* 37:245-266.
- Sukenik A, Bennett J, Falkowski PG. 1987. Light-saturated photosynthesis - limitation by electron transport or carbon fixation? *Biochim Biophys Acta* 891:205-215.
- Tanada T. 1951. The photosynthetic efficiency of carotenoid pigments in *Navicula minima*. *Am J Bot* 38:276-283.
- Terry KL. 1986. Photosynthesis in modulated light: Quantitative dependence of photosynthetic enhancement on flashing rate. *Biotechnol Bioeng* 28:988-995.
- Thimijan RW, Heins RD. 1983. Photometric, radiometric, and quantum light units of measure: A review of procedures for interconversion. *HortScience* 18:818-822.

- Torzillo G, Sacchi A, Materassi R, Richmond A. 1991. Effect of temperature on yield and night biomass loss in *Spirulina platensis* grown outdoors in tubular photobioreactors. *J Appl Phycol* 3:103-110.
- Torzillo G, Carlozzi P, Pushparaj B, Montaini E, Materassi R. 1993. A two-plane tubular photobioreactor for outdoor culture of *Spirulina*. *Biotechnol Bioeng* 42:891-898.
- Torzillo G, Accolla P, Pinzani E, Masojidek J. 1996. *In situ* monitoring of chlorophyll fluorescence to assess the synergistic effect of low temperature and high irradiance stresses in *Spirulina* cultures grown outdoors in photobioreactors. *J Appl Phycol* 8:283-291.
- Tredici MR, Zittelli GC. 1998. Efficiency of sunlight utilization: Tubular versus flat photobioreactors. *Biotechnol Bioeng* 57:187-197.
- Tredici MR. 1999. Bioreactors, Photo. In: Flickinger MC, Drew SW, editors. *Encyclopedia of bioprocess technology : Fermentation, biocatalysis, and bioseparation*. John Wiley & Sons, Inc. p 395-419.
- Usui N, Ikenouchi M. 1997. The biological CO<sub>2</sub> fixation and utilization project by RITE.1. Highly-effective photobioreactor system. *Energ Convers Manage* 38 Suppl. S:S487-S492.
- Vacha F. 1995. The role of oxygen in photosynthesis. *Photosynthetica* 31:321-334.
- Vonshak A, Torzillo G, Tomaseli L. 1994. Use of chlorophyll fluorescence to estimate the effect of photoinhibition in outdoor cultures of *Spirulina platensis*. *J Appl Phycol* 6:31-34.
- Walsh P, Legendre L. 1982. Effets des fluctuations rapides de la lumière sur la photosynthèse du phytoplancton. *J Plankton Res* 4:313-327.
- Weissman JC, Goebel RP, Benemann JR. 1988. Photobioreactor design: Mixing, carbon utilization, and oxygen accumulation. *Biotechnol Bioeng* 31:336-344.
- Yoshihara KI, Nagase H, Eguchi K, Hirata K, Miyamoto K. 1996. Biological elimination of nitric oxide and carbon dioxide from flue gas by marine microalga NOA-113 cultivated in a long tubular photobioreactor. *J Ferment Bioeng* 82:351-354.



## Samenvatting

Fototrofe ééncellige micro-organismen zoals algen en cyanobacteriën ('blauw-groene algen') kunnen ons voorzien van vele waardevolle componenten, zoals voedingssupplementen en stoffen met farmaceutische werking. Voor veel van deze toepassingen is het gebruik van gesloten bioreactoren noodzakelijk. Alleen in steriliseerbare reactoren, afgesloten van de buitenwereld, is het mogelijk gedurende lange tijd monoculturen van gewenste microalgen te kweken.

In dit proefschrift is beschreven hoe ééncellige algen reageren op licht-donkercycli zoals deze voorkomen in fotobioreactoren. Lichtenergie is de enige energiebron voor fototrofe micro-organismen. Daarom zijn fotobioreactoren voorzien van transparante wanden, zodat zoveel mogelijk zonlicht in de kweekvloeistof kan doordringen. De lichtvoorziening in deze fotobioreactoren is dan ook de belangrijkste ontwerpparameter. Licht is het groei-limiterend 'substraat'. Alle andere substraten - koolstofdioxide, stikstof- en fosfaatverbindingen - zijn makkelijk en tegen lage kosten toe te voeren aan de waterige kweekvloeistof.

De lichtvoorziening in een fotobioreactor is gecompliceerd. Aan de reactorwand worden algen blootgesteld aan zonlicht ( $1000 - 2000 \mu\text{mol fotonen m}^{-2} \text{s}^{-1}$ ) en diep in de reactor, weg van de wand, bevinden de algen zich nagenoeg in het donker. Dit laatste wordt veroorzaakt doordat al het licht wordt geabsorbeerd door algen dicht bij de wand: de één zit in de schaduw van de ander. Als gevolg van menging van de kweekvloeistof worden de algen verplaatst door deze lichtgradiënt en worden ze blootgesteld aan licht-donkercycli. Dit fluctuerende lichtregime zou een grote invloed kunnen hebben op de efficiëntie waarmee algen de geabsorbeerde lichtenergie aanwenden voor groei. Deze efficiëntie wordt ook wel de fotosynthese-efficiëntie genoemd.

In de praktijk is deze efficiëntie te laag. Zelfs in het geval dat algen worden blootgesteld aan zwak zonlicht ( $100 - 200 \mu\text{mol fotonen m}^{-2} \text{s}^{-1}$ ) kan slechts een deel van de energie worden verwerkt. Het restant gaat verloren als warmte of fluorescentie. Alleen onder zeer zwak licht gaan algen uiterst efficiënt met licht om. Als er zonlicht wordt gebruikt, is een snelle afwisseling tussen korte periodes van hoge lichtintensiteit en donkere periodes de enige praktische manier om de 'gemiddelde' lichtintensiteit te 'verlagen'. In de jaren vijftig is namelijk al aangetoond dat hoogfrequent fluctuerend licht ( $> 10 \text{ Hz}$ ) leidt tot 'lichtintegratie': algen gekweekt onder fluctuerend licht met lichtflitsen van hoge intensiteit gaan veel

efficiënter met lichtenergie om dan algen gekweekt onder continue belichting van dezelfde hoge intensiteit. Dit fenomeen wordt ook wel het ‘flitslichteffect’ genoemd.

Het is zeer lastig om gebruik te maken van het ‘flitslichteffect’ in fotobioreactoren van grote schaal. Slechts in reactoren met een diepte van enkele centimeters die ook nog intensief worden gemengd door middel van beluchting, kan lichtintegratie worden verkregen. Het kweekvolume van zulke reactoren is beperkt en de constructie is complex. Dit is de reden waarom in dit onderzoek een studie is gemaakt van het effect van langere licht-donkercycli met een lengte van 6 tot 100 seconden. Dit zijn licht-donkercycli zoals die voor zullen komen in fotobioreactoren van grotere schaal.

In deze studie is duidelijk aangetoond dat er geen lichtintegratie plaatsvindt onder licht-donkercycli van 6 seconden of meer. De fotosynthese-efficiëntie is lager onder blootstelling aan licht-donkercycli dan onder continu licht. Bij deze vergelijking is de lichtintensiteit onder continu licht altijd gelijk gehouden aan die tijdens de lichtperiode van de corresponderende licht-donkercycli. Verschillende soorten algen, *Chlamydomonas reinhardtii*, *Chlorella sorokiniana* en *Dunaliella tertiolecta*, zijn in het laboratorium gekweekt onder een aantal cycli. Als referentie zijn ze ook onder continu licht gekweekt. Onder elk lichtregime is de biomassa-toename, gemeten als eiwit, per hoeveelheid geabsorbeerde lichtenergie bepaald. Deze biomassa-toename op lichtenergie is een goede maat voor de fotosynthese-efficiëntie. De gebruikte algen zijn modelorganismen die vaak worden gebruikt in het laboratorium en waarvan veel bekend is. *Chlamydomonas* en *Chlorella* zijn groene zoetwateralgen en *Dunaliella* is een groene zoutwateralg.

In aanvullende experimenten is naast de biomassa-toename ook de zuurstofproductiecapaciteit van *Chlamydomonas* bepaald. De zuurstofproductiecapaciteit bleek lager te zijn wanneer *Chlamydomonas* was opgekweekt onder een licht-donkercyclus dan wanneer deze onder continu licht was opgekweekt. De zuurstofproductiecapaciteit is een maat voor de maximale snelheid van fotosynthese. Dit resultaat correleert goed met de lagere biomassa-toename op lichtenergie onder licht-donkercycli.

De efficiëntie waarmee de fotosynthese-machinerie van algen licht benut, kan ook worden gemeten met ‘pulse amplitude modulation’ (PAM) fluorometrie. Het fotosysteem van een alg fluoresceert een (kleine) fractie van het geabsorbeerde licht. Deze fluorescentie kan worden gemeten met behulp van de PAM-techniek en hiermee kan de zogenaamde fotochemische efficiëntie van fotosysteem II worden berekend. Net als de biomassa-toename op lichtenergie was de fotochemische efficiëntie lager tijdens kweek onder licht-donkercycli dan onder continu licht.

Algen zijn heel flexibel en kunnen de structuur van hun fotosynthese-machinerie aanpassen aan het heersende lichtregime. Deze machinerie, in de chloroplast van een algencel, bestaat uit een groot aantal fotosystemen. Elk fotosysteem bestaat uit een antenne van pigmentmoleculen die is gekoppeld aan een reactiecentrum. In het reactiecentrum wordt de ingevangen lichtenergie omgezet in chemische energie die bruikbaar is voor de cel. Wanneer de lichtintensiteit wordt verlaagd, worden hetzij meer fotosystemen aangemaakt door de cel, hetzij de antenne's van de bestaande fotosystemen vergroot. Dit proces wordt fotoacclimatisering genoemd.

In deze studie is aangetoond dat *Chlamydomonas* en *Dunaliella* hun specifiek absorptieoppervlak vergroten als ze worden opgekweekt onder licht-donkercycli in plaats van onder continu licht. De overgang van continu licht naar licht-donkercycli leidt tot een verlaging van de beschikbaarheid van (licht)energie. Waarschijnlijk treedt als gevolg hiervan fotoacclimatisering op en vergroten de algen hun fotosystemen.

Het optreden van fotoacclimatisering kan de lagere fotosynthese-efficiëntie onder licht-donkercycli verklaren. Omdat het specifiek absorptieoppervlak is vergroot, wordt tijdens de lichtperiode van de licht-donkercyclus meer licht geabsorbeerd dan onder het overeenkomstige continu-lichtregime. Blijkbaar kunnen de algen deze extra hoeveelheid energie niet verwerken en gaat deze verloren als warmte. Fotoacclimatisering is dus niet gewenst in het geval van een fluctuerend lichtregime.

Een tweede proces dat in het onderzoek is meegenomen, is fotoinhibitie. Fotoinhibitie treedt op bij zeer hoge lichtintensiteiten en wordt veroorzaakt door een overdosis van geabsorbeerde lichtenergie. Een deel van de fotosystemen raakt beschadigd en de capaciteit en efficiëntie van fotosynthese nemen af. In deze studie is de lichtintensiteit gevarieerd tot maximaal  $1200 \mu\text{mol fotonen m}^{-2} \text{s}^{-1}$ . Onder deze hoge lichtintensiteit bleek fotoinhibitie nog geen grote rol te spelen voor *Chlamydomonas* en *Dunaliella*.

In deze studie is het duidelijk aangetoond dat voor het kweken van microalgen licht-donkercycli met een lengte van 6 seconden of meer, minder aantrekkelijk zijn dan continu licht. De fotosynthese-efficiëntie is lager dan de toch al lage efficiëntie onder continu licht. Desalniettemin zijn deze cycli soms onvermijdelijk in fotobioreactoren. Dit is de reden dat de biomassatoename op lichtenergie is gemodelleerd als functie van cyclusduur en de relatieve lengte van de lichtperiode in een licht-donkercyclus: de lichtfractie. Er is een statistisch model gebruikt omdat het systeem voorlopig nog te complex is om een theoretisch model te ontwikkelen. Het model was voor *Dunaliella* in staat de biomassatoename op lichtenergie te



beschrijven in een raamwerk met een cyclusduur van 10 tot 100 seconden en een lichtfractie van 0,1 tot 1 (1 = continu licht).

De omstandigheden tijdens de experimenten waarmee de modelparameters zijn bepaald, zijn aangepast in vergelijking tot de andere experimenten. De lichtintensiteit in de lichtperiode was namelijk niet constant, maar de algen waren blootgesteld aan een lichtgradiënt. De lichtintensiteit varieerde van 1200 tot 50  $\mu\text{mol fotonen m}^{-2} \text{s}^{-1}$ . Op deze manier is het model een goede beschrijving van de praktijk. In fotobioreactoren is de lichtintensiteit in de belichte zone namelijk niet constant. De intensiteit neemt af van de intensiteit van zonlicht aan de reactorwand tot een zeer lage lichtintensiteit ter hoogte van de (arbitraire) grens van de belichte en donkere zone.

Ook onder deze meer natuurlijke lichtgradiënt-donkercycli was het duidelijk dat de fotosynthese-efficiëntie lager was onder deze cycli dan onder continu licht. Maar als de donkere periode korter is dan één derde van de cyclusduur, is de biomassatoename op lichtenergie ongeveer gelijk aan die onder continu licht.

Aangezien lichtintegratie niet optreedt onder licht/donker cycli groter dan 6 seconden is de cyclusduur verder verlaagd tot 0,19 seconden. Onder deze omstandigheden is wel lichtintegratie waargenomen. De biomassatoename op lichtenergie onder deze cyclus was namelijk hoger dan die onder het corresponderende continu-lichtregime. Deze resultaten ondersteunen het reeds bekende fenomeen dat lichtintegratie optreedt bij licht-donkercycli van 0,1 seconden of minder (= 10 Hz).

Als slot van deze studie zijn de belangrijkste fotobioreactoren geëvalueerd met betrekking tot het lichtregime en fotosynthese-efficiëntie. Het is duidelijk aangetoond dat een hoge fotosynthese-efficiëntie alleen haalbaar is in fotobioreactoren met een zeer korte lichtweg (= geringe diepte), een zeer hoge biomassaconcentratie (= korte lichtflits) en een zeer intensieve menging door middel van beluchting (= korte cyclusduur). Dit zijn de zogeheten vlakke paneelreactoren. Er moet echter geconcludeerd worden dat deze reactoren en ook de andere bestudeerde fotobioreactoren zeer slecht zijn op te schalen. Daarom is voorgesteld lichtinvang te scheiden van de bioreactor. Via spiegels en glasvezels kan licht worden ingevangen en naar een compacte gesloten bioreactor worden geleid. Deze compacte bioreactor zou dan bestaan uit een groot aantal vlakke paneelreactoren die van elkaar gescheiden zijn door lichtverspreidende platen. Door deze eenheden op een slimme manier met elkaar te verbinden, kan de bioreactor worden opgeschaald. Op basis van de huidige kennis zou in een dergelijk nieuw reactorontwerp een zeer hoge fotosynthese-efficiëntie haalbaar moeten zijn.

## Nawoord

Het schrijven zit er bijna op, Joepie! Ik ben erg blij dat mijn proefschrift klaar is. De laatste twee jaren waren zwaar. Het combineren van een ‘pre-doc’ post-doc positie met de laatste loodjes van een proefschrift viel niet mee. Voor de duidelijkheid, van januari 1996 tot en met december 1999 heb ik het praktisch werk verricht wat tot dit proefschrift heeft geleid. Na een vakantie in Afrika ben ik in maart 2000 begonnen als post-doc onderzoeker aan een nieuw 3-jarig onderzoek, waterstofproductie uit biomassa met behulp van fotosynthetische bacteriën. In mijn ‘vrije’ tijd kon ik mooi mijn proefschrift schrijven. Dat is dus gelukt!

Ik woon ondertussen al bijna dertien jaar in Wageningen. In 1989 ben ik reeds met mijn studie Milieutechnologie begonnen. Mijn enthousiasme voor het onderzoek is ontstaan in de laatste jaren van de studie toen ik afstudeeronderzoeken ging doen. Zelfstandig werken en nadenken vond ik veel leuker dan vakjes leren en examens doen. Mijn eerste afstudeervak was leuk, mijn tweede afstudeervak was nog veel leuker. Ik was de eerste student die bij de sectie Proceskunde met algen mocht werken. Ik vond het fantastisch licht en koolstofdioxide te gebruiken om algen te kweken. In die tijd wilden we de algen gaan gebruiken om zware metalen uit afvalwater te verwijderen. Het praktisch werk was nieuw en uitdagend en toen al kreeg ik van mijn begeleider René Wijffels alle ruimte en tijd om mijn eigen weg te gaan.

Het is dan ook niet vreemd dat ik tijdens mijn stage in de Verenigde Staten meteen ja zei op een aanbod van René om als onderzoeker in opleiding verder te werken aan het algenonderzoek. Het was het plan om eerst te kijken of algen efficiënter gekweekt kunnen worden in air-lift reactoren waarin je bepaalde licht/donker cycli kunt opleggen. Daarna zouden de algen geïmmobiliseerd moeten worden in kleine bolletjes zodat afvalwater met grote snelheid door de reactor gepompt kon worden terwijl de algen de zware metalen zouden verwijderen. Als je het proefschrift, of alleen de samenvatting, hebt gelezen zal je opvallen dat ik me beperkt heb tot het eerste deel van de oorspronkelijke onderzoeksvraag.

Dit onderzoek had ik in mijn eentje natuurlijk nooit kunnen doen. Ook bij het schrijven heb ik veel hulp gehad. Als eerste wil ik daarom graag mijn co-promotor René Wijffels bedanken. Een betere begeleider en baas kon en kan ik me niet wensen. Hans Tramper, mijn promotor, had in het begin moeite met de algen en fotosynthese, net als ik veel moeite had met schrijven. Menig concept artikel kwam terug met het commentaar, ‘dit begrijp ik niet’. Hans, toch ben ik erg blij dat je zo kritisch was en mij telkens dwong me beter te formuleren. Ook je

warme aandacht voor al die leuke opstellingen in Lab 632 was erg motiverend. Luuc Mur, mijn tweede co-promotor, wil ik graag bedanken voor zijn frisse blik van buitenaf.

Een groot deel van het praktisch werk is verricht door studenten die bij mij een afstudeeronderzoek hebben gedaan. Tjibbe Chris, Bram, Michel, Saskia, Bas, Michiel, Marcel, Matty, Teun, Lucas, Peter en Nienke dank jullie wel voor jullie geweldige inzet en enthousiasme! Ook alle andere studenten die Lab 632 hebben bevolkt wil ik graag bedanken voor hun plezierige aanwezigheid en voor menig gezellig uurtje buiten werktijd. Met name Cindy bedankt voor het coachen van de 'Proceskunde Heren Roeiploeg'.

Die andere studenten hadden natuurlijk ook een andere begeleider: Catrinus, mijn kamergenoot. Catrinus, ik vond het erg leuk met je samen te werken. Nooit hoorde ik jou mopperen en ik kon vaak mijn klaagzang bij jou doen. Ook vond ik het erg prettig dat je 'GVC-5' een paar jaar lang naar een hoger niveau wist te tillen. Ik had nooit gedacht dat zo'n lange Fries zo makkelijk een tegenstander kon 'poorten', veel succes op de 'Lange Leegte'!

Speciale aandacht verdient ook Ronald, die net als mij allemaal nieuwe dingen moest verzinnen in het lab... Ronald, vooral ook bedankt dat je me door de moeilijke uren van mijn promotieonderzoek hebt geholpen. En natuurlijk wil ik graag het zonnetje in huis, Maria, bedanken voor haar altijd plezierige aanwezigheid. Maria, ik ben je natuurlijk ook nog erg dankbaar dat je samen met Nienke verder bent gegaan met mijn onderzoek en mij Hoofdstuk 5 gegeven hebt!

Rouke, ook jij bedankt voor je enthousiasme en inzet voor de 'mariene biotechnologie groep' voor de 'borrels' en het 'zaalvoetbal', veel succes met je eigen promotie. Fred, Gerrit en Jos, hartstikke bedankt voor jullie adviezen en hulp, de 'O' in OBP'er is meer dan verdiend! Rolf, ook al ben je geen OBP'er je staat altijd voor iedereen klaar en je bent een echte Collega! Verder wil ik de mensen van de werkplaatsen bedanken, Jan, Evert, Eric, André, Reinoud, Peter en Hans, jullie kunnen echt iets toevoegen aan toegepast onderzoek. Hopelijk kunnen jullie het werk blijven doen wat jullie zo leuk vinden en wat zo belangrijk is voor de universiteit. Tenslotte wil ik graag al mijn collega's van Proceskunde bedanken voor de gezelligheid en de erg plezierige werkomgeving.

Naast mijn collega's zijn het natuurlijk mijn vrienden die het leven leuk maken. Als eerste de 'Troellies', Martin en Wilbert, ik vond het top tijdens mijn 'oio'-jaren bij jullie in huis te hebben gewoond. We hebben echt erg veel leuke dingen gedaan, teveel om op te noemen, samen met Hanneke, Martijn, Mariska en Sybren. Het was een mooie tijd! Jeroen, jij ook bedankt voor je humor, scherpzinnigheid, kleine pesterijtjes en het organiseren van leuke 'uitjes'. Tenslotte Wilbert S., ik ben erg blij dat je die prachtige Scania bus hebt gekocht van

Tinus om mee naar Gambia te rijden, en dat ik zomaar in kon stappen. Het was een tocht om nooit te vergeten. Alle vrienden die ik niet genoemd heb, allemaal hartstikke bedankt voor al die mooie momenten die het leven zo leuk maken.

Ik wilde het kort houden, maar helaas dat gaat toch niet lukken want ik wil natuurlijk mijn familie nog bedanken. Pap en mam, ik ben jullie erg dankbaar dat jullie mij de kans hebben gegeven naar de universiteit te gaan en het onderzoek in te gaan. Zonder jullie stimulans en hulp was dit nooit gelukt. Ik ben erg trots op jullie. Anja, je bent mij voorgegaan in Wageningen en je woont nog steeds slechts een paar straten verder. Ik vind het erg fijn dat ik je in de buurt heb af en toe lekker over het werk, het voetbal en andere dingen kan praten. Het proefschrift is af, de zondag is weer vrij.

Lieve Dorien, een miljoen knuffels voor jouw steun. Onze relatie is gelukkig niet als een licht/donker cyclus, maar een altijd aanwezig mooi en fel licht naast mij. Het is fantastisch dat ik jou ben tegengekomen. Ik zie de toekomst stralend, met een hoge intensiteit, tegemoet...

This work was carried out at Wageningen University, Department of Agrotechnology and Food Sciences, Food and Bioprocess Engineering Group, P.O. Box 8129, 6700 EV Wageningen, The Netherlands.

This research was sponsored in part by the Netherlands Organization for Scientific Research, Council for Chemical Sciences (NWO-CW) and was part of the research program of the Graduate School OSPT (Process Technology).



## **Curriculum Vitae**

Marcel Janssen werd geboren op 8 september 1971 in Horst. Hij begon in 1983 met de middelbare school opleiding aan het Boschveldcollege in Venray. In 1989 werd het VWO-diploma behaald. In het najaar van 1989 is hij van start gegaan met de studie Milieuhygiëne aan de Landbouwniversiteit Wageningen met als oriëntatie Milieutechnologie. In de doctoraalfase heeft hij afstudeeronderzoeken uitgevoerd bij de vakgroep Milieutechnologie (Prof. G. Lettinga en Dr. S. Rebac) en de sectie Proceskunde (Prof. J. Tramper en Dr. R.H. Wijffels). Van april tot en met september 1995 werd een stage verricht bij de University of Notre Dame (Prof. R.L. Irvine en Dr. P.J. Hirl) in de Verenigde Staten. In januari 1996 werd het doctoraaldiploma behaald.

Van januari 1996 tot en met december 1999 deed hij een promotie-onderzoek aan de sectie Proceskunde van het Departement Agrotechnologie en Voedingswetenschappen van Wageningen Universiteit. Dit promotie-onderzoek is uitgevoerd onder begeleiding van Prof. J. Tramper, Dr. R.H. Wijffels en Prof. L.R. Mur en de inhoud staat beschreven in dit proefschrift. Vanaf maart 2000 is hij werkzaam als postdoctoraal onderzoeker bij de sectie Proceskunde binnen het EU project 'Biohydrogen', ofwel 'waterstofproductie uit biomassa'.

## **Daglicht / Dag licht**

**Ik leef,  
heen en weer geslingerd  
tussen licht en donker,  
tussen hoop en vrees.**

**Duisternis  
verstikt me. Ik voel een gemis.  
Het gemis van leven,  
gevoed door licht.**

**Licht bundelt haar krachten  
en ik absorbeer  
de kracht te strijden. Tegen het lot  
dat het telkens weer ...**

**donker wordt.**

**Dorien**